DUBLIN CITY
UNIVERSITY
Ollscoil Chathair Bhaile Atha Cliath
DUBLIN 9, IRELAND.

DEVELOPMENT OF SOME CAPILLARY ELECTROPHORETIC SEPARATIONS AND ENZYME-BASED SENSORS FOR SUBSTANCES OF PHARMACEUTICAL AND BIOMEDICAL INTEREST

by

Gemma M. Robinson BSc.

Thesis submitted for the Degree of Doctor of Philosophy

Supervisor: Prof. Malcolm R. Smyth

Dublin City University February 1997

I hereby certify that this material, which I now submit for assessment on the programme of study leading to the award of Doctor of Philosophy (PhD.) is entirely my own work and has not been taken from the work of others save and to the extent that such work has been cited and acknowledged within the text of my own work.

Signed: Gemma Robinson ID No.: 93700601

Date:

To my family

Acknowledgments

I wish to thank my supervisor Prof. Malcolm R. Smyth for his guidance and support and for all the social events throughout the past three years. I am indebted to him for providing me with the opportunity to carry out research at both The University of Kansas and l'Université de Montréal.

Thanks to Dr. Donal Leech at l'Université de Montréal for sharing his in-depth knowledge of electrochemistry with me and also to all the postgrads there, who made me feel so welcome at all times.

I would also like to thank Dr. Craig E. Lunte at the University of Kansas for his direction and numerous discussions, chemistry and otherwise ! and also to Dr. Susan M. Lunte and to all the Lunte Research group for their kindness.

A big word of thanks to all the staff and postgrads in the Chemistry Dept. at DCU, especially to Siobhan (recommended for any map-reading excursions in the States), Caroline, Brendan, and Stephen for their entertainment and endless cups of coffee, and to former members of Malcolm's research group: Michaela, Declan, Enda, Mick, Brian, Bumni and Eithne. A special word of thanks to Dr. Emmanuel I. Iwuoha for all his positive criticisms with the electrochemical work.

Thanks to the '*Mullingar crew*' and also to Trish, Dopey and Netty for the '*craic*' over the years and having confidence in me (even when I didn't). Not forgetting my long-time friends Mary and AnnMarie for keeping the phone-lines open at all hours.

I am extremely grateful to my parents and family for all their love and support over the years and finally to Martin for his patience, understanding and love throughout the ups and downs of this work.

TABLE OF CONTENTS

		Page No.
TITLE PAGE		I
DECLARATION		II
DEDICATION		III
ACKNOWLEDGEMENTS		IV
TABLE OF CONTENTS		V
ABSTRACT		XIII

CHAPTER 1.

AN INTRODUCTION TO CAPILLARY ELECTROPHORESIS FOR THE SEPARATION OF PHARMACEUTICAL AND BIOMEDICALLY IMPORTANT COMPOUNDS 1

1.1.	INTRODUCTION	2
1.2.	FUNDAMENTALS OF CAPILLARY ELECTROPHORESIS	3
1.3.	SEPARATION MODES IN CE	8
1.3.1.	Capillary Zone Electrophoresis	8
1.3.2.	Capillary Isoelectric Focusing	8
1.3.3.	Capillary Gel Electrophoresis	9
1.3.4.	Capillary Isotachophoresis	9
1.3.5.	Micellar Electrokinetic Chromatography	10
1.4.	APPROACHES TO OBTAIN OPTIMUM SELECTIVITY AND EFFICIENCY IN CE	11
1.4.1.	Choice of appropriate buffer	11
1.4.1.1.	Buffer concentration	12

1.4.1.2.	Buffer pH	12
1.4.2.	Voltage and Temperature control	13
1.4.3.	Buffer Additives	13
1.4.3.1.	Organic solvents	14
1.4.3.2.	Ion Pairing Interactions in CE	15
1.4.3.3.	Host Guest Complexation Reagents	16
1.4.3.3.1.	Cyclodextrins	16
1.4.3.3.2.	Crown ethers	18
1.4.3.3.3.	Macrocyclic Antibiotics	19
1.4.3.4.	Metal Ions	20
1.5.	CAPILLARY TYPES USED IN CE SEPARATIONS	20
1.5.1.	Use of polymer coatings to prevent protein adsorption to capillary wall	21
1.5.2.	Polyacrylamide coatings	21
1.5.3.	Polyoxyethylene coatings	21
1.6.	DETECTION STRATEGIES IN CE APPLICATIONS	22
1.6.1.	Overview	22
1.6.2.	UV Spectroscopic Detection	22
1.6.3.	Fluorescence and Laser Induced Fluorescence Detection	24
1.6.4.	Mass Spectrometry	25
1.6.5.	Electrochemical Detection	25
1.7.	REFERENCES	27

CHAPTER 2.

CAPILLARY ELECTROPHORETIC METHOD DEVELOPMENT FOR NSG-PEPTOID COMBINATORIAL LIBRARIES 32

2.1.	INTRODUCTION TO COMBINATORIAL CHEMISTRY	33
2.1.1.	Synthesis of Combinatorial Libraries	33
2.1.2.	Low molecular weight combinatorial libraries	34
2.1.3.	Combinatorial peptoids	34
2.1.4.	Applications of NSG-peptoids	35
2.1.5.	Recognition of an active site	36
2.1.6.	Analytical Techniques for Combinatorial Library Analysis	36
2.1.7.	Aims of Research	37
2.2.	EXPERIMENTAL	38
2.2.1.	Chemicals	38
2.2.2.	Instrumentation	39
2.2.2.1.	Capillary Electrophoretic System 1	39
2.2.2.2.	Capillary Electrophoretic System 2	39
2.2.3.	Preparation of buffer solution	40
2.3.	RESULTS AND DISCUSSION	40
2.3.1.	Optimisation of separation conditions for the peptoid library: CHIR 4580.1	40
2.3.1.1	Effect of buffer pH	40
2.3.1.2.	Effect of increasing the ionic strength of the buffer	43
2.3.1.3.	Effect of ion-pairing agents on separation	45
2.3.1.4.	Addition of organic solvent to effect separation	47
2.3.1.5.	Combined effect of organic solvent sand ion-pairing agent on separation	49
2.3.1.6.	Effect of cyclodextrin	51
2.3.1.7.	Optimised Separation	54

2.4.	SEPARATION OF THE REMINING FIVE LIBRARIES USING THE SEPARATION METHOD DEVELOPED FOR THE NSG-PEPTOID LIBRARY CHIR 4580.1	55
2.4.1.	Peptoid libraries which were separated using the pre-existing method	56
2.4.1.1.	NSG-peptoid library CHIR 4582.1	57
2.4.1.2.	NSG-peptoid library CHIR 5216.1	59
2.4.1.3.	NSG-peptoid library CHIR 4555.1	60
2.5.	PROBLEMATIC LIBRARIES	63
2.5.1.	Development of a cyclodextrin-modified micellar based separation method	63
2.5.1.1.	NSG-peptoid library CHIR 2003.1	63
2.5.1.2.	NSG-peptoid library CHIR 4567.1	67
2.5.2.	Investigation of a bile salt for the separation of CHIR 4567.1	69
2.6.	INDIVIDUAL NSG-PEPTOIDS AS MARKER COMPOUNDS	70
2.6.1.	Overview	70
2.7.	CONCLUSION	75
2.8.	REFERENCES	78

CHAPTER 3.

A STUDY OF THE MELANISATION PATHWAY OF L-DOPA USING CAPILLARY ELECTROPHORESIS WITH DIODE ARRAY DETECTION AND AN INVESTIGATION OF SOME PROPERTIES OF THE MELANIN POLYMER FORMED BY ELECTROCHEMICAL TECHNIQUES 81

3.1.	INTRODUCTION	82

3.2.	EXPERIMENTAL	84
3.2.1.	Chemicals	84
3.2.2.	Capillary Electrophoresis system	85
3.2.3.	Spectroelectrochemical instrumentation	85
3.2.4.	Electrochemical apparatus	86
3.2.5.	Buffer preparation	86
3.3.	RESULTS AND DISCUSSION	87
3.3.1.	Optimisation of the separation conditions for L-tyrosine and L-dopa	87
3.3.2.	Sample stacking	87
3.3.2.1.	Buffer concentration differences to mediate stacking effects	88
3.3.2.2.	pH mediated stacking	88
3.3.3.	Tyrosinase oxidation of L-tyrosine	93
3.3.4.	Oxidation by sodium periodate	98
3.3.5.	Choice of suitable internal standard	106
3.4.	SPECTROELECTROCHEMISTRY OF DOPACHROME FORMATION	109
3.4.1.	Cyclic voltammetry of L-dopa	109
3.4.2.	Spectroelectrochemistry	110
3.5.	ELECTROCHEMISTRY OF MELANIN POLYMER	113
3.5.1.	Effect of buffer pH on the volumetric behaviour of L-dopa	114
3.5.2.	Effect of electrolyte ion	119
3.5.2.1.	Perchlorate based electrolytes	119
3.5.2.2.	Sulphate-based electrolyte	121
3.6.	CONCLUSIONS	123
3.7.	REFERENCES	125

CHAPTER 4

AN INTRODUCTION TO RECENT DEVELOPMENTS IN BIOSENSOR TECHNOLOGY, IN PARTICULAR RELATED TO BIOMEDICAL APPLICATIONS 127

4.1.	INTRODUCTION TO BIOSENSORS	128
4.2.	ENZYMES AS CATALYSTS FOR RECOGNITION	128
4.2.1.	Behaviour of immobilised enzymes at electrode surfaces	129
4.2.2	Types of redox enzymes used	130
4.3.	REDOX POLYMER MOIETIES FOR IMMOBILISATION ONTO ELECTRODE SURFACES	131
4.3.1.	Pre-assembled monomer units	132
4.3.2.	In-situ assembly	132
4.3.3.	Ion-Exchange polymers	133
4.3.4.	Advantages offered by electroactive polymers	134
4.4.	IMPROVEMENTS TOWARDS BETTER ELECTRICAL COMMUNICATION	134
4.4.1.	Electrical communication via relays	135
4.4.2.	Electrical 'wiring' of redox enzymes to the electrode via redox polymer chains	135
4.4.3.	Ferrocene containing redox mediators for biosensor use	137
4.4.4.	Electrochemically deposited polymers for biosensor application	138
4.4.5.	Layer thickness and enzyme loading; effects on kinetic parameters	138
4.4.6.	Membrane technology	139
4.4.7.	Mediator fine-tuning towards an improved biosensor design	139
4.5.	BIOSENSORS FOR ENVIRONMENTAL HEALTH MONITORING	141

4.5.1.	Toxin sensors	141
4.6.	METHODS USED TO STUDY CHARGE TRANSPORT WITHIN MULITLAYER BIOSENSORS	143
4.6.1.	Cyclic voltammetry	143
4.6.2.	Rotating disk voltammetry	145
4.6.3.	Potential step techniques	146
4.6.3.1.	Chronopotentiometry	146
4.6.3.2.	Chronoamperometry	147
4.6.3.3.	Chronocoulometry	147
4.7.	REFERENCES	148

CHAPTER 5

REAGENTLESS TYROSINASE ELECTRODE FOR THE DETECTION OF RESPIRATORY POISONS 152

5.1.	INTRODUCION	153
5.1.1.	Osmium and Group VIII metal redox polymers for biosensor applications	153
5.1.2.	Tyrosinase	154
5.1.3.	Atomic Absorption Spectrometry studies	156
5.2.	EXPERIMENTAL	157
5.2.1.	Apparatus for Atomic Absorption analysis	157
5.2.2.	Reagents and Materials	157
5.2.3.	Standard solution preparation	158
5.2.4.	Procedure for Atomic Absorbtion analysis	158
5.2.5.	Apparatus for Electrochemical experiments	159
5.2.6.	Redox polymer modified electrode preparation	159

5.2.7.	Homogenous inhibition studies	160
5.3.	RESULTS AND DISCUSSION	161
5.3.1.	Atomic Absorption analysis for the estimation of the copper content in the tyrosinase enzyme	161
5.3.2.	Osmium based redox compounds as artificial mediators	163
5.3.3.	Redox behaviour of tyrosinase	166
5.3.3.1.	Determination of kinetic parameters for a reversible electron-transfer system	167
5.3.3.2.	Enzyme Kinetic analysis	171
5.3.3.3.	Effect of Temperature, pH , and Ionic strength	173
5.3.3.4.	Homogenous inhibition of the tyrosinase enzyme using the complex $[Os(bpy)_2(MeIm)]PF_6^{2+/+}$ as mediator with sodium azide as a model inhibitor	177
5.3.3.5.	Immobilised enzyme inhibition electrode-Heterogenous inhibition	178
5.3.3.6.	Effect of enzyme concentration on inhibition	181
5.3.3.7.	Effect of polymer concentration on inhibition	182
5.3.4.	Determination of the kinetic parameters of the tyrosinase electrode using rotating disc electrode experiments	184
5.4.	CONCLUSIONS	188
5.5.	REFERENCES	189

CHAPTER 6

CONCLUSIONS/FUTURE TRENDS 191

APPENDIX

PUBLICATIONS A

ABSTRACT

Development of Some Capillary Electrophoretic Separations and Enzyme-based Sensors for Substances of Pharmaceutical and Biomedical Interest

Gemma M. Robinson

The development of Capillary Electrophoresis (CE) over the past decade has witnessed continued expansion, and it is now recognised as a powerful analytical technique. In Chapter 1 the concepts of CE are introduced and the various separation modes available to CE are discussed. Combinatorial Chemistry is a technique that is rapidly re-shaping the drug discovery process. This novel and cost-effective approach is capable of synthesising vast numbers of chemical variants all at one time, followed by the screening of these molecules for their bio-activity. This growing interest in combinatorial chemistry by the pharmaceutical industry has influenced the development of new analytical techniques for the analysis of such complex molecules. In Chapter 2 a CE method was developed for the separation of NSG-peptoid combinatorial libraries. In total, six libraries were examined. The separation power and versatility of CE makes it an ideal tool for the analysis of such libraries. A particular attraction is the ease with which the selectivity can be manipulated to bring about the efficient separation of these libraries. Chapter 3 discusses a CE method for the separation and analysis of products and intermediates of L-Dopa oxidation with Diode Array Detection (DAD). L-Dopa is one of the most important pre-cursors in the melanogenesis pathway. In this study both the tyrosinase enzyme and sodium periodate were used to catalyse several key steps in this pathway. Because of the instability of several of the intermediates formed, the detection and isolation of these compounds has remained problematic. Herein the advantages offered by CE are discussed and comparisons made with spectroelectrochemical techniques. Cyclic voltammetry and chrononcoulometric methods were used for the characterisation of the final polymeric product, melanin, and its utility as a sensor/biosensor assessed.

Recent advances in biosensor development are discussed in Chapter 4, in particular, for the detection and monitoring of toxins. The suitability of electroactive redox polymers as artificial mediators is examined and the concepts of charge propagation through such polymers. Recent trends have been to 'wire' a redox enzyme to an electrode via the use of these redox polymer chains. The development of a 'reagentless' immobilised enzyme inhibition sensor for respiratory poisons is described in Chapter 5. This system was based on the co-immobilisation of tyrosinase and a redox polymer, $[Os(bpy)_2\ (PVI)_{10}Cl]Cl$ (OsPVI), where bpy is the 2,2'-bipyridine ligand and the $(PVI)_{10}$ is poly-N-vinylimidazole indicating a ratio of co-ordinated redox sites to free pendant groups of 1:10. The hydrogel enzyme electrode allows 'reagentless' sampling of the enzyme activity by electrochemically 'switching on' the enzymatic reduction of oxygen through

electrochemical reduction of the immobilised osmium redox couple. This tyrosinase based sensor is capable of detecting any modulator of enzyme activity. Both homogenous and heterogeneous enzyme inhibition were investigated. The respiratory poison azide, which inhibits the tyrosinase enzyme, was selected as a model inhibitor to demonstrate the feasibility of the approach. It is envisaged that this system can be extended for the detection of other inhibitors of tyrosinase such as cyanide.

Finally, Chapter 6 discusses the conclusions reached during the course of this research and looks at possible areas for future research.

CHAPTER 1

AN INTRODUCTION TO CAPILLARY ELECTROPHORESIS FOR THE SEPARATION OF PHARMACEUTICAL AND BIOMEDICALLY IMPORTANT COMPOUNDS

1.1 INTRODUCTION

Developments in capillary electrophoresis (CE) have progressed at a phenomenal rate since its revival by Jorgensen and Lukacs [1], who demonstrated high separation efficiencies when a high electric field strength was applied to a capillary of 75 μm diameter. However, the popularity and widespread use of this technique has only commenced with the onset of commercially available instrumentation. A number of comprehensive reviews, discussing the various modes of CE, the principles of separation, sample introduction, and detection strategies, are available [2,3]. CE embraces the powers of traditional electrophoresis, chromatography and capillary technology. Several important features offered by CE include speed of analysis, ease of automation, minute sample and reagent consumption, and flexibility [4]. Advances in CE technology are so rapid that the importance of traditional HPLC methods are now being questioned.

The utility of CE as a diagnostic tool and separation technique has witnessed continued expansion, particularly in areas such as biomedical and pharmaceutical analyses [5,6]. A key feature in CE separations is the ease with which the selectivity can be modified. Initial studies were mainly centred around the analysis of charged molecules, and as the majority of drugs are either acidic and/or basic water soluble compounds, CE fitted the requirements quite well. However, the advent of micellar electrokinetic chromatography (MEKC) [7] has added a new dimension to CE separation technology, and highly efficient separations of uncharged molecules, which may be problematic with conventional HPLC methods, have now been realised. The addition of additives, such as organic solvents, ion pairing agents and cyclodextrins, to the run buffer has demonstrated tremendous versatility in CE separations, and hence, MEKC offers great potential for future applications. Other areas where CE has carved a niche include the analysis of food [8], water [9], analysis of inorganic ions [10], single cell analysis [11,12], enzyme technology [13,14] and peptide and protein applications [15,16].

1.2. FUNDAMENTALS OF CAPILLARY ELECTROPHORESIS

The basic configuration of a CE system is relatively simple and inexpensive to construct (Figure 1.1). It consists of a separation column (generally a fused silica capillary between 50-100 μm i.d.), a high voltage power supply, and a detection system; ultra-violet spectroscopy (UV) or laser induced fluorescence (LIF) detection being the most common. The design of these particular detectors require an optical window on-column, while end-column detection is more suited for mass spectrometry or electrochemical detection based systems. Samples are generally introduced into a buffer filled capillary from the anodic end, either by electromigration or hydrodynamically, and detected either on-column or end-column at the cathodic end. This capillary is positioned between the two buffer reservoirs, and electrical connection is made by placing two electrodes, one in each buffer reservoir, which are linked to the high voltage supply.

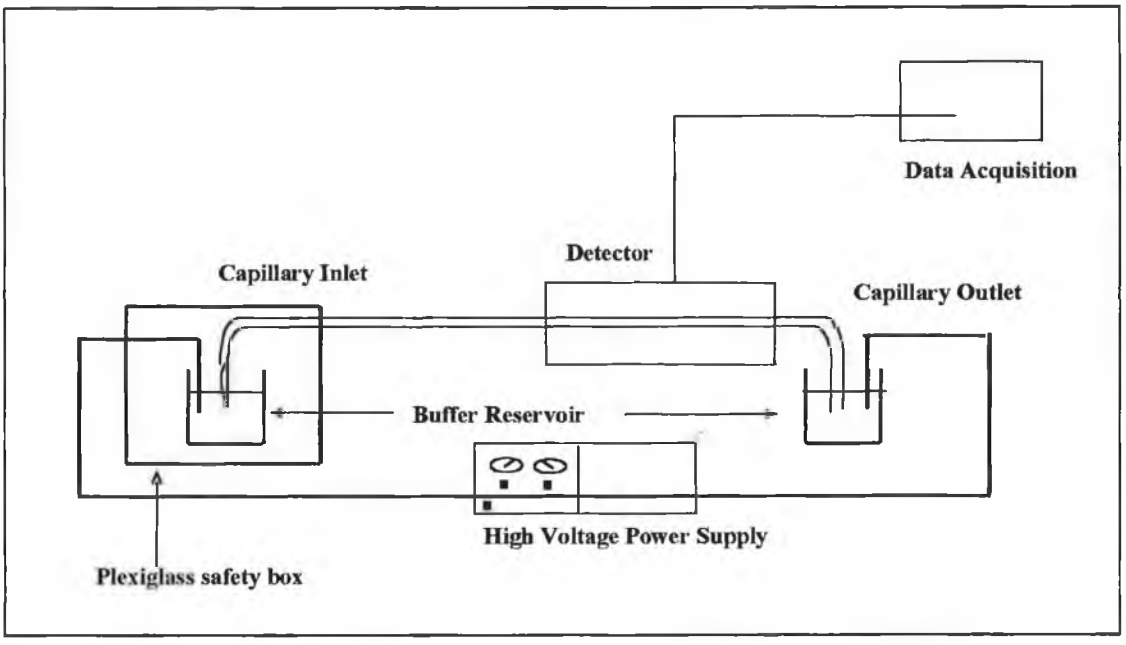

Figure 1.1. Schematic of a capillary electrophoresis system.

Separations in CE are based on differences in the electrophoretic mobilities between compounds upon the application of a high voltage to the system. The electrophoretic mobility; μ_{ep}, is determined from the Debeye-Huckel-Henry equation:

$$\mu_{ep} = q/6\pi\eta R \qquad (1.1)$$

where q is the net charge, R is the Stokes Radius and η is the viscosity of the buffer.

The velocity, ν, of any particular compound is denoted by the following equation:

$$\nu_{ep} = \mu_{ep} \times E = (q/6\pi\eta R) \times E \qquad (1.2)$$

where E is the potential applied across the capillary.

Hence the migration time, t_m, of a particular compound to travel a capillary of length, L, from the point of injection to the detector window is:

$$t_m = L/\nu = L/E \times 6\pi\eta R/q \qquad (1.3)$$

Thus, from the above equation, it can be seen that separation in CE is due to differences in the charge and the Stokes radii of the compounds of interest. Two compounds of opposite charge will be completely separated, as the direction of their migration will be opposite, while compounds of the same polarity may be separated depending on the number of charges and their respective radii.

The other important feature which permits separation of a range of compounds in CE is the electroosmotic flow (EOF). The EOF is a function of the applied potential and the potential drop across the interface between the capillary wall and the diffuse region within the capillary. The EOF is defined by:

$$\nu_{EOF} = (\varepsilon\zeta/4\pi\eta) E \qquad (1.4)$$

where ε is the dielectric constant, and ζ is the zeta potential measured at the plane of shear close to the liquid-solid interface.

For fused silica capillaries, the wall is negatively charged (when in contact with solutions of pH > 2). The higher the pH, the greater the deprotonation of the silanol groups on the surface of the capillary wall. The negatively charged wall thus attracts positively charged ions from the buffer solution, thereby creating an electrical double layer. When a voltage is applied across the capillary, cations in the diffuse portion of the double layer migrate in the direction of the cathode. The result is a net flow of buffer solution in the direction of the negative electrode. The mobility of a compound along a capillary will then be due to the combined effect of the electrophoretic and electroosmotic flows. The EOF can be quite robust, and makes possible the analysis of cations, neutrals and anions in a single analysis. Although the μ_{ep} directs anions in opposition to the EOF, the EOF is sufficiently stronger then μ_{ep} (particularly at neutral to alkaline pH), that it pulls the anions towards the cathodic end of the capillary. The elution profile of such charged and uncharged ions is illustrated in Figure 1.2.

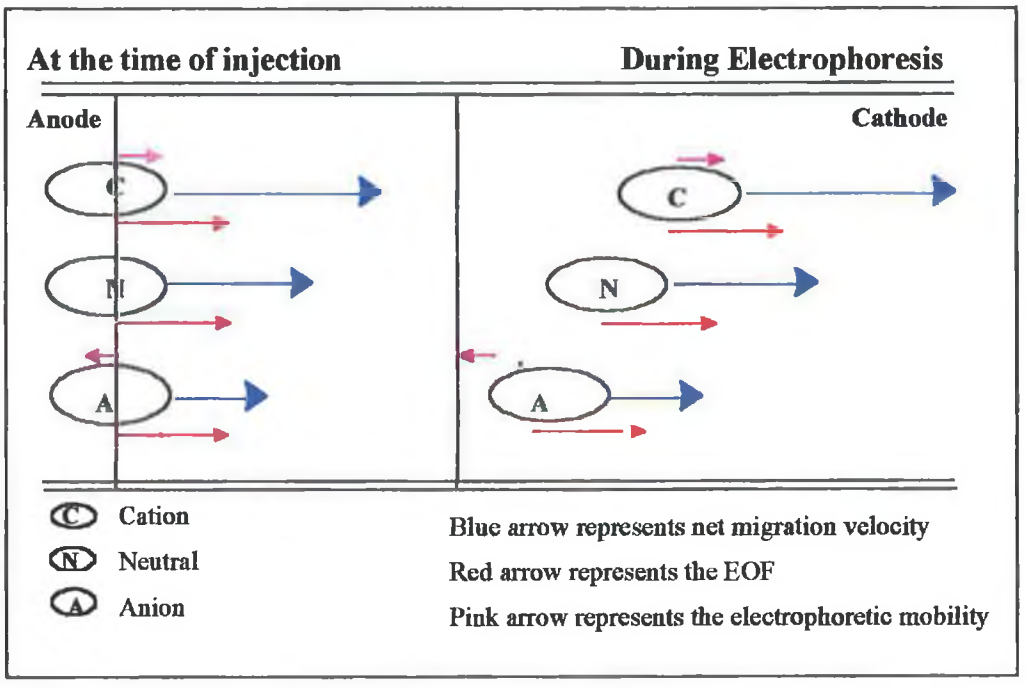

Figure 1.2. The order of migration of cations, neutrals and anions in CE, which is illustrated by the net migration due to the EOF and the electrophoretic mobility.

Although CE allows the separation of charged cations or anions due to differences in their Stoke radii, or due to differences in the number of their charges, neutral compounds will not be separated, as they migrate with the same velocity as the

EOF. Another mode of CE is required, namely micellar electrokinetic chromatography, for separation of such compounds which is discussed in detail later.

Several methods have been described to measure the EOF in CE [17-19]. For instance, Huang *et al.* [17] measured the drop in current as the electrolyte progressed along the capillary. This method also incorporated a conductivity detector to monitor changes in conductivity with time. Poor reproducibility of analyte migration times, however, has prevented the use of CE as a method for high accuracy identification of molecules, due to huge variations in the EOF. Huang [20] describes a model to explain the pH hysteresis of EOF in fused silica capillaries. He noted that the establishment of an equilibrium state for the silica-solution interface depends on the mode of capillary pre-conditioning employed, which can produce variations in the zeta potential, and hence a variation in the EOF. A theoretical model for electroosmotic flow has recently been described [21] where the behaviour between ion-selective membranes with the double-layer structure of the fused-silica capillary were compared.

The resolution, R_s, of two molecules in CE can be expressed by the following:

$$R_s = \frac{1}{4}\frac{(\mu_1 - \mu_2)}{\mu_{ave}} (N)^{1/2} \qquad (1.5)$$

where μ_1 and μ_2 are the respective electrophoretic mobilites of the two molecules, μ_{ave} is the average electrophoretic mobility of the two molecules, and N is the number of theoretical plates. By substituting for N (when $N = \mu_{ep}V/2D$), a new expression for the resolution can be obtained where

$$R_s = 0.177\ (\mu_1 - \mu_2)[V/\ D\ (\mu_{ave} + \mu_{EOF}]^{1/2} \qquad (1.6)$$

where V is the applied voltage and D is the diffusion coefficient of one of the molecules being separated.

From this expression it is clear that several factors limit the resolution which can be achieved. Increasing the voltage by a factor of four only doubles the resolution; however, the resulting increase in current (therefore Joule heat) limits the enhancement of resolution. Control of the pH is the most powerful parameter in CE separations in achieving the appropriate resolution as it controls the selectivity of the compounds to be separated and the dispersion between two compounds which is known as the efficiency term. Kenndler *et al.* [22] have described how selection of the appropriate pH is critical, especially for compounds with closely related pK_a values. Small pH differences close to the pK_a of the analytes can have deleterious effects on resolution.

Jorgensen and Lukacs [1] assumed that the only source of zone broadening in CE was due to diffusion; however a number of factors contribute to zone broadening which tend to limit the extent to which the highest resolution is possible. Schure *et al.* [23] observed that for medium sized or large molecules being separated, in short capillaries using high velocities, the presence of adsorption can be devastating. Even in small diameter capillaries, tailing reduces resolution considerably. In long capillaries with low velocity, no extra additional loss in resolution will be experienced through use of large diameter capillaries for medium or large molecules. The length of sample plug injected onto a capillary causes serious distortions to peak symmetry in CE [24]. For sufficient capillary lengths, N approaches a constant value, and becomes independent of plug size. At shorter capillary lengths, the fraction of the capillary occupied by the sample is greater and has a more marked effect on efficiencies, resulting in poor reproducibility. This arises because the injection field strength, E_{inj}, is inversely proportional to the capillary length. Another cause of zone broadening is the existence of temperature gradients within the capillary. Loss of heat from the capillary wall to the surrounding environment causes a radial temperature gradient, resulting in a viscosity gradient within the capillary. The magnitude of the temperature difference between the centre of the capillary and the wall is roughly proportional to the square of the diameter; hence wider diameter capillaries give rise to large temperature gradients, with less efficient heat dissipation. Depending on the ionic strength of the buffer, temperature differences as large as 38°C have been observed [25]. Hence the

requirement for efficient cooling mechanisms in CE technology is a prerequisite for good separations.

1.3. SEPARATION MODES IN CE

1.3.1. Capillary Zone Electrophoresis (CZE)

This technique, also known as free solution capillary electrophoresis (FSCE), is the simplest form of CE. The name capillary zone electrophoresis and capillary electrophoresis are almost synonymous. The separation mechanism is based on differences in charge-mass ratio, which have been discussed in detail in the previous section. The fundamental criteria for CZE separations are homogeneity through the buffer solution and a constant electric field strength applied throughout the entire length of the capillary. Capillaries of 50-100 μm i.d. are normally used, with lengths ranging from 20-100 cm or greater.

1.3.2. Capillary Isoelectric Focusing (CIEF)

This technique differs substantially from CZE on the basis of the pH gradient that is created inside the capillary when a voltage is applied to the carrier ampholytes. For zwitterionic compounds, separations occur as follows; at a pH below the pI of the molecule under investigation, the molecule is positively charged and migrates towards higher pH gradients, i.e. to the cathode. At a certain point the molecule will reach a region where the pH of the ampholyte equals the pI of the molecule. Migration ceases and the molecule will remain at this point. For a negatively charged molecule, i.e. when the pH is greater than the pI of the molecule, the molecule will migrate toward the anode entering lower pH gradients. Again migration ceases when it encounters a pH gradient which is the same as its own iso-electric point, pI. In CIEF, the EOF is minimised to prevent the molecules being swept past the detector before focusing. This technique is used quite substantially in modern applications [26,27] and has been reviewed recently [28].

1.3.3. Capillary Gel electrophoresis (CGE)

In this technique a capillary is filled with a gel-like matrix, i.e. a porous polymeric material dissolved in buffer, e.g. polyacrylamide or methylcellulose. When a potential is applied to the system, the molecules under investigation will migrate towards the appropriate electrode. Separation in gel electrophoresis is based on differences in size of molecules. Large biomolecules travel through the pores of the gel in a long and arduous path. Commercially available gels are used more frequently than home-made gels, due to problems with bubble formation and unstable currents which give rise to electrical discontinuity. CGE can also be used to estimate molecular weights of compounds. Proteins are usually denatured first, i.e. by reduction of the disulphide bonds. After this process, proteins have roughly the same shape and charge density. SDS is usually used to denature proteins via electrostatic and hydrophobic interactions. As SDS is anionic, it confers a negative charge to the protein; hence migration will be towards the anode. The mobility of the protein is then compared with several other size standards, which are used to calibrate the gel. This technique has been particularly useful for the separation of glycoproteins and high molecular weight biopolymers such as DNA fragments [29,30].

1.3.4. Capillary Isotachophoresis (CITP)

In CITP, the EOF is minimised, as in CIEF, and the buffer system is heterogeneous in nature [31,32]. Before an experiment is started, the capillary is filled with a leading electrolyte that has a mobility greater than the those of the sample components to be determined. The sample is then injected, followed by loading a terminating electrolyte into the opposite reservoir which has a mobility lower than any of the sample components. Initially, all samples are at the same point within the capillary, but as the run progresses, separation of the components will arise in the space between the two electrolytes. Migration will be determined by the mobility of the individual components. For a highly mobile sample component, the applied potential, E, and hence the electrophoretic velocity, ν_{ep}, will be reduced, and for sample components with low mobility, E will be greater and hence the ν_{ep} will also be increased.

A feature of CITP is its focusing capabilities; this arises when a diffuse band enters a neighbouring zone, which will cause its velocity to either increase or decrease, resulting in peak compression. This feature enables one to carry out quantitative analysis, based on the length of the zone. As adjacent bands are in contact with each other, spacers are often added, whose mobility are intermediate to the mobility of the two components of interest. This method is carried out when UV detection is used. Spacers which do not absorb at the detection wavelength are usually recommended. This technique is also used as a pre-concentration technique for CE applications [33].

1.3.5. Micellar Electrokinetic Chromatography (MEKC)

This technique was first introduced by Terabe [7]. Essentially, it consists of adding surfactant molecules, composed of long hydrophobic 'tails' and polar 'head groups'to the run buffer, to allow separation of uncharged molecules. Micelles are formed when a certain concentration (cmc) is reached; the surfactant molecules then aggregate and form spherical structures. The hydrophobic tails face inwardly in aqueous solutions with the polar head groups extending outward. Micelles that exist in this type of situation form what is known as a 'pseudophase'. Separations will be based on the interaction of a solute between the background electrolyte and the micelles, both of which exhibit different velocities.

SDS is by far the most widely used surfactant molecule; being anionic in nature, it will migrate toward the anode when a potential is applied. In untreated capillaries, the EOF is toward the cathode, hence the net migration velocity will be reduced. In neutral to alkaline pH, the EOF is substantially stronger, and the net flow will be still be in the direction of the cathode. When a sample is introduced into this type of system, it may partition into the micellar core, depending on its charge and size. Molecules which partition into the micelle will have a reduced velocity and hence, migrate with the micelle. Negatively charged molecules will be excluded from the micelle and will be swept toward the detector uninhibited, while neutral molecules will partition into the micelle. These molecules may then be separated based on hydrophobic interactions. Positively charged molecules may form electrostatic interactions with the micelle and will have the largest migration times. Hence the

migration order of charged molecules in MEKC will be the reverse of that observed in CZE. (Figure 1.3). Cationic surfactants have also been used; in this case, reversal of polarity of the power supply is necessary, because these surfactants bind to the negatively charged silanol sites on the capillary wall, and hence induce a positive charge to the fused silica wall.

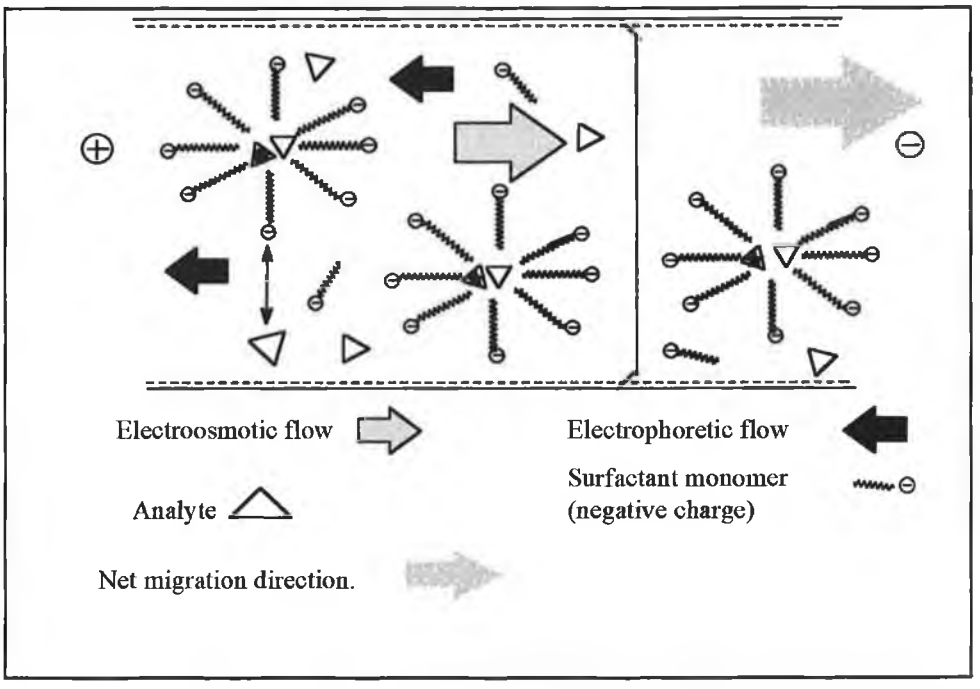

Figure 1.3. Separation mechanism in MEKC using an anionic surfactant..

1.4 APPROACHES TO OBTAIN OPTIMUM SELECTIVITY AND EFFICIENCY IN CE

1.4.1. Choice of the appropriate buffer

The first and most important step in any CE separation is the correct choice of buffer. The buffer determines the charge on the analyte of interest and hence its migration velocity. The majority of CE separations are performed using UV detection, and because of this, a fundamental parameter when selecting a buffer for CE is that it has a low UV absorbance. For the low pH range, dihydrogen phosphate and citrate buffers are commonly used, while at high pH, hydrogenphosphate and borate buffers are used. Zwitterionic buffers such as Tris, Taps and Caps are also recommended, as these

buffers offer lower conductivity values, hence give rise to lower current and less Joule heating. Another important parameter for CE separations is that the buffers be filtered through 0.45 μm filters.

1.4.1.1. Buffer concentration

The concentration of buffer that can be used will be controlled by the capillary length, diameter, the applied electric field and the effectiveness of the cooling system for the CE apparatus. High ionic strengths are desirable as they suppress ionic interactions between the charged analyte and the ionisable silanol surface of the capillary wall. However, the higher the ionic strength, the greater the problems associated with Joule heat, and hence loss in resolution. Joule heating can be minimised by use of low conductivity buffers, reducing the electric field strength, by reducing the inner diameter of the capillary, or by increasing the length of the capillary. The easiest and most effective situation is to increase the capillary length; however, this increases the time required for analysis and the probability of band broadening.

High ionic strength buffers allow for increased sample loading capacity which result in an on-capillary stacking effect. This will be discussed in detail later. Kuhn *et al.* [34] have described how borate buffers influence the electrophoretic mobilities of underivatised carbohydrates and glycopeptides. They demonstrated how increased concentrations of borate caused complexation to take place with native forms of the sugars without any derivatisation. This method showed increased sensitivity in the low UV range.

1.4.1.2. Buffer pH

The impact of pH on the analyte can be substantial, particularly for complex zwitterionic compounds such as proteins or peptides. The charge on these molecules is governed by the pH of the electrolyte, and hence governs the selectivity of separation. Generally a pH of at least two units above or below the pK_a of the analyte is used to ensure complete ionisation. At high pH values, the EOF is so strong that often

incomplete separation of the analytes may result. Certain protein separations can be performed at acidic pH. Under these conditions, the capillary wall will be uncharged and as the proteins are positively charged, no electrostatic interactions will occur, however, hydrophobic interactions may be present. A problem of low pH buffers is the increased migration times due to the reduced EOF. The effect of pH on separation of benzoic acids was described by Kenndler [22], who demonstrated how critical pH is for optimum separation. The composition of the buffer used is critical for control of the magnitude of the EOF [35] and hence the quality of separation.

1.4.2. Voltage and Temperature control

The effect of increasing voltage and temperature has already been mentioned briefly. As can be inferred from equations 1.2 and 1.4, both the electrophoretic velocity and the EOF are directly proportional to the applied electric field strength applied. Thus the higher the voltage applied, the shorter the migration times, and hence the higher the efficiencies (i.e. the extent of diffusion will be minimal). A consequence of using high voltages is Joule heating. A simple method for determining the optimum working voltage for a particular buffer system is the Ohms law plot. A linear plot of observed current versus applied voltage is indicitative of temperature control; the point where the linearity is lost shows where the thermostatting capacity of the system is lost [36]. Many commercially available CE instruments have incorporated efficient cooling devices into the basic unit, and are capable of maintaining excellent temperature control, even when high concentration buffers and large bore capillaries are utilised.

1.4.3. Buffer Additives

In addition to varying the ionic strength and pH of the buffer to achieve separation, various buffer additives can be employed to enhance the selectivity and efficiency of separations. In CE, some of the commonly used buffer additives include, organic solvents, ion-pairing agents, cyclodextrins, urea, inorganic ions and surfactants. These are simply dissolved in the running buffer, the column is conditioned as for a normal separation buffer and electrophoresis is carried out. This means of changing the selectivity for CE applications is rather inexpensive, when compared with classical

HPLC applications, where either large quantities of a reagent or a new column are required.

1.4.3.1. Organic Solvents

Miscible organic solvents are often added to the aqueous run buffer in CE separations to improve analyte resolution or to reduce analyte ion-capillary wall interactions [37-39]. Concentrations ranging from 0-30% (v/v) methanol or acetonitrile or 1-2% THF are the most commonly used, while formamide and DMSO are also used. Their mode of action is a speculative one, but it is believed that alcohols, in particular, interact strongly with the capillary wall, resulting in a higher concentration of alcohol within the double layer [35]. Salomon *et al.* [37], observed that the charge at the capillary wall increased when methanol was present in the buffer possibly due to the presence of methanol, which may have minimsed the repulsion between negatively charged silanol groups on the capillary surface, thus allowing more charge to exist in a given area when methanol was present. This increased cation concentration at a particular area, leads to a reduced value for the EOF. Methanol has a lower viscosity than water or other aqueous systems. By changing the viscosity, linear diffusion (which is a common problem in HPLC applications) is reduced, and hence the EOF. Changing the concentration of the organic solvent also changes the degree of protonation, which ultimately affects the dielectric constants of compounds, as well as the zeta potential of the capillary wall also leading to a reduced flow.

Schützner *et al.* [40] explored the effect of increasing acetonitrile on the separation of diastereomers. They noticed a shift in pK_a's of these diastereomers to higher values, with up to 1 pH unit of a difference with increasing acetonitrile from 0-50%. More recently, CE applications have been extended to purely non-aqueous solvents and this area is now known as non-aqueous capillary electrophoresis (NACE) [41,42]. This variant is particularly suited to the analysis of hydrophobic ionic substances, which have proven to be rather problematic in HPLC and also in normal CZE separations. Wang *et al.* [43] noticed that when NACE was used in conjunction with cyclodextrins, that the maximum enantioselectivity for racemic amines occurs

over a wider range; hence the selection of the optimum concentration was not as critical when compared to that in aqueous media. A problem encountered with organic solvents ,when used with UV detection, is the increased noise level, due to the high UV absorbance of these solvents at low wavelengths [44]. However, methanol and acetonitrile can be used at these lower wavelengths (around 210 nm) without any significant effects on the limit of detection.

1.4.3.2. Ion Pairing Interactions in CE

Ion-pair chromatography was first introduced to HPLC applications in the 1970's [45] and has been used extensively to study the retention behaviour of hydrophobic cationic and anionic compounds [46,47]. Selectivity in HPLC is determined by differences in the distribution equilibrium of analytes between a hydrophobic stationary phase and a polar mobile phase. Horvarth *et al.* [48] have demonstrated the addition of suitable counter ions to the mobile phase with substantial hydrophobic moieties. These counter ions have the potential to ion-pair with the charged analytes and thus may distribute themselves between either the non-polar stationary phase or the mobile phase with a significant increase in retention. Alternatively, ion-exchange materials may be used as the stationary phase, resulting in relatively strong retention mechanisms with the ion-exchanging stationary phase.

To extend the application of CE to the analysis of hydrophobic compounds, ion-pairing agents have been investigated by McLaughlin *et al.* [49]. They observed a significant enhancement in resolution for peptides, which they believe was caused by the fact that the hydrophobic alkyl side chains of the hexane sulphonic acid interact with the hydrophobic portion of the peptide, thereby decreasing aggregation. An increase in migration times was also observed, which may be attributed to the increased negative charges from the sulphonic acid groups. Ion-pair formation of polyammonium ions with aromatic disulphonates have recently been described by Okada [50]. An important factor observed for the formation of a stable ion-pair was the distance between ionic sites of the molecules involved. If the ammonium ion chains were too far removed from the sulphonate sites, then no interaction occurs. Furthermore, bulky ammonium ions were trapped within some aromatic disulphonates

due to steric hindrance. Enhanced selectivity was achieved when a tetravalent polyammonium ion was used, possibly attributing to a reduction in the overall mobility of the resulting ion-pair. Recently Kornfelt *et al.* [51] used phytic acid as an ion-pair reagent for the separation of positively charged amino acids. This compound is unlike the alkylsulphonic acids and the polyammonium ions which can change both hydrophobicity and the charge of the compound. Phytic acid on the other hand is of a polyanionic nature, with virtually no hydrophobic character. The ionic interaction with a positively charged species will therefore result in a change in their net charge in a negative direction.

1.4.3.3. Host Guest Complexation Reagents

1.4.3.3.1. Cyclodextrins

By far the most popular of all the complexing agents used in CE separations are the cyclodextrins (CD). Many of these applications concern the enantioselectivity of pharmaceutical drugs [52-54]. CD, first isolated in 1891 by Villiers, are formed by the enzymatic digestion of starch by cyclodextrin transglycosylase [55]. Natural α-, β- and γ-CDs are cyclic oligosaccharides containing 6,7 and 8 glucopyranose units respectively.

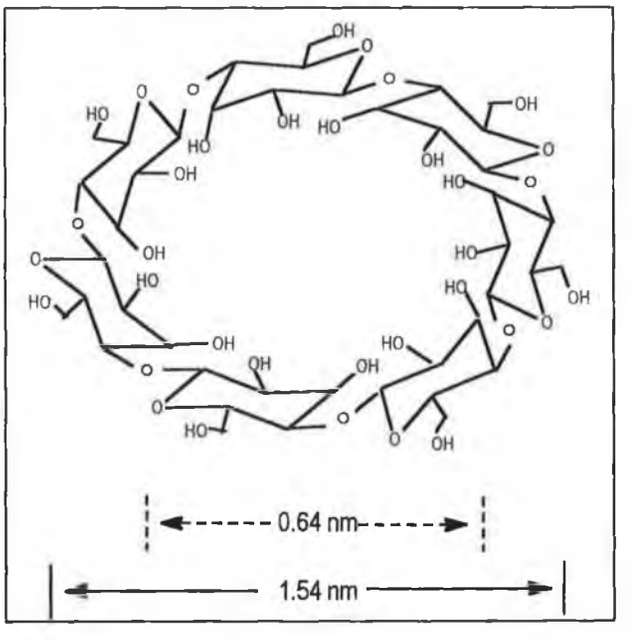

Figure 1.4 Structure of a β-cyclodextrin molecule, illustrating the width of the inner and outer diameter.

The most extensively used is β-CD, the structure of which is illustrated in Figure 1.4. These molecules have unusual stability [56], due to intramolecular hydrogen bonding between the C2 hydroxyl and the C3 hydroxyl of adjacent glucopyranose units. CDs have an electron rich hydrophobic inner cavity with exterior hydrophilic sites lining the entrance to the cavity. They can selectively complex with, or indeed, encapsulate entire molecules, depending on the chemical structure of the molecule. They can also reduce self-aggregation and adsorption tendencies due to hydrophobic interactions with the hydrophobic loci of the CD. It is this ability to selectively form host-guest interactions that many researchers have been exploring. Enantioselectivity is based on the inclusion of an aromatic or alkyl functionality into the cavity and additional hydrogen bonding between secondary hydroxyl groups around the opening of the cavity and substituents of the guest molecule. Host-guest interactions with the neutral CD cavity and a basic guest molecule leads to a reduction of the 'guests' migration velocity relative to the bulk flow. The stronger the interaction formed, the longer the migration will be. As even the slightest difference in the analytes structure will result in a slightly different complex, thus enantiomer separation can be realised.

The β-CD molecule has poor solubility. However, by chemically derivatising the exterior hydroxyls with hydrophilic or apolar substituents, the solubility characteristics are remarkably improved [56]. Fanali [57] investigated the effect of methyl β-CD derivatives on the separation of sympathomimetic drugs. He found that the correct fit is a necessary element for adequate complexation, and hence enantioseparation. It is generally accepted that α-CD has inner dimensions suitable only for the separation of aliphatic and mono-cyclic aromatic molecules. However, Sepaniak *et al.* [55] demonstrated that by chemically modifying the exterior rim of the CD, separation of bi-naphtyl enantiomers was made possible. They explained this phenomenon by considering the mouth of the CD to be 'stretched'; hence this changed the steric qualities required for host-guest interactions. They also observed that at a CD concentration, a maximum value for resolution was obtained followed by a decrease in resolution with increasing concentration of the CD further.

Recently, a polyanionic CD derivative was introduced [58]. This derivative is anionic over the entire pH range suited for CE applications, and hence exhibits a countercurrent mobility, which is believed to provide a substantially 'wider' separation window. This type of chiral selectivity is particularly suited for the separation of molecules which are unstable or are insufficiently resolved at high pH. Already, there have been numerous applications regarding this negatively charged-β-CD for instance in forensic drug analysis [59], polycyclic aromatic hydrocarbons [60] and a large variety of pharmaceutical compounds [51]. The number of applications using cyclodextrins in CE separations is enormous, that a molecular database is currently being created, in anticipation of a faster and more rational approach for chiral selectors [61].

1.4.3.3.2. Crown ethers

Crown ethers are another member from the family of host-guest complexating reagents. Kuhn *et al.* [62] reported the use of 18-crown-6 tetracarboxylic acid, the structure of which is illustrated in Figure 1.5(A). This macrocyclic polyether ring system is composed of six oxygen atoms, spaced intermittently with ethylene bridges. It has an inner diameter range of 0.26-0.32 nm. Four carboxylic acid groups lie perpendicular to a plane formed by oxygen atoms. Inclusion complexes with potassium, ammonia and primary alkylamine cations are formed within the ring cavity [63]. The mechanism of chiral selection is still speculative, but it has been proposed that the carboxylic acid pairs on opposite sides of the ring act like a chiral barrier, dividing the space available for substituents of the chiral carbon atom adjacent to the amine functionality into two domains. Like the CDs, the complex formed will depend on the size and the three dimensional structure of the guest molecule. It is also thought that the carboxylic acid groups can electrostatically interact with substituents of the guest molecule [63].

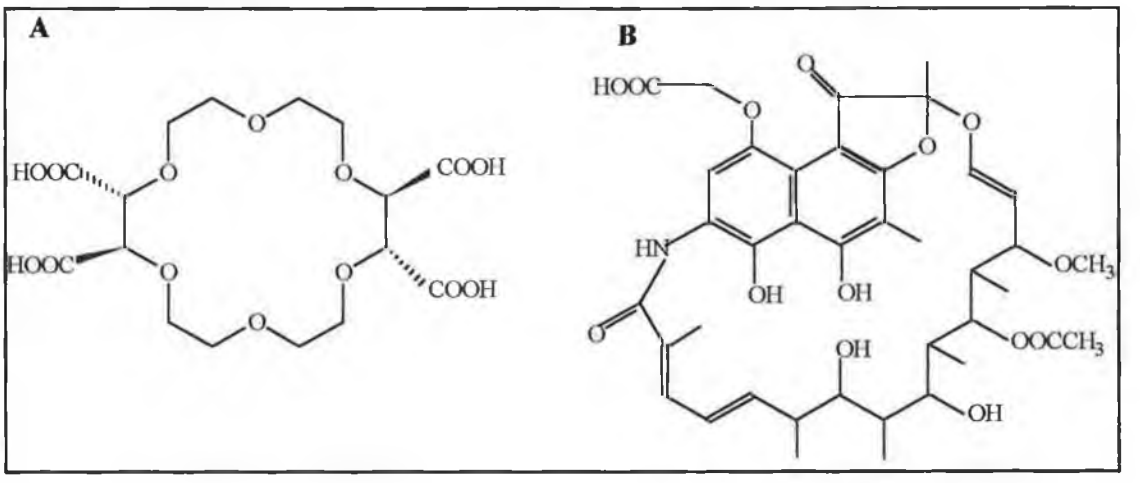

Figure 1.5. Chemical structure of (A) 18-crown-6 tetracarboxylic acid and (B) Rifymaycin B.

1.4.3.3.3. Macrocyclic Antibiotics

A new class of chiral selectors capable of host-guest interactions, i.e. ansamycins, have recently been introduced [64]. Rifamycins, being one of the better known members of ansamycins, are macrocyclic antiobiotics. They have a characteristic ring structure, surrounded by an aliphatic chain, as illustrated in Figure 1.5(B). The location and type of substituent on the naphthohydroquinone ring differs in each rifamycin. Rifamycin B, exists as a dibasic acid, with pK_a's of approximately 2.8 and 6.7. It has nine stereogenic centers, including four hydroxy groups, a carboxylic acid group and an amide bond, many of which are ionisable and capable of chiral recognition [64]. Rifamycin B is an anionic compound; hence electrophoretic mobility will oppose the EOF, and any interactions with this molecule will have an overall reduced mobility. Armstrong *et al.* [64] used Rifamycin B to selectively separate enantiomers of amino alcohols. A feature of Rifamycin B is its highly absorbing characteristics in both the UV and visible regions, with maxima at 220, 304 and 425 nm; hence indirect detection is best suited for such applications. Unlike CDs, Rifamycin B has several ionisable functional groups which are affected by changes in pH. Alteration of pH may induce changes in the molecular structure and properties of the molecule; hence careful consideration of operating parameters is advised when carrying out CE separations.

1.4.3.4. Metal Ions

Metal ions such as Cu(II), Zn(II), Mg(II) and Fe(II) have been used to co-ordinate with proteins, peptides and oligonucleotides, containing; nitrogen , oxygen or sulphur [65,66]. Divalent metal ions can be electrostatically attracted to the surface of an anionic surfactant and differential metal complexation of some oligonucleotides (being negatively charged) has lead to separation of complex samples [66]. Issaq *et al.* [67] used Zn(II) for adequate separation of small peptides. Interaction with these metal ions causes a reduction of the analyte's mobility relative to the uncomplexed species. A copper-aspartame complex [68] was used to perform chiral separation of dansylated amino acids. The formation of a weak complex between copper(II) and the aspartame was broken and replaced by an amino acid, leading to the formation of a ternary complex. Specific hydrophobic interactions between the aspartame phenylalanine residue and the amino acid side-chain can take place. This method in the presence of an anionic surfactant, could be extended for the separation of neutral amino acids. A problem associated with this method, and which may have prevented its widespread use, is the extremely long time required for conditioning of the capillary wall, which was necessary to remove any metal hydroxide precipitate which may form on the silica wall.

Other additives include either anionic or cationic surfactants, [69, 70], mixed micellar phases [71], bile salts [72] or even divalent amines [73] to separate very hydrophobic compounds.

1.5. CAPILLARY TYPES USED IN CE SEPARATIONS

The vast majority of CE separations are carried out using uncoated, fused-silica capillaries. The external polyimide coating which protects the otherwise fragile, thin-walled glass capillary, does not alter the properties of the capillary significantly, and thus make it ideal for electrophoretic separations. Good run-run reproducibility is generally obtained by rinsing the capillary with a consistent method, which is usually successful for a diverse array of molecules. The ability to separate molecules by CE

reproducibly may, however, be dependent on the complexity of the analyte and its potential to form secondary interactions with the negatively charged silanol groups on the capillary wall, or with other molecules. Protein molecules tend to be the most problematic, and an alternative approach is required for their efficient separation.

1.5.1. Use of Polymer Coatings to prevent protein adsorption to capillary wall.

Much research has been devoted to strategies to minimise solute-wall interactions in CE. Various additives such as salts, zwitterions and surfactants have been used in buffers to compete with proteins for adsorption sites and to minimise adsorption, with little success. Protein adsorption to the capillary wall results in band broadening and poor efficiencies. This is mainly due to the attraction of the charged sites on the protein molecules for the fixed negatively charged sites on the capillary wall, or through hydrophobic forces. An alternative approach to improve protein separations in CE is to chemically bond a polymer to the capillary wall [74]. Several different approaches have been demonstrated, but a common theme among the studies carried out thus far is to use the silanol groups on the capillary wall to anchor the polymeric chains.

1.5.2. Polyacrylamide coatings

Polyacrylamide coatings were first described by Hjerten [75]. This method involved attaching a coupling reagent i.e. γ-methacryloxypropyltrimethoxysilane (MAPTMS), to the fused silica wall, followed by polymerisation of tetramethylethylenediamine (TEMED). Problems such as column instability at high pH and irreproducibility of migration times has lead to continued method development. A more efficient method evolved [76], which involved coating two layers onto the silica wall. Efficiencies were greatly improved using this approach, although column stability remained a problem.

1.5.3. Polyoxyethylene coatings

These type of coatings were first demonstrated by Bruin *et al.* [77]. This method consisted of modifying the capillary wall using a similar reagent to that used by Hjerten

[75], followed by covalently bonding polyethyleneglycol chains via reaction with an epoxide. Zhao *et al.* [78] investigated the effect of film thickness on column efficiencies. They found that low film thickness (<50 nm) gave rise to poor efficiency, possibly due to incomplete coverage of the silanol groups on the capillary wall. High film thicknesses (120 nm) also gave rise to poor column efficiency, which may be as a result of radial diffusion of the proteins into the polymer layer. Towns and Regnier [79] demonstrated that use of small polyoxyethylene surfactant head groups suffered from reduced efficiency and poor peak symmetry, possibly due to protein interactions with the hydrophobic surface of the capillary. By addition of small amounts of surfactant in the running buffer, the concentration of the coating on the capillary wall was maintained, hence providing better masking of the negatively charged wall.

1.6. DETECTION STRAGIES IN CE APPLICATIONS

1.6.1. Overview

Developments in CE separations took place so rapidly, that several aspects inherent to its progress were ignored in the early years. One area which was poorly addressed, was in the detection of such well separated analytes. Low concentration sensitivity is regarded as a major drawback in CE analyses [80]. While impressive mass detection limits have been reported for CE applications (e.g. femtomole to attomole range), the concentration detection limits are typically in the high μM range. This problem is due to the extremely small injection volume used (i.e. nL to pL range), and also to the small detection cell volume. Some of the more important modes of detection will be discussed here, however, in an extensive review by St Claire [2], the most recent modifications and improvements made in detector designs are discussed.

1.6.2. UV Spectroscopic Detection

UV Spectroscopic detection is by far the most popular means of monitoring CE separations. A primary reason for this is that, the vast majority of compounds absorb somewhere in the UV region. Another advantage is that no chemical modification of

the sample is required prior to analysis, hence many UV detectors can be housed on-line. The Beer-Lambert law:

$$\mathbf{I_0/I = A = \varepsilon cl} \qquad (1.7)$$

where I_0 is the intensity of radiation incident on the sample, I is the radiation emerging from the sample, A is the concentration of absorbance measured by the sample, ε is the molar extinction coefficient, c is the molar concentration of the sample in the flow cell and l is the pathlength.

describes the various parameters that influence the detection sensitivity achievable using an absorbance mode detection.

A fundamental problem with CE-UV detection is that the amount of light energy reaching the photomultiplier tube is an order of magnitude less than in typical HPLC detectors, due to the limited path length. Limits of detection are governed by geometric constraints imposed by small capillary dimensions, the separation channel and the inherently insensitive nature of absorbance detection [81]. Limited sensitivity in UV absorbance detection is expected because the optical pathlength is restricted by the capillary inner diameter. Typically used capillaries have a diameter range from 10-100 μm. Several approaches have been introduced to try and improve these limitations in CE-UV detectors. For instance, Tsuda *et al.* [82] have used rectangular capillaries, which have increased the path length by 1 mm. They observed approximately a 15-fold increase in sensitivity. The increased surface area to volume ratio created a more efficient means of heat dissipation and the flat rectangular walls produced less optical scattering. This type of capillary design, however, is rather fragile and not very flexible, and the presence of high background noise limit its application. A 3 mm Z-shaped flow cell was constructed by Chervet *et al.* [83] as part of the capillary column. Theoretical gains in sensitivity up to 80-fold were expected; however, only a 6-fold improvement was reported. This huge loss in sensitivity may be attributed to chemical noise and spectral scatter. Use of high power lasers as the UV source have also been

documented [84] for the analysis of individual neuronal cells. Limits of detection in the nM range were reported using a HeCd laser, with an optical line of 354.5 nm.

Multiwavelength detectors such as photo diode array (PDA) and scanning UV detectors are valuable because spectral as well as electrophoretic information can be displayed. PDA detectors are used to assist in peak assignment confirmation, which is regarded as a very valuable tool in the pharmaceutical industry; however, these detectors are frequently less sensitive when used in the scanning mode, since signal averaging must be carried out more rapidly than for a single-wavelength detection. Nevertheless, despite the inherent problems associated with sensitivity and limit of detection, UV continues to be the detector of choice for many CE applications.

1.6.3. Fluorescence and Laser Induced Fluorescence detection (LIF)

Fluorescence detection is likely the most sensitive detection mode available for CE at the present time, boasting detection limits as low as 10^{-12} M (attomole). Unlike UV absorbance detection, the ultimate sensitivity obtained from fluorescence is not strictly pathlength dependent, and laser-based systems can be focused into even the smallest diameter capillaries. One of the first fluorescence detectors described was that constructed by Jorgensen and Lukacs [1]. While not very sensitive, it demonstrated that fluorescent detectors were quite simple to construct and the enormous potential that they held. The degree of sensitivity of fluorescent detectors depends on the intensity and stability of the light source and on the similarity between the fluorophore and the wavelength of the light source. This strong inter-relationship has lead to the more prominent use of laser-based fluorescent detectors. Only a small fraction of analytes under investigation, however, naturally lend themselves to this detection mode; therefore derivatising reagents are typically required. The argon ion and HeCd laser dominate this area. The 488 nm emission line of the argon ion laser closely matches the 490 nm absorption maximum of the fluorescein-based label, while the 325 nm line of the HeCd laser is best suited for the detection of o-phthalaldehyde (OPA) and the 442 nm line is compatible with napthalene dicarboxylic acid (NDA). These lasers are easy to use and inexpensive. Detection mechanisms can be based on either pre-column, on-column, or end-column [85-88] technology, and many of these

approaches described are capable of 10^{-10} M (attomole) detection limits and several extend below the 10^{-12} M (zeptomole) level.

1.6.4. Mass Spectrometry (MS)

The coupling of mass spectrometry to the outlet end of a CE capillary is considered by many to be the most optimum mode of detection for CE. CE-MS affords powerful methodology for structural determination of low concentration analytes; however optimal performance can only be achieved when both CE and MS are considered as an integral technique. Even today, most MS instruments can only accommodate volatile CE buffers, and the highest sensitivity is obtained when using narrow bore capillaries (5-10 μm i.d.) [89], which is particularly suited for electrospray ionisation only. Therefore, although MS affords good sensitivity, the inability to load more than a few pL to nL of sample onto the capillary exacerbates the issue of poor CE concentration limit of detection (CLOD). Several techniques to enhance the limits of detection in CE-MS have been reviewed recently [90], which include sample stacking techniques, isotachophoresis as an on-line concentration pre-treatment step and use of solid phase C_{18} materials. However, while it may allow enhanced CLOD, the performance will ultimately be affected, and problems such as loss of resolution and peak tailing are common.

1.6.5. Electrochemical Detection

The use of electrochemical techniques as a detection mode with CE applications has gained much acceptance in recent years [91]. Compared with LIF or other rival detection modes providing similar or better limits of detection, electrochemical detection (EC) can be used for a far greater number of applications, without the need for derivatisation or pre-concentration. Since its conception by Wallingford and Ewing [92], enormous interest has evolved in this relatively inexpensive and simple instrumental design. Their work largely focused on the analysis of cytoplasmic neurotransmitters in single nerve cells. Carbohydrate chemistry has been extensively studied by Zare *et al.* [93], while pharmaceutical and biomedical compounds continue

to dominate this field [91], with detection sensitivities in the attomole range. A problem commonly encountered with CE-EC systems, has been the high noise arising from the CE system, which limits detection. A recent report [94] using a Nafion joint to electrically isolate the electrochemical cell from the CE system was described. This method offered improved detection limits with low dead volume. Electrochemical analysis for CE serves as a highly sensitive and selective detection method, for a wide range of applications; however, as yet it is mainly confined to laboratories within academic institutions.

In addition to the detection modes described, several other, less well documented techniques exist. These include: CE with conductivity detectors, nuclear magnetic resonance (CE-NMR), refractive index detection (CE-RI), and indirect detection with either UV or LIF.

1.7 REFERENCES

1. Jorgenson, J. W.; Lukacs K. D. *Anal. Chem.* **53** (1981) 1298-1302.
2. St. Claire, R. L. *Anal. Chem.* **68** (1996) 569R-586R.
3. Monnig, C. A.; Kennedy, R. T. *Anal. Chem.* **66** (1994) 280R-314R.
4. Lauer, H. H.; Ooms, J. B. *Anal. Chim. Acta.* **250** (1991) 45-60.
5. Perret, D.; Ross, G. Trends *Anal. Chem.* **11** (1992) 156-163.
6. Xu, Y. *Anal Chem.* **65** (1993) 425R-433R.
7. Terabe, S.; Ozaki, K.; Ichikawa, A; Tsuchiya, A.; Ando, T. *Anal. Chem.* **56** (1984) 111-113.
8. Zeece, M. *Trends Food Sci. Technol.* **3** (1992) 6-10.
9. Nielen, M. W. F. *Trends Anal. Chem.* **12** (1993) 345-356.
10. Jackson, P . E., Haddad, P. R. *Trends Anal. Chem.* **12** (1993) 231-238.
11. Wallingford, R. A.; Ewing, A. G. *Anal. Chem.* **60** (1988) 1972-1975.
12. Olefirowicz, T. M.; Ewing, A. G. *Anal. Chem.* **62** (1990) 1872-1876.
13. Chen, F. T. A. *Anal. Biochem.* **225** (1995) 341-345.
14. Craig, D.; Arriga, E. A.; Banks, P.; Zhang, Y.; Renborg, A.; Palcic, M.M.; Dovich, N. J. *Anal. Biochem.* **226** (1995) 147-153.
15. Hilser, V. J.; Freire, E. *Anal. Biochem.* **224** (1995) 465-485.
16. Vonguyen, L.; Wu, J. Q.; Pawliszyn, J. *J Chromatogr. Biomed. Appl.* **657** (1994) 333-338.
17. Huang, X.; Gordon, M. J.; Zare, R. N. *Anal. Chem.* **60** (1988) 1837-1838.
18. Altria, K. D.; Simpson, C. F. *Anal. Proc.* **23** (1986) 453-454.
19. Hayes, M. A.; Ewing, A. G. Ewing, *Anal. Chem.* **64** (1992) 512-516.
20. Huang, T. L. *Chromatographia* **35** (1993) 395-398.
21. Tavares, M. F. M.; Mcguffin, V. L. *Anal. Chem.* **67** (1995) 3687-3696.
22. Kenndler, E.; Friedl, W. *J Chomatogr.*, **608** (1992) 161-170.
23. Schure, M. R.; Lenhoff, A. M. *Anal. Chem.*, **65** (1993) 3024-3037.
24. Delinger, S. L.; Davis, J. M. *Anal. Chem.* **64** (1992) 1947-1959.
25. Grushka, E.; McCormick, R. M.; Kirkland, J. J. *Anal. Chem.* **61** (1989) 241-246.

26. Zhu, M., Hansen, D.; Burd, S.; Gannon, F. *J. Chromatorg.* **480** (1989) 311-319.

27. Bossi, A.; Gelfi, C.; Orsi, A.; Righetti, P. G. *J. Chromatogr.* **686** (1994) 121-128.

28. Weinberger, R. *Practical Capillary Electrophoresis*, Academic Press, Inc. UK. (1993).

29. Guttman, A.; Herrick, S. *Anal. Biochem.* **235** (1996) 236-239.

30. Guttman, A. *Trends Anal. Chem.* **15** (1996) 194-198.

31. Mazereeuw, M.; Tjaden, U. R.; Reinhoud, N. J. *J. Chrom. Sci.* **33** (1995) 686-697.

32. Smith, R. D.; Loo, J. A.; Barinaga, C. J.; Edmonds, C. G.; Udseth, H. R. *J. Chromatorg.* **480** (1989) 211-232.

33. Stegehuis, D. S.; Irth, H.; Tjaden, U. R.; Van Der Greef, J. *J. Chromatogr.* **538** (1991) 393-402.

34. Hofstetter-Kuhn, S.; Paulus, A.; Gassman, E.; Widmer, H. M. *Anal. Chem.* **63** (1991) 1541-1547.

35. VanOrman, B. B.; Liversidge, G. G.; McIntire, G. L.; Olefirowicz, T. M.;and Ewing. A. G. *J. Microcol. Sep.* **2** (1990) 176-180.

36. Nelson, R. J.; Paulus, A.; Cohen, A. S.; Guttman, A.; Karger, B. L. *J. Chromatogr.* **480** (1989) 111- 127.

37. Salomon, K.; Burgi, D. S.; Helmer, J. C. *J. Chromatogr*, **549** (1991) 375-385.

38. Wallingford, R. A.; Ewing, A. G. *Anal. Chem.* **61** (1989) 98-100.

39. Liu, J.; Cobb, K. A.; Novotony, M. *J. Chromatogr.* **468** (1988) 55-65.

40. Schützner, W.; Fanali, S.; Rizzi, A.; Kenndler, E. *J. Chromatogr. A*, **719** (1996) 411-420.

41. Salimi-Moosavi, H.; Cassidy, R. M.; *Anal. Chem.* **68** (1996) 293-299.

42. Björnsdottir, I.; Hansen, S. H. *J. Pharm. Biomed. Anal.* **13** (1995) 1473-1481.

43. Wang, F.; Khaledi, M. G. *Anal. Chem.* **68** (1996) 3460-3467.

44. Lu. W.; Poon. G. K.; Carmichael, P. L.; Cole, R. B. *Anal Chem.* **68** (1996) 668-674.

45. Eskborg, S.; Schill, G. *Anal. Chem.* **45** (1973) 2092-2100.

46. Melin, A. T.; Ljungcrantz, M.; Schill G. *J. Chromatogr.* **185** (1979) 225-239.

47. Knox, J. H.; Laird, G. R. *J. Chromatogr.* **122** (1976) 17-34.

48. Horvath, C.; Melander, W.; Molnar, I. Molnar, P. *Anal. Chem.* **49** (1977) 2295-2305.

49. McLaughlin, G.M.; Nolan, J. A.; Lindhall, J. L.; Palmieri, R. H.; Anderson, K. W.; Morris, S. C.; Morrison, J. A.; Bronzert, T. J. *J. Liq. Chrom.* **15** (1992) 961-1021.

50. Okada, T. *Anal. Chem.* **68** (1996) 1158-1163.

51. Kornfelt, T.; Vinther, A.; Okafo, G.; Camelleri, P. *J. Chromatogr. A* **726** (1996) 223-228.

52. Stalcup, A. M.; Gahm, K. H. *Anal. Chem.* **68** (1996) 1360-1368.

53. Li, F.; Cooper, S. F.; Mikkelsen, S. R. *J. Chromatogr. B* **674** (1995) 277-285.

54. Peterson, T. E. *J. Chromatogr.* **630** (1993) 353-361.

55. Sepaniak, M. J.; Cole, R. O.; Clark, B. K. *J. Liq. Chrom.* **15** (6&7), (1992) 1023-1040.

56. Strattan, C. E. *Biopharm.* **4** (1991) 44-51.

57. Fanali. S. *J. Chromatogr.* **474** (1989) 441-446.

58. Tait, R. J.; Thompson, D. O.; Stella, V. J.; Stobaugh, J. F. *Anal Chem.* **66** (1994) 4013-4018.

59. Lurie, I. S.; Klein, R. F. X.; Dal Cason, T. A.; LeBelle, M. J.; Brenneisen, R.; Weinberger, R.E. *Anal. Chem.* **66** (1994) 4019-4026.

60. Brown, R. S.; Luong J. H. T.; Szolar, O. H. J.; Halasz, A.; Hawari, J. *Anal. Chem.* **68** (1996) 287-292.

61. Bingcheng, L.; Yibing, J.; Yibing, C.; Epperlein, U.; Koppenhoefer, B. *Chromatographia*, **42** (1&2), (1996) 106-110.

62. Kuhn, R.; Stocklin, F.; Erni, F. *Chromatographia*, **33** (1992) 32-36.

63. Kuhn, R.; Erni, F.; Bereuter, T.; Hausler, J. *Anal. Chem.* **64** (1992) 2815-2820.

64. Armstrong, D. W.; Rundlett, K.; Reid (III), G. L. *Anal. Chem.* **66** (1994) 1690-1695.

65. Mosher, R.A. *Electrophoresis* **11** (1990) 765-769.

66. Cohen, A. S.; Terabe, S.; Smith, J. A.; Karger, B. L. *Anal. Chem.* **59** (1987) 1021-1027.

67. Issaq, H. J.; Janini, G. M.; Atamna, I. Z.; Muschik, G.M.; Lukszo, J. *J. Liq. Chrom.* **15** (1992) 1129-1142.

68. Gozel, P.; Gassman, E.; Michelsen, H.; Zare, R. N. *Anal. Chem.* **59** (1987) 44-49.

69. Janini, G. M.; Issaq, H. J.; *J. Liq. Chrom.* **15** (1992) 927-960 .

70. Ahuja, E. S.; Foley, J. P. *J. Chromatogr. A*, **680** (1994) 73-83.

71. Dobashi, A.; Ono, T.; Hara, S.; Yamaguchi, J. *Anal. Chem.* **61** (1989) 1986-1988.

72. Nishi, H.; Fukuyama, T.; Matsuo, M.; Terabe, S. *J. Chromatogr.* **513** (1990) 279-295.

73. Lauer, H. H.; McManigill, D. *Anal. Chem.* **58** (1986) 166- 170.

74. Bruin, G. J. M.; Paulus, A. *Anal. Meth. Instrum.* **2** (1995) 3-26.

75. Hjerten, S. *J. Chromatogr.* **347** (1985) 191-198.

76. Schmalzing, D.; Piggee, C. A.; Foret, F.; Carrilho, E.; Karger, B. L. *J. Chromatogr. A.* **652** (1993) 149-

77. Bruin, G. J. M.; Chang, J. P.; Kuhlman, R. H.; Zeegers, K.; Kraak, J. C.; Poppe, H. *J. Chromatogr.* **471** (1989) 429-436.

78. Zhao, Z.; Malik, A.; Lee, M. L. *Anal. Chem.* **65** (1993) 2747-2752.

79. Towns, J. K.; Regnier, F. E. *Anal. Chem.* **63** (1991) 1126-1132.

80. Schulc, M. C.; Krull, I. S. *J. Chromatogr.* **659** (1994) 231-245.

81. Landers, J. P. *Handbook of Capillary Electrophoresis*, CRC Press, UK.

82. Tsuda. T.; Sweedler, J.V.; Zare, R.N. *Anal. Chem.* **62** (1990) 2149-2152.

83. Chervet, J. P.; Van Soest, R. E. J.; Ursem, M. *J. Chromatogr.* **543** (1991) 439-449.

84. Shippy, S. A.; Jankowski, J. A.; Sweedle, J. V. *Anal. Chim. Acta.* **307** (1995) 163-171.

85. Gilman, S. D.; Ewing, A. G. *Anal. Chem.* **67** (1995) 58-64.

86. Zhou, S. Y.; Zuo, H.; Stobaugh, J. F.; Lunte, C. E.; Lunte, S. M. *Anal. Chem.* **67** (1995) 594-599.

87. Nickerson, B.; Jorgenson J. W., *J. Chromatogr.* **480** (1989) 157-168.

88. Mank, A. J. G.; Beekman, M. C.; Velthorst, N. H.; Brinkman, U.A. Th.; Lingeman, H. Gooijer, C. *Anal. Chim. Acta.* **315** (1995) 209-216.

89. Smith, R. D.; Barinaga, C. J.; Udseth, H. R. *Anal. Chem.* **60** (1988) 1948-1952.

90. Tomlinson, A. J.; Guzman, N. A.; Naylor, S.; *J. Cap. Electrophoresis* **2** (1995) 247-266.

91. Lunte, S.M.; O' Shea, T. J. *Electrophoresis*, **15** (1994) 79-86.

92. Wallingford, R. A.; Ewing, A. G. *Anal. Chem.* **59** (1987) 1762-1766.

93. Colón, L. A.; Dadoo, R.; Zare, R. N. *Anal. Chem.* **65** (1993) 476-481.

94. Park, S.; Lunte, S. M.; Lunte, C. E. *Anal. Chem.* **67** (1995) 911-918.

CHAPTER 2

CAPILLARY ELECTROPHORETIC METHOD DEVELOPMENT FOR NSG-PEPTOID COMBINATORIAL LIBRARIES

2.1 INTRODUCTION TO COMBINATORIAL CHEMISTRY

Combinatorial chemistry has captivated the imagination of both the medicinal chemists and the molecular biologists because of its potential to revolutionise the drug discovery process. In combinatorial chemistry, a chemical library (a large collection of structurally diverse compounds) is produced by sequentially linking different molecular building blocks or by adding substituents to a core structure, such as a polycyclic compound [1]. Such libraries have been synthesised many different ways: (i) by solid phase synthesis, where the molecules are often covalently linked to a solid support; (ii) assembled on the surface of micro-organisms; or (iii) in solution phase; where the molecules produced exist free in solution. The number of molecules that can be synthesised very rapidly is immense, and hence a problem exists to identify active compounds within a particular library both swiftly and accurately. For those libraries that contain vast numbers of molecules, encoding schemes have been devised, or deconvoluting methods are used for those with smaller numbers of molecules. Traditional information management strategies are futile and several new software systems have been devised to handle such a plethora of information. This rapid generation of combinatorial libraries, along with the convergence of several technologies, appears to be the way forward in the search for new drug candidates.

2.1.1. Synthesis of Combinatorial libraries

The synthesis of a combinatorial library is generally performed by either (i) split synthesis, or (ii) parallel synthesis.

Split synthesis is generally used to produce small quantities of a large number of compounds. In this method, the molecules are arrayed on the surface of beads [2], with each bead containing a single molecule. Synthesis involves a series of steps, which split up the beads to add a new building block, followed by recombining them again. This process is repeated a number of times until the desired combinatorial library is produced. As these beads can be physically moved, isolation and identification of an active molecule is quite easy to accomplish.

Parallel synthesis is used to produce large quantities of a relatively smaller number of compounds. For instance Geysen *et al.* [3] utilised a 96-well microtitre plate to synthesise more than 3,000 peptides a week. In this method, polyethylene rods were assembled in these plates and the appropriate reagents were added in a pre-defined manner. This method allows several tests to be carried out on a particular well and is ideal for the generation of a complete set of all possible variants. This process is fast becoming the method of choice, because it can be performed on a solid-phase or in solution, and is easily automated. Solid-phase methods can use excess reagents to drive reactions to completion, and excess reagents can easily be washed away from beads or microparticles afterwards. Solution-phase synthesis is a very versatile method, because many organic solution based reactions have not been adapted for solid-phase synthesis.

2.1.2. Low molecular weight combinatorial libraries

Over the past number of years, scientists have come to realise that peptides have limited utility as bioavailable therapeutic agents, because they generally cannot be taken orally and have rapid physiological clearing times. More recently, the driving force has been to produce non-polymeric low molecular weight combinatorial libraries. In 1992, Ellman [4] synthesised non-polymeric benzodiazepine derivatives; one of the most important classes of bioavailable therapeutic agents. This discovery has led the way for the synthesis of many similar classes of small organic molecules by combinatorial methods.

2.1.3. Combinatorial Peptoids

Another facet of low molecular weight combinatorial libraries are the NSG-peptoids. Oligo N-(substituted)-glycines (NSG-peptoids) are synthetic oligomers which have a common backbone structure, with a variety of functional groups. These functional groups are generally attached at the amide nitrogen instead of the α-carbon, as associated with natural peptides [5]. The functional groups on the achiral backbone are spaced at intervals comparable to those of naturally occurring peptides (Figure 2.1).

Each N-substituted glycine monomer is assembled from two readily available 'submonomers' in the course of extending the NSG polymer. The first step involves an acylation stage, followed by nucleophilic displacement [6].

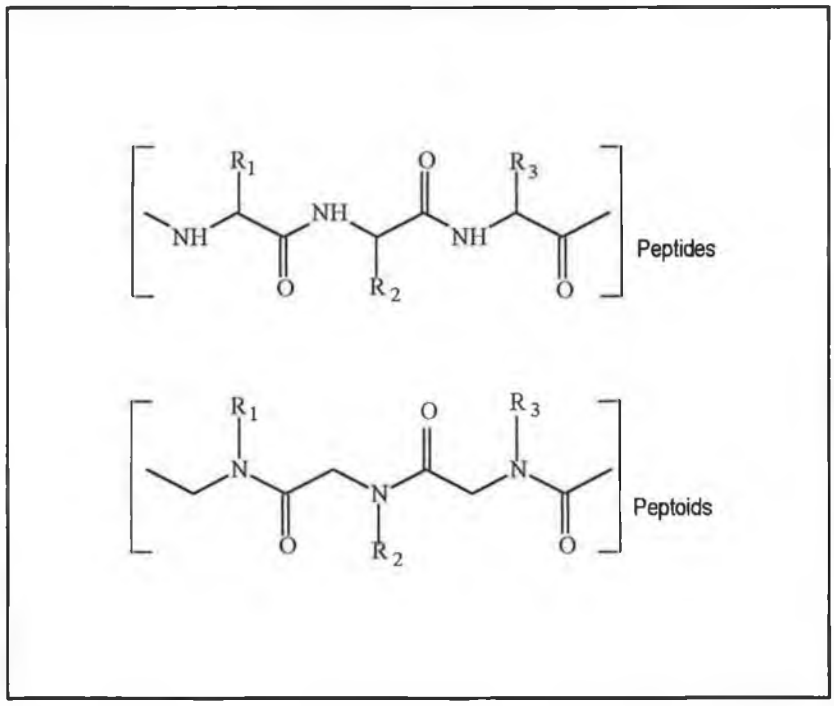

Figure 2.1. Schematic representation of a peptide and a peptoid chain. Similar features which exist between these chains include an achiral backbone with functional groups attached at regularly spaced intervals.

An important feature of these peptoids is their resistance to enzymatic cleavage, which is a major advantage for their bioavailability. Miller *et al.* [7] investigated the stability of these NSG-peptoids by subjecting them to a range of major proteases and found that they remained essentially unchanged. The choice of side-chain functionalities that can be attached is virtually limitless [5], from functionally diverse and commercially available primary amines, to functional groups with unusual steric or electronic configurations.

2.1.4. Applications of NSG-peptoids

The primary application envisaged for these NSG-peptoids is in screening of diverse mixtures for identification of a favourable array of functional groups for binding to an enzyme or receptor. Already, several potent pharmacophores have been discovered

from a library containing almost 5000 synthetic NSG-peptoids [8]. These ligands bind to receptors in the 7-transmembrane G-protein-coupled receptor (7TM/GPCR) family. The absence of substituted backbone carbons and of amide hydrogens removes the intramolecular hydrogen bonding capabilities, and hence changes the steric interactions that induce the secondary structure in peptides. As a result it can be assumed that characteristic differences between both peptides and peptoids will arise, and the binding properties associated with peptides will not be the same in the NSG-peptoids.

2.1.5. Recognition of an active site

When a compound library is determined to have biological activity, a method must be used to determine which molecule(s) in the library is (are) active. Large libraries have been screened by the use of encoding techniques, which involves the covalent attachment of a radiofrequency tag [9,10] or label [11,12] to the compounds in a particular library. This often involves the attachment of the compounds to a solid support. This mechanism of screening for activity may interfere with the molecular structure or binding properties of the compound. Screening of smaller combinatorial libraries is generally based on deconvolution methods. One strategy, i.e. 'SURF' [13], was used to investigate the binding properties of RNA hybridisation as a model system. Martin *et al.* [14] used a set of structural descriptors to indicate whether a series of compounds should be explored further. The information gained from these analyses can then be stored in one of the many commercially available computer databases, e.g. SPECS, Daylight etc. [15].

2.1.6. Analytical Techniques for Combinatorial Library Analysis

Analytical control over the chemistry and in the identification of the compounds is a further step required to characterise these combinatorially synthesised molecules as therapeutic drug agents. Traditionally, HPLC [5,8] and MS [16,17] methods have been used as a qualitative technique for the analysis of these libraries. Direct identification of active small-molecule libraries by MS coupled with a suite of techniques for molecular weight confirmation or fragmentation pattern analysis have recently been documented [16,17]. However, the diversity of probe libraries investigated were quite small and

library constituents with different molecular weights were chosen to avoid problems associated with isobaric compounds. The complexity of the mass spectra produced often make analysis difficult, i.e. some molecules make be poorly ionised and hence hidden by noise, or suppressed by the presence of the stronger proton acceptor or proton donor. Peak intensity cannot be directly related to the relative concentration of compounds in the mixture due to different ionisation efficiencies.

2.1.7. Aims of Research

In this chapter, the utility of capillary electrophoresis (CE) for the analysis of several NSG-peptoid combinatorial libraries was evaluated. This involved developing a CE separation method for one particular NSG-peptoid library (CHIR 4580.1), and assessing the ruggedness of this separation method for the remaining five libraries. All libraries were donated by Chiron Corporation. These libraries contain functional groups ranging from long hydrocarbon chains to aromatic hydrophobic moieties to secondary amines. With reversed-phase HPLC, large diverse functionalities present a significant challenge for separation, and often require elaborate gradient elution methods for adequate separation [5,18]. Separation in CE is based on differences in charge and size providing significantly higher efficiencies than typical with HPLC. CE is frequently documented as an analytical technique capable of high resolution with theoretical plates of the order of several hundred thousand [19,20]. In addition, the sample requirement is considerably smaller for CE relative to HPLC. CE was therefore thought to provide advantages for the analysis of peptoid based combinatorial libraries.

The initial study involved developing a separation method for one particular NSG-peptoid library, namely CHIR 4580.1. The various parameters affecting the separation of the peptoids in CE were examined. Mixed mode separations, in which run buffer additives were used to add partitioning character to the separation was also investigated. The second part of this chapter then describes how the separation method developed for CHIR 4580.1 was applied to five different peptoid combinatorial libraries; i.e. CHIR 4582.1, CHIR 5216.1, CHIR 4555.1, CHIR 2003.1 and CHIR 4567.1. All five libraries have a different backbone structure, but with the same twenty-four functional groups as before. Each library represents a physical and

chemically diverse set of compounds. It was found that three of the five libraries were resolved using the method developed for CHIR 4580.1, having to make only minor modifications. The remaining two libraries were resolved using yet another mixed-mode system; involving cyclodextrin and a micelle. The advantage of using CE applications over other complimentary techniques is the ease with which the selectivity can be changed. Different buffer additives can simply be added to the mobile phase to alter the chromatographic conditions considerably and bring about efficient separation, while remaining relatively inexpensive. Finally a brief look at some individual NSG-peptoid marker compounds was carried out. These may be used as internal standards in the NSG-peptoid method development, or simply as a guide to explain the behaviour of such large hydrophobic molecules when subjected to an electric field.

2.2. EXPERIMENTAL

2.2.1. Chemicals

The following peptoid combinatorial libraries were kindly donated by Chiron Corp. (Emeryville, CA, USA): CHIR 4580.1, CHIR 4582.1, CHIR 4555.1, CHIR 4567.1, CHIR 5216.1 and CHIR 2003.1. All libraries were 1 mM in DMSO and were diluted 1:2 with deionised water, with the exception of CHIR 4580.1 which was 1 mM in ethanol and was diluted tenfold with deionised water. Deionised water was obtained by passing distilled water through a NANOpure water system (Sybron-Barnsted, Boston, MA, USA). Methyl-β-cyclodextrin was obtained from Aldrich Chemical Co. (Milwaukee, WI, USA) and 1-heptane sulphonic acid (HSA) was obtained from Sigma Chemical Co. (St. Louis, MO, USA). o-Phosphoric acid (85%), sodium lauryl sulphate, ammonium acetate, sodium borate, sodium hydrogen phosphate sodium dihydrogen phosphate and any organic solvents used were all obtained from Fisher Chemicals (Fair Lawn, NJ, USA).

2.2.2. Instrumentation

2.2.2.1.Capillary Electrophoresis System 1 (used for the analysis of CHIR 4580.1)

The capillary electrophoresis apparatus was home-made using a Spellman high-voltage dc (0-30 kV) CE 1000R power supply (Spellman, High Voltage Electronics Corp., Plainview, NJ, USA). The anodic (high voltage) end of the capillary was isolated in a Plexiglas box fitted with a safety interlock device. A 50 μm fused silica capillary from Polymicro Technologies, (Tuscon, AZ, USA) was used for separation of the mixture with a total length of 60 cm and 40 cm length to the detector window. A voltage of 15 kV was applied through platinum electrodes immersed in the buffer solutions at both ends for all experiments. The capillary was first flushed with 0.1 M sodium hydroxide for 20 minutes followed by conditioning of the capillary with the run buffer for a further 30-45 minutes prior to use. The peptoid mixture was hydrodynamically injected into the capillary by applying a pressure of 2.5 psi for 5-8 seconds. Detection was performed using an ISCO, Model CV^4 Capillary Electrophoresis UV detector, with a detection wavelength of 210 nm and a Hewlett Packard 3396 Series II Integrator was used for data acquisition.

2.2.2.2. Capillary Electrophoresis System 2 (used for the analyses of the remaining five libraries)

A commercially available capillary electropherograph (Model 3850) from ISCO (Lincoln NE, USA), connected with a Spectra Physics Model SP4400 Integrator for data acquisition, was used for the analyses of these libraries. Data was collected in ASCII format and any processing of data was performed using Origin 3.5 (Microcal. Software, Northhampton, MA, USA). 50 μm id fused silica capillaries from Polymicro Technologies (Tucson AZ, USA) was used for all separation of these libraries with a total length of 80 cm and 45 cm to the detection window. Capillary columns were rinsed as described previously. Sample introduction using this equipment could be performed either by electromigration or by the vacuum technique. To avoid sample

discrimination (of charged or smaller molecules), vacuum injection was applied throughout the experiments for a period of 15 seconds.

2.2.3. Preparation of buffer solution

1 M Phosphoric acid buffer, pH 2.0, was prepared by diluting the appropriate volume of concentrated phosphoric acid and adjusting to pH 2.0 with 0.1 M sodium hydroxide. The pH was monitored daily and adjusted as needed with 0.1 M sodium hydroxide. Phosphate buffer with ion-pair reagent was prepared by dissolving the appropriate amount (HSA) in 250 mM phosphoric acid buffer. The solution was then sonnicated for 30 minutes to ensure complete dissolution of the HSA and the pH adjusted to 2.0 with 0.1 M sodium hydroxide. Phosphate buffer with cyclodextrin was prepared by dissolving the appropriate amount of methyl-β-CD in 250 mM phosphoric acid buffer and the pH adjusted to 2.0 with 0.1 M sodium hydroxide. Borate-phosphate buffer solution pH 8.0 was prepared by mixing 100 mM sodium tetraborate solution and 250 mM sodium dihydrogen phosphate solution in an appropriate ratio to indicate pH 8.0. The SDS and CD buffer solutions were prepared by dissolving the required accurate weight of each in the borate-phosphate buffer solution followed by sonnication for 30 minutes and adjusting the pH where necessary. All solutions were filtered through a 0.2 μm nylon Acrodisc 13 mm syringe filter (Fisher Fair Lawn, NJ) prior to use.

2.3. RESULTS AND DISCUSSION

2.3.1. Optimisation of separation conditions for the peptoid library: CHIR 4580.1

2.3.1.1. Effect of buffer pH

The net charge on a peptoid molecule can be manipulated by modification of the buffer pH, particularly near the pK_a values of the amino terminal or carboxy terminal side

group. The first peptoid library investigated was CHIR 4580.1, with the backbone structure illustrated in Figure 2.2.

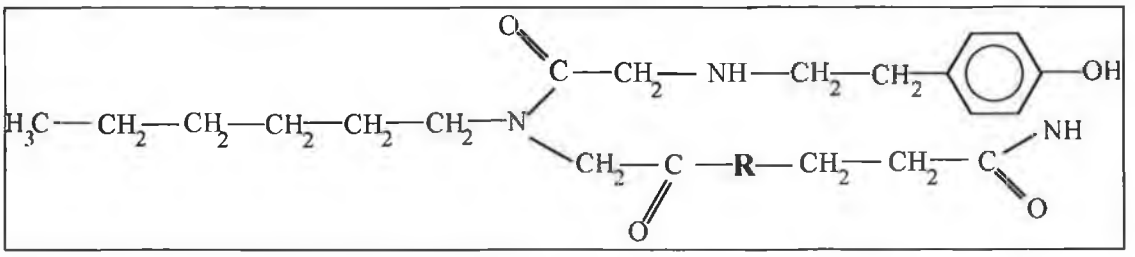

Figure 2.2. Backbone structure of the NSG-Peptoid library; CHIR 4580.1

This library has 24 different functional groups attached at position **R**. These functional groups range in character from simple hydrocarbon chains to large hydrophobic aromatic groups as shown in Figure 2.3.

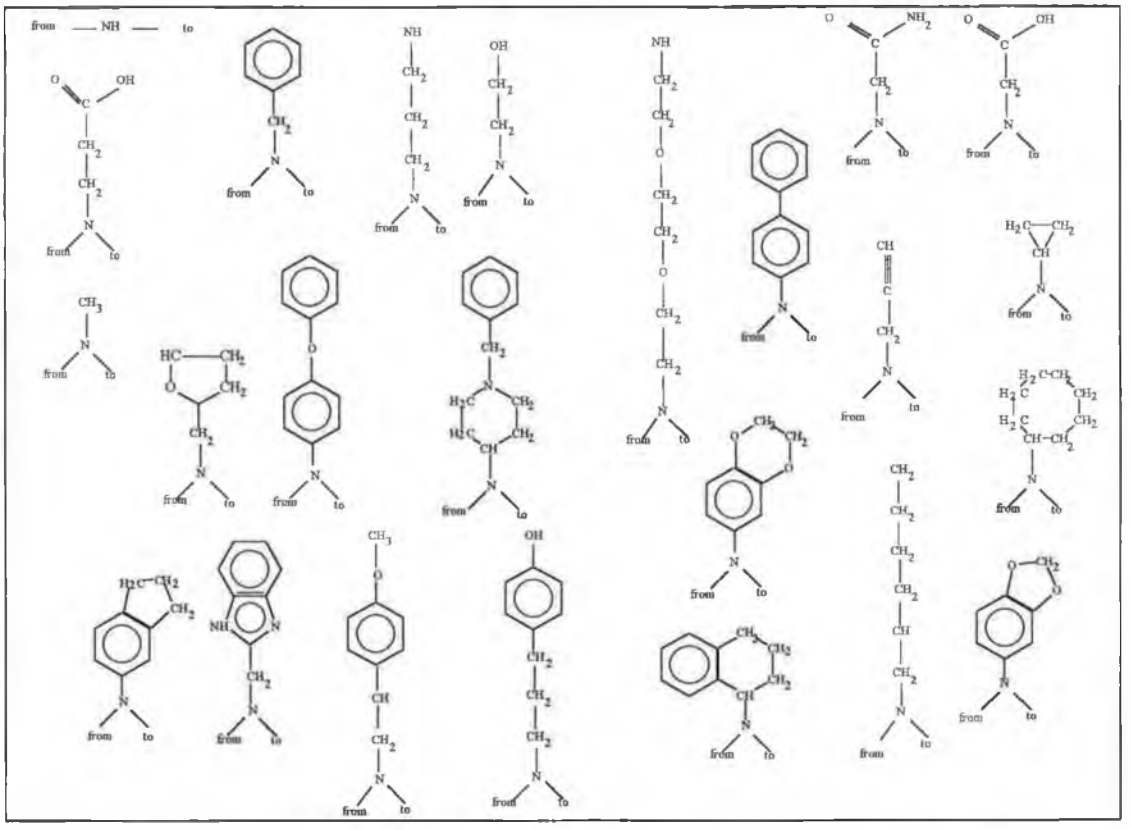

Figure 2.3. The range of functional groups which are attached at position **R** of CHIR 4580.1

CHIR 4580.1 has a molecular weight range of 392 to 581 Da. It has a pK_a range from 3.4 to 10.11 and a pK_b range from 7.6 to 9.8 [18]. Buffer pH also affects the electroosmotic flow (EOF), with a larger flow at the higher pH. The effect of run buffer pH over the range of 2 to 10 was investigated (Figure 2.4). At pH values greater than 11 the peptoid library has an overall negative charge and has a tendency to migrate towards the cathode. However, the EOF is very large at high pH, which results in very short times to achieve separation. Using borate buffer at pH 10, the test library elutes so fast, that almost none of the individual peptoid molecules are separated, because of the overwhelming effect of the EOF. Phosphate and acetate buffers were also used to study the pH range from 4 to 8; however, the NSG-peptoids are minimally charged in this range and clearly these pH values are of no benefit for analysis. To induce an overall negative charge on this library, buffers with a pH greater than the pK_a are required.

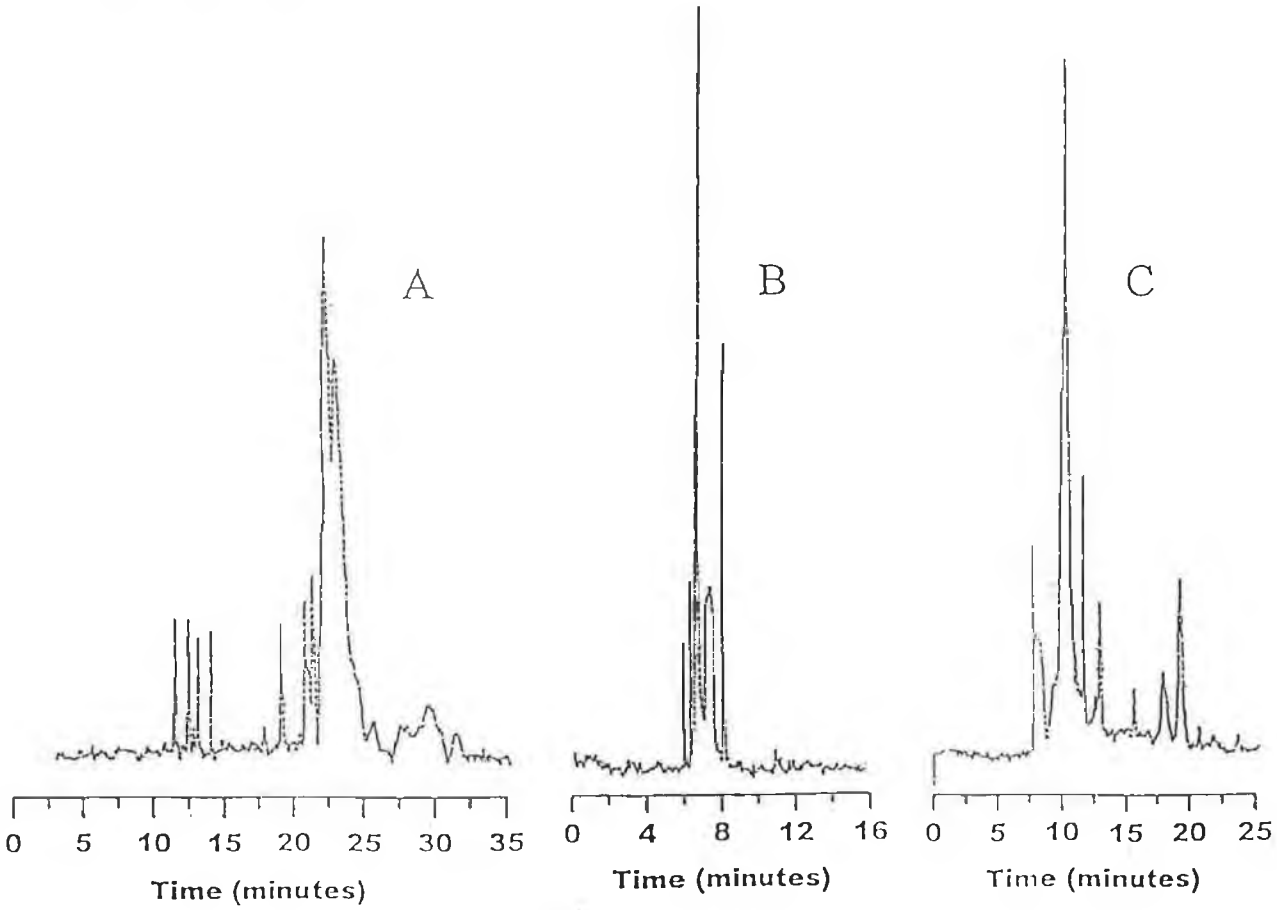

Figure 2.4. The effect of buffer pH on the separation of the NSG-peptoid library 4580.1. The buffers used were (A) 100 mM trihydrogen-phosphate buffer, pH 2.0; (B) 100 mM sodium phosphate buffer, pH 7.0 and (C) 100 mM sodium borate buffer, pH 10.0.

However, the EOF is so strong at such high pH that it would be quite difficult to achieve separation of twenty four components which have very different structural and chemical characteristics. At a pH less than 3, the peptoid library has an overall positive charge, and migrates toward the cathode. However, at this pH the EOF is very small resulting in relatively long analysis times to achieve separation. Both peptoid electrophoretic migration and the EOF are toward the negative electrode. Due to the much slower movement of the bulk solution it allows greater scope for separation of this library. Solutions of both pH 2 and 3 yielded good separation of the test library. A buffered solution of trihydrogen-phosphate at pH 2.0 was therefore selected for this method to provide greater ruggedness for a range of peptoids.

2.3.1.2. Effect of increasing the ionic strength of the buffer

Increasing the ionic strength of the run buffer decreases the EOF, and as a result peak resolution is improved. This effect can be seen in Figure 2.5, where various concentrations of trihydrogen-phosphate buffer, all at pH 2.0, were used. While in theory the higher the ionic strength the greater the resolution that should be attained, in practice the use of high ionic strength buffers is limited by increased Joule heating at higher ionic strength (lower resistance). Smaller bore capillaries or longer capillary columns reduce this effect somewhat, otherwise elaborate cooling systems are required to regulate the temperature. In this experiment, increasing the buffer concentration from 150 mM to 250 mM phosphate, pH 2.0, doubled the electrophoretic current. The optimum ionic strength was found to be 250 mM which allowed maximum efficiency without inducing Joule heating problems. Using a run buffer of 250 mM tri-hydrogen phosphate, pH 2.0, 14 individual peaks were identified from the library containing 24 compounds. The larger aromatic NSG-peptoids are very hydrophobic and have a greater tendency to self-aggregate or form strong electrostatic interactions with the silica wall, hence the large unresolved clump at higher migration times. Because of the complexity of combinatorial libraries, buffer additives are required to increase their resolving power in CE. In this application, organic solvents, ion-pairing agents and cyclodextrins were investigated as suitable buffer additives for the further resolution of this peptoid library.

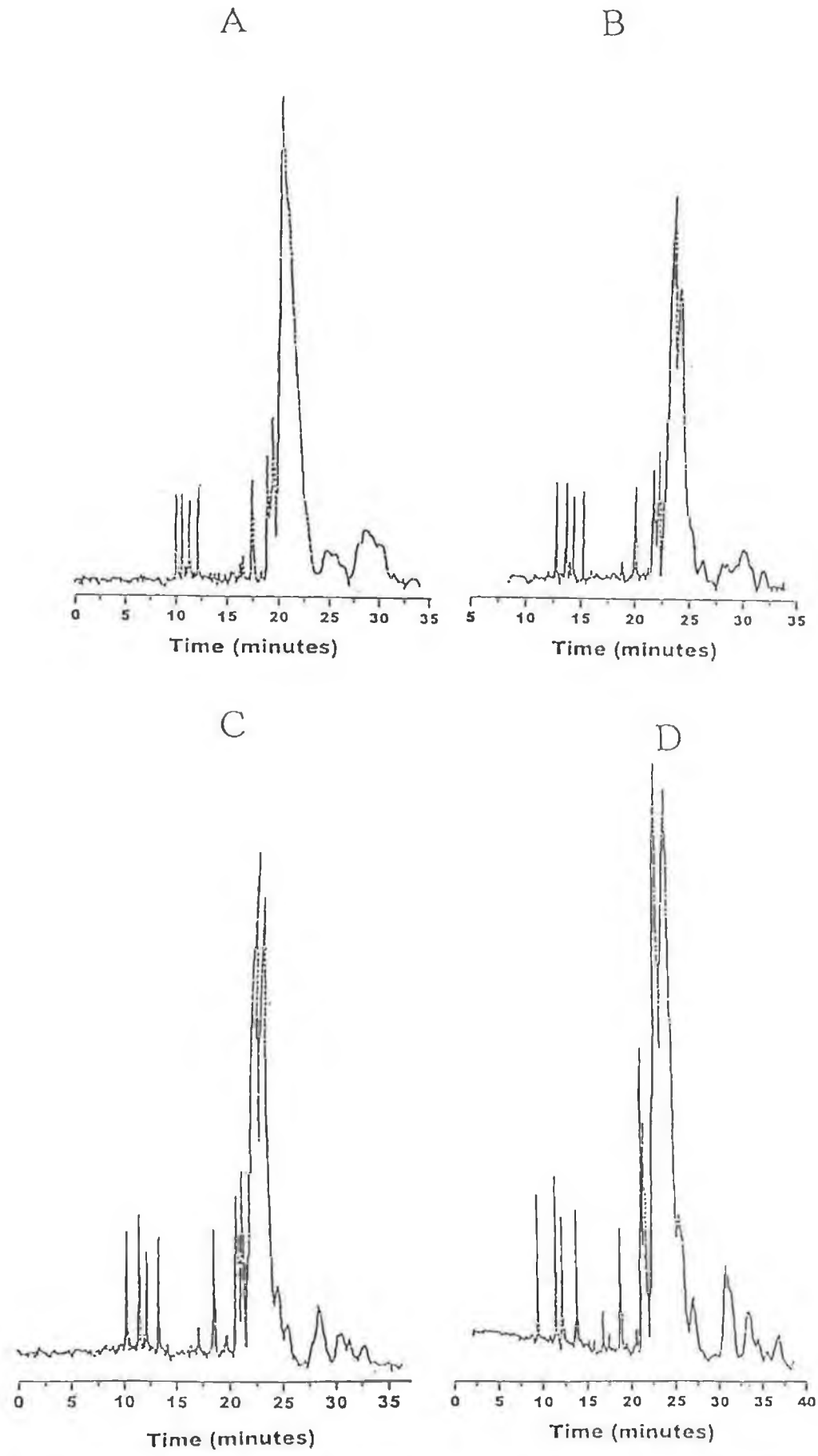

Figure 2.5. The effect of ionic strength on the separation of individual NSG-peptoids from the library CHIR 4580.1 using (A) 50 mM; (B) 100 mM; (C) 150 mM and (D) 250 mM trihydrogen-phosphate buffer, pH 2.0.

*2.3.1.*3. Effect of ion-pairing agents on separation.

Recently, separation of peptides and synthetic peptides have been achieved using ion-pairing agents in CE analyses [21,22]. In this study, heptane sulphonic acid (HSA) was used as an ion-pairing agent for the separation of these individual peptoids. Rather than the classical ion-pair formation or the dynamic ion-exchange mechanism of HPLC, in this system the HSA is thought to form a hydrophobic interaction between the alkyl chains of the sulphonate and the hydrophobic surfaces of the peptoid molecule. This is thought to decrease self-aggregation and provide better electrophoretic separation [22]. At a certain concentration below the critical micelle concentration (cmc), the alkyl chains of the ion-pairing agent surround the hydrophobic moieties of the peptoids and induce a repulsion for their self-aggregation and any interactions with the silica wall. In addition, due to the sulphonic acid groups of HSA, the adduct has an overall negative charge which contributes to an increase in migration times. It is also possible that the HSA can ion-pair, as in traditional HPLC applications, with positively charged peptoids. This would also decrease the net charge of the peptoid molecules and disrupt any interactions with the negatively charged capillary wall.

Upon addition of 25 mM HSA, much sharper resolution is achieved when compared with the separation obtained with phosphate buffer alone (Figure 2.6). The resolution of the large band of hydrophobic molecules was improved quite substantially, though some self-aggregation was still apparent. Upon increasing the concentration from 50 to 75 mM, better separation was achieved, and resolution of previously co-eluting peaks was observed. However, HSA alone is not sufficient to competitively interact with these strongly hydrophobic molecules.

A consequence of increasing the HSA concentration was to increase the current and hence Joule heating. Increasing the concentration of HSA from 25 mM to 75 mM increased the current from 30 μA to 78 μA. A concentration of 25 mM HSA was chosen for further experiments, as it gives rise to the lowest Joule heating. This concentration is also sufficient to reduce hydrophobic interactions considerably as the increased concentrations had no dramatic improvement. This concentration of HSA resulted in sixteen of the twenty four NSG-peptoids being resolved. (Figure 2.6).

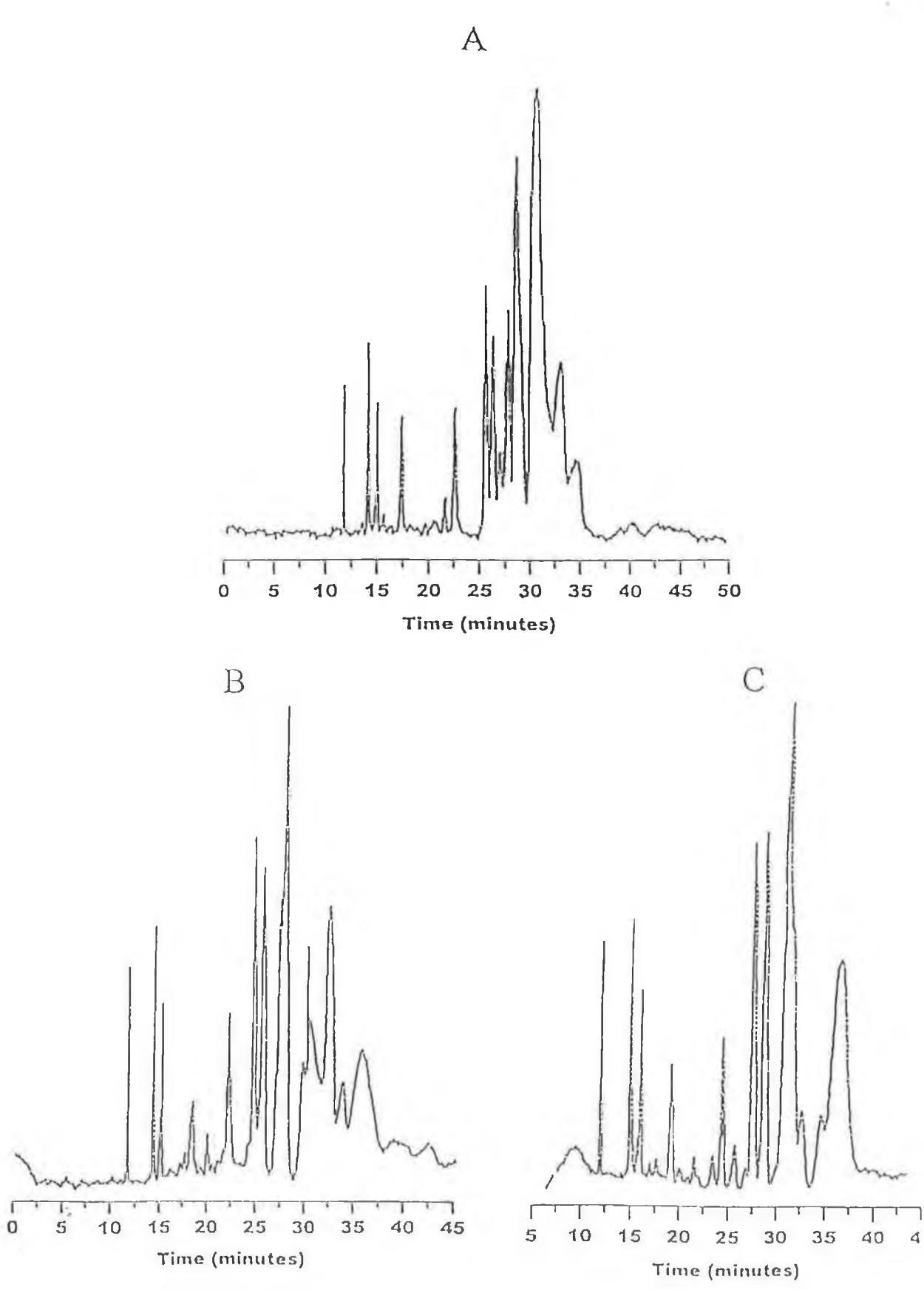

Figure 2.6. The effect of the ion-pairing agent, heptane sulphonic acid, HSA, on the separation of individual NSG-peptoids from the library CHIR 4580.1. Run buffers were 250 mM trihydrogen-phosphate buffer, pH 2.0 with (A) 25 mM HSA, (B) 50 mM HSA and (C) 75 mM HSA.

2.3.1.4. Addition of organic solvents to effect separation

Miscible organic solvents, such as methanol and acetonitrile, have been added to the aqueous run buffer to improve separations and to extend the applicability of CE to a wider range of compounds having low solubility in water. At low pH, there are potentially significant hydrophobic interactions occurring between the hydrophobic peptoids. Both methanol (a protic solvent) and acetonitrile (an aprotic solvent), despite their significant differences in properties, compete with these hydrophobic intramolecular interactions and offer an increase in analyte solubility [23]. Greater solubility means less self-aggregation of the hydrophobic analytes and also less self propensity for capillary wall adsorption.

The competitive nature of methanol with this hydrophobic peptoid library is shown in Figure 2.7. At low concentrations of methanol (3% v/v), the altered viscosity of the buffer is evident from the increased migration times of the individual peaks. This becomes more pronounced as the concentration of methanol is increased. The larger hydrophobic molecules are also solubilised slightly (see effect of methanol concentration at 14 and 16% (v/v). However, the tendency of these molecules to self-aggregate is so strong that methanol alone is not sufficient to break down these highly hydrophobic interactions. Tsuda *et al.* [24] stated that the μ_{eo} value for methanol was lower than that for water, while the μ_{eo} value for acetonitrile was higher. In this study, it is apparent that the μ_{eo} is reduced with increasing concentration of methanol.

The effect of acetonitrile on the separation of this library was also investigated. Unlike methanol, it had no significant effect on the EOF, with the migration times of the individual NSG-peptoids remain relatively unchanged even at high acetonitrile concentrations. The resulting peaks were sharper hence hydrophobic interactions of these peptoids molecules were reduced, however no concentration of acetonitrile alone, was sufficient to reduce these strong hydrophobic forces. It must also be remembered that with the increasing organic solvent concentration, that a decrease in salt concentration results. This effect was not studied on this occasion, but it is known that the concentration of charge in the buffer solution will have altered. Using 250 mM

tri-hydrogen phosphate buffer, pH 2.0 with 3% (v/v) methanol or 16% (v/v) methanol, 15 of the NSG-peptoids were resolved, however, the migration times at these conditions differ considerably (Figure 2.7).

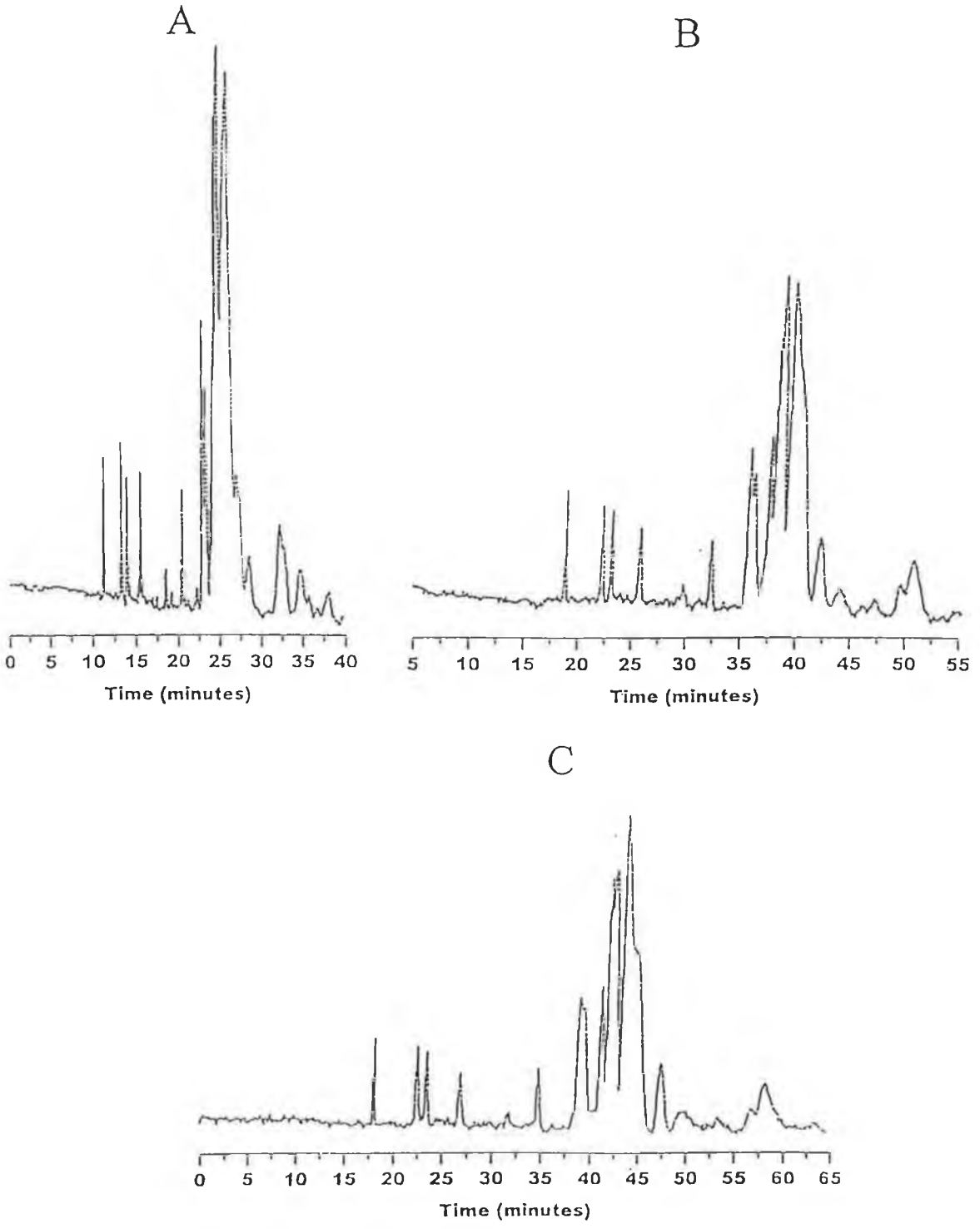

Figure 2.7. Effect of increasing methanol concentration on the migration times of individual NSG-peptoids from the library CHIR 4580.1. All run buffers contained 250 mM trihydrogen-phosphate buffer, pH 2.0, with (A) 3% (v/v); (B) 14% (v/v) and (C) 16% (v/v) methanol.

2.3.1.5 Combined effect of organic solvents and ion-pairing agent on separation

The effect of the organic modifier was much more effective when used in conjunction with the ion-pairing agent, HSA. Methanol and HSA interacted more effectively with the strong hydrophobic forces of the larger molecules and separate the individual peptoids substantially with increasing concentration of methanol (Figure 2.8). Low concentrations of HSA were sufficient to bring about sufficient resolution. At the highest concentration of methanol studied (16% v/v), the peak heights are relatively uniform, but many of the later eluting peaks have shoulders indicating that there are still many components of this mixture co-eluting. Peak efficiency is not as good at the higher concentrations, and the migration times are also quite long; hence it is unlikely that higher concentrations of methanol would improve separation. Acetonitrile in conjunction with HSA was also studied, and while improving the solubility of the components, it did not have quite as dramatic an effect on separation as methanol. Using 250 mM tri-hydrogen phosphate buffer, 25 mM HSA, at a pH of 2.0 and 16% (v/v) methanol, approximately 16 peaks were well resolved (Figure 2.8).

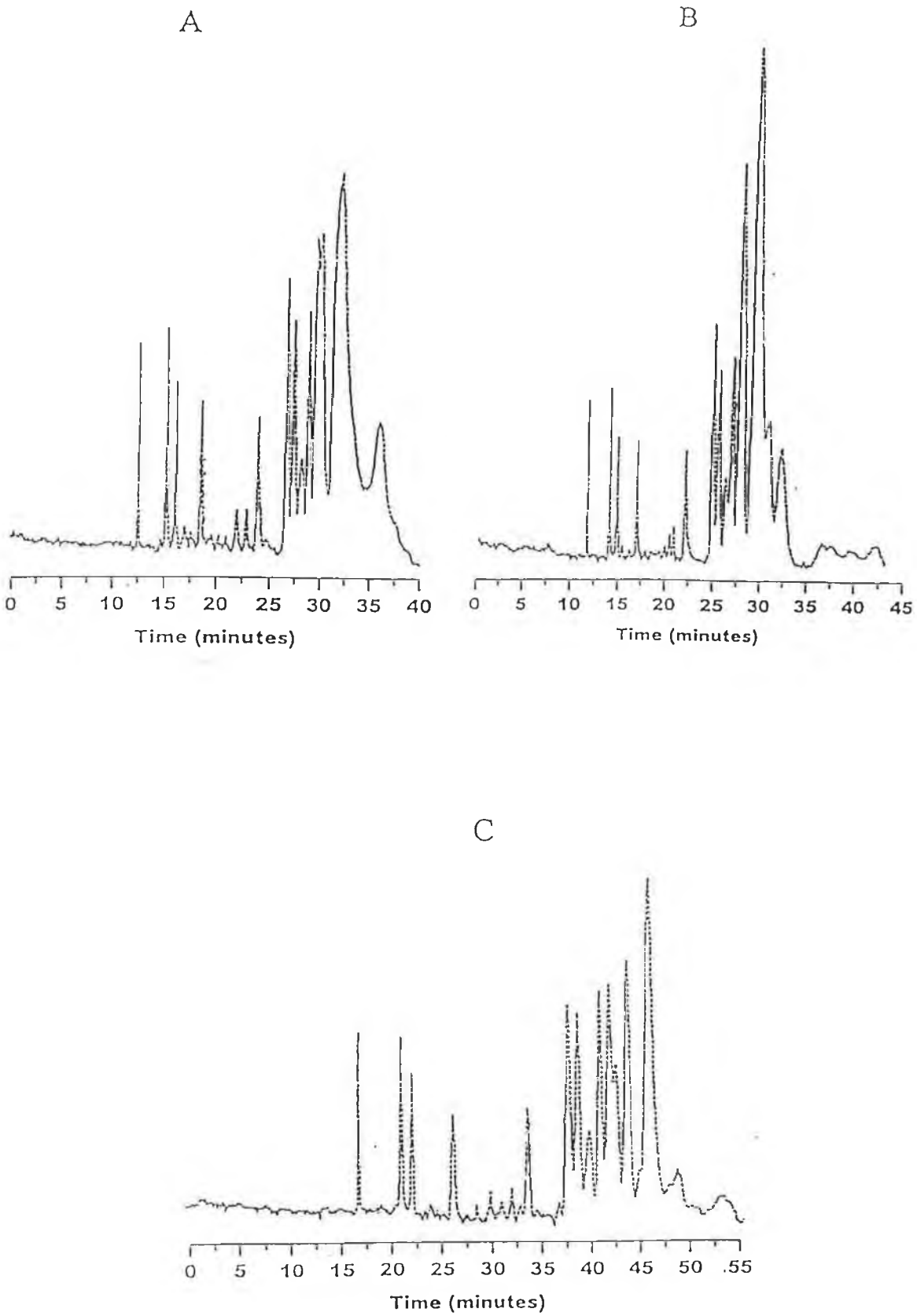

Figure 2.8. Combined effect of HSA and methanol on the separation of CHIR 4580.1. All run buffers contained 250 mM trihydrogen-phosphate buffer, pH 2.0, with 25 mM HSA and (A) no methanol; (B) 3% (v/v); (C) 14% (v/v).

D

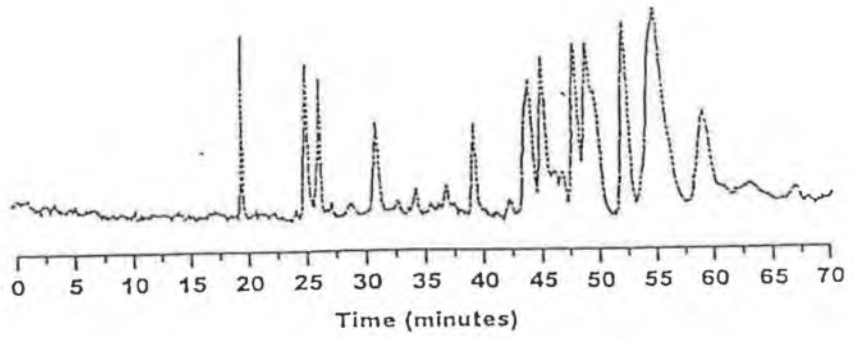

Figure 2.8 (D). Combined effect of HSA and methanol on the separation of CHIR 4580.1. Run buffer was 250 mM trihydrogen-phosphate buffer, pH 2.0, with 25 mM HSA and 16% (v/v) methanol.

2.3.1.6. Effect of cyclodextrin

CDs are water-soluble cyclic-oligosaccharides formed by the enzymatic digestion of starch by cyclodextrin transglycosylase [25]. The most commonly used CD consist of 6,7 and 8 glycopyranose units corresponding to α, β, and γ-CD [26] and are illustrated in Figure 2.9. They possess a toroidal structure with an apolar inner cavity allowing them to form host guest inclusion complexes with many hydrophobic compounds, such as peptoids. Several derivatised cyclodextrins have been synthesised to increase their solubility and reduce hydrogen bonding capabilities, A wide range of these derivatised cyclodextrins are commercially available from companies such as Sigma and Aldrich. Peterson [27] and Brown et al. [28] have investigated several derivatised forms, demonstrating that the type of cyclodextrin employed plays an important role in resolution. The physical size of these molecules can be exploited to effect separation. α-CD selectively allows a single aromatic ring or smaller, whereas β-CD allows naphthalene-like compounds and γ-CD can accommodate molecules as large as a four-fused benzene-ring [25].

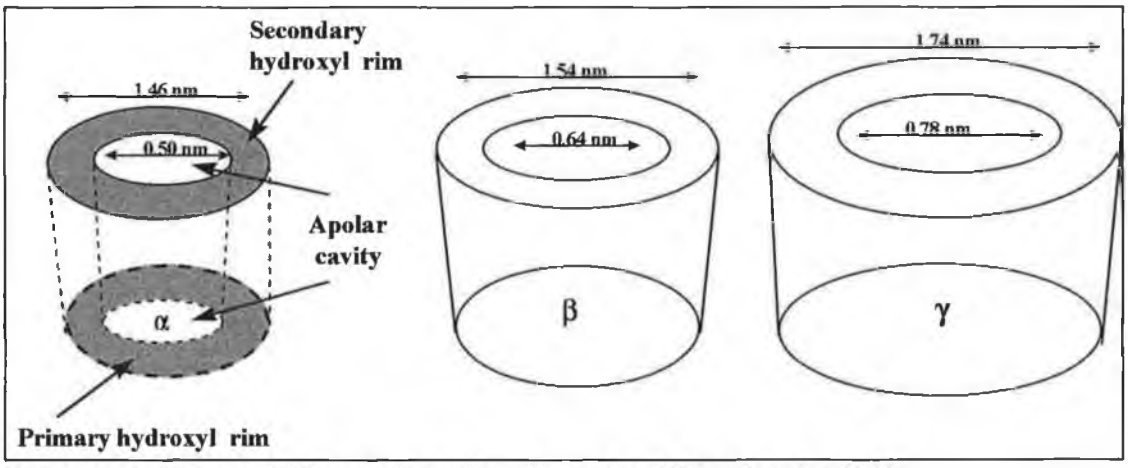

Figure 2.9. Schematic illustration of α-, β-, and γ-CD molecules [26].

The β-CD was chosen because of its suitable inner cavity dimensions, it was thought that the inner cavity dimensions of the γ-CD would be too large and would possibly accommodate several molecules without inducing efficient separation. β-CD is only poorly soluble, hence a better approach is to use a derivatised form. Methyl-β-CD was chosen in this application to effect separation of the peptoid library at acidic pH. At low pH the EOF is extremely slow and the CD molecule migrates with the EOF because it is neutral. The peptoid molecules are protonated at this pH and move towards the detector (cathodic end). Peptoid molecules with the correct fit will partition into the methyl-β-CD cavity and will migrate at a modified rate. When the concentration of methyl-β-CD was increased, an increase in the overall elution time of the peptoid library was observed with a slight improvement in the resolution of individual peptoids. However, above 60 mg/ml, no further increase in resolution was observed. Nishi *et al.* [29] have observed that beyond a certain concentration of CD, resolution begins to deteriorate because of decreased efficiency due to increased elution time. Using a run buffer of 250 mM trihydrogen-phosphate, pH 2.0, with 60 mg/ml methyl-β-CD, separation of the test library resulted in the resolution of approximately 17 NSG-peptoids with a much improved separation efficiency than before.(Figure 2.10).

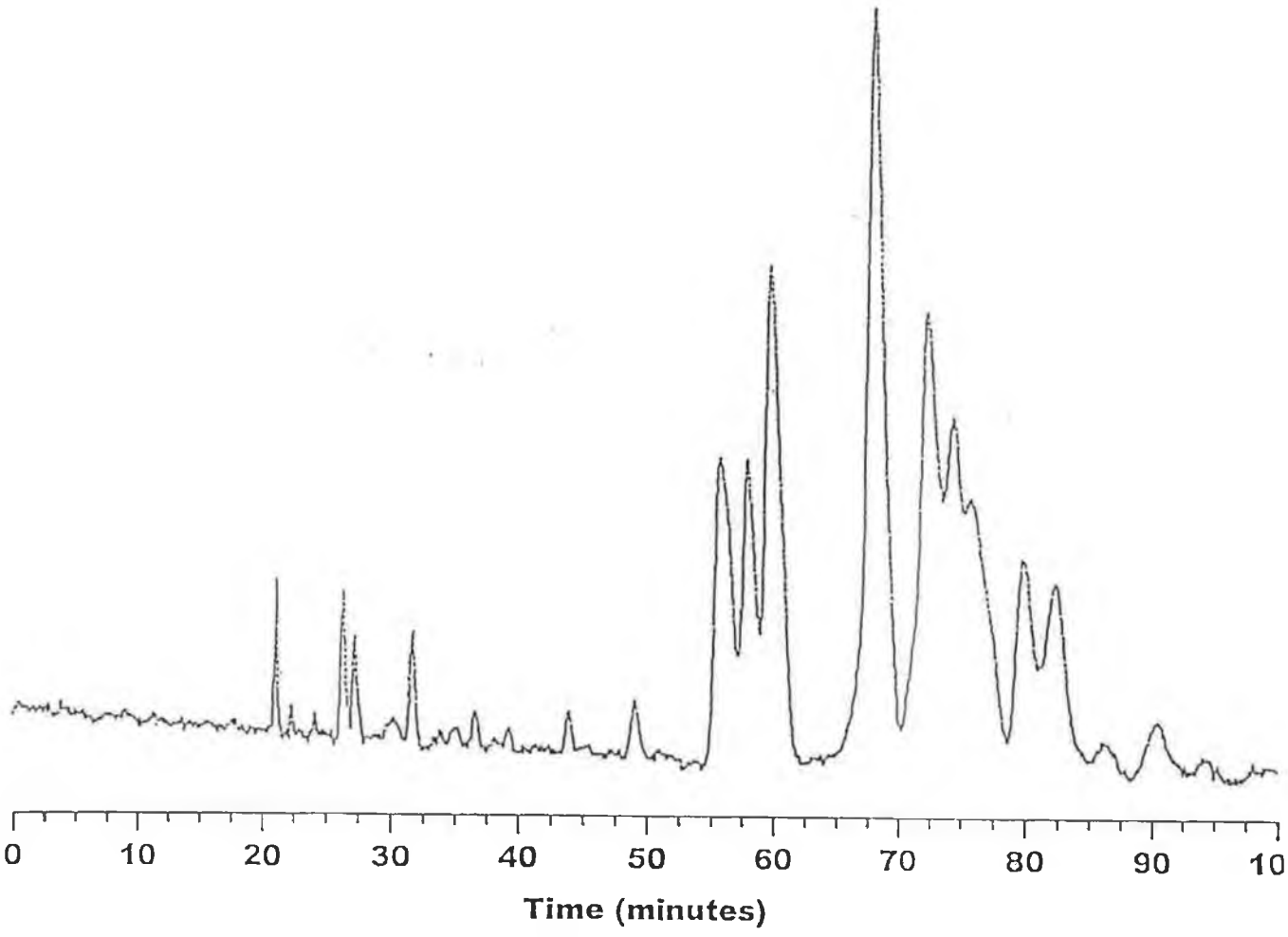

Figure 2.10. The effect of the host guest interaction capabilities of cyclodextrin on the separation of the individual NSG-peptoid library CHIR 4580.1 using 250 mM trihydrogen-phosphate buffer, pH 2.0 with 60 mg/ml methyl-β-CD.

2.3.1.7. Optimised Separation

It was noticed, however, that when methyl-β-CD was employed in conjunction with the ion-pairing agent HSA, a very powerful separation mechanism was realised for the separation of the test peptoid library. The primary role of the HSA was to solubilise the large hydrophobic molecules and reduce the self-aggregation of these peptoids, while the role of the methyl-β-CD was to bring about their efficient separation. The conditions which achieved optimum resolution of this library were 250 mM tri-hydrogen phosphate, 25 mM HSA and 40 mg/ml methyl-β-CD, pH 2.0. Under these conditions 21 of the required 24 peptoids were resolved efficiently (Figure 2.11).

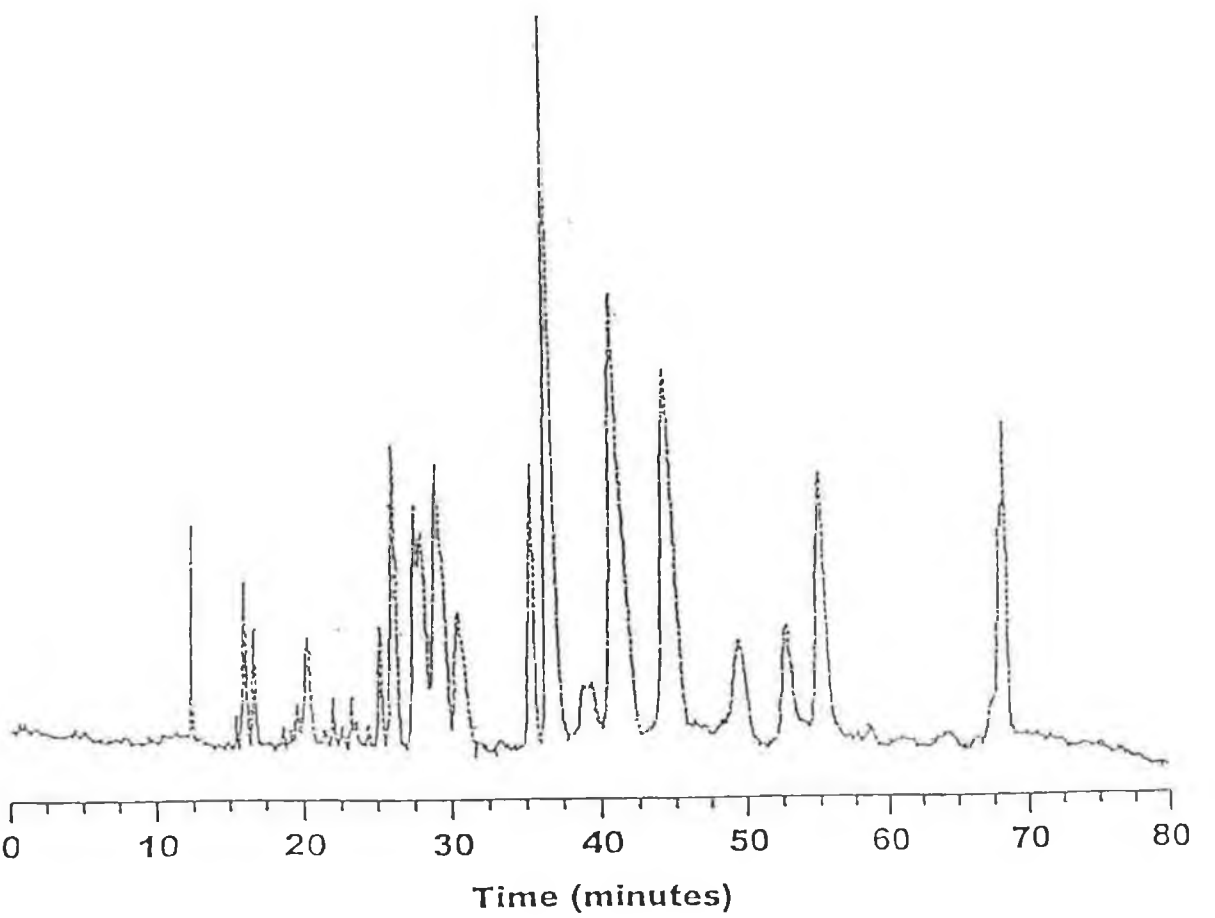

Figure 2.11. The optimised separation of the NSG-peptoid library CHIR 4580.1. The conditions used were 250 mM trihydrogen-phosphate buffer, pH 2.0, with 25 mM HSA and 40 mg/ml methyl-β-CD. Current = 72 μA, for an applied voltage of 15 kV.

2.4. SEPARATION OF THE REMAINING FIVE LIBRARIES USING THE SEPARATION METHOD DEVELOPED FOR THE NSG-PEPTOID LIBRARY CHIR 4580.1

The method developed in 2.3. was then applied to five new peptoid libraries; CHIR 4582.1, CHIR 5216.1, CHIR 4555.1, CHIR 4567.1 *(all linear molecules)* and CHIR 2003.1 *(cyclic)*. Each library has a different backbone structures ranging from increased aromaticity to cyclic peptoid molecules (Figure 2.12) but each library contains the same 24 functional groups attached at position R as before.

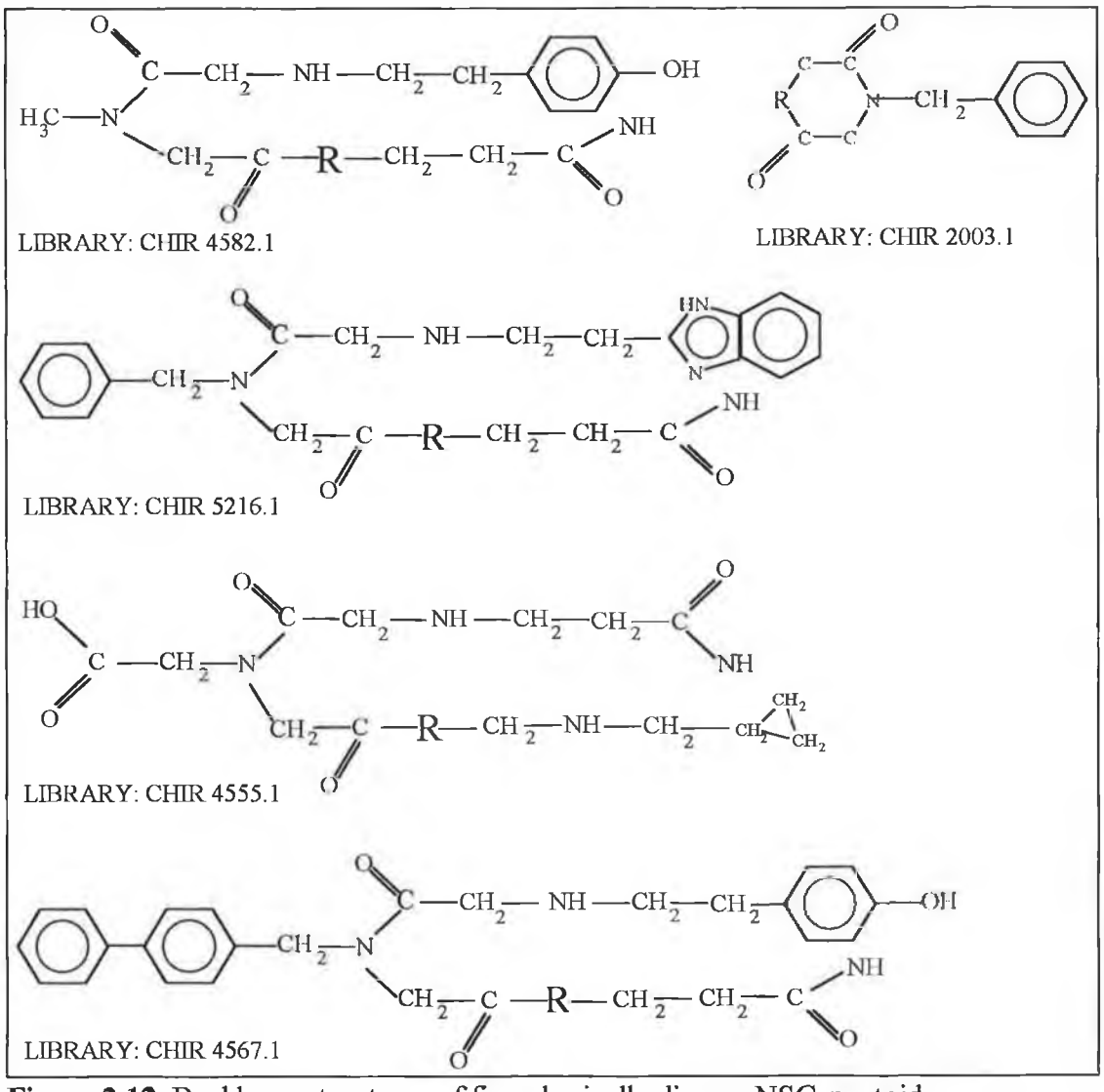

Figure 2.12. Backbone structures of five physically diverse NSG-peptoids.

These libraries exhibit differences in their physico-chemical characteristics defined by their shape, hydrogen boding capabilities, molecular weight, Log D values and pK_a values. These are illustrated by their molecular structure (Figure 2.12) and as summarised in Table 2.1. The apparent octanol/PBS distribution coefficient (log $D_{O/PBS}$) and pK_a values were determined for Taylor *et al.* [18] of Chiron Corporation by Compudrug Chemistry Ltd., Budapest, Hungary.

Peptoid Library	**apK_a**	**bpK_a**	**log $D_{O/PBS}$**	**MW range**	**Structure class**
CHIR 4580.1	3.4 - 10.1	9.8 - 7.6	-2.5 - 4.5	392-581	linear
CHIR 4582.1	3.4 - 10.1	9.8 - 7.6	-5.0 - 1.9	322-495	linear
CHIR 4555.1	3.1 - 3.3	9.8 - 7.6	-5.0 - 0.6	300-473	linear
CHIR 5216.1	3.4 - 6.8	9.8 - 7.6	-2.0 - 3.1	408-581	linear
CHIR 4567.1	3.4 - 10.1	9.8 - 7.6	-1.3 - 5.6	460-633	linear
CHIR 2003.1	3.4 - >14	9.8 - <1	-3.7 - 3.1	204-377	cyclic

Table 2.1. Physical and chemical characteristics of each of the NSG-peptoid libraries investigated.

2.4.1. Peptoid libraries which were separated using the pre-existing method

Efficient separation of three libraries namely CHIR 4582.1, CHIR 5216.1 and CHIR 4555.1, was achieved using the previously described method. These three libraries are linear trimeric molecules, with variations in their backbone structure which define a variety of physical and chemical characteristics for each one. It can be observed that these conditions, described in section 2.3, resolve many of the individual NSG-peptoids, although some of the molecules need to be more efficiently resolved. With this objective in mind it was hoped that by more careful fine-tuning of the existing method, that all twenty four compounds could be separated.

All experiments performed on the NSG peptoid library CHIR 4580.1 were achieved using a home-built apparatus (System 1). The capillary was housed in a Plexiglas box fitted with a safety interlock device and connected to a high-voltage dc

(0-30kV) power supply. For the following five libraries studied, a commercially available ISCO Model 3850 system was used which contained a cooling device to protect the capillary from Joule heating effects (System 2). This facilitated the use of higher concentrations of the ion-pair reagent HSA. Increasing the concentration of HSA from 25 mM to 75 mM in conjunction with CD had a substantial improvement on the separation of individual NSG-peptoids. The ionic strength of the phosphate buffer was reduced from 250 mM to 200 mM, pH 2.0. This was done to maintain sufficiently low currents. By reducing the concentration of the CD, the migration times of the individual peptoids decrease and as a result sharper peak widths are obtained without altering the separation efficiency achieved. The conditions which were deemed the most suitable for separation of all three libraries was 200 mM tri-hydrogen phosphate, 75 mM HSA and 30 mg/ml methyl -β-CD, pH 2.0. The currents while quite high (72-78 μA), were permitted because of the cooling apparatus. While the conditions were altered from the original one, no major changes have been implemented and hence the applicability of this method for NSG-peptoid separations is demonstrated.

2.4.1.1. NSG-peptoid library CHIR 4582.1

This particular library is very similar to the first library studied, i.e. CHIR 4580.1, the only difference being a shorter alkyl side chain on this library. The previous conditions of 250 mM trihydrogen-phosphate, 25 mM HSA and 40 mg/ml methyl-β-CD, pH 2.0, gave rise to adequate separation of this particular library with approximately 19 of the 24 compounds separated. In Figure 2.13(a) the separation achieved using the previous conditions is illustrated. When the modified conditions of 200 mM trihydrogen-phosphate, 75 mM HSA and 30 mg/ml methyl-β-CD, pH 2.0 were used for the separation of this library a major difference was observed (Figure 2.13(b)). The individual NSG-peptoid peaks 5, 6 and 10 have all split, and clearly three new peptoids are resolvable. Hence by increasing the concentration of the HSA from 25 mM to 75 mM, the propensity to form intramolecular interactions is reduced and the potential to separate these molecules is made possible.

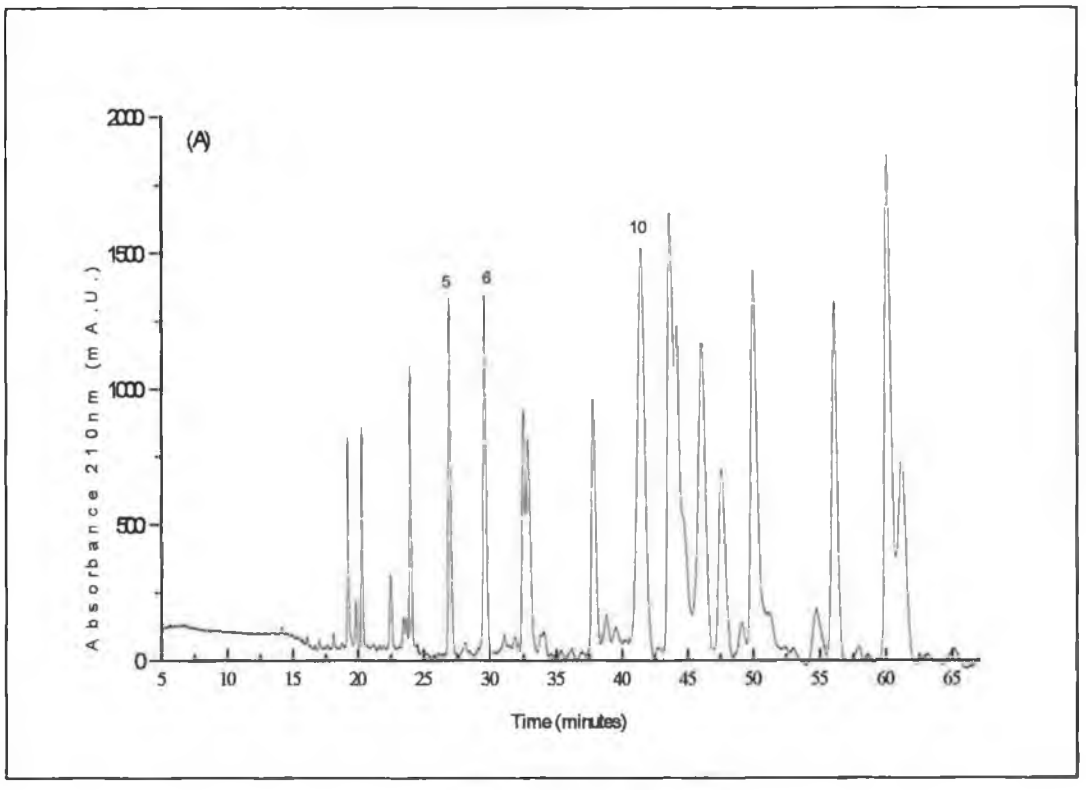

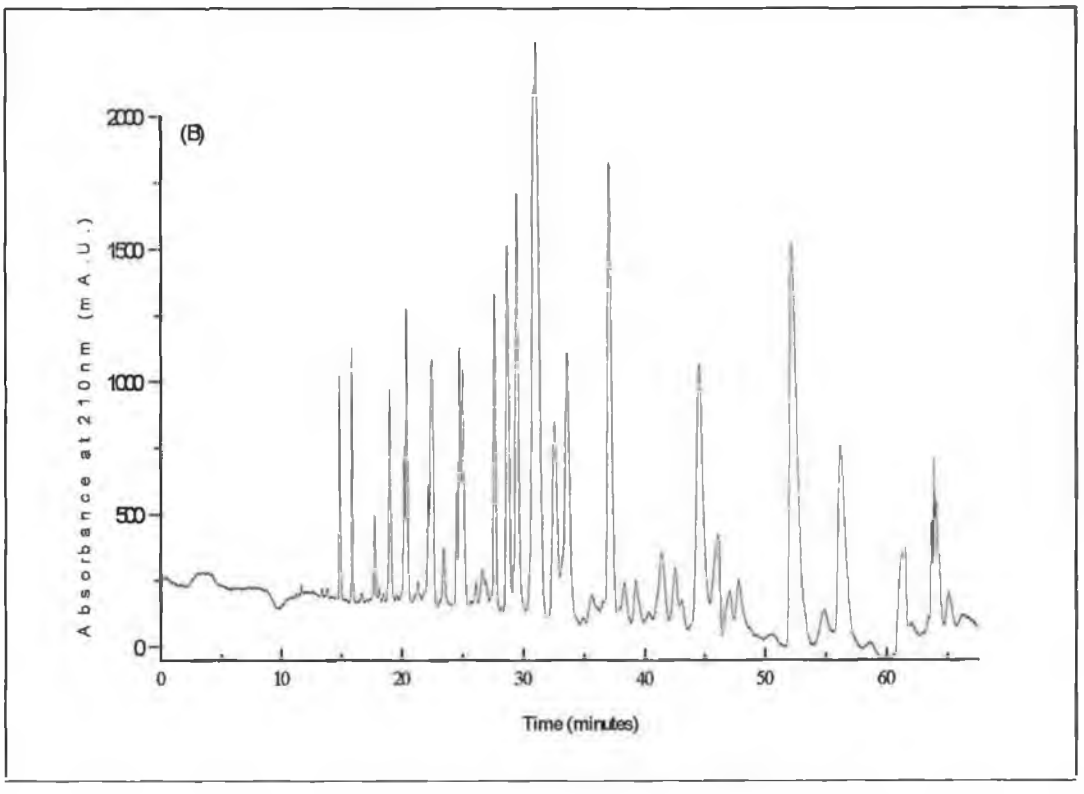

Figure 2.13. Separation of the linear trimeric NSG-peptoid library; CHIR 4582.1. Running buffer conditions were: (A) 250 mM trihydrogen-phosphate, 25 mM HSA, and 40 mg/ml methyl-β-CD, pH 2.0. (B) 200 mM trihydrogen-phosphate, 75 mM HSA and 30 mg/ml methyl-β-CD, pH 2.0.

2.4.1.2. NSG-peptoid library CHIR 5216.1

This linear trimeric library has similar molecular weight and chemical characteristics as CHIR 4580.1. The long alkyl chain associated with CHIR 4580.1 has been replaced by an aromatic ring and the phenol group by a phenylimidazole group. These groups act merely as protecting agents for the library to prevent attack by strong cleaving proteases. Using the old conditions of 250 mM trihydrogen-phosphate, 25 mM HSA and 40 mg/ml methyl-β-CD, pH 2.0, the peak shapes are very sharp but the resolution could be improved (Figure 2.14(A)).

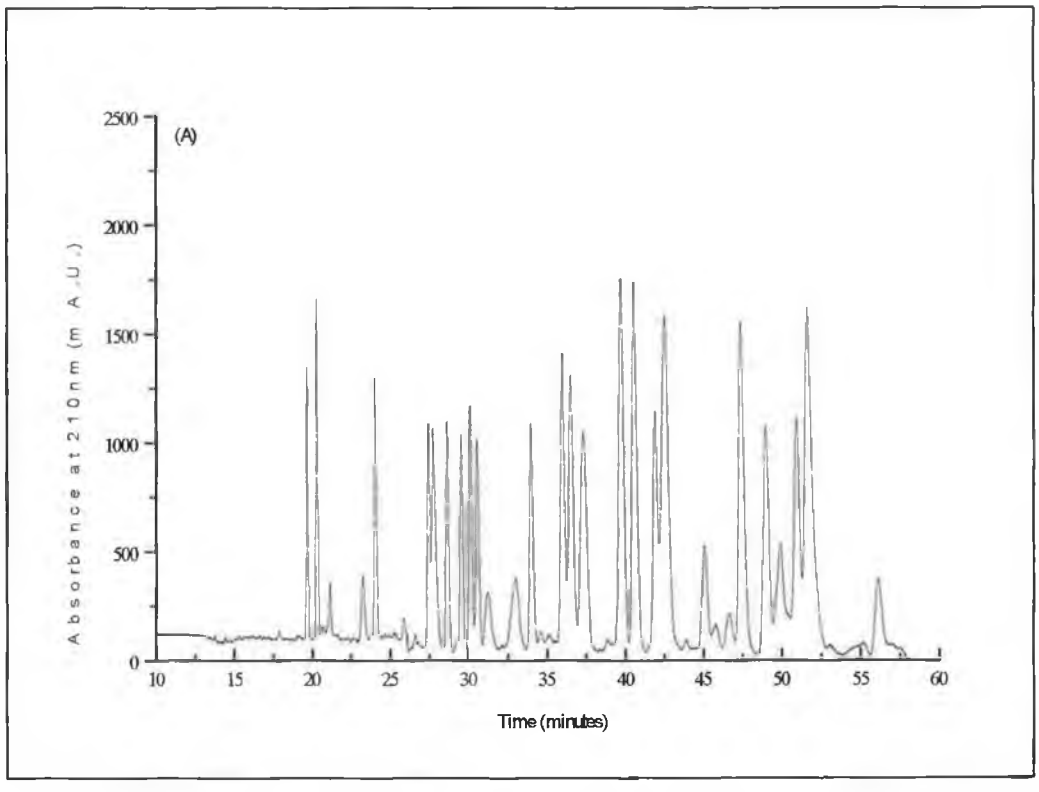

Figure 2.14(A). Separation of the linear trimeric NSG-peptoid library CHIR 5216.1. Running buffer conditions were 250 mM trihydrogen-phosphate, 25 mM HSA, and 40 mg/ml methyl-β-CD, pH 2.0.

When the modified method was applied, the resolution of the individual NSG-peptoids was much improved, notably for those peaks which migrate between 23 and 30 minutes. As the ionic strength of the phosphate buffer is now reduced from 250 mM to 200 mM, the peak widths are broadened and the separation between 17.5 and 21 minutes is not as good as that obtained using a concentration of 250 mM. It was not practical, however, to use the high ionic strength buffer with the higher

concentration of HSA, as the Joule heating effect becomes too large. Increasing the concentration of HSA from 25 to 75 mM, while keeping the other conditions the same, increased the current from 45 to 89 μA, hence a trade-off between high buffer concentration and low HSA concentration or reduced buffer concentration while using higher HSA concentration may be used depending on the requirement. Using the modified method, approximately 25 peaks are well resolved as is illustrated in Figure 2.14(B).

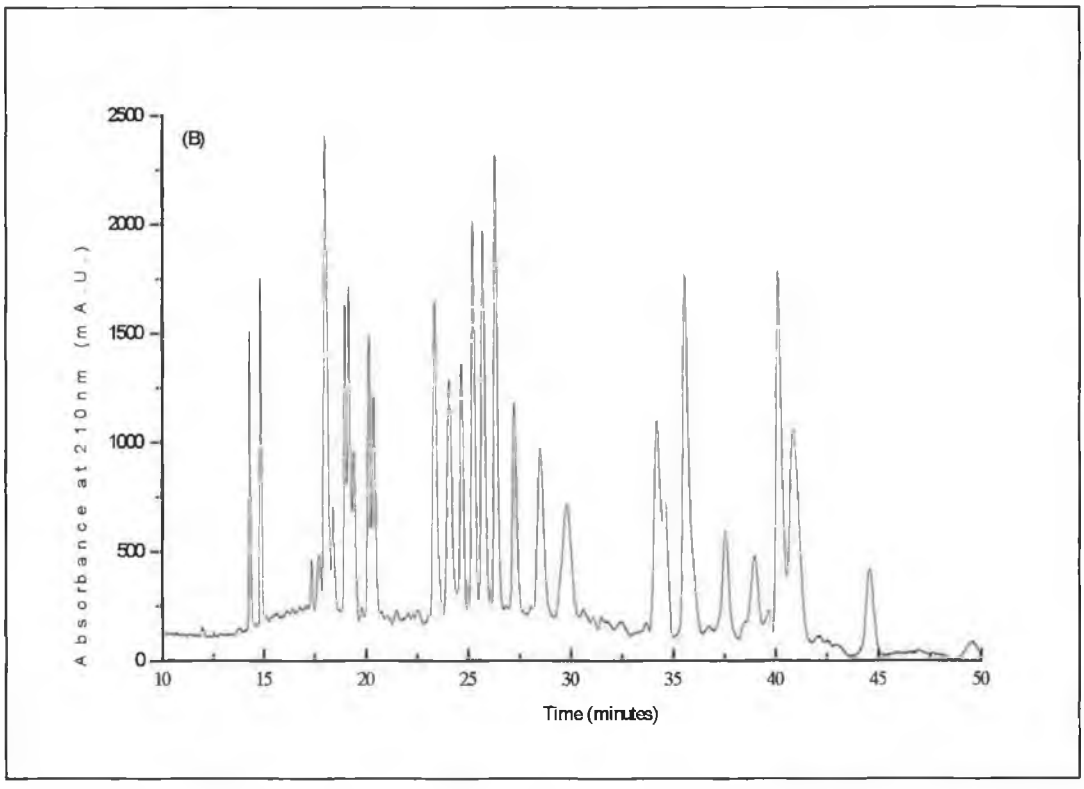

Figure 2.14(B). Separation of the linear trimeric NSG-peptoid library CHIR 5216.1. Running buffer conditions were 200 mM trihydrogen-phosphate, 75 mM HSA and 30 mg/ml methyl-β-CD, pH 2.0.

2.4.1.3. NSG-peptoid library CHIR 4555.1

This library again is quite different to the previous two libraries investigated. The phenol group has now been replaced by a saturated cyclopentane group and the alkyl chain has been replaced by a carboxylic acid. The presence of the carboxylic group on one end of this peptoid backbone and the absence of phenol or other aromatic groups explain its low apK_a value. Using the previously described conditions of 250 mM trihydrogen-phosphate, 25 mM HSA and 40 mg/ml methyl-β-CD, pH 2.0, only 15 of

the 24 NSG-peptoids were actually separated, many of which are not baseline resolved (Figure 2.15(A)).

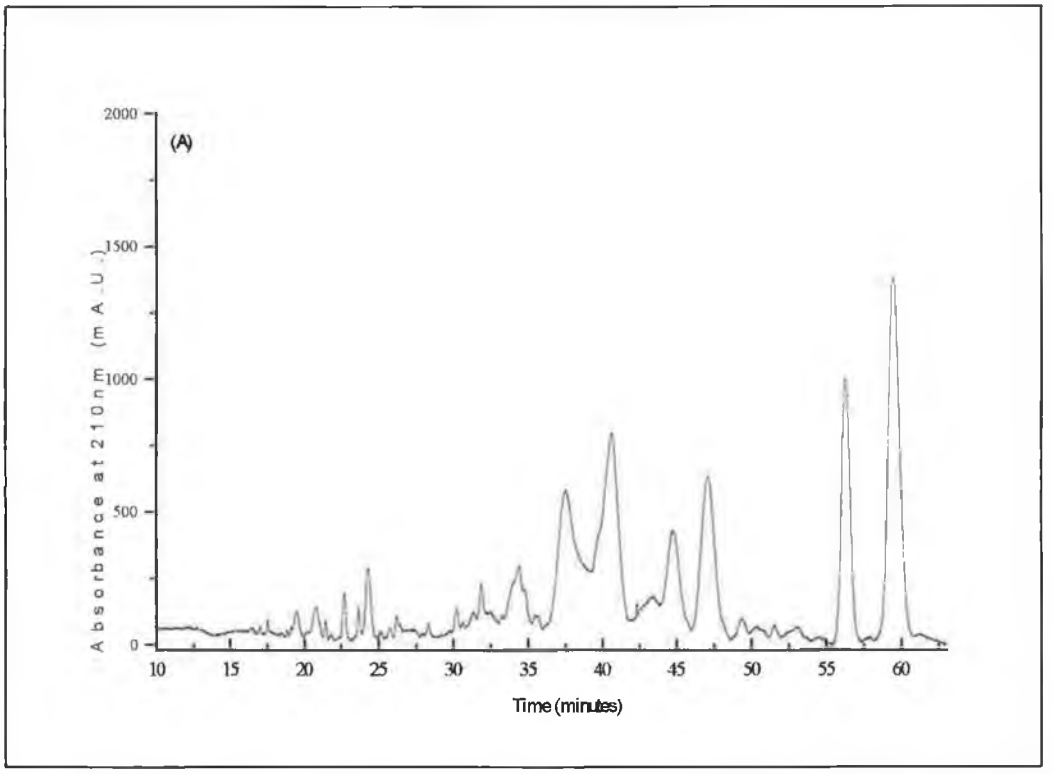

Figure 2.15(A). Separation of the linear trimeric NSG-peptoid library CHIR 4555.1. using 250 mM trihydrogen-phosphate, 25 mM HSA, and 40 mg/ml methyl-β-CD, pH 2.0.

Upon increasing the HSA concentration to 75 mM the separation of the individual NSG-peptoids is improved and approximately 20 peaks are detected. The peak base widths are characteristically narrow with the later eluting peaks showing peak broadening. This may be attributed to co-eluting peaks (Figure 2.15(b)). The final two eluting peaks are broad due to their increased migration times; however, they both exhibit a shoulder indicating that there are still some co-eluting molecules. This particular library may require some further fine-tuning to efficiently resolve the hidden peaks.

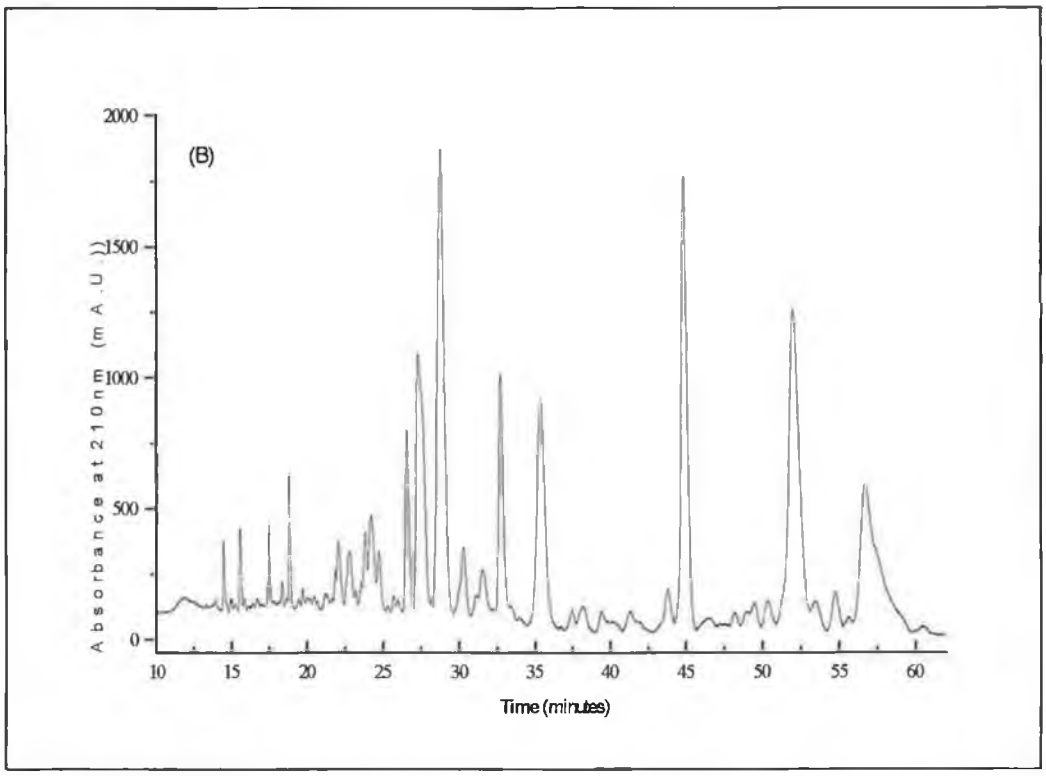

Figure 2.15(B). Separation of the linear trimeric NSG-peptoid library CHIR 4555.1. using the modified conditions of 200 mM trihydrogen-phosphate, 75 mM HSA and 30 mg/ml methyl-β-CD, pH 2.0.

In conclusion, this modified method, consisting of 200 mM trihydrogen-phosphate, 75 mM HSA and 30 mg/ml methyl-β-CD, pH 2.0. separates linear trimeric peptoid libraries quite well. Table 2.2. illustrates the number of peaks resolved, for the three libraries by using the existing method compared with the newly modified method.

Peptoid Library	Previous Conditions	Modified Conditions
CHIR 4582.1	18	24
CHIR 5216.1	25	25
CHIR 4555.1	15	20

Table 2.2. Improvements achieved in the resolution (i.e. the number of individual NSG-peptoids actually separated) of the three libraries; (CHIR 4582.1, CHIR 5216.1, and CHIR 4555.1) through modification of the run buffer conditions developed for CHIR 4580.1.{Previous conditions consisted of 250 mM trihydrogen-phosphate, 25 mM HSA and 40 mg/ml methyl-βCD, pH 2.0. New conditions consisted of 200 mM trihydrogen-phosphate, 75 mM HSA and 30 mg/ml methyl-βCD, pH 2.0}

2.5. PROBLEMATIC LIBRARIES

2.5.1. Development of a cyclodextrin-modified micellar based separation method

Two libraries were poorly separated using the method developed initially for CHIR 4580.1. The first library was a dimeric cyclic NSG-peptoid library (CHIR 2003.1) and the second was a linear trimeric library (CHIR 4567.1).The backbone structures of these libraries are illustrated in Figure 2.12. These libraries were resolved using a micellar phase which replaced the ion-pair reagent.

2.5.1.1 NSG-peptoid library CHIR 2003.1

The absence of a tertiary amine and no ionisable functional groups on the backbone structure of this library implied that yet another sophisticated method was required for its efficient separation.

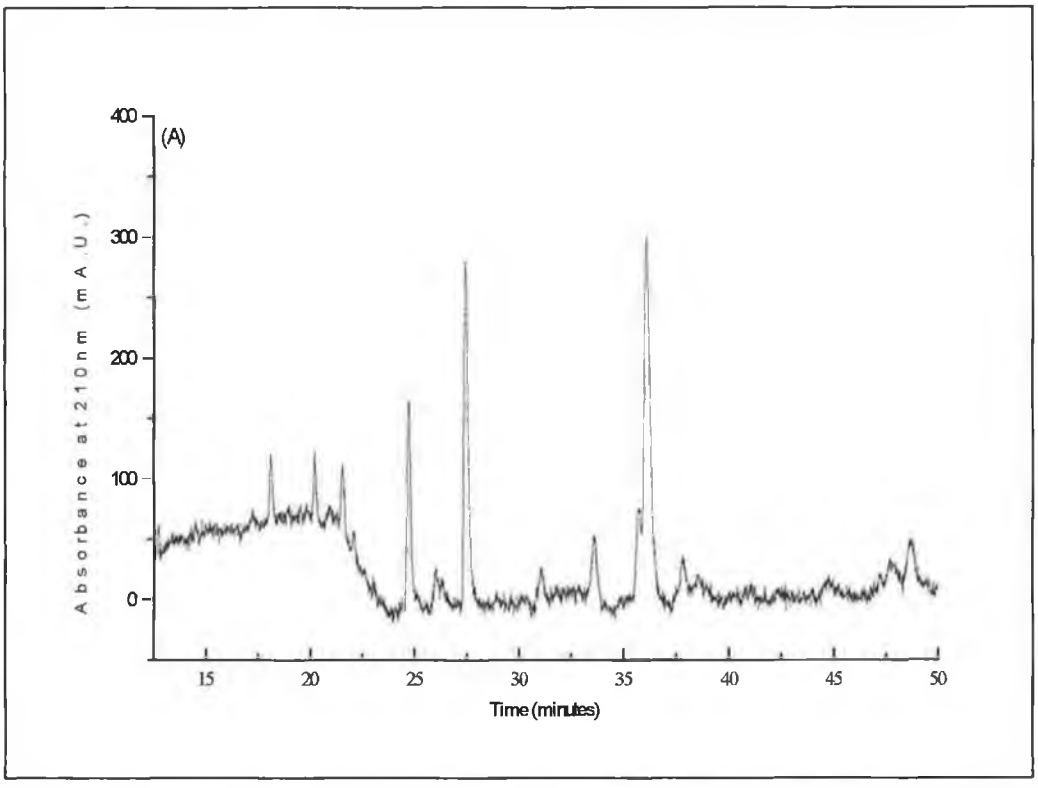

Figure 2.16. Separation of the cyclic dimeric NSG-peptoid library CHIR 2003.1. The running buffer consisted of 250 mM trihydrogen-phosphate, 25 mM HSA, and 40 mg/ml methyl-β-CD, pH 2.0.

This library has an apK_a range of 3.4 to 14, and a bpK_a range from 9.8 to <1, and hence will remain relatively uncharged at any pH. Using the conditions developed for CHIR 4580.1, approximately 12 peaks were resolved. Based on this fact that the library remains relatively uncharged at any pH, the idea of using a micellar phase was considered. Micelles, first introduced to CE by Terabe [30], are aggregates of surfactant molecules which possess both hydrophilic and hydrophobic regions that are spatially separated [31]. Micelles provide a pseudophase by which neutral molecules through their varying affinities for the pseudophase can be separated [32].

Micellar electrokinetic chromatography (MEKC) is especially suited for small neutral molecules. Efficient separation of large hydrophobic molecules would create a more exciting challenge. Very hydrophobic molecules tend to remain on the inner hydrophobic core of the micelle and eventually co-elute with the micelle. This is illustrated in Figure 2.17. A large hydrophobic band is observed between 12-18 minutes and some separation is achieved between 40 and 45 minutes.

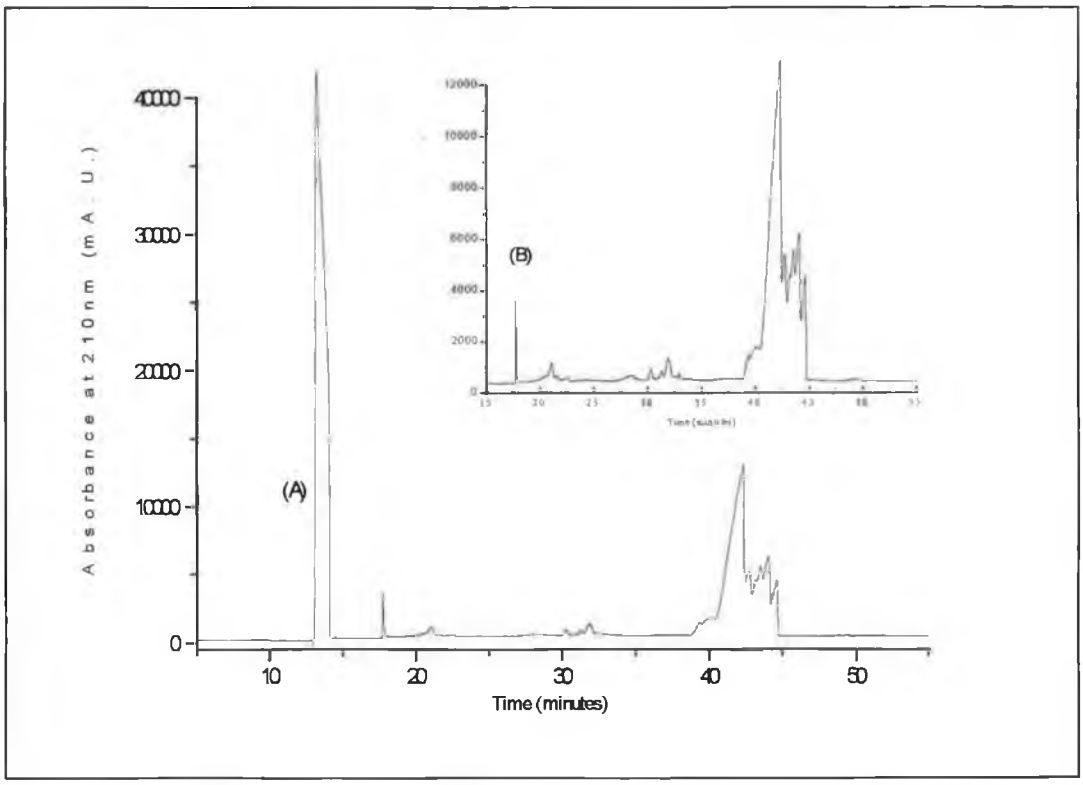

Figure 2.17. Separation of the cyclic dimeric NSG-peptoid library CHIR 2003.1. The run buffer conditions used were (A) 75 mM di-sodiumhydrogen-phosphate, 25 mM sodium borate and 75 mM SDS, pH 8.0.and inset (B) same conditions with reduced y-axis scale.

The large hydrophobic band at 10 minutes may be explained by strong intermolecular and intramolecular interactions between several NSG-peptoids which may be too large to spatially fit inside the hydrophobic micellar core, and hence elute with the EOF. The poorly resolved peaks between 40 and 45 minutes are those hydrophobic molecules that actually fit inside the micellar core with varying degrees of hydrophobic interactions evident.

It was found that by the addition of additives to the run buffer, the affinity of the hydrophobic molecules for the aqueous based run buffer was increased. CD-modified MEKC, in which CD is added to a micellar solution, was developed by Terabe [33] for the separation of electrically neutral and highly hydrophobic compounds. Due to the outer hydrophilic nature of the CD molecule it will not interact with the micellar solution. Therefore a new state exists where the CD will behave as a separate phase against the micelle. When highly hydrophobic and large ionic molecules such as an NSG-peptoid library is injected into the CD-modified MEKC system, the molecules distribute between three phases, namely the aqueous phase of the run buffer, the micellar phase and form host-guest inclusion complexes with the CD.

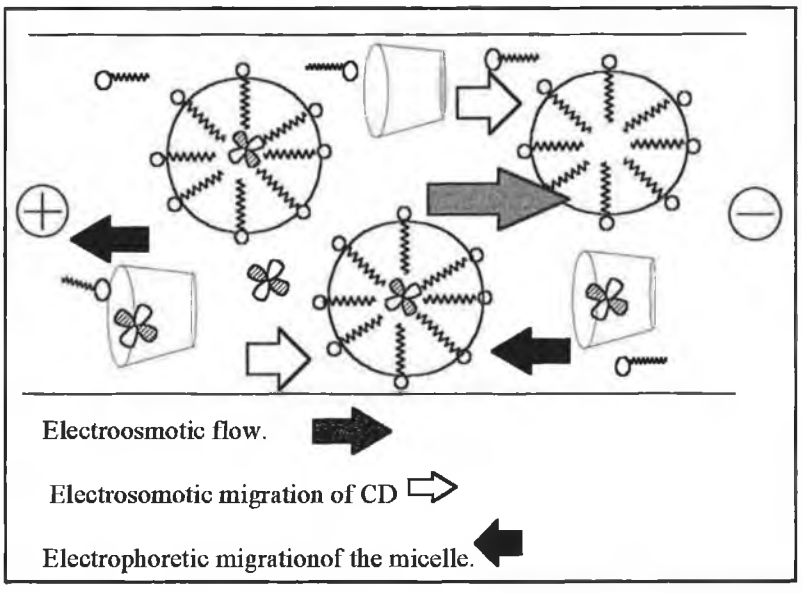

Figure 2.18. Schematic of the basis of separation of CD-modified MEKC, adapted from [30].

The degree of partitioning of these molecules into the micelle will depend on their hydrophobicity, but the inclusion complexes formed between the NSG-peptoid and the

CD will depend on the agreement of the molecular size with the inner diameter of the CD in addition to its hydrophobicity. This distribution of the peptoid molecules between the various phases is very evident in Figure 2.19. The hydrophobic band is still visible at 10 minutes, but sharp well resolved peaks follow. This region between 10 and 25 minutes is due to the resolving nature of the CD and the high concentration of phosphate buffer. Increasing the buffer concentration induces better separation efficiency. The later eluting more broadened and less well resolved peaks are due to the affinity of the NSG-peptoids for the SDS micelle. Between the region of 23 and 33 minutes there are approximately 5 peaks which are centrally split. This may indicate equal proportions of very closely related compounds. Increasing the SDS concentration from 50 mM to 75 mM improved the resolution substantially, with much sharper peaks and greater separation of the later eluting large hydrophobic peptoids. Increasing the CD concentration from 0.02 to 0.04 g/ml reduced the separation time from 80 to 50 minutes. As a result the individual NSG-peptoids were more tightly compressed but had no detrimental effect on the overall resolution of the library.

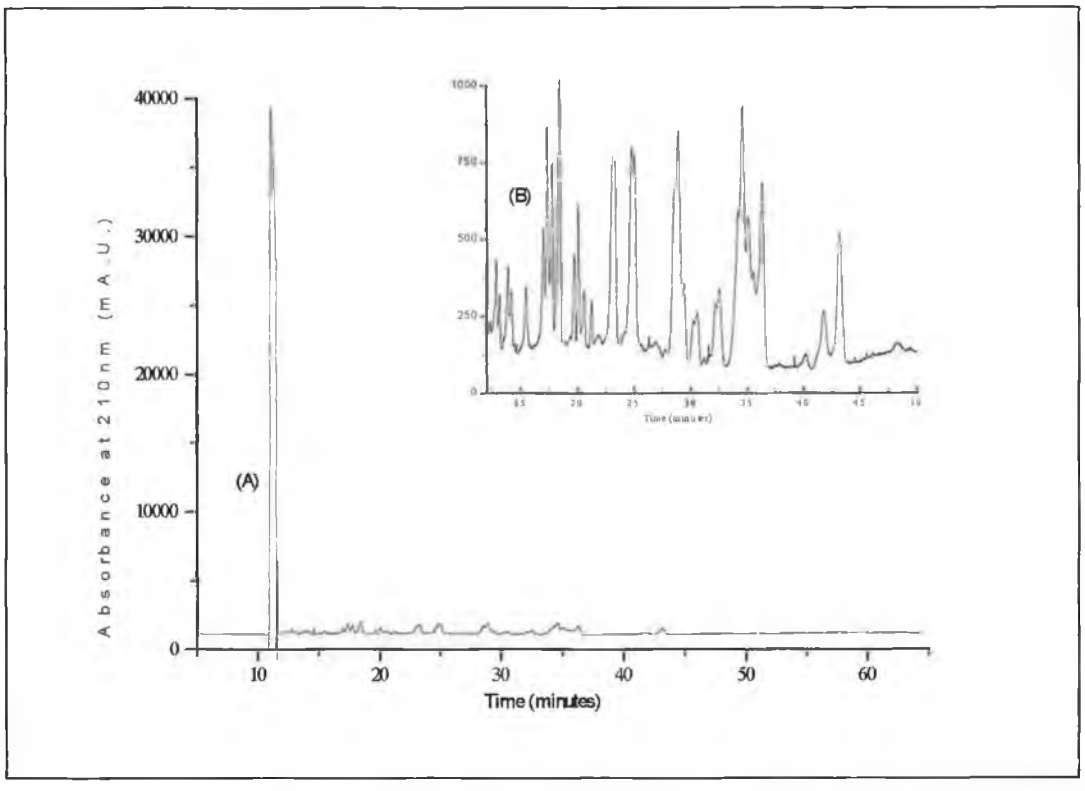

Figure 2.19. Separation of the NSG-peptoid library CHIR 2003.1. Run buffer conditions used were 75 mM di-sodiumhydrogen-phosphate, 25 mM sodium borate,75 mM SDS and 40 mg/ml methyl-β-CD, pH 8.0, and inset (B) same as (A) with reduced y-axis scale.

Presently more than the required number of compounds have been detected using a run buffer containing 75 mM phosphate, 25 mM borate, 75 mM SDS and 40 mg/ml methyl-β-CD, pH 8.0. As the purity of the sample is unknown, it is assumed that many of the these extraneous peaks may be impurity peaks from the synthesis or from the run buffer. This is as yet a preliminary investigation for the separation of cyclic NSG-peptoids and further optimisation is necessary but this approach appears quite promising.

2.5.1.2. NSG-peptoid library CHIR 4567.1

The final library which was studied was the highly aromatic, linear trimeric library, CHIR 4567.1. The separation conditions of 250 mM phosphate, 25 mM HSA and 40 mg/ml methyl-β-CD, pH 2.0, which was suitable for the separation of the other linear NSG-peptoid libraries, was not sufficient to separate this particular library. Using the conditions developed for CHIR 4580.1, only 10 peaks were resolved (Figure 2.20). A possible explanation why this library is more problematic than the other linear libraries investigated may be attributed to its increased aromaticity and steric hindrance. It has both a phenolic ring and a biphenyl group attached. The presence of the tertiary amine, however, indicates that this library may be charged below pH 3.4; however its increased molecular weight and greater aromaticity may induce stronger hydrophobic interactions thereby preventing its efficient separation.

Having separated the cyclic dimeric NSG-peptoid, CHIR 2003.1 using a CD-modified, MEKC system, it was decided to apply these electrophoretic conditions to this problematic library. Again a very similar situation was observed. Neither CD or SDS alone could solubilise these hydrophobic components to bring about their efficient separation. Yet, when these two additives were combined, a very powerful separation mechanism was achieved which was sufficient to resolve many of the 24 NSG-peptoid molecules in this library (Figure 2.22).

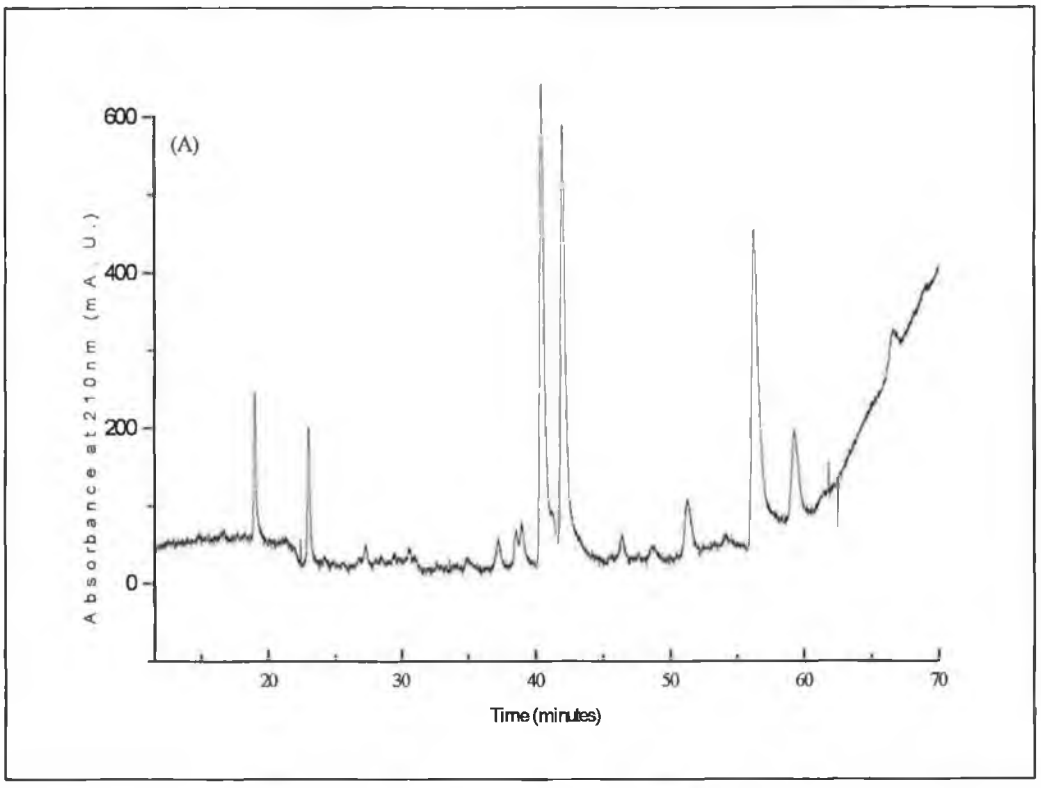

Figure 2.20. Separation of the NSG-peptoid library CHIR 4567.1 achieved using a run buffer of 250mM trihydrogen-phosphate, 25 mM HSA, and 40 mg/ml methyl-β-CD, pH 2.0.

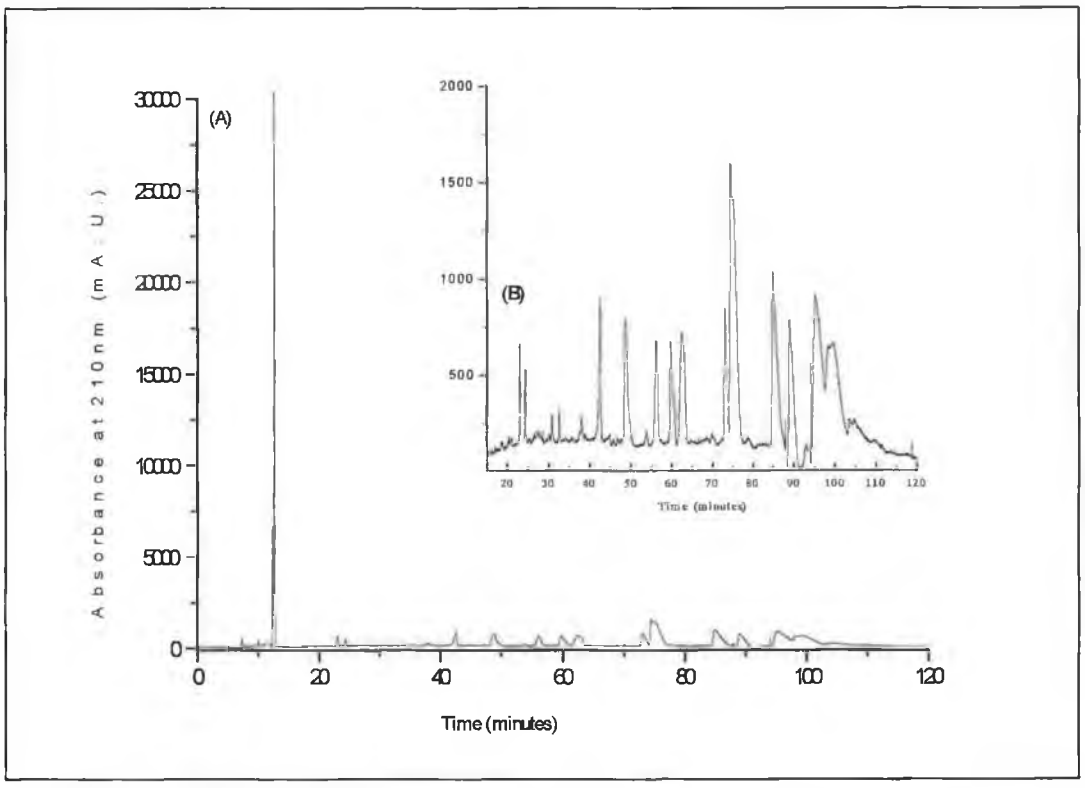

Figure 2.21. Separation of the NSG-peptoid library CHIR 4567.1. Buffer conditions were (A) 75 mM di-sodium phosphate, 50 mM sodium borate, 50 mM SDS and 40 mg/ml methyl-β-CD, pH 8.0, and inset (B) same as for (A) with y-axis scale reduced.

Hence it was demonstrated that micelles may also be used for the separation of hydrophobic molecules which are not successfully separated by CZE. This library is largely neutral at pH 8.0; therefore separation of the library is due to weak electrostatic interactions and hydrophobic interactions which affect its distribution coefficient. As this approach has resolved 17 of the required 24 components it certainly appears that by further fine-tuning of this approach that all 24 compounds will be resolved.

2.5.2. Investigation of a bile salt for the separation of CHIR 4567.1

Bile salts are often used to separate large hydrophobic molecules. For instance Nishi et al. [34] have used these naturally occurring surfactant molecules to separate corticosteriods and diltiazem related compounds with high theoretical plate numbers. Bile salts have both a hydrophilic and a hydrophobic face in the molecule and tend to combine with each other at the hydrophobic face in aqueous solutions. They can form a micelle with up to ten monomers. They have less solubilisation effect than SDS monomers and hence appear to be more beneficial for separating hydrophobic compounds.

The peptoid library CHIR 4567.1 was investigated briefly using taurocholic acid (sodium salt). This surfactant produced some rather dramatic results. Migration times of this peptoid library were reduced considerably from 120 minutes to less than 40 minutes. Selectivity was also greatly enhanced. The experiments were carried out at pH 7.4 (natural pH) and at pH 8.0, and operating conditions kept similar to what had been used previously. It was found that a run buffer of 75 mM di-sodium phosphate, 75 mM sodium borate, 100 mM taurocholic acid and 20 mg/ml methyl-β-CD, pH 7.4, gave rise to good selectivity with approximately 17-18 peaks resolved. Most of these peaks were resolved between 23 and 43 minutes (Figure 2.22(B)). The large hydrophobic band (as had been previously observed while using the CD-modified-SDS system) was again noted between 12-16 minutes.

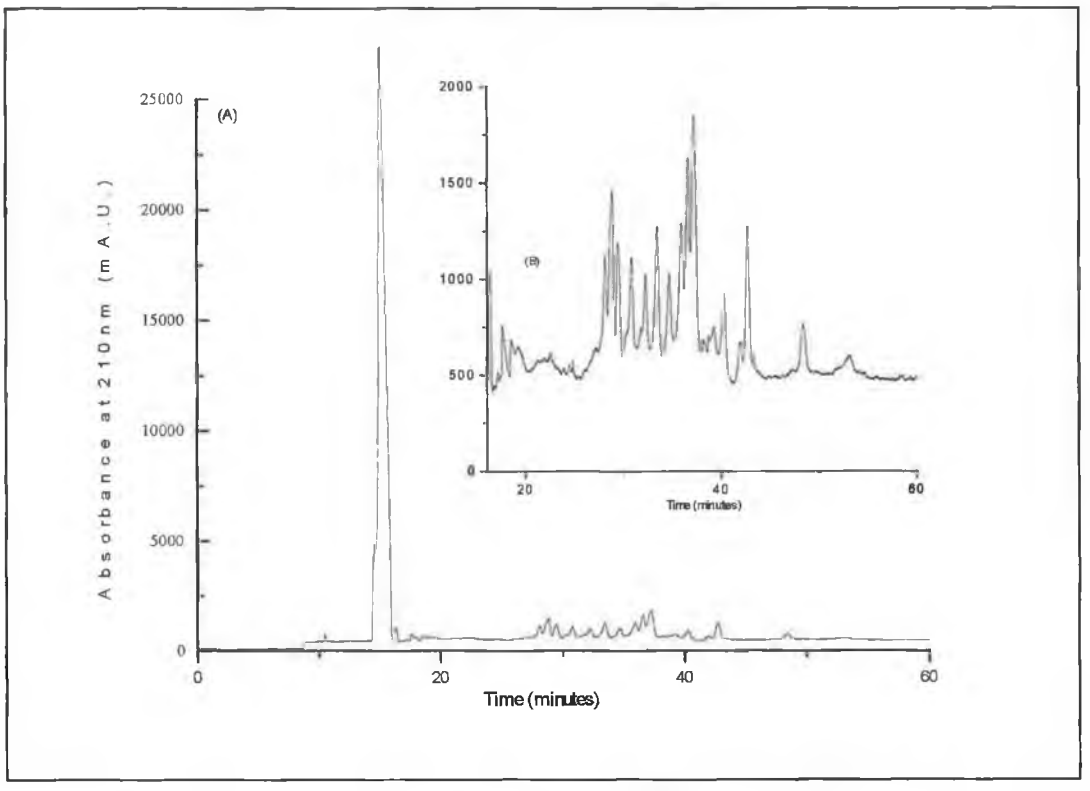

Figure 2.22. Effect of the bile salt taurocholic acid on the separation of CHIR 4567.1 Run buffer conditions were (A) 75 mM di-sodiumhydrogen-phosphate, 75 mM sodium borate buffer, pH 7.4 with 100 mM taurocholic acid (sodium salt) and 20 mg/ml methyl-β-CD, and inset (B) same conditions as (A) with reduced y-axis scale.

It is believed that the inner cavity diameter of the methyl-β-CD is sufficient to allow small NSG-peptoids and a surfactant monomer only to form host-guest interactions, the larger and more hydrophobic peptoids being excluded. This phenomena where the SDS monomer and the analyte can partition into the cavity of the CD was described by Nishi *et al.* [29]. The larger diameter offered by the γ-CD may be more suited for these CD-modified micellar-based applications to complete the separation of these libraries.

2.6. INDIVIDUAL NSG-PEPTOIDS AS MARKER COMPOUNDS

2.6.1. Overview

Marker techniques have been employed by Riekkola *et al.* [35] and Guiochon *et al.* [36] for high accuracy identification in CE. A number of individual NSG-peptoids were kindly donated by Chiron Corporation representing the very diverse nature of these peptoids analysed. It was hoped that these molecules would provide some qualitative

information, and help elucidate certain areas within an electropherogram of a given library. The molecular weight, apK_a, bpK_a and log $D_{O/PBS}$ values of those individual NSG-peptoids investigated are represented in Table 2.3. The separation conditions used for the analysis of these molecules was 75 mM di-sodium-hydrogen-phosphate, 25 mM sodium borate, 75 mM SDS and 40 mg/ml methyl-β-CD, pH 8.0.

NSG-peptoid	apK_a	bpK_a	log $D_{O/PBS}$	Molecular weight	Structure class
CHIR 5614	-	-	-2.8	257	linear
CHIR 5617	-	-	0.67	294	linear
CHIR 5920	10.1	7.6	2.3	575	linear

Table 2.3. Physical and chemical characteristics of individual NSG-peptoids.

CHIR 5614 and CHIR 5617 represent two very diverse NSG-peptoids both of which are neutral molecules, hence should be of benefit in the method development for the six combinatorial libraries studied. CHIR 5614 was a 10 mg/ml stock solution in acetonitrile and CHIR 5617 was a 5 mg/ml stock in ethanol, both of which were diluted ½ with distilled deionised water prior to analyses. The electropherograms obtained for each are illustrated in Figure 2.23 and Figure 2.24 respectively. The electropherogram of CHIR 5614 exhibits a number of peaks and it is assumed that the more dominant peak eluting at approximately 23 minutes is the active component of CHIR 5614, and the remaining unidentifiable peaks are impurity peaks due to the synthesis procedure.

CHIR 5617 is a slightly larger molecule with a molecular weight of 294, this compound however elutes at approximately 17 minutes. It is believed that a more favourable interaction with the cyclodextrin molecule occurred, hence more rapid elution.

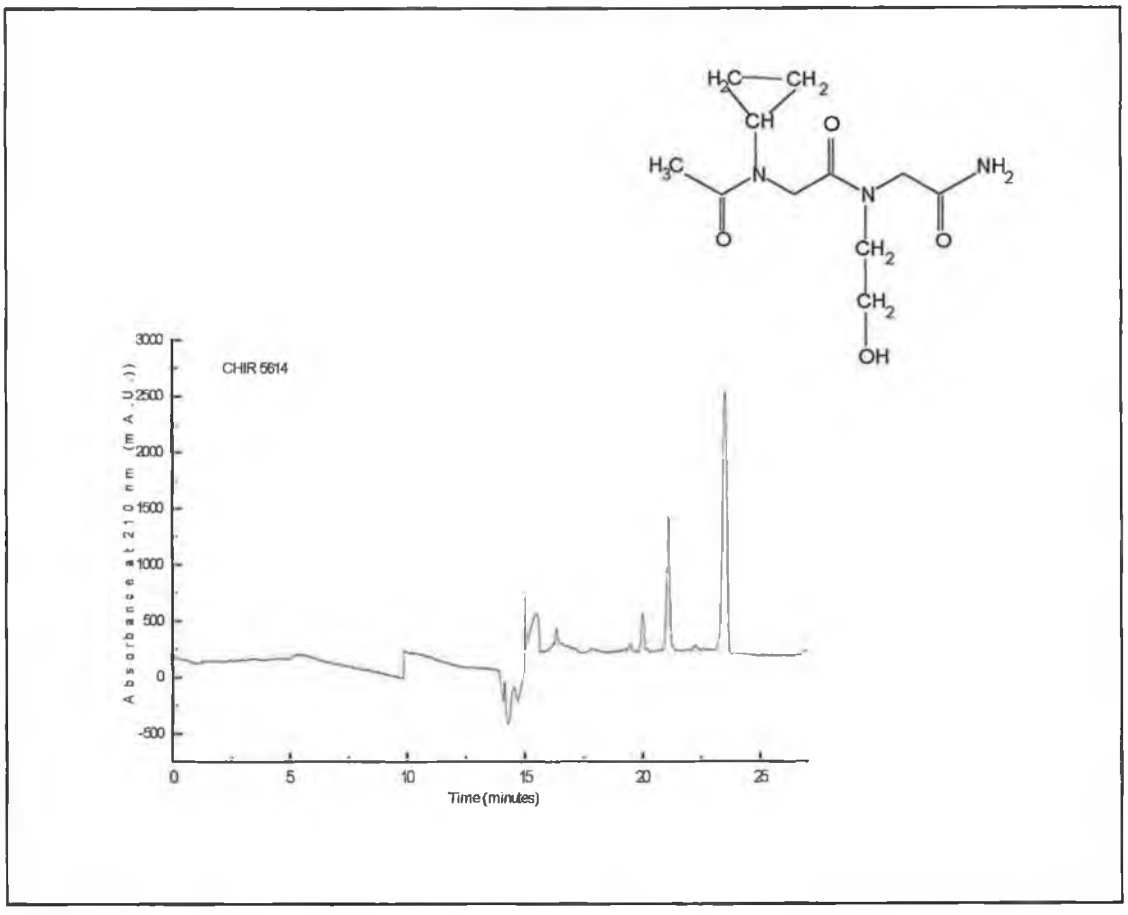

Figure 2.23. Electropherogram obtained for the individual NSG-peptoid CHIR 5614, using a run buffer of 75 mM di-sodium hydrogen-phosphate, 25 mM sodium borate, 75 mM SDS and 40 mg/ml methyl-β-CD, pH 8.0.

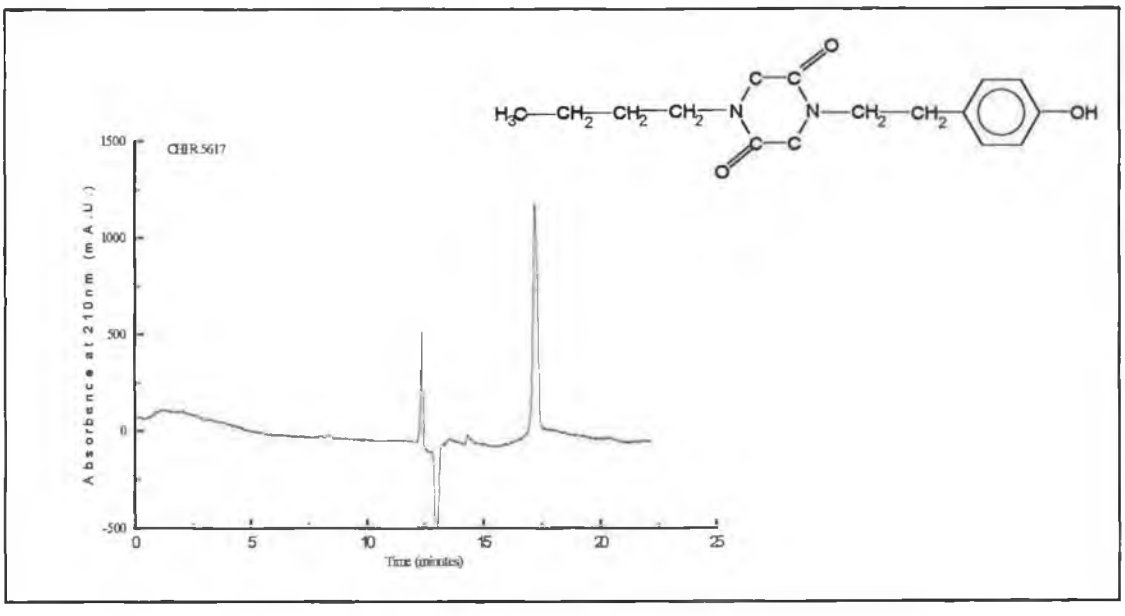

Figure 2.24. Electropherogram of the individual NSG-peptoid CHIR 5617 using separation conditions of 75 mM di-sodiumhydrogen-phosphate, 25 mM sodium borate, 75 mM SDS and 40 mg/ml methyl-β-CD, pH 8.0.

CHIR 5920 was diluted ½ with distilled deionised water from a stock solution of 5 mg/ml in ethanol. This rather large and bulky molecule with a molecular weight of 575 has a pK_b of 7.6, and hence may possess a slight negative charge at the separating conditions used. The peak detected for this compound had a migration time of approximately 47 minutes, but was very broad and the electropherogram was not typical of the peptoids studied thus far.

The increased migration time indicates no interaction with cyclodextrin. Its rather bulky side chain functionalities may have been too large for the β-cyclodextrin inner cavity, while the outer hydroxyl rim of the cyclodextrin molecule may have induced a repulsive force against the NSG-peptoid molecule. The separation conditions used were the same as those used for the separation of the library CHIR 2003.1, which indicated that separation was complete before 45 minutes. (Figure 2.19.) This molecule has a much greater molecular weight than any of the individual NSG-peptoids analysed in CHIR 2003.1 and hence may interact differently. Large hydrophobic molecules such as CHIR 5920 tend to remain in the inner hydrophobic core of the SDS micelle, and eventually co-elute with the micelle [30]. The migration time of this molecule indicates that such a process was possibly occurring (Figure 2.25).

This brief investigation of some individual NSG-peptoids will help in the CE method development for such peptoid combinatorial libraries by helping to predict migration times for other related but structurally diverse libraries, and may also be used as internal standards to correct for irreproducible migration times from run-to-run. Other structure related individual NSG-peptoids were available, but were not analysed at this time, however increased confidence in analyte behaviour can be gained with a greater number of standards.

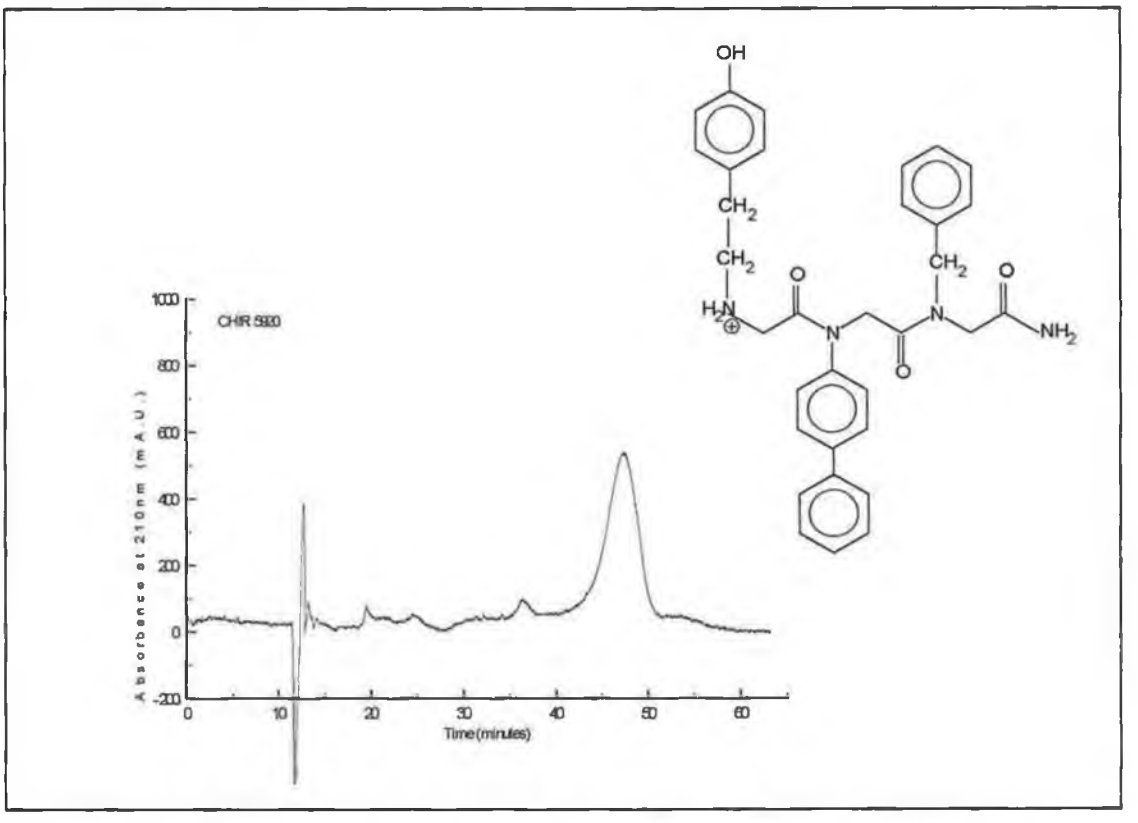

Figure 2.25. Electropherogram of the individual NSG-peptoid CHIR 5920 using separation conditions of 75 mM di-sodiumhydrogen-phosphate, 25 mM sodium borate, 75 mM SDS and 40 mg/ml methyl-β-CD, pH 8.0.

2.7. CONCLUSION

The separation power and versatility of CE makes it an ideal tool for many of the analytical challenges provided by the biopharmaceutical industries today. A particular attraction of the use of CE for analyses is the simplicity and speed with which separation conditions may be assessed. CE also has several advantages over traditional methods, both sample and reagent consumption being much less. Fused silica capillaries are used for the separation of a wide range of analytes, with the separations being effected by careful choice of buffer composition, pH, and ionic strength. Selectivity can easily be modified by the addition of one or more from a variety of different buffer additives to achieve the desired effect.

In this chapter, the applicability of CE for the separation of six NSG-peptoid combinatorial libraries has been shown. The aim of this project involved developing a CE separation method for one of these libraries and to test the ruggedness of this method by applying it to the remaining five libraries. Ruggedness may be defined by the ability to perform an analytical method effectively and in an acceptable manner each time that it is used [37]. Each library had a structurally diverse backbone with the same twenty four individual side chain functionalities attached. These side chains range from simple hydrocarbon chains to large branched and aromatic molecules. This complex combination of physical and chemical properties made the separation of these libraries by HPLC methods relatively impossible. Complex gradient elution methods have been used by Chiron Corp. but have remained problematic hence the interest to investigate CE.

Separation of the first peptoid library (CHIR 4580.1) involved using a mixed-mode buffer additive strategy. By careful manipulation of the buffer pH below the pK_a of this library complete ionisation was attained. A high ionic strength buffer was necessary to maintain separation efficiencies while the selectivity was controlled by the use of buffer additives. It was found that a combination of an ion-pairing agent (heptane sulphonic acid) and a cyclodextrin molecule were necessary to achieve separation of this largely hydrophobic library. The ion-pairing agent was elementary in

reducing the hydrophobic interactions and the cyclodextrin facilitated the formation of host-guest interactions with these individual hydrophobic NSG-peptoids. The conditions which were deemed optimum for the separation of this library consisted of 250 mM trihydrogen-phosphate, pH 2.0, 25 mM HSA and 40 mg/ml methyl-β-CD.

The second part of this project involved applying the method developed for CHIR 4580.1 to the remaining five libraries. These libraries were deliberately chosen because of their diverse physical and chemical properties and to cover as wide spectrum of diversity as possible within libraries. This method successfully separated three of the five libraries. Further fine-tuning of the existing method enhanced the selectivity of these libraries even more. The two remaining problematic libraries consisted of a dimeric-cyclic molecular backbone library and a trimeric-linear backbone library. The latter appeared to be similar to those previously investigated; however, its increased aromaticity and huge molecular weight combined to make this library more hydrophobic than previously encountered. Due to the lack of ionisable functional groups on the cyclic library it was anticipated that a micellar phase would be most effective for its separation. It was found that a CD-modified MEKC system generated greater separation of this library. Similarly the large trimeric library was most efficiently resolved using this CD-modified MEKC system.

As the separation of these two libraries are only in the preliminary stages, it is anticipated that by further fine-tuning of the system the entire resolution of these libraries may be attained. Areas to investigate further are the use of cyclodextrins with a larger inner cavity diameter and a range of micelles. Nishi *et al.* [29] reported that surfactant monomers could be incorporated into the CD cavity. This appears to be occurring in the separation of both CHIR 2003.1 and CHIR 4567.1, creating a competitive reaction with the peptoid molecules to form host-guest interactions with the CD. It is possible that the smaller peptoid molecules may be able to fit alongside with an SDS monomer inside the CD cavity; however the ability of larger molecules to form host-guest interactions with the CD is now reduced due to the interfering monomers. An alternative is to investigate the capabilities of a γ-CD (which has a larger inner cavity diameter) to separate these problematic libraries.

Bile salts have also been documented [34] to yield selectivities significantly different from the long alkyl chain surfactants, and are especially useful for the separation of very hydrophobic compounds. Bile salts have both a hydrophilic and a hydrophobic face with a relatively smaller solubilisation effect compared with SDS micelles. Taurocholic acid (sodium salt) was briefly investigated. Two major differences were observed: (i) the migration times were reduced dramatically from 120 minutes to 40 minutes, hence allowing faster analysis of several libraries; and (ii) the selectivity was also improved quite substantially. The large hydrophobic band which was noted while using the SDS-based system (elutes within 10-12 minutes) was again observed using the taurocholic acid-based system. This leads to the opinion that a larger cavity diameter cyclodextrin is required to attain separation of compounds within this region.

Finally a brief look at some individual NSG-peptoids which would be suitable as internal standards for these libraries studied, was carried out. While only three individual NSG-peptoids were analysed, the diverse physical and chemical characteristics of the compounds studied demonstrated their usefulness as markers to aid in the identification of individual peptoids within a given library. As it is anticipated that only few of the actual peptoids synthesised will contain the active ingredient required for the intended application, then markers such as these have an even greater role to play.

In effect, the separation powers of CE have been demonstrated as a powerful mechanism for the analysis of peptoid combinatorial libraries. The ease with which the selectivity can be changed has been demonstrated to obtain efficient separation of all five libraries investigated. Combinatorial synthesis yields vast numbers of molecules in very small quantities. CE is ideal for the separation and analysis of such compounds as it requires only nanoliters for a single injection, and can analyse very diverse libraries quite easily.

2.8. REFERENCES

1. Borman, S. *C& E News*, February (1996) 29-54.
2. Lam, K. S.; Salmon, S. E.; Hersh, E. M.; Hruby, V. J.; Kazmierski, W. M.; Knapp, R. J. *Nature*, **354** (1991) 82-84.
3. Geysen, H. M.; Meloen, R. H.; Barteling, S. J. *Proc. Natl. Acad. Sci. USA*, **81** (1984) 3998-4002.
4. Bunin, B. A.; Ellman, J. A. *J. Am. Chem. Soc.*, **114** (1992) 10977-10998.
5. Simon, R. J.; Kania, R. S.; Zuckermann, R. N.; Huebner, V. D.; Jewell, D. A.; Banville, S.; Ng, S.; Wang, L.; Rosenberg, S.; Marlowe, C. K.; Spellmeyer, D. C.; Tan, R.; Frankel, A. D.; Santi, D. V.; Cohen, F. E.; Bartlett., P. A.; *Proc. Natl. Acad. Sci. USA*, **89** (1992) 9367-9371.
6. Zuckermann, R. N.; Kerr, J. M.; Kent, S. B. H.; Moos, W. H. *J. Am. Chem. Soc.* **114** (1992) 10646-10647.
7. Miller, S. M.; Simon, R. J.; Ng, S.; Zuckermann, R. N.; Kerr, J. M.; Moos, W. H. *Bioorg. Med. Chem. Let.*, **4,** 22 (1994) 2657-2662.
8. Zuckermann, R. N.; Martin, E. J.; Spellmeyer, D. C.; Stauber, G. B.; Shoemaker, K. R.; Kerr, J. M.; Figliozzi. G. M.; Goff, D. A.; Siani, M. A.; Simon, R. J.; Banville, S. C.; Brown, E. G.; Wang, L.; Richter, L. S.; Moos, W. H. *J. Med. Chem.* **37** (1994) 2678-2685.
9. Moran, E. J.; Sarshar, S.; Cargill, J. F.; Shahbaz, M. M.; Lio, A.; Mjalli, A. M. M.; Armstrong, R. W. *J. Amer. Chem. Soc.* **117** (1995) 10787-10788.
10. Nicolaou, K. C.; Xiao-Yi Xiao, Parandoosh, Z.; Senyei, A.; Nova, M. P. *Angew. Chem. Int. Ed. Engl.* **34**, 20 (1995) 2289-2291.
11. Kerr, J. M.; Banville, S. C.; Zuckermann, R. N. *J. Amer. Chem. Soc.* **115** (1993) 2529-2531.
12. Olhmeyer, M. H. J.; Swanson, R. N.; Dillard, L. W.; Reader, J. C.; Still, W. C. *Proc. Natl. Acad. Sci. USA*. **90** (1993) 10700-10704.
13. Frier, S. M.; Konings, D. A. M.; Wyatt, J. R.; Ecker. D. J. *J. Med. Chem.* **38** (1995) 344-352.
14. Martin, E. J.; Blaney, J. M.; Siani, M. A.; Spellmeyer, D. C.; Wong, A. K.; Moos, W. H. *J. Med. Chem.* **38** (1995) 1431-1436.

15. Krieger, J. H. *C&EN*, February (1996) 67-73.

16. Brummel, C. L.; Vickerman, J. C.; Carr, S. A.; Hemling, M. E.; Roberts, G. D.; Johnson, W.; Weinstock, J.; Gaitanopulos, D.; Benkovic, S. J.; Winograd, N. *Anal. Chem.* **68** (1996) 237-242.

17. Dunayevskiy, Y.; Vouros, P.; Carell, T.; Wintner, E. A.; Rebek, J. *Anal. Chem.* **67** (1995) 2906-2915.

18. Taylor, E.; Braeckman, R. *in press* (1996).

19. Jorgenson, J.W. and Luckacs, K.D. *Science.* **222** (1983) 266-272.

20. Jorgenson, J.W. and Luckacs, K.D. *Anal. Chem.* **53** (1981) 1298-1302

21. Kornfelt, T.; Vinther, A.; Okafo, G. N.; Camilleri, P. *J. Chromatogr. A.* **726** (1996) 223-228.

22. McLaughlin, G. M.; Nolan, J. A.; Lindhal, J. L.; Palmieri, R. H.; Anderson, K. W.; Morris, S. C.; Morrison, J. A.; Bronzert, T. J. *J. Liq. Chrom.* **15** (1992) 961-1021.

23. Schützner, W., Fanilli, S., Rizzi, A., and Kenadler, E., *J. Chromatogr. A.* **719** (1996) 411-420.

24. Tsuda, T.; Nomura, K.; Nakagawa, G. *J. Chromatogr.* **248** (1982) 241-247.

25. Sepaniak, M.J., Cole, R.O., and Clark, B.K. *J. Liq. Chrom.* **15** (1992) 1023-1040.

26. Strattan, C. E. *Biopharm.* **4**, (1991) 44-51.

27. Peterson, T.E., *J. Chromaogr.* **630** (1993) 353-361.

28. Brown, R. S., Luong, J. H. T., Szolar, O. H. J., Halasz, A., and Hawari, J. *Anal. Chem.* **68** (1996) 287-292.

29. Nishi, H.; Fukuyama, T.; Terabe, S. *J. Chromtogr.* **553** (1991) 503-516.

30. Terabe, S.; Otsuka, K.; Ichikawa, K.; Tsuchiya A.; Ando, T. *Anal. Chem.* **56** (1984) 111-113.

31. Janini, G. M.; Issaq, H. J.; *J. Liq. Chrom.* **15** (1992) 927-960.

32. Oda, R. P.; Madden, B. J.; Morris, J. C.; Spelsberg, T. C.; Landers, J. P. *J. Chromatogr. A.* **680** (1994) 341-351.

33. Terabe, S.; Miyashita, Y.; Shibata, O.; Barnhart, E. R.; Alexander, L. R.; Patterson, D. G.; Karger, B. L.; Hosoya, K.; Tanaka, N. *J. Chromatogr.* **516** (1990) 23-31.

34. Nishi, H.; Fukuyama, T.; Matsuo, M.; Terabe. S. *J. Chromatogr.* **513** (1990) 279-295.

35. Riekkola, M-L.; Jumppanen, J. H. *Anal. Chem.* **67** (1995) 1060-1066.

36. Dose, E. V.; Guiochon, G. A. *Anal. Chem.* **63** (1991) 1154-1158.

37. Jenke, D. R. *J. Liq. Chrom. And Res. Technol.* **19**, (12) (1996) 1873-1891.

CHAPTER 3

A STUDY OF THE MELANISATION PATHWAY OF L-DOPA USING CAPILLARY ELECTROPHORESIS WITH DIODE ARRAY DETECTION AND AN INVESTIGATION OF SOME PROPERTIES OF THE MELANIN POLYMER FORMED BY ELECTROCHEMICAL TECHNIQUES

3.1. INTRODUCTION

Extensive research has been carried out throughout this century by various research groups to elucidate the structure of melanin and the melanogenesis pathway [1-3]. The structure of melanin remains uncertain, containing a mixture of 5,6-dihydroxyindole units of different oxidation levels, and to a lesser extent of pyrrole units, linked randomly by carbon-carbon bonds. This polymer, or mixture of polymers, precipitates as a black amorphous, highly hygroscopic powder, the elemental composition of which varies [3].

The impetus for studies of melanins has come mainly from clinical and biomedical interest. Biosynthesis of melanins occurs in humans and other mammals as well as fruits and plants. The familiar darkening of our skin on exposure to sunlight, or blackening of various fruits, including mushrooms, bananas, apples etc., on exposure to air is a result of enzymatic oxidation. The enzyme responsible for these processes is known as tyrosinase and its properties are discussed in greater detail in Chapter 5. Tyrosinase is capable of catalysing the direct aerobic oxidation of monophenols, the most frequently studied being the amino acid, tyrosine. This type of activity is known as cresolase or monophenolase activity. This enzyme is also responsible for the second step in this reaction, commonly regarded as catecholase or diphenolase activity, where the product of the first reaction, L-dopa, is oxidised to form dopaquinone, followed by a series of complex chemical reactions which occur almost instantaneously to produce dopachrome. This particular compound signals the formation of a polymeric compound called melanin [4] (Figure 3.1).

The significance of the melanogenesis pathway stems not only from the cosmetic and social aspects, but also from the intrinsic importance of related biological phenomena at a cellular level, i.e. to processes which lead to the formation of malignant melanoma. In this chapter, CE was used to probe the biosynthesis of melanin towards a better understanding of this process.

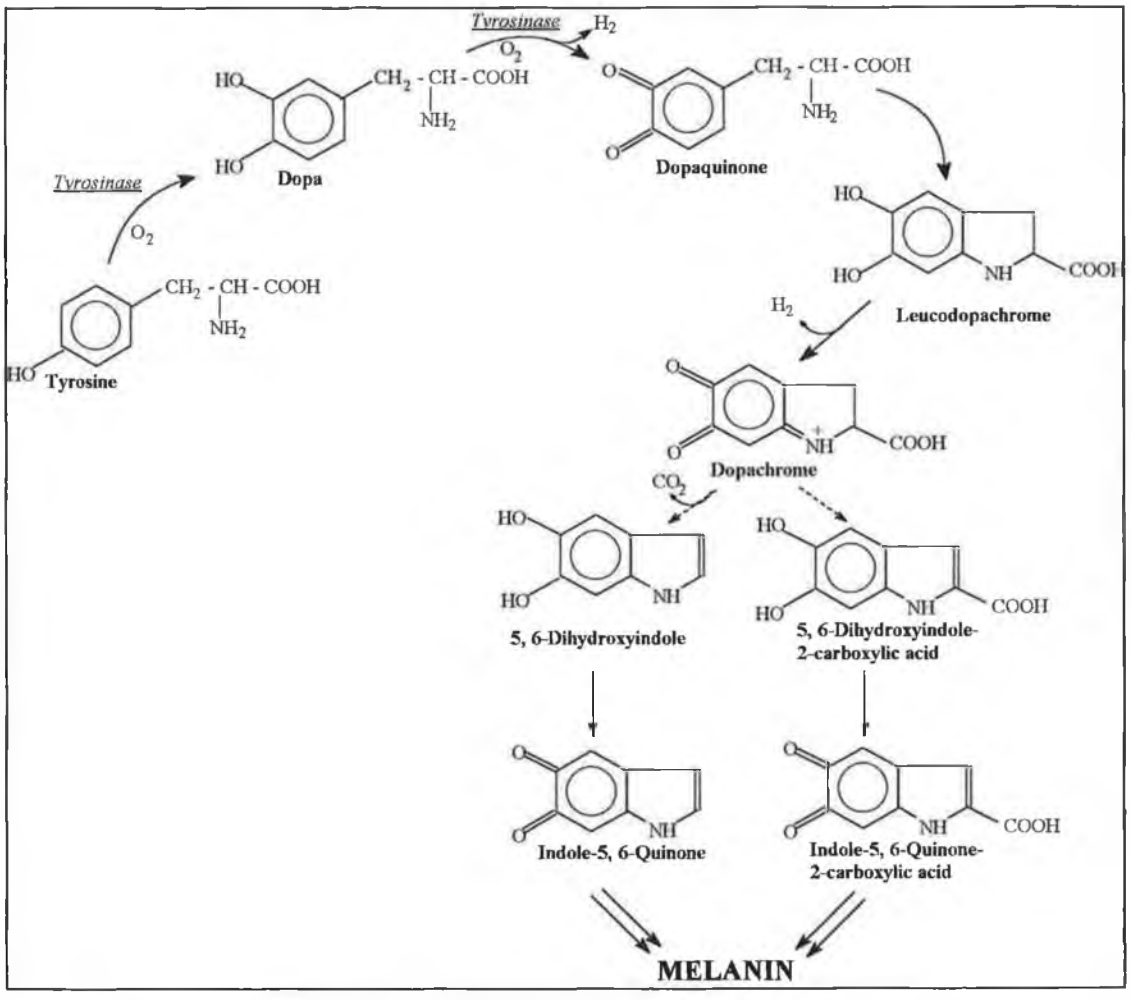

Figure 3.1. Schematic pathway of the melanogenesis pathway as it is currently envisioned.

Raper and Mason [1,2] both proposed the production of dihydroxyindole (DHI) and dihydroxyindole carboxylic acid (DHICA) following dopachrome formation. Recently Avoca *et al.* [5], presented a new procedure to prepare dopachrome using sodium periodate. This method offers a fast, easy and quantitative way to produce dopachrome, which involved following the increase in absorbance at 308 nm (instead of the commonly accepted 475 nm), proceeded by the formation of DHI and DHICA. The use of both tyrosinase and sodium periodate were investigated as catalysts towards the oxidation of L-dopa.

Both HPLC with fluorimetric detection [6] and GC-MS [7] have been used to identify the structures of some of the metabolites; however these methods require time-consuming extraction procedures, and derivatisation using expensive labels, all of which have proven to be unsuitable for the analysis of these highly unstable

compounds. In this study Diode Array Detection (DAD) was used as an alternative detection scheme, to facilitate the rapid monitoring of this reaction, while short capillaries were used to maintain greater control over the reaction process.

In addition, some electrochemical studies have been carried out to assess the potential of the melanin biopolymer for use as a chemical sensor or biosensor. Electrochemical polymerisation of various monomers has been studied quite extensively by Lowe *et al.* [8] and Bartlett *et al.* [9]. This method allows precise control over the thickness of the polymer film formed, and deposition can be followed by monitoring the charge passed. This minimises the batch to batch variation commonly encountered with other sensor designs. Electrochemical deposition of this melanin polymer onto an electrode surface can also be used to entrap enzyme molecules, such as glucose oxidase, and hence its potential as an enzyme-based sensor can be envisaged.

3.2. EXPERIMENTAL

3.2.1. Chemicals

The following reagents were obtained from Sigma Chemical Co. (St. Louis, MO, USA): tyrosinase (polyphenol oxidase E.C. 1.14.18.1, Activity: 4,400 Units/mg solid) from Agaricus bisporus, L-tyrosine; [L-3 (4-hydroxyphenylalanine], L-dopa; [L-3,4, dihydroxyphenylalanine], Topa, [2,4,5-trihydroxyphenylalanine], L(+)-lactic acid (2-hydroxypropionic acid) and di-sodium tetraborate decahydrate. Uracil, sodium periodate, citric acid dihydrate (Analar grade) sodium-dihydrogen phosphate and disodium-hydrogenphosphate (Analar grade) were obtained from BDH Chemicals Ltd. (UK). Reagents used in the electrochemical experiments include acetonitrile, obtained from Labscan (Stillorgan Industrial Estate, Dublin), perchloric acid (70%) from Riedel de Häen (AG D-3016, Seelze, Germany) and lithium perchlorate from Aldrich Chemical Company (Dorset, England, UK).

3.2.2. Capillary Electrophoresis system

The capillary electrophoresis apparatus consisted of a Beckman P/ACE system 5000 (Beckman Instruments, Irl.), which contained the basic elements as discussed in Chapter 1: and in addition a temperature regulated capillary column, an automated sample injection system, and a diode array absorbance detection system. The unmodified fused silica capillary (20 cm × 50 μm) was located within a temperature-regulated cartridge (between 15-50 °C). Temperature regulation was achieved by constant re-circulation of a thermostatted heat transfer fluid through the capillary cartridge. This effective means of controlling the temperature is essential for run-run reproducibility of migrating ions. A variation of 1 °C causes a change of 2% in electrophoretic mobility [10]. A high-voltage power supply capable of delivering up to 250 μA at potentials ranging from 1-30 kV, was connected to the separation channel by means of platinum electrodes. The polarity of these electrodes was easily reversed, hence enabling both negative and positive modes of CE separation. Either UV or a diode array detection system completed the assembly. The latter system assists in rapid peak assignment. Data was captured and analysed using Beckman's System Gold software (Version 8.1), interfaced with an Elonex PC-466 computer.

3.2.3. Spectroelectrochemical instrumentation

Electrochemical measurements were performed using an EG & G Princeton Applied Research, Model 362 scanning potentiostat. This was connected to a UV-Vis-NIR recording spectrophotometer (Shimadzu Scientific Instruments Inc., Model UV-3100) and interfaced with an Elonex PC-466/1. The spectroelectrochemical software used with this instrument was UVPC Version 3.5, personal spectroscopy software by Shimadzu Scientific Instruments Inc. The electrochemical cell consisted of a three-electrode thin-layer design, which was placed in the sample cavity of the spectrometer, to record the absorption spectra of the electrogenerated species. A requirement of this particular design is a suitable optically transparent working electrode, that enables the light beam to pass directly through the electrode and the adjacent electrolyte solution. The type of transparent electrode used in this particular assay consisted of a platinum

gauze, where the transparency is due to the physical holes in the minigrid structure. An inert platinum counter electrode and an anodised silver wire (in KCl) as reference completed the assembly.

3.2.4. Electrochemical apparatus

A glassy carbon electrode (0.0707 cm^2), obtained from Bioanalytical Systems (BAS, West Lafayette, IN, USA), was used throughout all electrochemical experiments. Electrode preparation involved successive polishing of the electrode with finer grades of an alumina slurry of 1.0, 0.3 and 0.05 μm from Buehler, Micropolish (Lakebluff, IL, USA). The final polishing step, involving the 0.05 μm alumina particle diameter slurry, was repeated before each scan. An Ag/AgCl reference electrode and a platinum wire completed the assembly. A BAS 100-W Electrochemical Analyser, (BAS Instruments Inc., West Lafayette, IN, USA) was used for all electrochemical experiments, interfaced with BAS software, Version 1.0. The electrochemical cell was flushed with argon for 15 minutes, prior to each electrochemical experiment and protected by an argon blanket throughout each experiment.

3.2.5. Buffer preparation

A 0.1 M stock solutions of borate buffer, pH 9.05, was prepared by dissolving the required amount of di-sodium tetraborate decahydrate in distilled deionised water and made up to 250 ml. Phosphate buffer (P.B.) was prepared by adding a stock solution (usually 0.1 M each) of potassium di-hydrogen phosphate to di-potassium hydrogen phosphate until the desired pH was reached. Standards of L-tyrosine and L-dopa were prepared in 0.05 M borate/0 025 M phosphate, pH 7.4 unless otherwise stated. All buffer and standard solutions were filtered before use with 0.45 μm Whatman filter paper. Stock tyrosinase solutions of 2200 Units/mg solid were prepared in P.B., pH 7.4.

3.3. Results and Discussion

3.3.1. Optimisation of the separation conditions for L-tyrosine and L-dopa

A wide variety of buffers can be employed for CE separations. These buffers are most effective within one or two units of their pK_a e.g. phosphate is used around pH 2.5 and 7, while borate is used around pH 9.0. Typical buffer concentrations range from 0.025-0.1 M. The pK_a's of L-tyrosine are 2.30, 9.28 and 10.28 [11] and for L-dopa are; 2.31, 8.71, 9.74 and 13.4 [12]; hence buffers used for their efficient separation should carefully consider their pK_a values. Both L-tyrosine and L-dopa are neutral species at physiological pH (i.e. pH 7.4), hence their effective mobilities are too close for them to be efficiently separated at this pH. This was evidenced by the migration times obtained for each; 0.98 minutes and 0.99 minutes for L-tyrosine and L-dopa respectively, when a run buffer of 0.025 M P.B. pH 7.4 was used. Using a run buffer of 0.025 M borate, pH 9.0 both compounds should have a slight negative charge. L-tyrosine elutes first, being slightly less negative than L-dopa at this pH. As expected the migration times increased due to the increased electrophoretic mobility towards the anode. However, Raper [1] described that the tyrosinase enzyme (which oxidises L-tyrosine to L-dopa), is most active between pH 6 and 8, and that outside these limits the activity is small, ceasing finally at pH 5 and 10. Hence, using the borate buffer at pH 9.0, would be inefficient to follow the progress of the reaction in an attempt to understand the complex melanisation pathway involving tyrosinase.

3.3.2. Sample stacking

Sample stacking is a method often used in CE to improve the LOD and peak efficiencies, This phenomenon occurs due to matrix differences between the plug of injected sample and the surrounding buffer which makes ions of the sample accelerate towards the adjacent buffer zone when a separation voltage is applied. As these fast moving ions leave the sample zone and enter into the buffer zone, a small local electric field is produced. This reduces the velocity of the ions, and hence a compression of these ions into the buffer zone results. Matrix differences that can generate a different

electric field required for implementation of sample stacking can be a change in the solution pH and or a change in the concentration of the buffer ions in the separation buffer relative to the sample buffer.

3.3.2.1. Buffer concentration differences to mediate stacking effects

This idea has largely been utilised by Chien *et al.* [13,14] and involves injection of a long sample plug contained in a low-concentration buffer into a buffer filled capillary of higher concentration but of the same composition. Electrophoretic separations are then induced by the application of an electric field. Because the low-concentration sample buffer has a higher resistivity than the run buffer, the electric field strength within the sample plug will be higher than the rest of the capillary. As a result the ions of the sample zone will migrate faster towards the sample/run buffer boundary. Once the sample ions reach this concentration boundary, they immediately start to slow down, causing a narrowing of the sample ion zone in the run buffer region. This stacking mechanism occurs for both positive and negative ions and is illustrated in Figure 3.2. The degree of stacking is determined by the differences in resistivities of the two buffers.

3.3.2.2. pH mediated stacking

A second approach to sample enrichment is based on differences in pH of the sample zone relative to the run buffer and has been described by Aebersold *et al.* [15]. An overall negative charge is induced on the sample ions by choosing a buffer pH 1-2 units above the pK_a of the sample ions (or positively charged by choosing a buffer pH 1-2 units below the pK_a of the ions). These anions will migrate in the direction of the anode, when an electric field is applied, until they are intercepted by the run buffer, where they are slowed down. If this buffer is of lower pH than the sample zone buffer, the negatively charged sample ions will eventually become positively charged and migrate towards the cathode as a sharp zone.

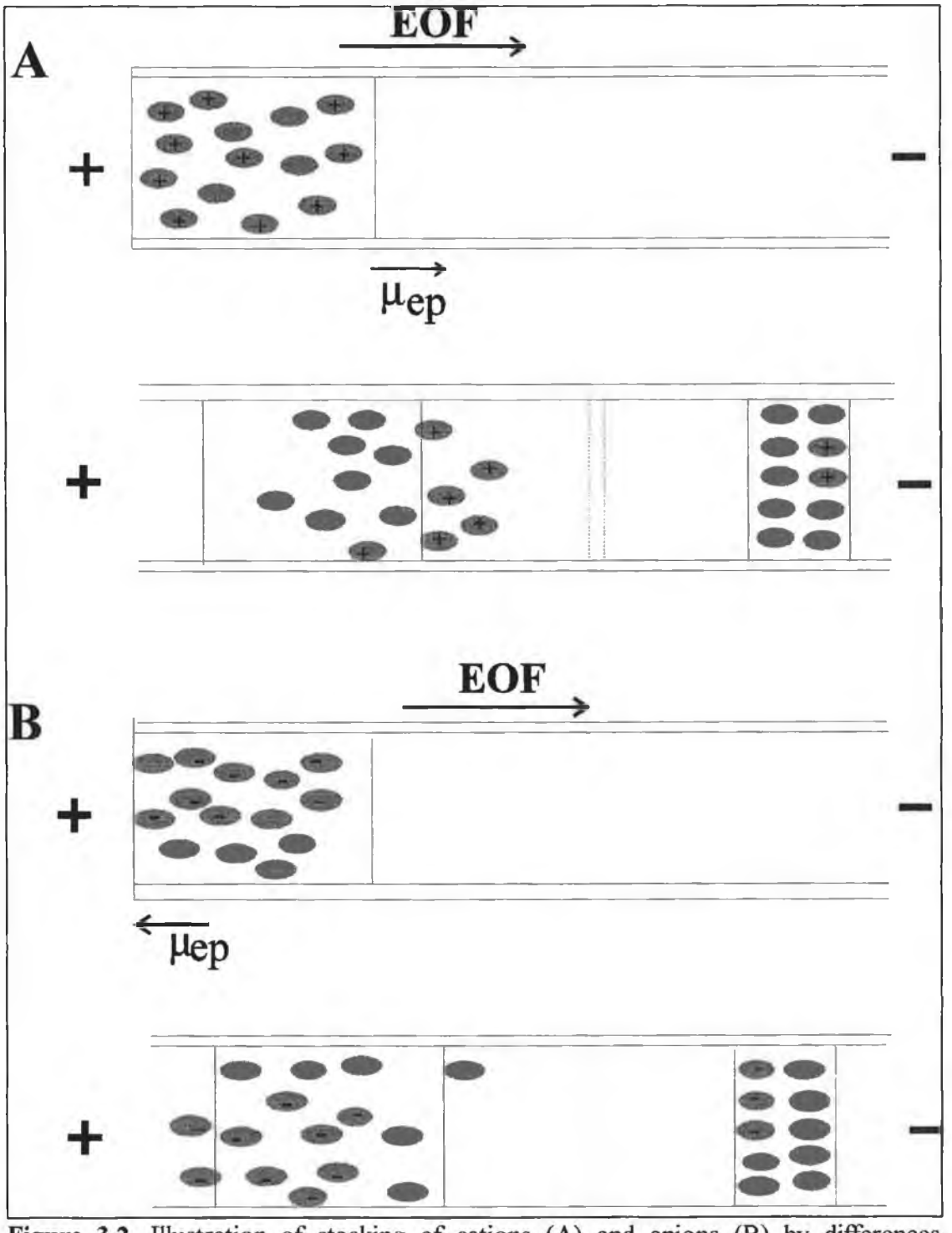

Figure 3.2. Illustration of stacking of cations (A) and anions (B) by differences between the ionic strength of the sample buffer and the run buffer [16].

By preparing the standards of L-tyrosine and L-dopa in phosphate buffer pH 7.4 and separating them using borate buffer, it was found that considerable band broadening and considerable fronting resulted with increased migration times of 1.36 and 1.96 for L-tyrosine and L-dopa respectively (Figure 3.3(A)). Upon injection, the neutral ions will electrophoretically migrate together towards the cathode; however when they

encounter the negatively charged buffer zone, they will gradually become negatively charged and the direction of their mobility will be reversed, dragging them back towards the anode. However the EOF is overwhelming at this pH (i.e. pH 9) that everything is driven towards the cathode. The negatively charged silanol groups on the capillary wall also have an attraction for positively charged ions and may also contribute to this band broadening observed. McCormick [17] has also described that phosphate groups can bind to the capillary wall, further decreasing the activity of the silanol groups and decreasing the electrophoretic mobilities of these compounds.

The effect of varying the composition of phosphate and borate, while maintaining a neutral pH of 7.4 as the sample medium which contained the two standards was then investigated (Figure 3.3(B,C)and in Table 3.1). Increasing the borate concentrations as run buffer produced excessive Joule heating (150 μA) within the capillary, and this was not continued. The separation conditions which maintained low current values, with rapid separation efficiency of the two standards of L-tyrosine and L-dopa was 0.025 M borate, pH 9.0, as the run buffer while the standards were prepared in 0.05 M borate/0.025 M phosphate, pH 7.4. The high concentrations of borate in the sample buffer may reduce ionic interactions with the silica wall and also reduce the electrophoretic mobility differences experienced previously. This pH-effect of stacking is observed in Figure 3.3C. The effect of the various buffer compositions on the migration behaviour of the two standards are illustrated in Table 3.1.

The capillary was rinsed with 0.1 M NaOH for 2 minutes, followed by a 3-4 minute rinse with the run buffer, prior to each injection. It was found that more reproducible migration times were obtained when the capillary was rinsed as described while using separate buffer vials to rinse the capillary and to perform CE separations improved this consistency. Samples were injected by pressure for 5 seconds using the automated Beckmann P/ACE 5000 system.

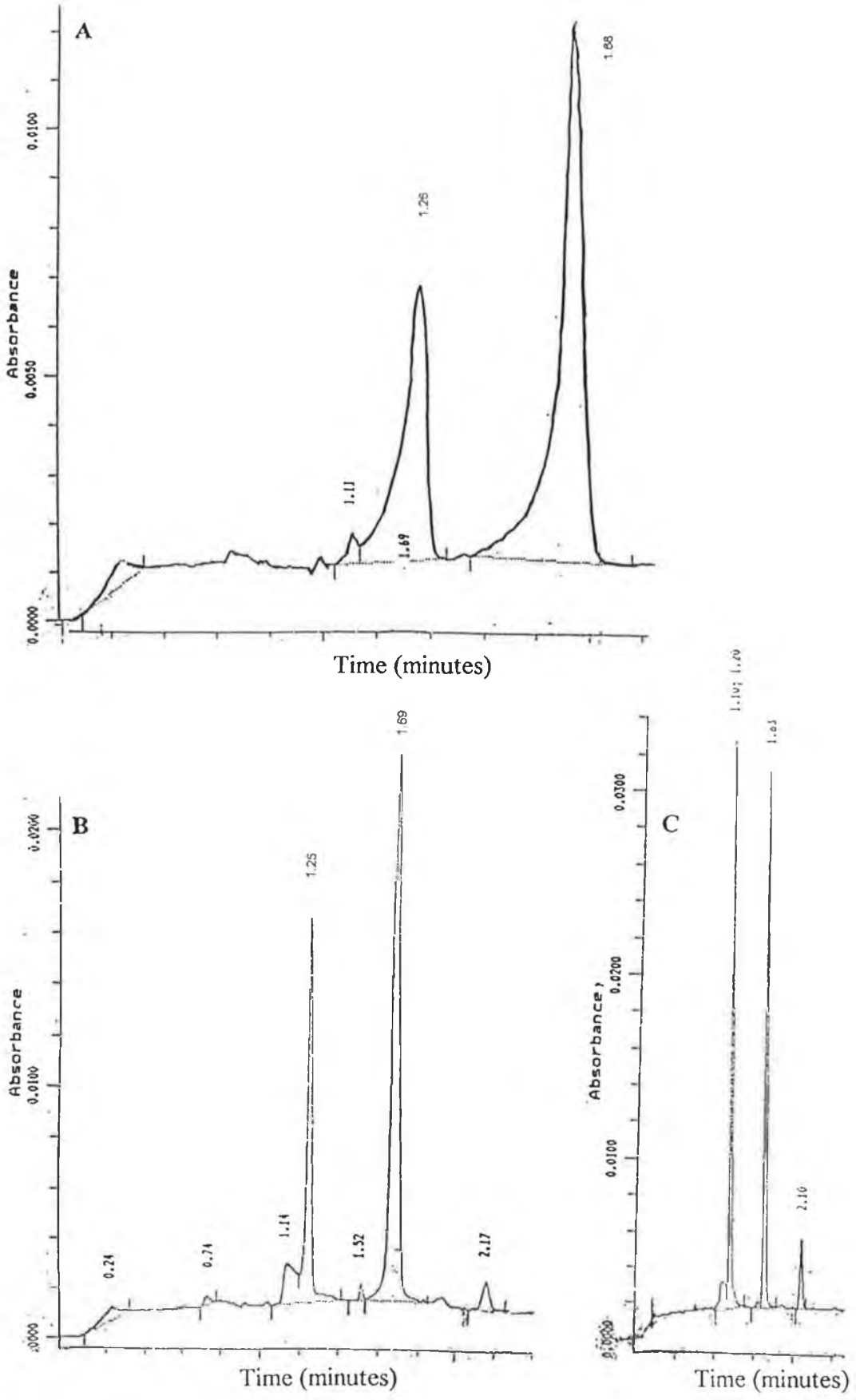

Figure 3.3. Effect of buffer composition and pH on the separation of L-tyrosine and L-dopa using a run buffer of 0.025 M borate buffer, pH 9, and a sample preparation buffer of 0.025 M phosphate, pH 7.4; (A), using both a run buffer and sample preparation buffer of 50:50 0.05 M borate/ 0.05 M phosphate, pH 7.4; (B), and a run buffer of 0.025 M borate and a sample preparation buffer of 0.05 M borate/ 0.025 M phosphate, pH 7.0; (C).

Run Buffer	Sample preparation buffer	Migration Time /min	
		L-tyrosine	*L-dopa*
0.025 M phosphate, pH 7.4	0.025 M phosphate, pH 7.4	0.98	0.99
0.025 M borate, pH 9.0	0.025 M borate, pH 9.0	1.26	1.68
0.025 M borate, pH 9.0	0.025 M phosphate, pH 7.4	1.4	1.94
0.05 M borate, pH 9.0	0.025 M borate/ 0.025 M phosphate, pH 7.4	1.59	2.48
0.05 M borate/0.05 M phosphate, pH 7.4	0.05 M borate/ 0.05 M phosphate, pH 7.4	1.25	1.69
0.025 M borate, pH 9.0	0.05 M borate/ 0.025 M phosphate, pH 7.4	1.10	1.43

Table 3.1. Migration times observed using various phosphate and borate buffer compositions for the separation of L-tyrosine and L-dopa, using a 50 μm × 20 cm capillary. Separation voltage was 20 kV, with a 3 second pressure injection of sample.

3.3.3. Tyrosinase oxidation of L-tyrosine

The run buffer consisting of 0.025 M borate, pH 9.0, while the standards were prepared in 0.05 M borate/0.025 M phosphate, pH 7.4. as just described, were used as optimum for the oxidation of L-tyrosine by tyrosinase. It is generally accepted that the first product of L-tyrosine oxidation by tyrosinase is L-dopa. This is followed by the production of dopaquinone, and because of its instability, this compound is rapidly converted to leucodopachrome and finally to dopachrome. This final product exhibits a red colour in solution and is relatively stable. The intermediate compounds because of their instability have not been detected and isolated during enzyme-mediated oxidation of L-tyrosine. Recently, an HPLC-EC detection system was described [17] for the separation and detection of these intermediates. This method was rather complicated, which involved oxidation by tyrosinase followed by reduction using ascorbate and sodium borohydride. Herein, an alternative method using CE with UV and diode array detection (DAD) is described which follows the direct oxidation of L-tyrosine and is capable of detecting all species produced in a single analysis instantaneously.

L-tyrosine, prepared in 0.05 M borate/ 0.025 M phosphate buffer, pH 7.4, was subjected to enzymatic oxidation by the addition of mushroom tyrosinase in the reaction vial (capillary inserts). Samples from this oxidation process were then injected directly onto the buffer filled capillary without any pre-treatment procedures i.e. filtration or centrifugation, and analysed immediately. As only nanolitres of sample were injected per analysis, no change was expected to occur in the amounts of intermediate and final products produced. The reaction progress was monitored by UV detection at 280 nm, with repeated injections from the sample vial at t = 0, 1, 5 and 10 minute intervals afterwards. The concentration of tyrosinase used was critical for sufficient oxidation of L-tyrosine. When a tyrosinase concentration of 22 units/mg solid was used, the oxidation of L-tyrosine was rather slow and L-dopa production was not observed following a period of incubation of one hour (Figure 3.4(A)). Eventually, L-dopa production was noticed after almost 2 hours and two further peaks with migration times of 1.71 and 1.95 minutes were also observed (possibly dopaquinone and dopachrome), but remained in relatively small quantities, see Figure 3.4(B). Li and Christensen [18], in their HPLC-EC study, could not detect any of the

intermediate compounds other than dopachrome when they followed the enzymatic oxidation of L-tyrosine.

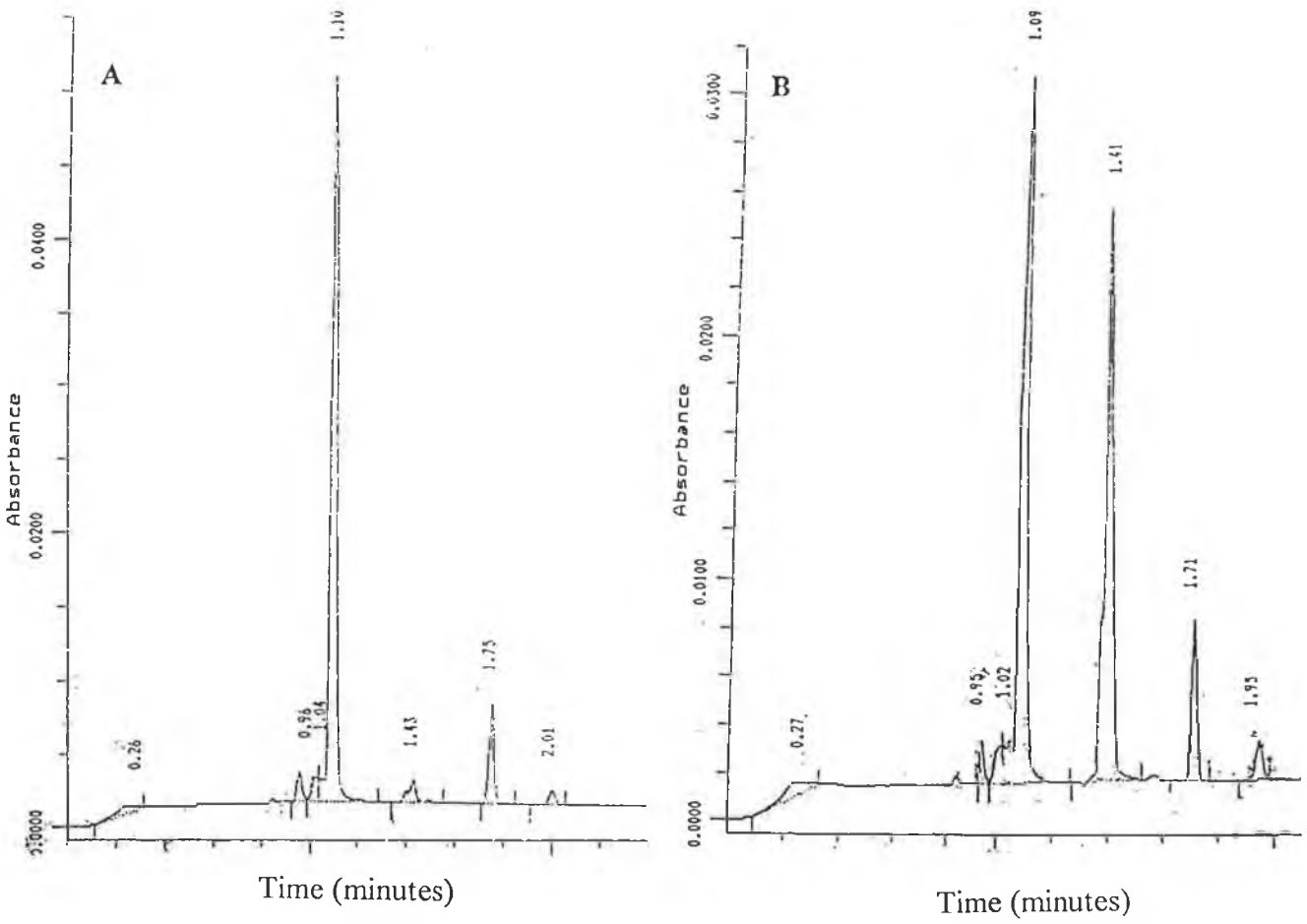

Figure 3.4. The oxidation of 2 mM L-tyrosine using mushroom tyrosinase (22 units/mg solid). Detection of product formation at t = 60 minutes (A), and 150 minutes (B) using 0.025 M disodium tetraborate decahydrate, pH 9.0, as run buffer.

When the activity of tyrosinase was doubled (44 units/mg solid), the reaction advanced more rapidly, with an L-dopa peak being observed as early as 5 minutes (Figure 3.5(A)), after tyrosinase addition. The production of L-dopa progressed steadily with a gradual decrease in the concentration of L-tyrosine and further production of intermediate compounds at approximately 1.6 and 1.8 minutes. The peak with a migration time around 1.6 minutes decreased slightly with further incubation containing tyrosinase, while that around 1.8 was not detected following a two hour incubation period with tyrosinase. (Figure 3.5). As these compounds elute after L-tyrosine and L-dopa, one can assume that these intermediate compounds are even

more negative than the two standard compounds. No further peaks were observed following incubation at 25 °C for three hours and it was believed that complete oxidation of L-tyrosine was not occurring, possibly due to the auto-degradation of tyrosinase. Increased concentrations of tyrosinase did not enhance the progress of the melanisation process; rather it inhibited the detection sensitivity due to the turbidity of the reaction vial and it appeared that the increased concentration of tyrosinase was adhering to the capillary wall. Various concentrations of L-tyrosine were also investigated: it was found that a 1 mM standard solution gave the highest yield of L-dopa with greater amounts of the two later eluting peaks being produced also.

Control experiments, which involved the incubation of L-tyrosine prepared in 0.05 M borate/ 0.025 M phosphate buffer, pH 7.4 at 25 and 37 °C were also carried out. The L-tyrosine standard remained stable even after 15 hours at these elevated temperatures. A control experiment on L-dopa prepared in the same buffered solution demonstrated reduced stability, however, and after 30 minutes at 37 °C in this buffered solution, small amount of auto-oxidation products with migration times of 1.52 and 1.68 minutes respectively were formed. This is consistent with that observed by Lerner *et al.* [18], who reported that L-dopa is readily oxidised at pH above 7 even in the absence of enzyme. While the peak height of L-dopa never decreased substantially and the peak heights of these products formed remained rather small, the lack of stability of L-dopa in borate/phosphate buffer, pH 7.4 was worrying. Low pH buffers such as citrate buffers at pH 4.0 and a phosphate/citrate buffer, pH 6.0, offered improved stability of L-dopa even after 16 hours, as is illustrated in Figure 3.6.

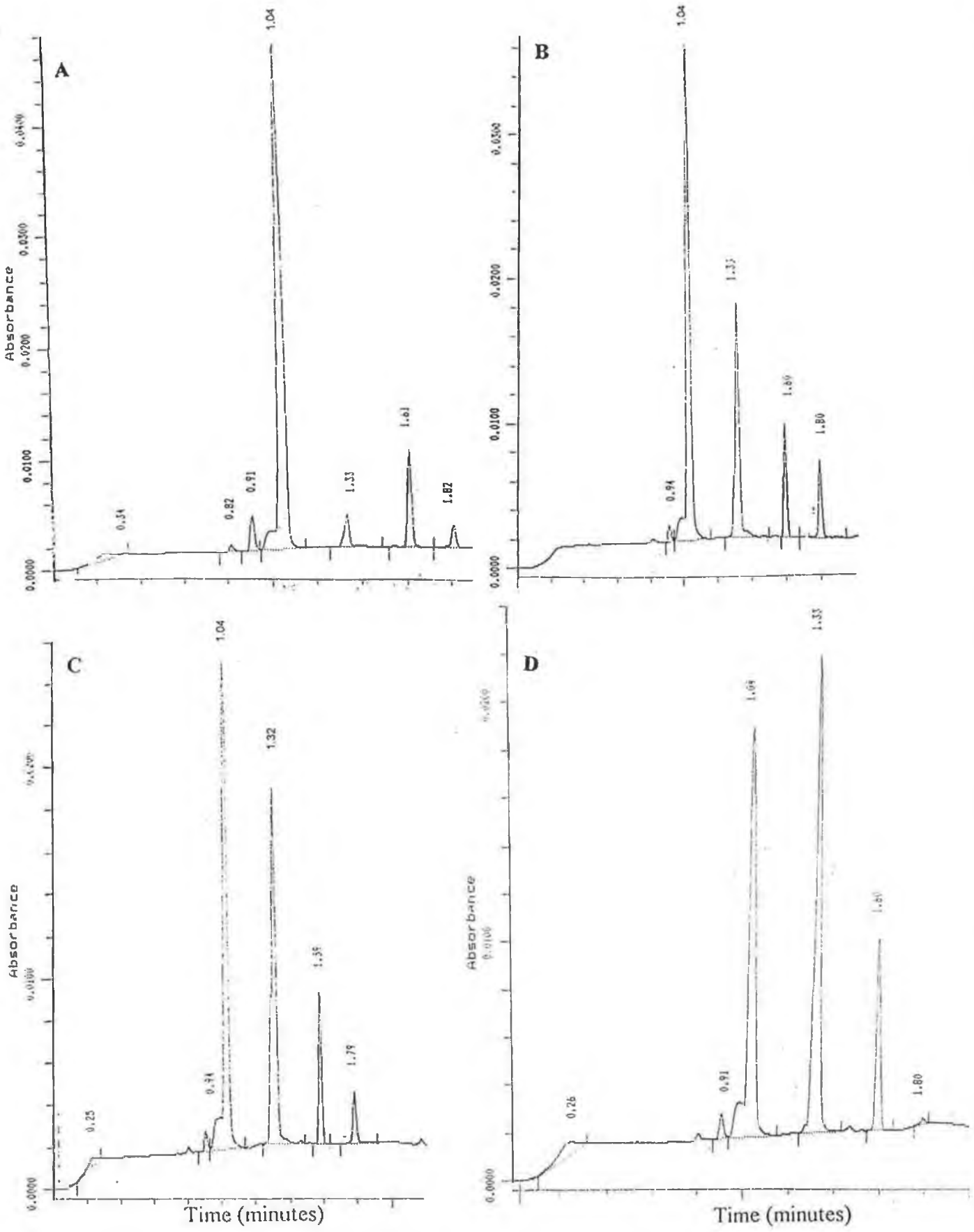

Figure 3.5. Oxidation of L-tyrosine using mushroom tyrosinase (44 Units/mg solid) with detection of product formation after t = 5 (A), 30 (B), 60 (C) and 150 (D) minutes respectively.

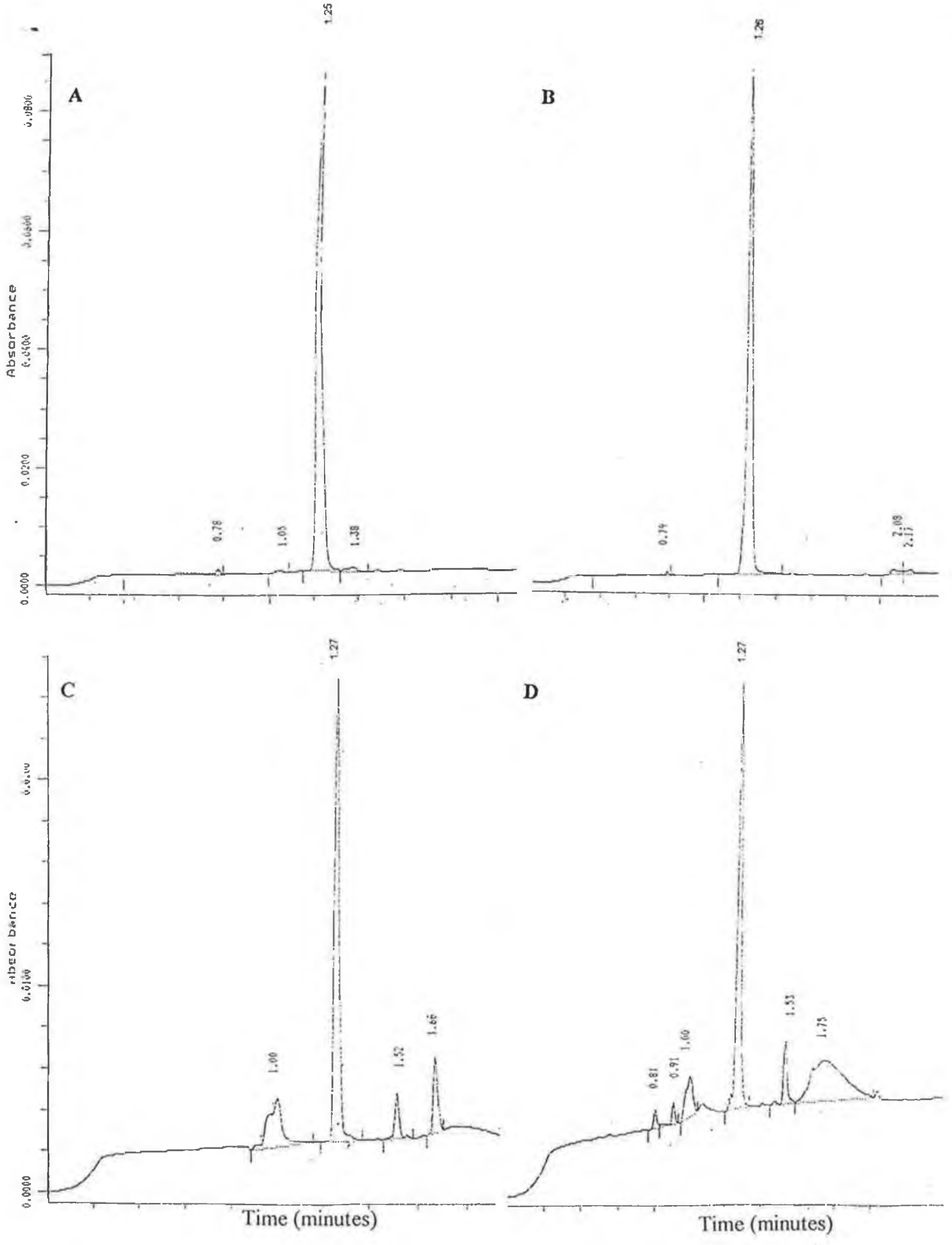

Figure 3.6. Control experiments carried out on a L-dopa standard using 0.01 M citric acid/ 0.02 M disodium hydrogenphosphate, pH 4.0, after incubation at 37 °C for 30 minutes (A) and 16 hours (B) and using 0.05 M disodium boratedecahydrate/ 0.025 M P.B., pH 7.4 for 30 minutes (C) and 16 hours (D).

3.3.4. Oxidation by sodium periodate

Aroca *et al.* [5] demonstrated that dopachrome can be chemically prepared 'in-situ' by L-dopa oxidation involving sodium periodate. The oxidation of L-dopa by periodate is rapid and quantitative, leaving no L-dopa unreacted in solution. Initial studies involved the oxidation of L-tyrosine with a 2.5 mM solution of sodium periodate; the reaction vial turned pink almost immediately upon addition of sodium periodate, however, CE analysis revealed only L-dopa production. When L-dopa was used as substrate, a dramatic colour change was observed immediately upon periodate addition. A pale yellow colour, followed by a bright red, then a gradual browning of the solution and finally a black to colourless solution was noticed. This colour change is characteristic of dopaquinone formation followed by dopachrome conversion (red solution). The gradual darkening of the solution which leads to an insoluble black pigment being produced is due to the formation of melanin [1].

When analysed by CE, a number of peaks were observed. The advantage of using short capillaries and high voltages enabled rapid migration times and hence short analyses times per injection. Standard solutions of L-dopa were prepared in citric acid (0.01 M) /disodium hydrogen phosphate (0.02 M) buffer pH 2 to ensure stability of the compound, see Figure 3.7. Oxidation of L-dopa (2 mM standard) was generally performed in plastic epindorf vials to which sodium periodate (approximately 2 mM) was added. The lower pH offered by the citrate buffer facilitated greater control over the oxidation process. In high pH buffers, periodate rapidly converts L-dopa to dopachrome with only very slight production of intermediate compounds being detected. As the oxidation of L-dopa by periodate proceeds so fast, 1 µl aliquots were removed at approximately 30 seconds intervals for the first 2 minutes, then a further sample at 5 minutes followed by sampling every 5 minutes. The samples, once removed were subject to CE separation immediately upon completion of individual runs, hence the two-step rinse procedure for the capillary prior to each injection was not employed. This results in slight variations of individual peak migration times from run to run.

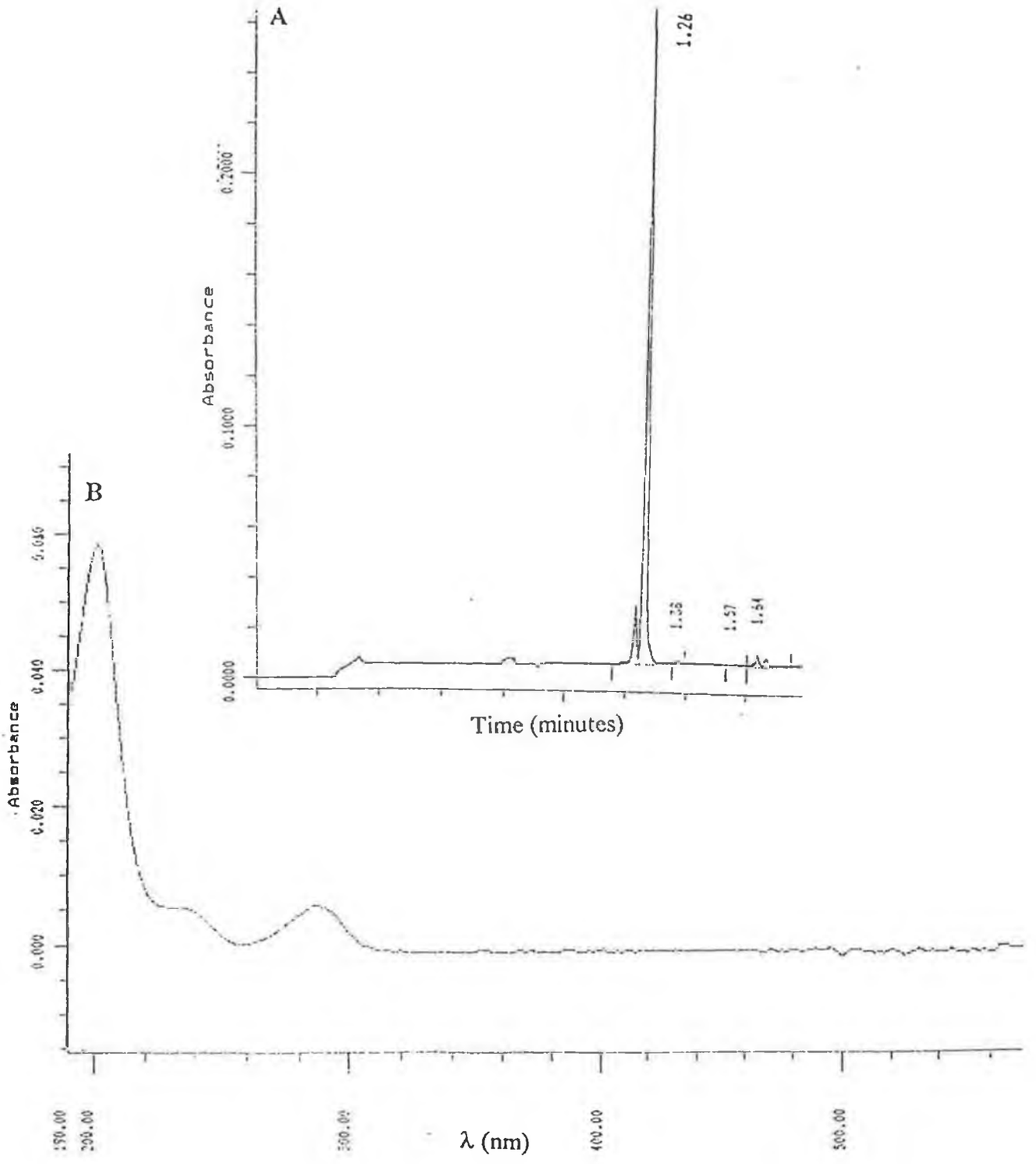

Figure 3.7. Electropherogram of a 2 mM L-dopa standard (prepared in 0.01 M citrate/ 0.02 M sodium dihydrogen phosphate buffer, pH 2.0), with a run buffer of 0.025 M disodium boratedecahydrate buffer, pH 9.0 (A), and accompanying UV-Vis spectrum using diode array detection (B).

The oxidation of L-dopa, proceeds so rapidly, that 15 seconds after periodate addition, three distinct peaks are detected in considerable quantities, with migration times of approximately 1.3, 1.7 and 2.25 minutes respectively. See Figure 3.8(A). Kagedal et al. [12] recently reported that dopachrome has three pK_a values: 0.8, 3.1 and 9.1. At a pH beyond 9.1, this compound has a net charge of minus 2, thus it is likely that under the CE separation conditions used here that the later eluting peak at 2.25 minutes, being most anionic of all compounds separated, is possibly dopachrome. At 45 seconds after periodate addition, Figure 3.8(B), three new peaks with migration times of 1.57, 1.62 and 2.17 minutes respectively are produced. Within 6 minutes after periodate addition, much of the oxidation of L-dopa is complete, with it's peak height decreasing rapidly, while the peak at 1.62 and the two peaks at 2.18 and 2.32 minutes increase as is illustrated in Figure 3.8(C-E). Thus, while CE offers rapid separation of these compounds, a suitable detection system is necessary to scan each of these individual peaks simultaneously to facilitate their identification. While fluorescence and electrochemical detection techniques offer improved sensitivity, labelling of these compounds would prove rather cumbersome and the possibility exists that the oxidation of L-dopa may be complete before sufficient amounts of labelled intermediates are produced for fluorescence detection. For electrochemical detection, the oxidation and reduction compounds are analysed separately. DAD, while less sensitive meets the requirements demanded by this particular assay.

The diode array scans as illustrated in Figure 3.9, reveal some important information regarding the formation of intermediate compounds in the oxidation of L-dopa. The first compound to elute; L-dopa has an absorbance maxima at 236 nm and 285 nm with no spectral features in the visible region. The middle region of the electropherograms (Figure 3.8B), containing three distinct peaks at 1.57, 1.62 and 1.69 minutes respectively are only detected for a short period after periodate addition, hence it may be assumed that these are converted to another stage in the melanisation pathway. Two of these compounds exhibit similar absorbance spectra i.e. an absorbance maxima at 218 nm and 272 nm is observed for the peak eluting at 1.57 minutes while the peak at 1.62 exhibits an absorbance maxima at 210 nm and 270 nm. The third peak (with a migration time of 1.69 minutes), has an absorbance maxima at

220 nm, 310 nm and 420 nm. This peak is very similar to the peak at 2.18 minutes which exhibits an absorbance maxima at 220 nm, 310 nm, and 475 nm.

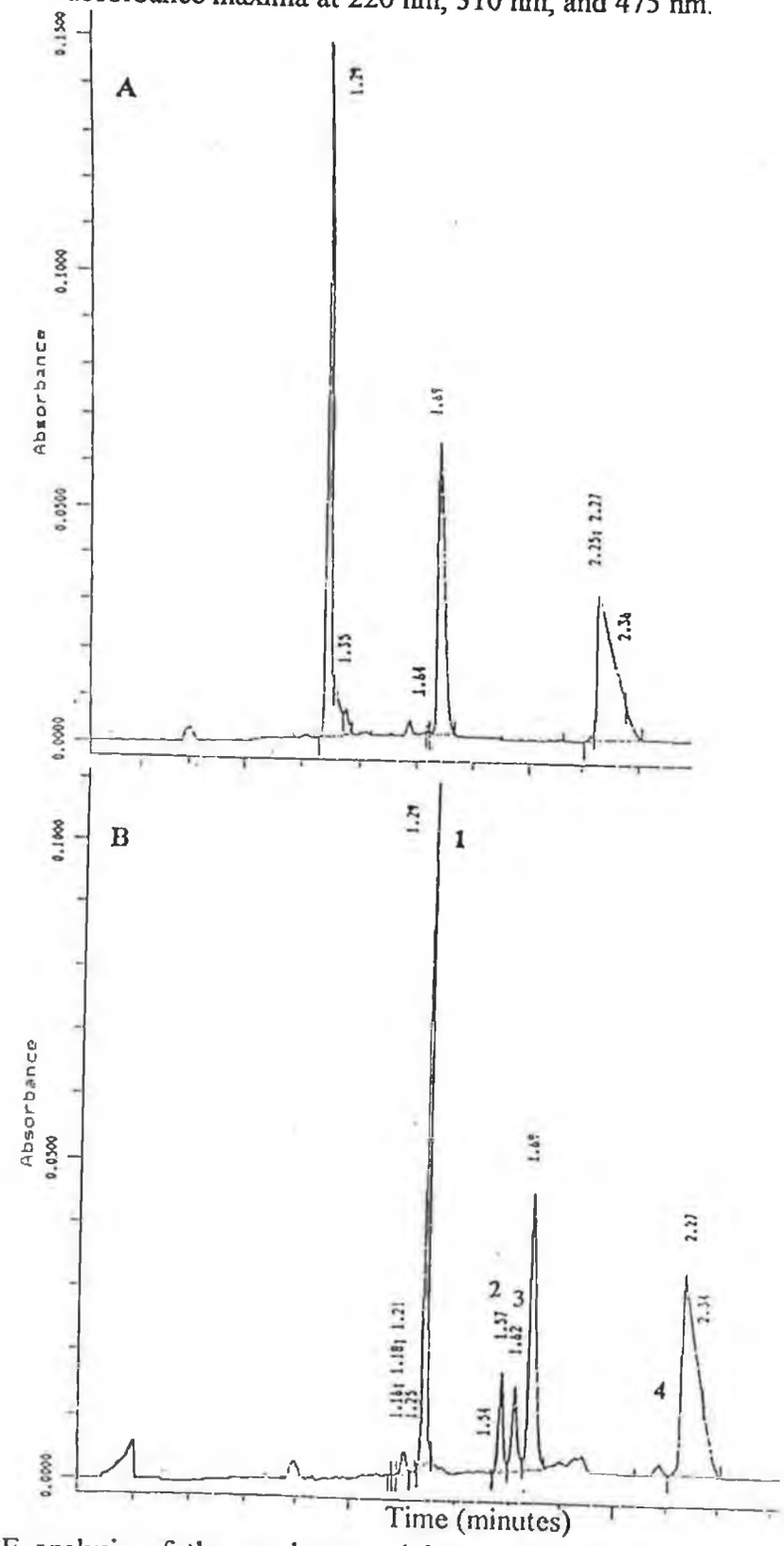

Figure 3.8. CE analysis of the products and intermediates formed during L-dopa oxidation (2 mM) by sodium periodate (2 mM) under strong acidic conditions (0.01 M citrate/ 0.02 M phosphate buffer, pH 2).Oxidation of L-dopa 15 seconds after periodate addition (A), 45 seconds (B)

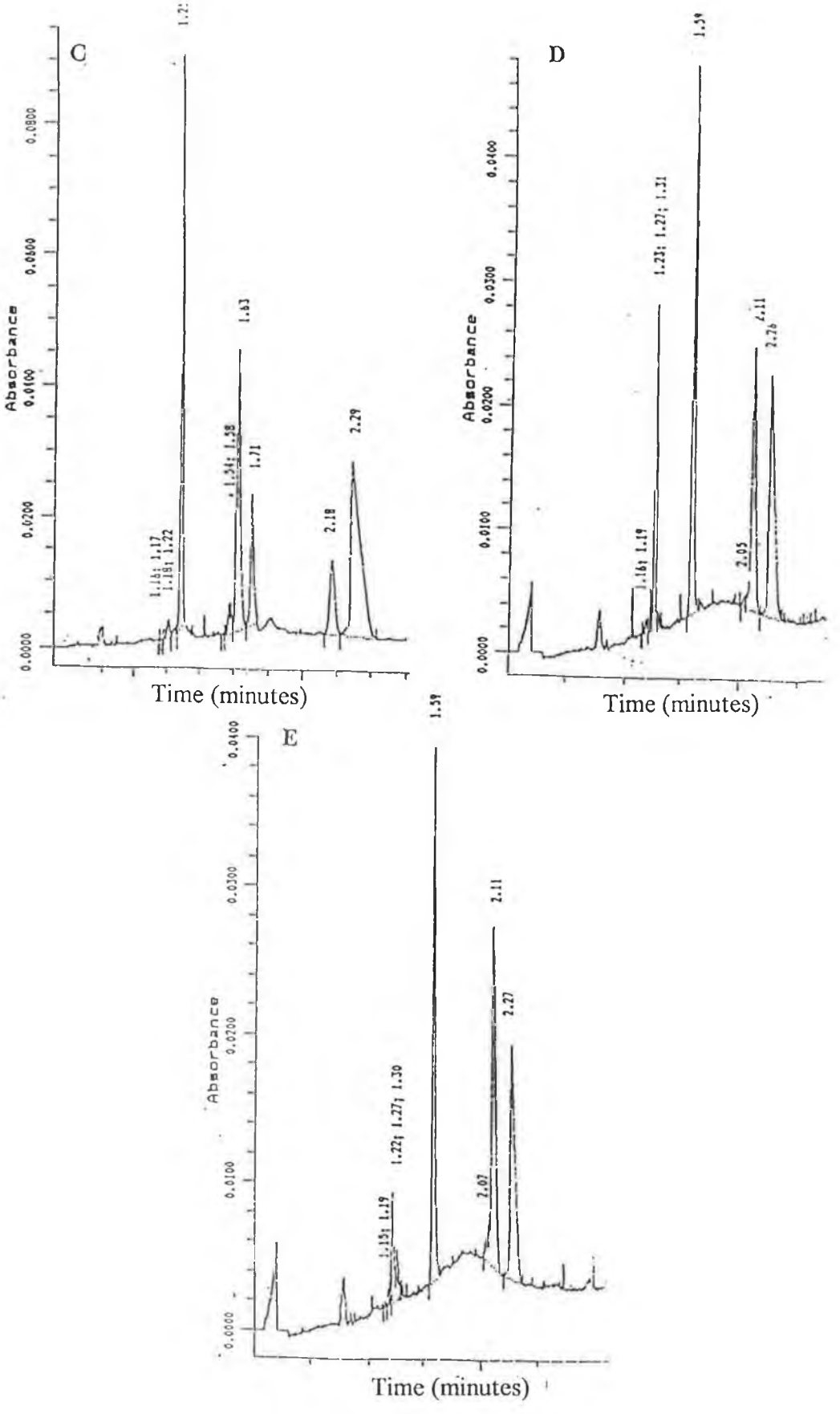

Figure 3.8.(continued) CE analysis of the products and intermediates formed during L-dopa oxidation (2 mM) by sodium periodate (2 mM) under strong acidic conditions (0.01 M citrate/ 0.02 M phosphate buffer, pH 2).after 5 minutes (C), 30 minutes (D) and 90 minutes (E). Separation were performed on a 20 cm × 50 μm i.d. capillary, with a separating voltage of 20 kV and a run buffer of 0.025 M disodium tetraborate decahydrate, pH 9.0.

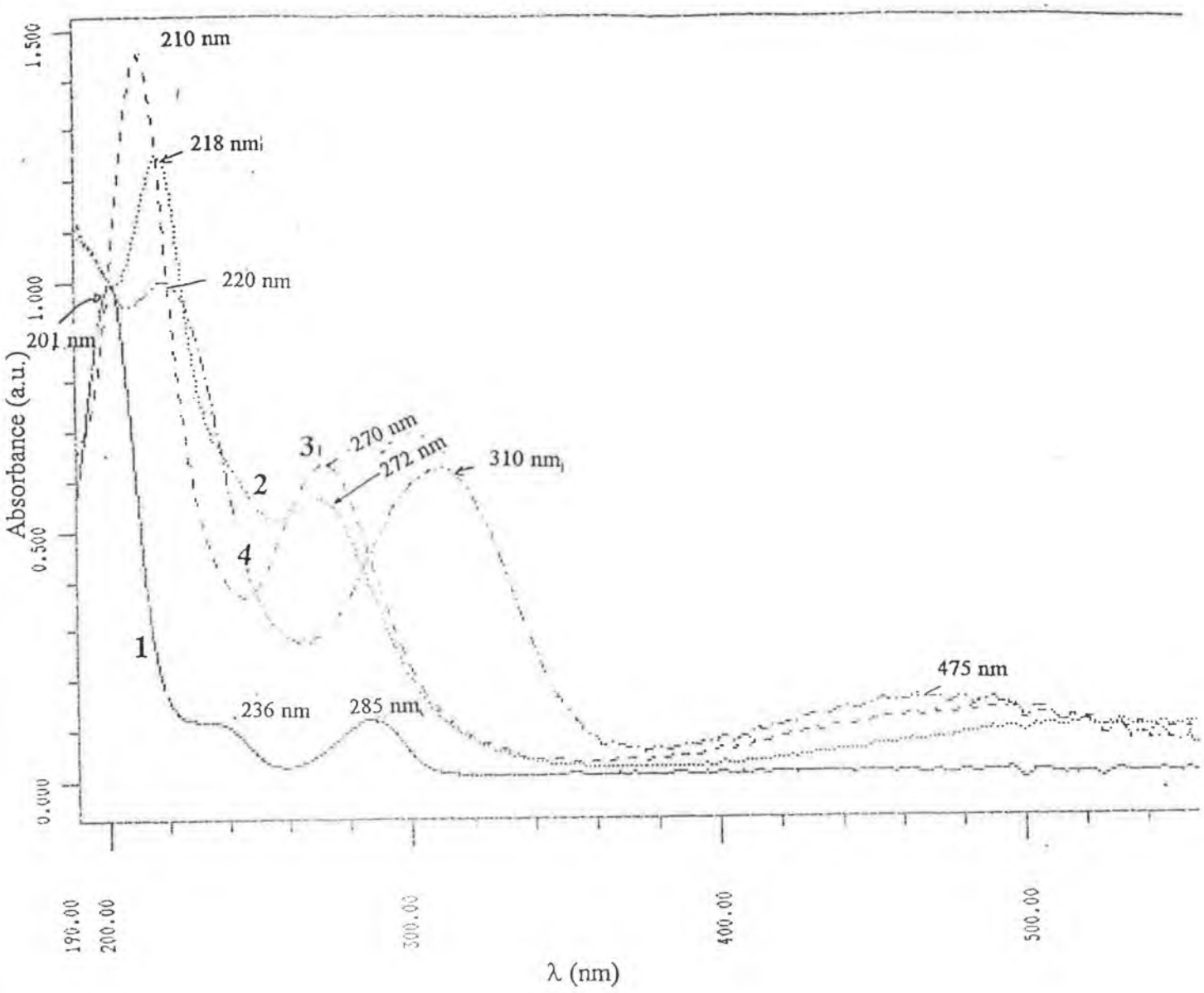

Figure 3.9. The utility of diode array detection is demonstrated where UV-Vis absorbance spectra of peaks 1-4 in Figure 3.8(B) are displayed.

Several research groups, [5,12] have reported that dopachrome absorbs at 310 nm and 475 nm hence it may be concluded that this particular peak at 2.18 minutes is in fact dopachrome. This would also be consistent with its elution order profile, because it possesses a greater net negative charge than the other products detected. Based on the information gained from its absorbance spectra, it may also be inferred that the peak detected at 1.69 minutes is leucodopachrome or some related dopachrome-based species.

When the oxidation of L-dopa is performed in-situ, using sodium periodate under acidic conditions, an additional compound, topa, is formed [5]. This compound is unlikely a component of the enzymatic oxidation reaction because of the restricted pH range for optimum tyrosinase activity. An authentic standard (2.5 mM) of L-topa prepared in distilled deionised water was subjected to CE analysis and is illustrated in Figure 3.10. The major peak at 1.34 minutes is the L-topa standard, which will co-elute with L-dopa if produced in significant quantities. Topa is also oxidised by periodate, to yield topaquinone, so the presence of topa in the reaction vial will remain small throughout. Topa is light sensitive, and has undergone auto-oxidation prior to injection, as evidenced by the broad second peak at 1.54-1.6 minutes. It is assumed that by preparation of this standard in citrate buffer, pH 2, that the stability of this standard would be enhanced. The peak symmetry, particularly of the oxidised component at 1.54 minutes, may also be improved. Thus, it may be concluded that the peaks detected at 1.57 and 1.62 minutes are topaquinone and dopaquinone respectively.

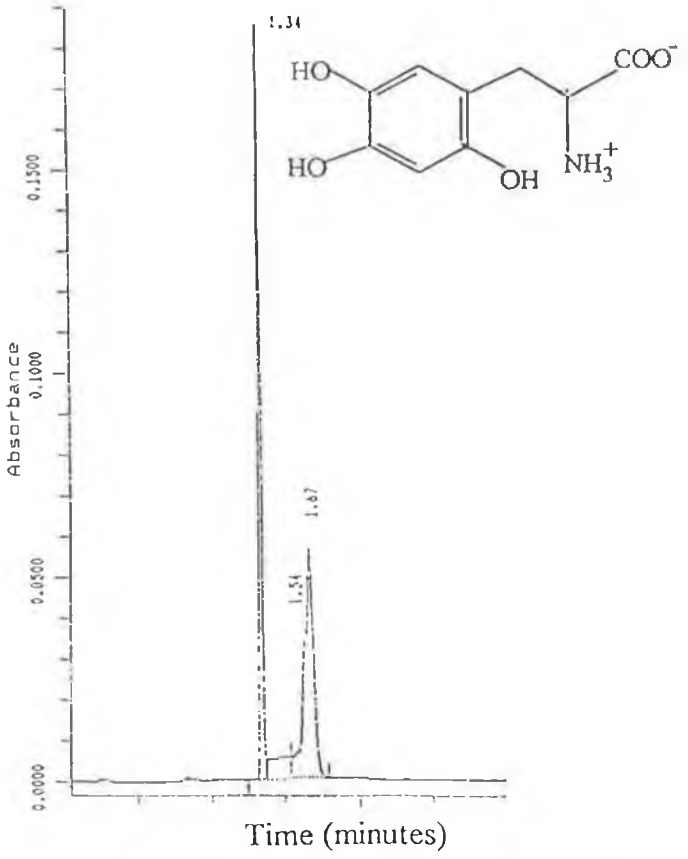

Figure 3.10. Electropherogram of a 2.5 mM standard of topa (prepared in distilled deionised water) using a run buffer of 0.025 M disodium tetraborate decahydrate. V= 20 kV.

Mason [2] suggested that two forms of the red pigment may exist; however this idea has never been firmly established. In this assay, two peaks with similar peak heights and peak areas remain after complete oxidation of L-dopa with migration times of approximately 2.11 and 2.26 minutes respectively and exhibit absorbance maxima characteristic of a dopachrome-based species. It was noticed, however, that a slight change of the run buffer pH, from 9.0 to 9.3 resulted in the co-elution of these peaks.

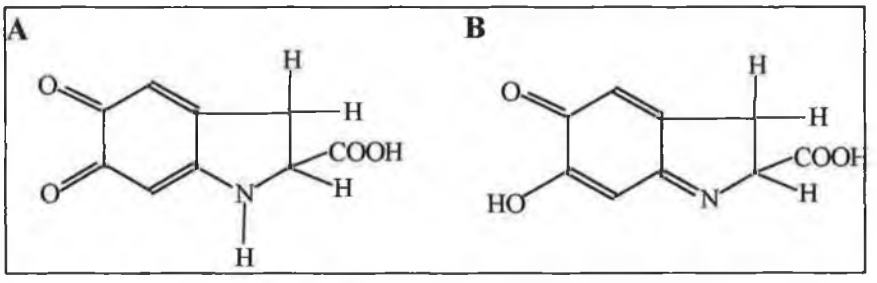

Figure 3.11. The structure of 2-carboxy-2,3-dihydroindole-5,6-quinone (A) and 2-carboxy-2,3-dihydro-6-hydroxy-indole-1,5-quinonimine (B), as postulated by Mason for the red pigment dopachrome [2].

The results obtained from the oxidation of L-dopa by sodium periodate using DAD are tabulated below. An advantage of CE over its chromatographic counterparts, is that it can rapidly analyse several components simultaneously, while closely mimicking the natural environment of these components.

Migration Time (minutes)	Absorbance Maxima (nm)			Possible Identity
1.25	236	285	-	Dopa
1.57	218	272	-	Topaquinone
1.62	210	270	-	Dopaquinone
1.69	220	310	420	Leucodopachrome
2.18	220	310	475	Dopachrome

Table 3.2. The migration times and their respective absorbance maxima of the products obtained by periodate oxidation of L-dopa using diode array detection. Data were derived from the electropherogram shown in Figure 3.8(B).

Using a run buffer of 0.025 M disodium tetraborate decahydrate, pH 9.0, facilitates rapid analysis times, while the citrate buffer, pH 2, maintains control over the rate of L-dopa oxidation by periodate. As the intermediate compounds formed during melanin biosynthesis are still speculative, diode array detection has proven beneficial for their identification. As the CE analyses were performed on samples removed from the reaction vial up to 30 minutes after periodate addition (retaining the red colour in solution), it was assumed that the second phase of melanogenesis never occurred, i.e. the re-arrangement of dopachrome to indole-quinones, which are colourless in solution.

3.3.5. Choice of Suitable Internal Standard

Variations in the migration times of the products of L-dopa oxidation were observed from run to run, with more pronounced variations from day to day. While it was believed that this effect was due to improper conditioning of the fused silica capillary and to a lesser extent to temperature irregularities. Jumppanen *et al.* [19] described that the repeatability of analyte migration times in fused silica capillaries is very poor, especially if new capillaries are used. This, he describes was mainly due to the nonrepeatable electroosmotic flow velocity (v_{eo}) caused by the unstable surface conditions of the capillary wall. Internal standards are often used to correct for variations that arise in the migration time of the analytes and hence improve the precision of a particular application. Choice of the correct internal standard is critical; it must not react with the analytes under investigation, be present in a concentration similar to the working standards and elute within the separation frame of the given assay. They can also be used to quantitatively calculate the concentration of the unknown components. This is usually represented by the following:

$$\mathbf{C_{sample} = (R_{sample}/R_{standard})\, C_{standard}} \qquad (3.1)$$

where C_{sample} and $C_{standard}$ are the concentrations of the sample and standard respectively and R_{sample} and $R_{standard}$ are the respective peak area ratios.

Several compounds were investigated for use as potential internal standards. Two compounds which were deemed suitable for this particular assay were uracil and L-lactic acid and are illustrated in Figure 3.12. Uracil, being one of the major pyrimidine bases found in nucleotides, should have no charge at pH 9.0. When subjected to CE analysis using borate buffer, pH 9.0 as the run buffer, a migration time of 1.08 minutes was obtained, eluting before L-dopa, which would have a slight negative charge. L-lactic acid, formed during glucose oxidation in muscle tissue, contains a single carboxylic acid group which will be ionised at pH 9.0. This compound, while less stable than uracil is a useful indicator for those compounds formed, that possess a net negative charge of -1. While it may be difficult to separate this compound from the quinone-based species at the initial stages of melanogenesis, it is quite easily identified at the latter stages of this reaction pathway. This is illustrated in Figure 3.12(B,C).

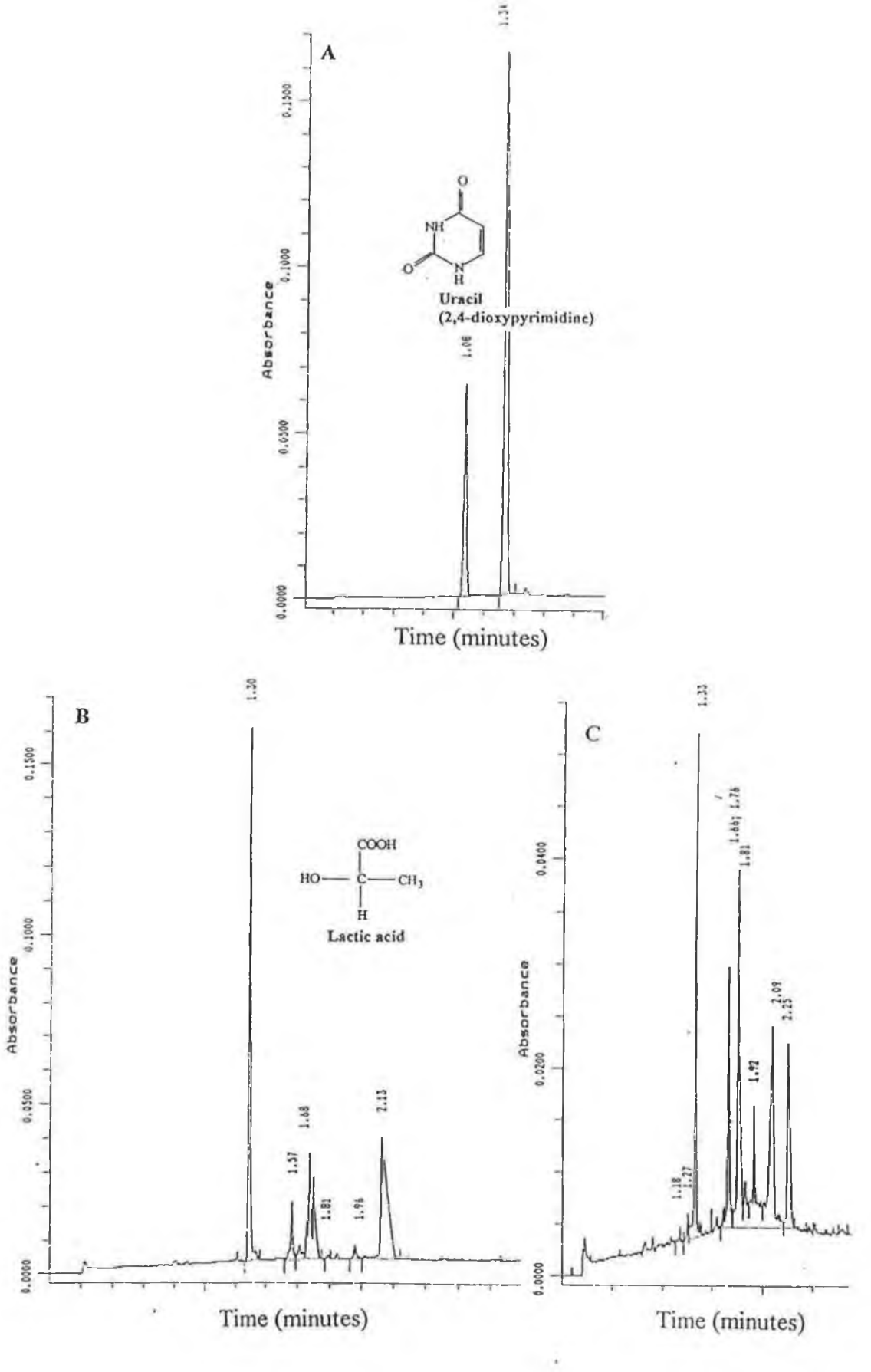

Figure 3.12. Electropherograms of possible internal standards for the anaysis of L-dopa oxidation by sodium periodate include; uracil (A) and lactic acid 5 seconds after periodate addition, B, and 40 minutes after periodate addition, C.

3.4. SPECTROELECTROCHEMISTRY OF DOPACHROME FORMATION

Spectroelectrochemistry; a combination of two very different techniques; electrochemistry and spectroscopy, is a powerful approach used to probe the consequences of spectral i.e. ultraviolet (UV), infrared (IR), or near-infrared (NIR) or redox potential phenomenon, upon application of a fixed potential. It is a most useful means of monitoring the electrogeneration of a product in aqueous or even non-aqueous media [20]. Herein, this technique was used to probe the fate of L-dopa upon the application a fixed potential, by monitoring the change in its absorbance spectra.

3.4.1. Cyclic voltammetry of L-dopa

A cyclic voltammogram (Figure 3.12), in which the potential applied to the working electrode is scanned and the current measured, shows two potential regions, where the current is observed due to the electrolysis of L-dopa. These potential regions indicate where oxidation and reduction of L-dopa occur: at +0.435 V and -0.455 V respectively with respect to Ag/AgCl.

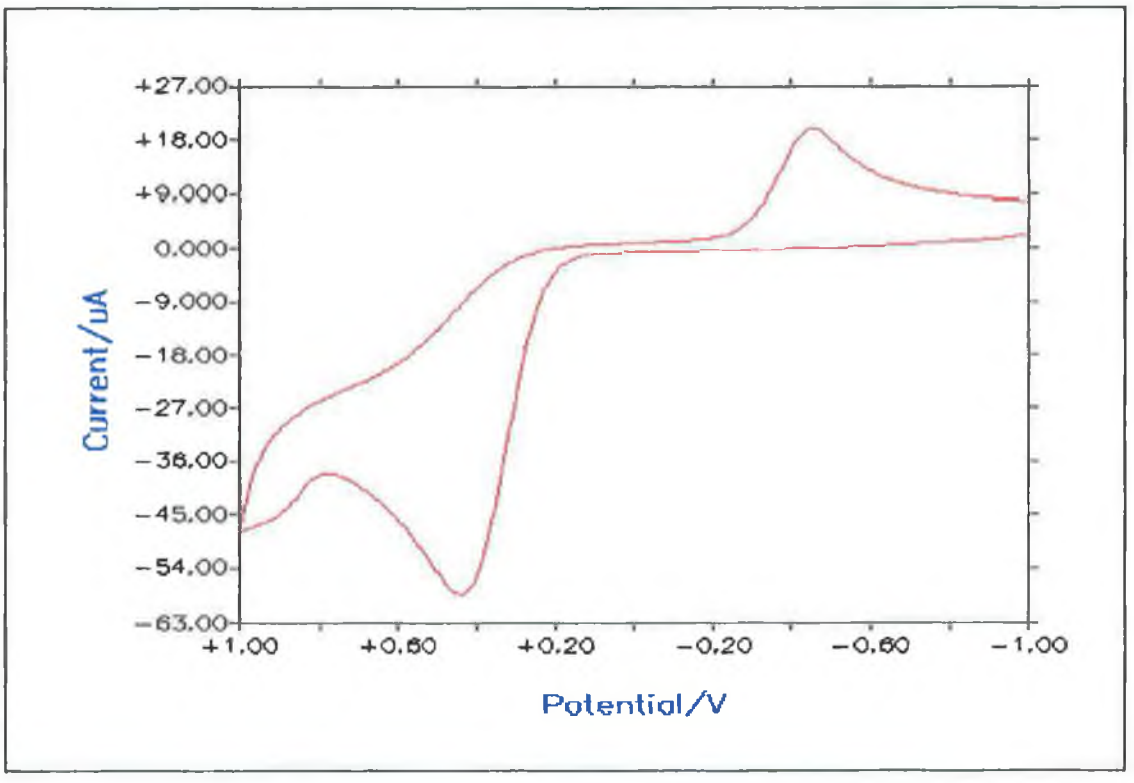

Figure 3.12. Cyclic voltammogram of a 2 mM L-dopa solution, prepared in 0.1 M P.B., pH 7.4. (degassed with argon for 15 minutes prior to analysis).$\nu = 0.1$ V s^{-1}.

3.4.2. Spectroelectrochemistry

Initial studies involved scanning a solution of L-dopa (in 0.1 M P.B. pH 7.4) in the range 200-600 nm at 0.00 V. The absorbance spectrum obtained was similar to that observed previously, with absorbance maxima at 230 nm and 280 nm. A potential was then applied from - 1.00 V to + 1.00 V, at 0.2 V intervals. No change in the absorbance spectrum was recorded, until the region where L-dopa oxidation was reached (i.e. + 0.435 V). This was evident by the appearance of absorbance peaks at ≈ 300 nm and ≈ 480 nm. A fixed potential of + 0.435 V was applied for 20 consecutive scans and the resultant change in absorbance recorded. Upon initial application of this potential, the solution turned yellow; further application of this potential caused the solution to turn red, followed by black-colourless, as was previously observed, following oxidation by sodium periodate. The absorbance spectra, illustrated in Figure 3.13, demonstrates an increase in absorbance at both 305 nm and 475 nm up to 10 scans due to the electro-oxidation of L-dopa to form dopachrome.

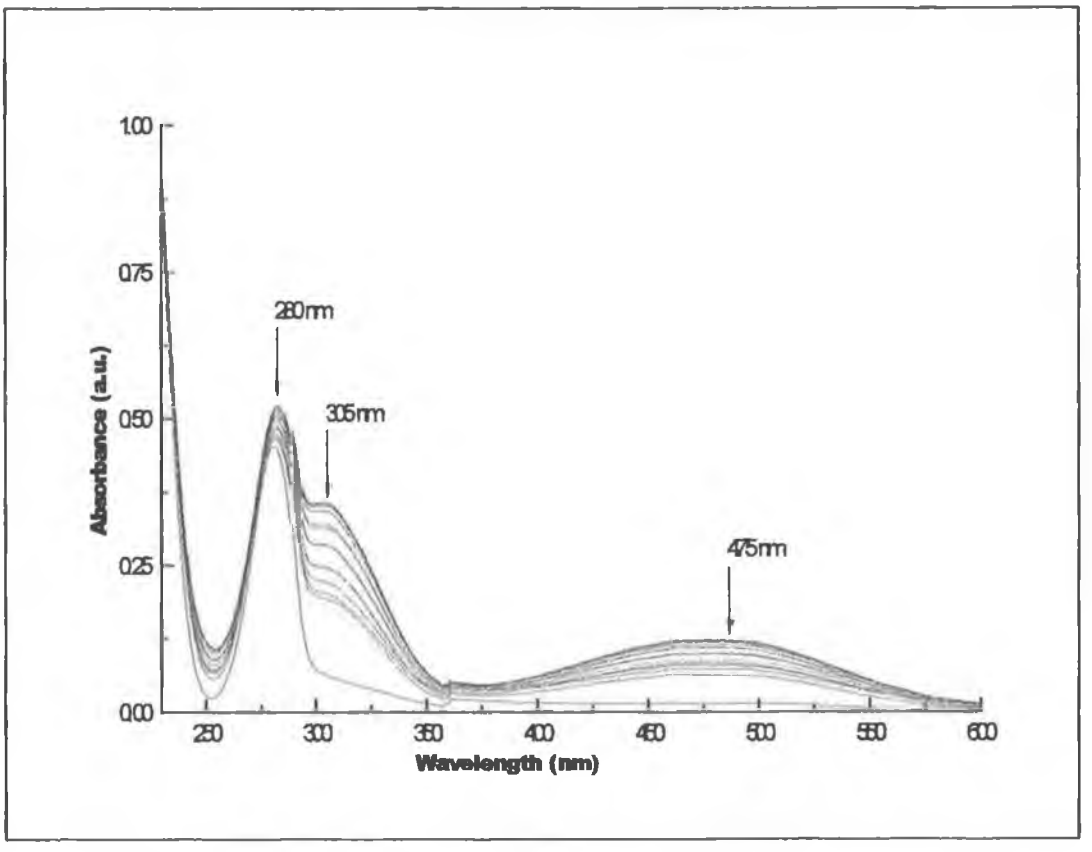

Figure 3.13. The UV spectrum obtained when a fixed potential of + 0.435 V was applied to a solution of L-dopa (approx. 2 mM) in 0.1 M P.B., pH 7.4.

The absorption spectra of dopaquinone or leucodopachrome were not evident, possibly due to the rapid rate of formation of dopachrome and greater quantities of this compound being formed may have masked the detection of the other intermediate compounds expected. A more rapid scanning spectrometer to record several hundred complete spectra per second could be utilised for obtaining such short-lived intermediate compounds. Further scanning of the absorbance spectra upon application of a potential of + 0.435 V, revealed a decrease in absorbance at 475 nm. This decrease, is due to the rearrangement of dopachrome with the loss of CO_2 at neutral pH to yield 5,6-di-hydroxyindole (DHI), or 5,6-dihydroxyindole 2-carboxylic acid (DHICA) in acidic milieu. The formation of DHICA is enhanced by the presence of certain metal ions [3] and the platinum gauze working electrode could contribute to its production. While the formation of these colourless compounds, DHI or DHICA is not easily observed in Figure 3.13, a second approach involving the oxidation of L-dopa at +0.435 V for 3 minutes, followed by its subsequent reduction at -0.455 V clearly demonstrate the formation of these compounds.

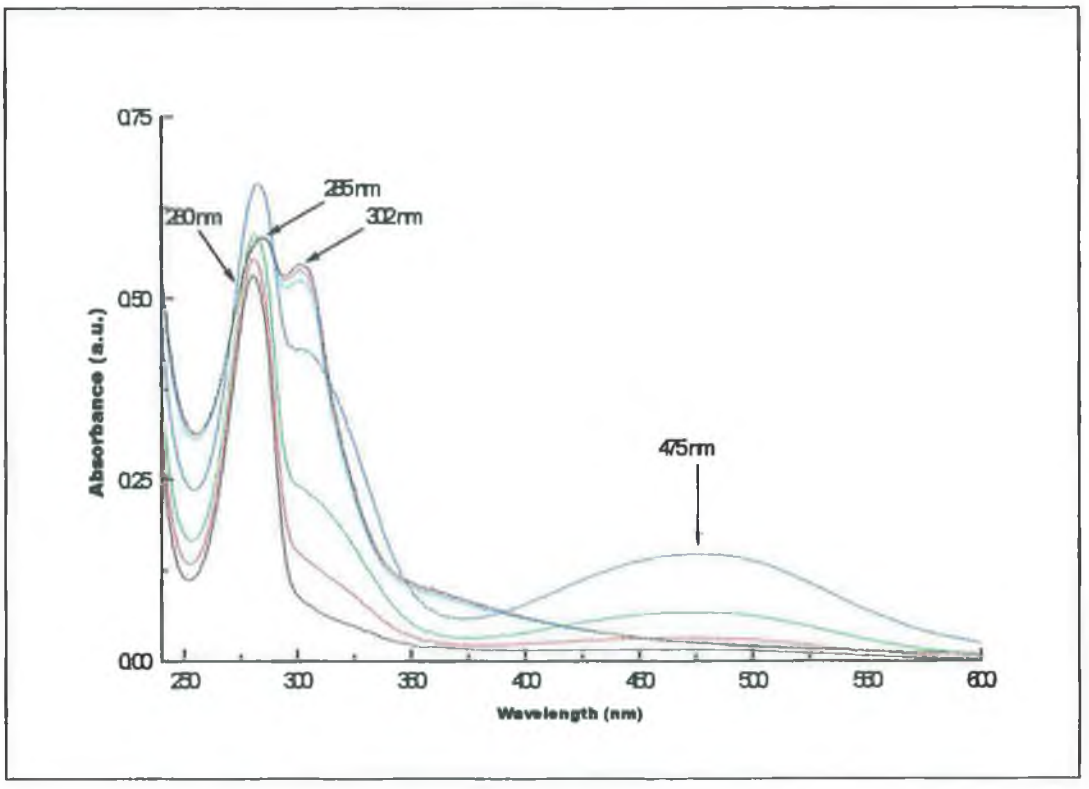

Figure 3.14. The oxidation of L-dopa at + 0.435 V leads to an increase in absorbance at 305 nm and 475 nm; however upon application of a reduction potential at - 0.455 V, the absorbance maxima at 475 nm is reduced, and a new spectra, with absorbance maxima at 285 nm and 302 nm, characteristic of di-hydroxyindole formation was evident [2].

While it may appear that the oxidation of L-dopa *in-vitro* is not indicative of the *in-vivo* mechanism, it has been demonstrated by several research groups [3,17], that the chemical properties of naturally occurring pigments are very similar to those of dopa melanin preparation *in-vitro*, indicating the presence of certain metal ions in the melanisation process *in-vivo*. When a 2 mM solution of L-dopa was subjected to a potential of - 0.455 V and the absorbance recorded, no change was observed indicating no product formation. Hence, only the reduction of dopachrome lead to the development of DHI. Further reduction at this potential lead to the formation of a black precipitate which adsorbed onto the platinum gauze working electrode i.e. production of melanin polymer, which made any further analysis difficult.

3.5. ELECTROCHEMISTRY OF MELANIN POLYMER

The idea that plastics could conduct electricity would have seemed completely irrational almost a decade ago, has since consumed endless hours of research in laboratories throughout the world, in an attempt to prove that polymeric materials are indeed electrically conducting. Conducting polymers, usually formed by means of an electrochemically induced polymerisation of the monomer in the absence of oxygen, have received considerable attention recently [21,22]. The most important of these electrochemically synthesised polymers include polypyrrole [8,23], polyaniline [24], polyindole [9,25] and polyacetylene [26]. A major advantage of electrochemically prepared polymer films is the exact localisation of the polymerisation reaction, the ability to control the properties and the thickness of the polymer film, deposited at the electrode surface. Fabrication of a microelectrode array [27] analogous to diodes and transistors, to the formation of biosensors, by entrapment of redox enzymes during the polymer growing process [28], are just some areas where these films have been applied to date.

This final section describes an attempt to electrochemically polymerise melanin, onto the surface of a glassy carbon electrode. As described in the previous section, the continuous oxidation of L-dopa in aqueous solution lead to the production of a black pigment (melanin), which appeared to adsorb onto the surface of the working electrode. This process, influenced the idea to investigate the properties of this polymer formed, with a view towards sensor-based applications. The effect of aqueous buffer pH, various organic-based supporting electrolytes and different concentrations of each, on the rate of charge propagation through these electrochemically prepared films were investigated using both cyclic voltammetry and chronocoulometry. The applicability of a polymer in areas of electrocatalysis, photoelectrochemistry and sensor technology may be determined by the rates of charge propagation through the redox polymer film. As described by Forster *et al.* [29], the rate of charge propagation can be controlled by one of several processes. These may be described as the flow of counterions in and out of the film, the intrinsic barrier to self-exchange for electron hopping to occur between adjacent redox centres and polymer chain motions which

may be required to bridge the intersite-separation in order for electron exchange to occur. The evaluation of charge transport rates for various electrolyte systems was investigated using chronocoulometry (CC). The theory and principles of operation of these techniques used to study the formation of the melanin polymer are discussed in chapter 4.

3.5.1. Effect of buffer pH on the voltammetric behaviour of L-dopa

The most striking feature in a series of cyclic voltammograms of L-dopa in the various pH solutions investigated, is the complete change between the first and the subsequent scans in a given direction as illustrated in Figure 3.15. The potential scan rate chosen for these and subsequent experiments was 0.1 V/s. This medium scan rate was most suitable for the observation of transient intermediates whose lifetimes are too short to be seen at higher sweep rates. The first scan, initiated at - 1.0 V and swept anodically towards + 1.0 V at 100 mV/s, shows that essentially no oxidation occurs until a potential of + 0.56 V is reached (using 0.1 M P.B., pH 6 as electrolyte, where P.B. is the addition of 0.1 M sodium-dihydrogen-phosphate to 0.1M disodium-hydrogen-phosphate to the required pH). This pronounced peak indicates the region where oxidation of L-dopa occurs. When the sweep direction is reversed, two reduction peaks i.e. at + 0.050 V and a broad peak at - 0.42 V are observed. On the second and all other subsequent cycles, an anodic peak at a potential of + 0.070 V is detected. This anodic peak, which appears after initial oxidation of L-dopa, immediately marks the system as one in which a chemical follow-up reaction has occurred after the initial charge transfer. The anodic and cathodic peaks at + 0.56 V and - 0.42 V respectively, slightly change shape and decrease until a steady state is achieved. Turner *et al.* [30] reported that quinones are electrochemically reduced at approximately - 0.15 V (vs Ag/AgCl), hence these more positive peak potentials as observed in Figure 3.15. are unlikely due to quinones alone, but may be a quinone- based polymer. Rivas and Solis [31] studied the electro-oxidation of both L-tyrosine and L-dopa, using McIlvaine buffer, pH 6.0 and suggested that L-dopa is easily oxidised to its corresponding o-quinone at +0.19 V and re-reduced at + 0.16 V (vs SCE). They assigned the electroreduction of dopachrome at - 0.35 V with corresponding re-oxidation at - 0.203

V. Their observations are markedly different from those described above, possibly due to the restricted narrow potential range studied (i.e. + 0.4 to - 0.4 V).

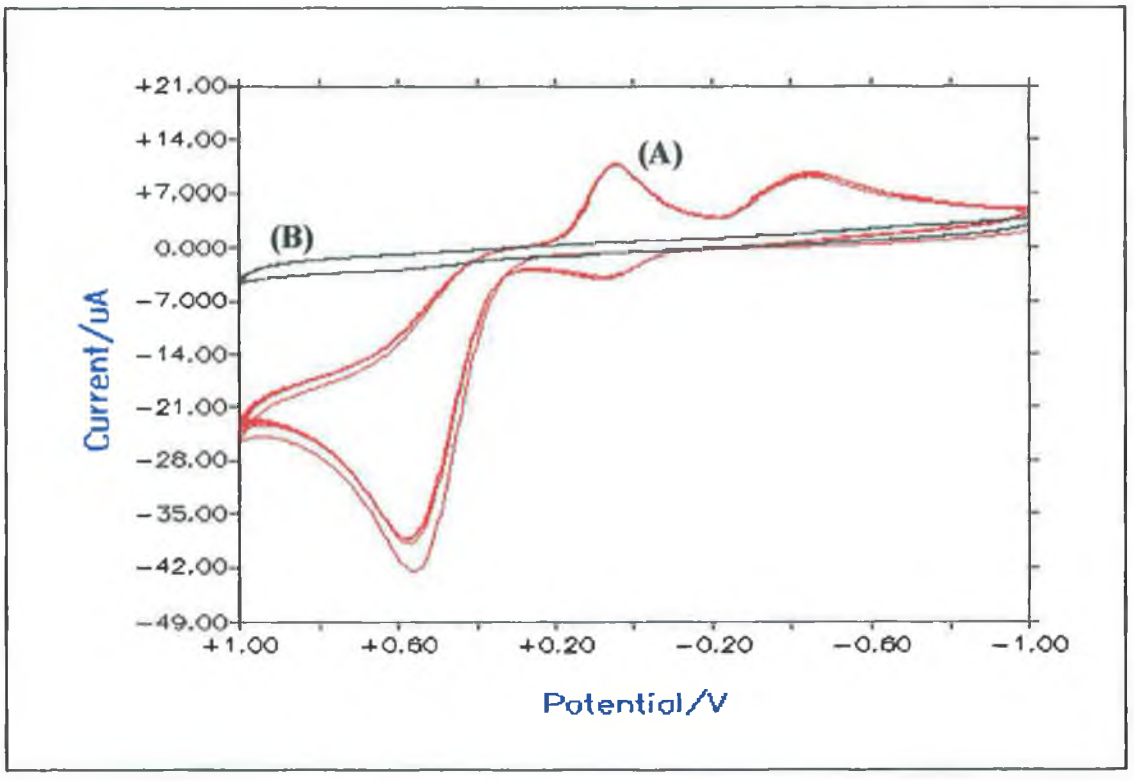

Figure 3.15. A typical cyclic voltammogram of a 2 mM L-dopa solution in P.B., pH 6 (A) for 10 complete cycles. The background solution prior to addition of L-dopa (B). Potential scan rate was 0.1 V/s.

Differences in electrochemical characteristics were observed at higher pH, the effect of a chemical follow-up reaction was yet again seen and general loss in electroactivity was observed at increasing pH (Figure 3.16). The first anodic scan for a P.B. solution at pH 7 and pH 8, again shows initial oxidation of L-dopa at + 0.515 V and + 0.445 V respectively. On the reverse scan, essentially no current appears, until a potential of - 0.509 V and - 0.51 V for each pH respectively. Subsequent scans reveal a second peak at + 0.06V and 0.0 V corresponding to re-oxidation of the reduced species. Using P.B. pH 7.4 as electrolyte, two oxidation peaks are observed (in the region between 0 and + 0.150 V). When the second anodic scan is initiated, peak potentials at - 0.018 V and + 0.14V were observed, upon subsequent scanning the peak at - 0.018 V decreases and is shifted to more positive potentials. This may be due to the formation of the melanin polymer, which becomes more and more non-conducting and hence more positive potentials are required for oxidation. After 20

cycles the oxidation potential has shifted to + 0.18 V. Meanwhile, the peaks at +0.505 V and - 0.509 V continue to decrease, indicating that less and less L-dopa is reaching the electrode surface, due to increasing thickness of the polymer film being formed there. These two peaks, which may constitute a redox couple indicate slow charge transfer, hence the irreversible nature of this system. A similar series of CVs were obtained when using the P.B. pH 8.0 buffer. This decrease in the peak potentials with increasing pH demonstrate that the oxidation processes involve the loss of hydrogen ions, therefore as pH increases (i.e. hydrogen ion concentration decreases), lower voltages are required for the oxidation process to occur. Melanin production involves loss of electrons from dopaquinone and dihydroxyindole as depicted in Figure 3.1. After several cycles, the hydrogen ion concentration at the electrode increases, thereby, making it difficult for the proton loss reaction to occur. This results in decreased current values and as increase in peak potential.

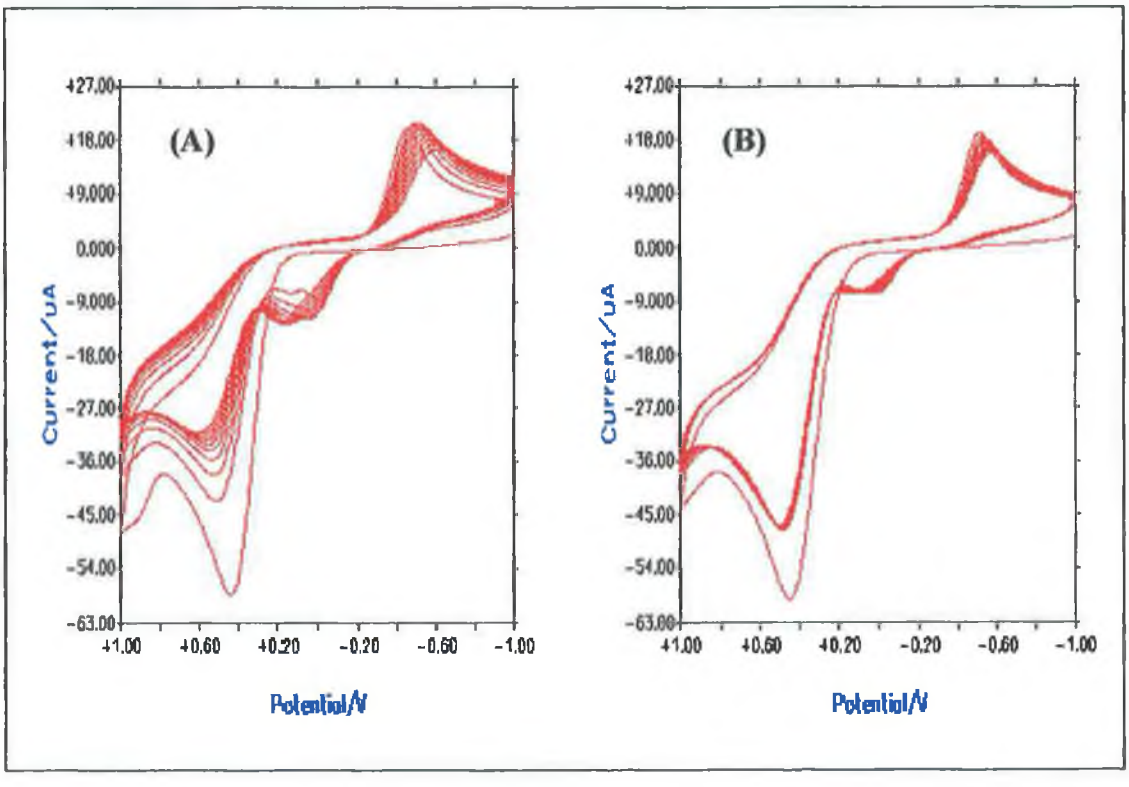

Figure 3.16. Cyclic voltammograms of a 2 mM L-dopa solution in 0.1 M P.B., pH 7; (A) and pH 8; (B). Scan rate was 0.1 V/s for 10 repeated cycles.

When sodium periodate (1 mM final concentration) was added to each of these buffered solutions containing L-dopa, immediate colour changes were observed, indicating oxidation of the remaining L-dopa in solution. Subsequent scanning of these solutions with a freshly polished electrode, demonstrated polymer growth at the electrode surface. A conducting polymer film was formed in P.B. solutions at pH 6 and 7, at pH 8 and a 25 mM disodium tetraborate buffer at pH 9.0; however, the films formed were less conducting. When the P.B. solutions at pH 6 and 7 were left to stand for approximately 1 hour to ensure complete oxidation of L-dopa, a conducting polymer was again produced as is illustrated in Figure 3.17.

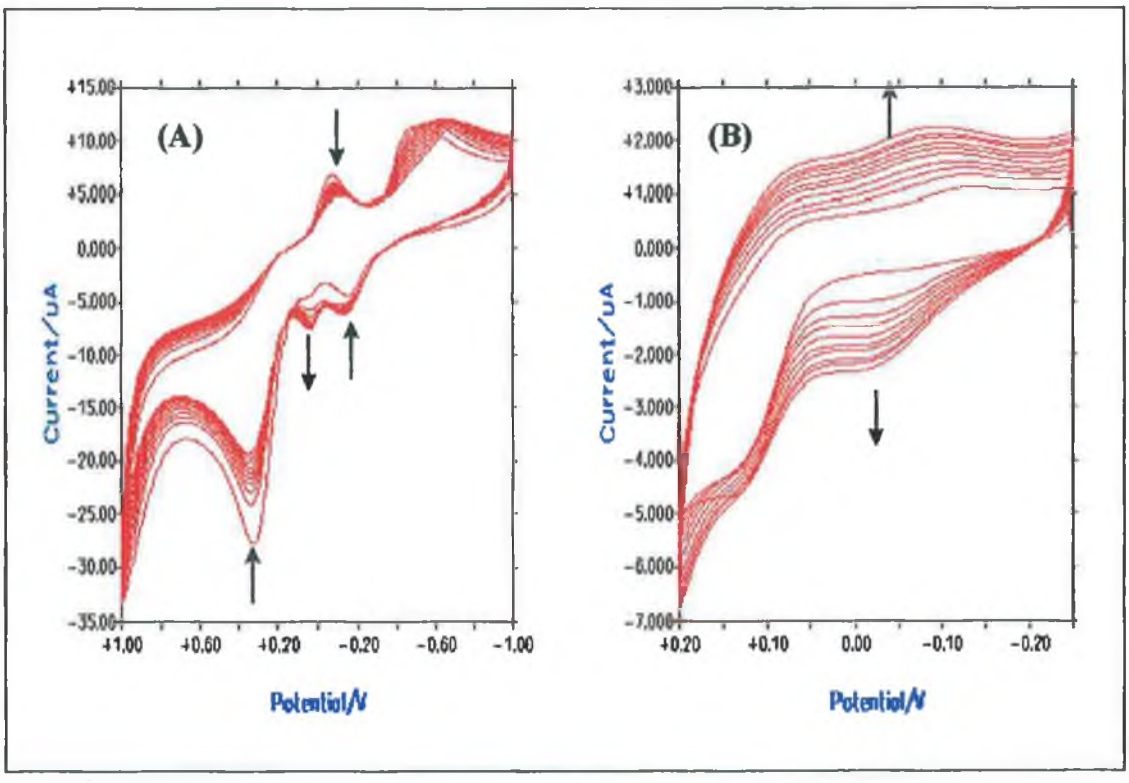

Figure 3.17. Growth of melanin polymer from a 2 mM L-dopa solution in P.B., pH 6 (A) and pH 7.4 (B), approximately 1 hour after sodium periodate addition at a scan rate of 0.1 V s^{-1} for 10 complete cycles.

The durability of the polymer formed was then investigated. This involved careful rinsing of the electrode in distilled deionised water, to remove any excess monomer on the electrode surface, followed by replacement of this electrode into an oxygen free P.B., pH 7 solution (without L-dopa). The potential was then scanned from - 1.0 V to + 1.0 V at various scan rates. Reduced electrical behaviour was

observed upon the initial cycle, with loss in electroactivity in subsequent cycles, indicating that the polymer was falling off the electrode surface.

The rate of charge transfer along the polymer film formed was estimated from potential step chronocoulometry experiments. It is assumed that electron transfer during the course of the experiment is controlled by semi-infinite diffusion of charge in the polymer. A plot of the chronocoulometric charge (Q) as a function of the square root of time ($t^{½}$) will be linear originating from the origin and the diffusion coefficient (D_e) can be calculated from the slope of the Anson plot according to the equation:

$$\mathbf{Q = (2nFAD_e^{1/2} C_{es} t^{1/2})/\pi^{1/2}} \qquad (3.1)$$

where Q is the reduction charge passed when the potential was stepped down from an initial potential (E_i) of + 1.0 V to a final potential (E_f) of 0 V, n is the number of electrons transferred (which is assumed to be 2), F is the Faraday constant (96500 C mol^{-1}), A is the area of the electrode surface (0.0707 cm^2), C_{es} is the concentration of the electroactive polymer bound at the electrode surface (mol cm^{-3}), t is the time required to carry out the charging process (seconds) and D_e is the diffusion coefficient (cm^2 s^{-1}). As the concentration of polymer formed is unknown, then values of $D_e^{½}C_{es}$ were calculated and are tabulated below. These results show that pH has no effect on the rate of electron transport in the conducting polymer.

pH	$D_e^{1/2}C_{es}$ (mol cm^{-2} $s^{-1/2}$)
6	2.46×10^{-9}
7	3.27×10^{-10}
8	2.24×10^{-9}
9	2.85×10^{-10}

Table 3.3. Effect of pH on the rate of charge transport through the polymer film formed at the electrode surface. 0.1 M P.B. was used for pH 6, 7 and 8 while 0.025 M disodium tetraborate decahydrate was used for the pH 9 experiments.

3.5.2. Effect of electrolyte ion

3.5.2.1. Perchlorate based electrolytes

The behaviour of L-dopa in perchlorate solutions i.e. using aqueous lithium perchlorate ($LiClO_4$) and perchloric acid solutions in acetonitrile (ACN) were examined. Typical solutions contained 2 mM L-dopa in 0.1 M $LiClO_4$ or 0.1 M $HClO_4$/ACN Cyclic voltammetry experiments carried out on the $LiClO_4$ based solution displayed a large oxidation peak at + 0.76 V and two reduction peaks at + 0.105 V and - 0.01 V respectively on the first cycle (Figure 3.18A). Subsequent cycling between - 1.0 V and + 1.0 V demonstrated the emergence of a single reduction peak at + 0.094 V. The film formed at the electrode surface was more stable than previous attempts and when this polymer-coated electrode was replaced into 0.1 M $LiClO_4$ without L-dopa, the polymeric characteristics are evident , see Figure 3.19(A and B).

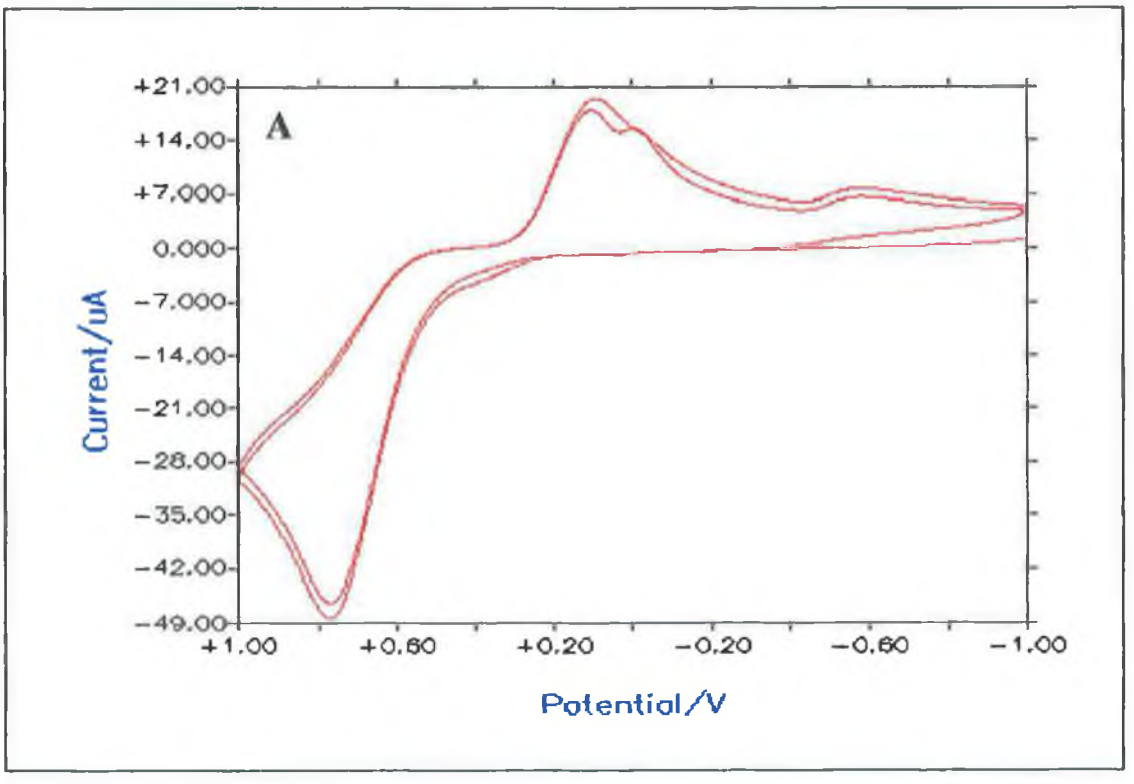

Figure 3.18. The effect of the perchlorate electrolyte ion on the electrooxidation of L-dopa (A). A 2 mM L-dopa solution in 0.1 M $LiClO_4$, Scan rate was 0.1 V s^{-1}.

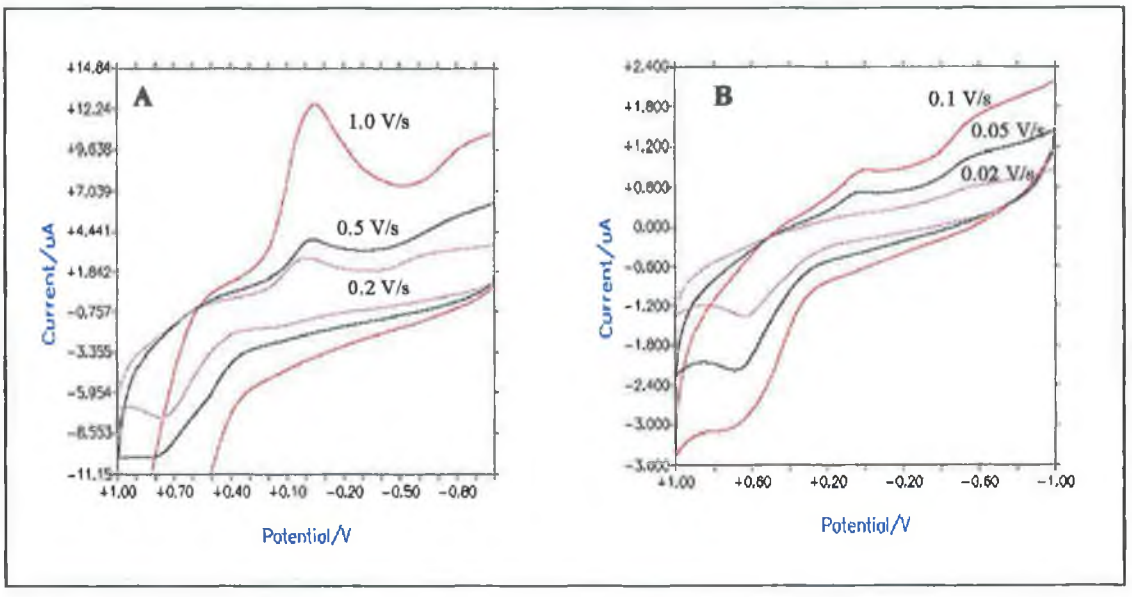

Figure 3.19. The cyclic voltammograms of the melanin polymer film in 0.1 M $LiClO_4$ at scan rates of 1.0, 0.5, and 0.2 V/s (A) and 0.1, 0.05 and 0.02 V/s (B).

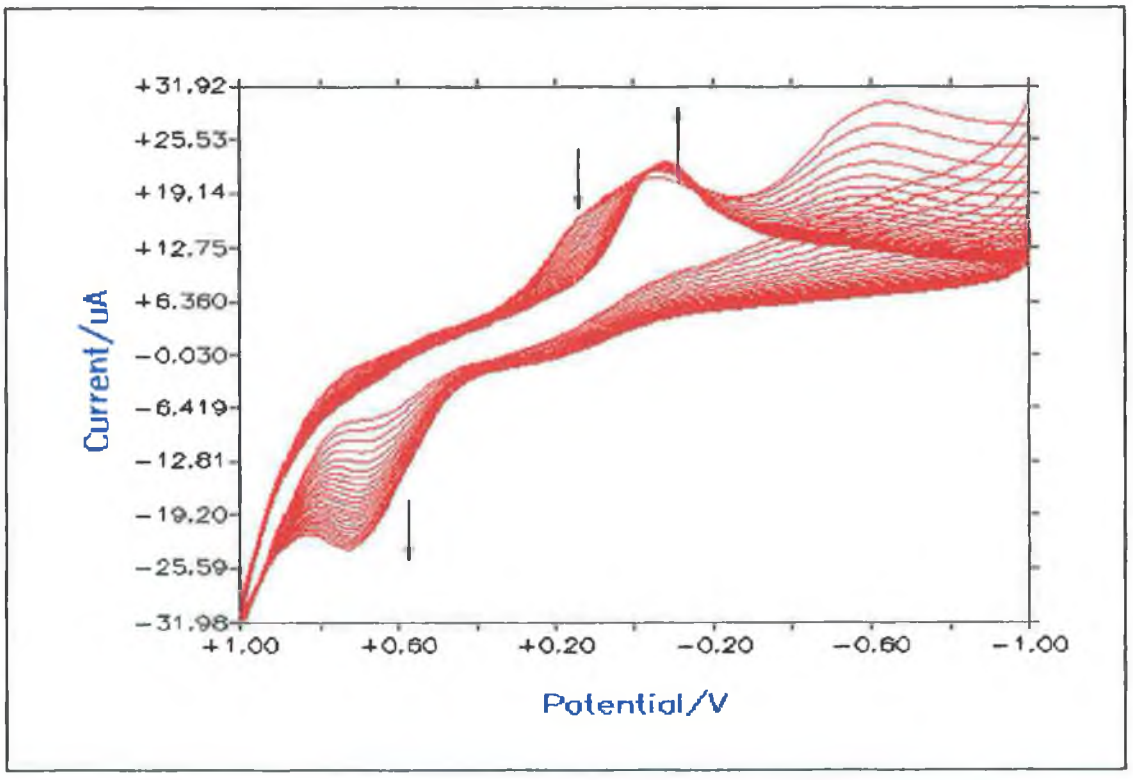

Figure 3.20. Effect of the perchloric acid electrolyte solution on the growth of melanin polymer.

The gradual increase of the reduction peak at (-0.08 V) and subsequent decrease at (+ 0.1 V) was more pronounced in the perchloric acid based system. A highly conducting polymeric film developed upon repeated cycling from - 1.0 V to + 1.0 V following

periodate addition (complete oxidation of all L-dopa in solution) and is illustrated in Figure 3.20. The effect of perchlorate concentration on $D_e^{1/2}C_{es}$ was evaluated as before, using chronocoulometry. These results showed no significant change in $D_e^{1/2}C_{es}$ with increasing concentration of $LiClO_4$ as supporting electrolyte. However, a profound effect in $D_e^{1/2}C_{es}$ values were observed with increasing perchloric acid concentration, hence affecting the electron transport properties of the polymer.

Concentration of supporting electrolyte (M)	$D_e^{1/2}C_{es}$ **(mol cm^{-2}s$^{-1/2}$)**	
	$LiClO_4$	**$HClO_4$**
0.1	2.65×10^{-9}	3.09×10^{-9}
0.2	2.60×10^{-9}	3.57×10^{-9}
0.4	2.65×10^{-9}	2.89×10^{-9}
0.6	2.60×10^{-9}	2.83×10^{-9}
0.8	2.60×10^{-9}	2.76×10^{-9}
1.0	2.66×10^{-9}	2.75×10^{-9}

Table 3.4. Effect of increasing perchlorate concentration on the rate of charge transport ($D_e^{1/2}C_{es}$), within the polymer film adsorbed onto the glassy carbon surface.

3.5.2.2. Sulphate-based electrolyte

The electrochemical behaviour of the film formed in 0.1 M tetraethylammonium-toluene-4-sulphonate (TEATS)/ACN was similar to those formed previously, insofar that they too were electroactive and electrochromic. (Figure 3.21). Colour changes from pale purple to red were observed upon repeated cycling of these solutions. Two peak oxidation potentials were recorded upon initial cycling at + 0.124 V and + 0.720 V respectively and a reduction peak at + 0.200 V. Subsequent cycles demonstrated a loss of this oxidation peak at + 0.124 V, possible a quinone intermediate; however upon repeated cycling, gradual development of a broad peak in the same region was again evident, due to the polymeric film being formed.

The charge transport diffusion parameters for various concentrations of (TEATS) were then investigated. This bulky molecule occupies a larger molar volume than those previously studied, hence one would expect a reduction in $D_e^{1/2}C_{es}$ if counter-ion transport alone is rate limiting. While an overall decrease in $D_e^{1/2}C_{es}$ was observed however, with increasing concentration, the actual value at 0.1 M TEATS was among the highest obtained for the systems studied thus far and are presented in Table 3.5 below. The results presented for $D_e^{1/2}C_{es}$ are all obtained from different electrode coatings. This avoids the problem of 'memory effects', where the rate of charge transport through a film would be dependent on the electrolyte to which it had been exposed previously.

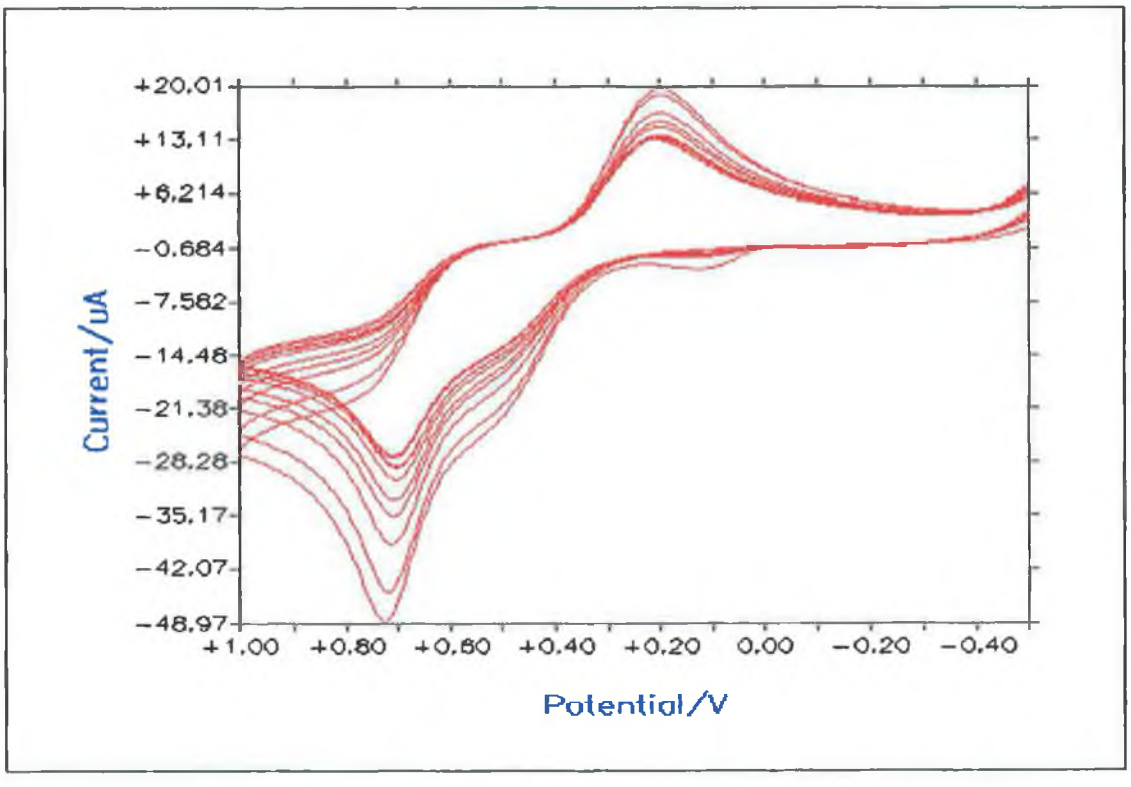

Figure 3.21. CV of 2 mM L-dopa solution in TEATS/ACN after 10 repetitive cycles at 0.1 V/s.

Conc. of TEATS in solution (M)	$D_e^{1/2}C_{es}$ (mol cm^{-2}s$^{-1/2}$)
0.1	3.83×10^{-9}
0.2	3.04×10^{-9}
0.4	2.80×10^{-9}
0.6	2.67×10^{-9}
0.8	2.49×10^{-9}
1.0	2.20×10^{-9}

Table 3.5. Effect of increasing TEATS concentration on the diffusion coefficient $D_e^{1/2}C_{es}$

The results obtained for the calculation of $D_e^{1/2}C_{es}$ agree with those of Forster *et al.* [32], where an increased supporting electrolyte concentration is likely to increase the electrolyte concentration within the film, as a result migration would be expected to have a greater contribution, while giving rise to larger apparent $D_e^{1/2}C_{es}$ values, when the supporting electrolyte concentration is low. A further explanation why a decrease in $D_e^{1/2}C_{es}$ is observed upon increasing electrolyte concentration, may be the increased distance between adjacent electroactive sites due to a swelling of the polymer film at these higher concentrations, which reduce electron hopping between sites.

3.6. CONCLUSIONS

The metabolism of L-dopa is a complex process, with many potential reaction pathways. This particular path chosen, while almost 100 years since the initial studies were carried out on the biosynthesis of melanin, still remain obscure and research continues towards a better understanding of the reaction mechanisms involved.

The CE-DAD analyses has shown to be useful for the analyses of transient intermediate compounds formed and for studies where sample volumes are limited, as described here. The spectroelectrochemistry experiments could only detect the

formation of dopachrome and could not distinguish if dopaquinone or leucodopachrome were actually formed. The latter part of this study describes an attempt to electrochemically polymerise melanin onto an electrode surface. This biopolymer would be envisaged to produce little/none side reactions with in-vivo biological experiments, hence this idea of developing melanin polymers towards biosensor based applications was extremely challenging. While the formation of polypyrrole[8] and polyaniline [24] is well documented as a radical cation mediated reaction process, the final products of melanin biosynthesis are as yet uncertain. Nevertheless, the electro-oxidation and reduction of this polymer was studied briefly and the effect of the rate of charge propagation by different electrolyte ions. Further studies envisaged, should include (i) a series of different cationic and anionic electrolytes as well as potential substituents to improve polymer stability and enhance its electrochemical properties, (ii) film thickness, (iii) spectral changes due to different films grown in different media.

3.7. REFERENCES

1. Raper, H. S. *Physiological Review* **8** (1928) 245-282.
2. Mason, H. S. *J. Biol. Chem.* **172** (1948) 83-99.
3. Prota, G. *Medicinal. Research Review* **8** (1988) 525-556.
4. Cabanes, J.; Garcia-Canovas, F.; Lozano, J. A.; Garcia-Carmona, F. *Biochim. Biophys. Acta.* **923** (1987) 187-195.
5. Aroca, P.; Solano, F.; Garcia-Borron, J. C.; Lozano, J. A. *J. Biochem. Biophys. Meth.* **21** (1990) 35-46.
6. Pavel, S.; Van Der Slik, W. *J. Chromatogr.* **375** (1986) 392-398.
7. Pavel, S. Trends *Anal. Chem.* **8**, (5) (1989) 177-183.
8. Foulds, N. C.; Lowe. C. R. *J. Chem. Soc. Faraday Trans.* **1** (82) (1986) 1259-1264.
9. Bartlett, P. N.; Farrington, J. *Bulletin Electrochemistry*, **8** (1992) 208-211.
10. Weine, R. J. *'Chromatography: A Laboratory Handbook of Chromatography and Electrophoresis Methods'*, Third Edition, van Nostrad, (NY, 1985).
11. Tominaga, T. T.; Imasato, H.; Nascimento, O. R.; Tabak, M. Anal. Chim. Acta. 315 (1995) 217-224.
12. Kagedal, B.; Konradsson, P.; Shibata, T.; Mishima, Y. *Anal. Biochem.* **225** (1995) 264-269.
13. Chien, R-L.; Burgi, D. S. *Anal. Chem.* **64** (1992) 1046-1050.
14. Chien, R-L.; Burgi, D. S. *Anal. Chem.* **64** (1992) 489A-496A.
15. Aebersold, R.; Morrison, H. D. *J. Chromatogr.* **516** (1990) 79-88.
16. McCormick, R. M. *Anal. Chem.* **60** (1988) 2322-2328.
17. Li, J.; Christensen, B. M. *J. Liq. Chrom.* **16** (1993) 1117-1133.
18. Lerner, A. B.; Fitzpatrick, T. B.; Calkins, E.; Summerson, W. H. *J. Biol. Chem.* **178** (1949) 185-195.
19. Jumppanen, J. H.; Riekkola, M-L. *Anal. Chem.* **67** (1995) 1060-1066.
20. Heineman, W. R. *Anal. Chem.* **50** (1978) 390A-402A.
21. Diaz, A. F.; Bargon, J. *Handbook of Conducting Polymers*, Chapter 3, Vol.1, Edited by Skotheim, T. A. (Dekker Press, NY USA) 1986.

22. Evans, G. P. *Advances in Electrochemical Science and Engineering*, **Vol. 1**, Edited by Gerischer, H.; Tobias, C. W. (VCH Publishers (UK) Ltd., Cambridge, UK) 1990.

23. Pickup, P. J. *J. Electroanal. Chem.* **225** (1987) 273-280.

24. Pekmez, N.; Pekmez, K., Yildiz, A. *J. Electroanal. Chem.* **370** (1994) 223-229.

25. Pandey, P. C. *J. Chem. Soc. Faraday Trans. I* **84** (1988) 2259-2265.

26. Roth, S.; Bleier, H.; Pukacki, W. *Faraday Discuss. Chem. Soc.* **88** (1989) 223-233.

27. Kittlesen, G. P.; White, H. S.; Wrighton, M. S. *J. Am. Chem. Soc.* **106** (1984) 7389-7396.

28. Schuhmann, W. *Mikrochim. Acta* **121** (1995) 1-29.

29. Forster, R. J.; Kelly, A. J.; Vos, J. G.; Lyons, M. E. G.; *J. Electroanal. Chem.* **270** (1989) 365-379.

30. Dennison, M. J.; Hall, J. M.; Turner, A. P. F. *Anal. Chem.* **67** (1995) 3922-3927.

31. Rivas, G. A.; Solis, V. M. *Anal. Chem.* **63** (1991) 2762-2765.

32. Forster, R. J.; Vos, J. G. *J. Electrochem. Soc.* **139** (1992) 1503-1508.

CHAPTER 4

AN INTRODUCTION TO RECENT DEVELOPMENTS IN BIOSENSOR TECHNOLOGY, IN PARTICULAR RELATED TO BIOMEDICAL APPLICATIONS

4.1. INTRODUCTION TO BIOSENSORS

The endeavours of technologically advanced societies are increasingly reliant on the sensing, monitoring and control of chemical and biochemical species, often at very low levels. In the last two decades, a sensing concept based on biological recognition was established, known as a *biosensor* [1]. A *biosensor* may be defined as "a device which can recognise an analyte in an appropriate sample, convert this target analyte to a molecular or an ionic product, which is then monitored by subsequent redox, potentiometric or other methods" [2]. The recognition system is usually an enzyme covalently bound or trapped near the electrode surface. The *biosensor* should be capable of selectively determining analytes in complex environments without the need for sample pre-treatment or separation.

In 1962, Clarke and Lyons [3] introduced the first immobilised enzyme electrode. Based on the principle of their oxygen electrode, the enzyme solution was trapped by a semi-permeable membrane held in front of the working electrode. This non-destructive and reusable enzyme electrode represented the birth of the biosensor era. This breakthrough has lead to an almost exponential growth in electrode developments in analytical chemistry [4,5], with more recent developments including incorporating polymeric bilayers for longer enzyme activity [6], greater selectivity and faster transfer kinetics [7]. Biosensors have also been integrated with flowing systems (FIA) [8-10], liquid chromatography [11,12], and more recently with capillary electrophoresis [13]. Hence this developing arena of biosensor design and technology have the potential to revolutionise analytical methodologies.

4.2. ENZYMES AS CATALYSTS FOR RECOGNITION

An understanding of the theoretical basis of enzyme function helps in explaining the response and performance of enzyme electrodes. The names Briggs and Haldane and Michaelis and Menten will always be synonymous with enzyme reaction kinetics [14], which can be illustrated by considering the simplest enzyme reaction scheme

$$E + A \underset{k_{-1}}{\overset{k_1}{\rightleftharpoons}} EA \xrightarrow{k_2} E + P \qquad (4.1)$$

The rate of reaction, v, can be represented by the following equation

$$v = (k_2 [E]_0 [A])/K_m + [A] \qquad (4.2)$$

where K_m is the Michaelis-Menten constant, [E] and [A] is the concentration of the enzyme and substrate respectively.

This type of reaction represents the homogenous case where the mediator and the enzyme are both freely diffusing in solution. In most analytical applications concerning amperometric enzyme electrodes, the enzyme is entrapped at the electrode surface in some form of matrix.

4.2.1. Behaviour of immobilised enzymes at electrode surfaces

The kinetics of enzyme reactions, where the enzyme is immobilised in a homogenous film (heterogeneous case), may differ considerably from the homogenous case. Bockris [15] has studied the effect of adsorption of the flavoprotein, glucose oxidase, on graphite electrodes. The redox potential of the immobilised enzyme appeared to have shifted somewhat from that of the freely diffusing species in solution. He deduced that the enzyme undergoes a radical conformational change, possibly involving unfolding of the enzyme structure, or even dissociation of the redox center from the protein, depending on the enzyme concentration used. At high enzyme concentrations, the entire electrode surface is covered and results indicate that structural transitions (of the tertiary structure) occur leading to enzyme inactivation. At low enzyme concentrations, some of the enzyme appeared to have retained its native conformation and responded to changes in glucose concentration.

The rates of reaction may be influenced to varying extents by pH and ionic strength. The optimum pH for an enzyme immobilised within a negatively charged (anionic) support moves to a more alkaline region, while for a positive (cationic) support, the acidic region is

favoured [16]. This is largely due to changes in the degree of ionisation of reactive amino acid residues at the active site.

Other factors which affect the kinetic behaviour of immobilised enzymes include :

1. *Partitioning effects*; where there is a variation in the equilibrium substrate concentration between the local and the bulk solution .
2. *Micro-environmental effects*; the native environment may be different to the local environment in which it is placed.
3. *Diffusional and Mass transport effects*; involving diffusional resistance to the translocation of the substrate / product to or from the site of enzyme reaction.

The immobilisation technique used may also reduce the enzyme activity, which would inevitably limit its application as a useful biosensor; thus the rates of reaction for the heterogenous case must be considered in addition to the homogenous case [17-19].

4.2.2. Types of redox enzymes used

A large proportion of the literature concerned with the development of amperometric biosensors use a class of enzymes termed the *Oxidoreductases* [20]. This class of enzyme requires the presence of metal atoms for catalytic activity. The metal atoms associated with catalysis are normally cations and often have more than one oxidation state. Alkali metal cations (e.g. Na^+, K^+) and alkali earth metal cations (e.g. Ca^{2+}, Mg^{2+}) are involved in enzymatic activation; however, the transition metals (e.g. Cu^{2+}, Fe^{2+}, Zn^{2+}, Co^{2+}) bind to enzymes much more strongly forming metalloenzymes. These enzymes are easier to study, and hence are a more popular choice for biosensor use. Oxidoreductases catalyse the transfer of hydrogen atoms, oxygen atoms or electrons from one substrate to another. They can be subdivided into oxidases, dehydrogenases, reductases, peroxidases and oxygenases. In general, oxidases use up oxygen and generate hydrogen peroxide; dehyrogenases uses up a pyridine nucleotide; peroxidases consume hydrogen peroxide; and oxygenases can be measured by a decrease in oxygen, but no production of hydrogen peroxide. Hence, the consumption of oxygen or the production of hydrogen peroxide, is an obvious choice used to monitor the enzyme-catalysed reaction.

However, a number of problems have been associated with these ideas for monitoring the reaction:

1. the response can be limited by the oxygen concentration at ambient conditions;
2. high overpotentials are required to oxidise hydrogen peroxide at most of the commonly used electrodes;
3. large amounts of hydrogen peroxide produced can degrade the enzyme.

The problems associated with hydrogen peroxide or oxygen detection have been alleviated somewhat by recent developments to observe direct electron transfer to redox enzymes by using low molecular weight redox species to mediate electron transfer and the modification of electrode surfaces. In 1979, Eddowes and Hill [21], in an innovative approach modified an electrode by adsorption of 4,4'-bipypyridyl, using the enzyme cytochrome c . Near reversible behaviour was observed. The bipyridyl molecule helped to mediate biological electron transfer. This initiated a huge interest in the modification of electrodes for use as enzyme electrodes.

4.3. REDOX POLYMER MOIETIES FOR IMMOBILISATION ONTO ELECTRODE SURFACES

Redox polymers consist of electronically localised electron donor and acceptor sites that are bonded or linked to a polymeric chain. They can be pre-assembled and then applied as a film to the electrode surface, or they can be assembled from mono-layers directly as a film on the electrode. The final result is a multi-molecular layer film on the electrode surface [22]. Generally, larger amounts of material are available through direct synthesis of the redox polymer, which allow relatively better analytical and structural characterisation. On the other hand, fabrication of very thin, uniform films from pre-assembled redox polymers can be difficult, since they are often multiply charged, reluctantly soluble [23], and the ratio of metal centres to polymer units is difficult to control and determine. In-situ assembly of redox polymers by hydrolytic or electrochemical polymerisation of monomers can yield very thin-film forming characteristics but often at the expense of a less thorough analytical characterisation.

4.3.1.Pre-assembled monomer units

The most common pathways are polymerisation of vinyl-substituted redox monomers, pendant attachment of a redox monomer to a suitably functionalised linear polymer, and condensation polymers involving redox monomers. Only a few vinyl-substituted redox monomers have been pre-assembled into polymers, such as poly(vinylferrocene) [24] and poly(4-nitrostyrene) [25]. Pendant group attachment is a much more flexible approach, wherein well characterised functionalised, linear polymers (poly (4-vinylpyridine)) are reacted with suitable substituted redox molecules [26,27].

4.3.2. In-situ assembly

Redox polymer formation in-situ, was first introduced by Wrighton [28], and Murray and Meyers [29,30]. The hydrolytically reactive monomers demonstrated by Wrighton, are based on attaching reactive organosilane functionalities such as ferrocenes and viologens, and all exhibit good electron transfer activity.

Redox polymers can also be formed by electrochemical polymerisation, the main requirements being that the monomer (a) has an oxidation potential which is accesible via a suitable solvent system; (b) will produce a radical cation which reacts more quickly with other monomers to form the polymer than it will with other nucleophiles in the electrolyte system; and (c) produces a polymer with a lower oxidation potential than that of the monomer [31-33]. The process of electropolymerisation is rather complex and involves diffusion of a monomer to the electrode surface, activating reduction or oxidation, and then competing diffusion away from the electrode and precipitation onto the electrode surface [34]. The monomers involved in the process are often quite bulky and allow permeability of small molecules and counterions through the interstices between monomer sites. Hence the polymer acts as a molecular sieve, selectively allowing molecules according to their molecular size. Pyrrole is commonly used in such processes, as its electronic charge is delocalised along the chain [35]. Ferrocene and ferrocenium groups in poly(vinylferrocene) are also used; the overall result is a 'conducting polymer' with facile transfer kinetics.

4.3.3. Ion-Exchange polymers

Coating an electrode with ion-exchange polymers was first introduced by Anson and co-workers [36,37], who adsorbed poly(vinylpyridine) onto graphite electrodes. Formation of ion-exchange layers involves coating an adherent film of the ion-exchange polymer onto the electrode in the presence of a suitable solvent which enables the polymer film to 'swell'. This condition is necessary to allow counterion movement into and out of the polymeric film. Nafion, a sulfonated perfluorinated poly(ether), was first developed by DuPont. It is a highly stable cationic ion conductor membrane, and is frequently used in sensor-based applications. An attractive feature of this compound is that it can be dissolved in ethanol and re-cast, but remains completely insoluble in water [38]. Nafion and other related perfluoropolymers have a large proportion of charged hydrophilic sites, with long segments of hydrophobic chains which remain flexible even after cross-linking. The charged sulfonate sites move away from the hydrophobic chains into water filled channels surrounded by coiled hydrophobic perfluoro-poly(ether) chains. This phase segregation greatly modifies Nafion's ion-exchange character whereby in-partitioning is governed by both charge and hydrophobicity of the redox ion [39].

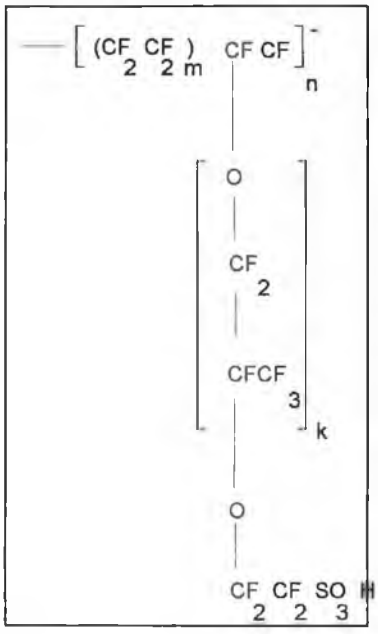

Figure 4.1. Ion-exchange polymer: Nafion , a perfluorosulfonic acid polymer.

4.3.4. Advantages offered by electroactive polymers

In electroactive polymeric films composed of electronically discrete redox sites, electrons are transported through the polymer by hopping between oxidised and reduced redox sites within the matrix [40]. The successful attempts to measure (within accuracy) the electron transfer rate constants between polymeric layers and electrode has provoked intensive research into electron self-exchange mechanisms [41,42]. It has been largely accepted that multilayer films survive a greater number of oxidation state turnovers than do monolayer films (formed by chemisorption, covalent bonding etc.). This indicates that redox sites in multilayer films have an enhanced stability which is important for electrocatalysis. Another attractive feature of these polymer films is their ease of preparation The larger signals yield more straightforward characterisation which is also amenable with these type of polymer films produced.

4.4. IMPROVEMENTS TOWARDS BETTER ELECTRICAL COMMUNICATION

In recent years the electronic industry has made considerable advances towards miniaturisation, while in biology there is now a greater understanding of many living systems at a molecular level. This has provided an even greater opportunity to monitor electrical communication between or within molecules and to sensor technology in sensing and selecting the presence and the concentration of biomolecules in a biochemical reaction. Most biological macromolecules of 50kDa or greater are 'electrical insulators'. The outer protein/glycoprotein layer serves merely as a protective shell, preventing indiscriminate electron exchange between other redox macromolecules and to stabilise the structure; therefore it is not a necessary element for electron exchange catalysis [43]. If this shell is chemically altered without interfering with the activity of the enzyme; forming conducting channels which facilitate electron transfer between enzyme and electrode. This transfer of electrons (current flow) decays exponentially with distance, but can be transferred across distances of 20-25 Å, at relatively high rates when the energy required to reorganise the nucleus is less than or equal to 1 eV [44].

4.4.1. Electrical communication via relays

A system resembling the 'telephone-relays' was proposed [43]. If relays are placed between the reactive centers of enzymes and the working electrode surface, then the rate of electron transfer should increase. This dependence on distance (d) is illustrated in the following equation:

$$k_{et} = 1 \times 10^{13} \exp[-\beta(d-3)] \exp[-(\Delta G + \lambda)^2/4\lambda RT] \qquad (4.3.)$$

where k_{et} is the electron transfer rate, β is a constant for a given electron /donor pair (usually a value of 0.91 Å s^{-1} is used), ΔG is the driving energy per change in free energy upon electron transfer and λ is the Marcus reorganisational energy.

The Marcus reorganisational energy (λ), maintains that for a given reorganisational energy, temperature, distance and in a given medium the rate of electron transfer increases [44]. Hence, as high self-exchange rates are needed, the relays must be capable of transferring and accepting electrons across substantial distances. Many suitable candidates have been investigated i.e. ferrocenes, ferrocenium [45], and ruthenium-based compounds [46]. A problem arose, however, with these relays, which required the orientation of the enzyme to be properly aligned close to the electrode surface for electron exchange.

4.4.2. Electrical 'wiring' of redox enzymes to the electrode via redox polymer chains

A better approach involves 'wiring' the redox enzyme to the electrode using a long polymer of high electron density. Polycationic redox polymers of 10^5 Da approx. with 100-200 redox centres can penetrate and bind with the polyanionic enzyme and also to the electrode. These electrostatic complexes formed between the positively charged relaying redox polymer and negatively charged zones of the enzyme form a rugged cross-linked electroactive film on the surface of the electrode. The electron transfer distance is reduced, eliminating the requirement for a membrane to contain the enzyme - redox polymer couple .

Heller *et al.* [47] have demonstrated electrical communication between redox centres of glucose oxidase and a glassy carbon electrode via electrostatic and covalent binding with a

co-polymer of poly(vinylpyridine)$Os(bpy)_2Cl$ and poly(vinyl-N-methyl pyridinium) chloride, where Os(bpy) is an Osmium bipyridine complex. The sensor stability was improved by forming an insoluble cross-linked film between the polymer and enzyme on the electrode surface [48]. This was achieved by using a cross-linking agent (triethylenetetramine) triene. In the presence of an enzyme and triene, this polymer forms a rugged three dimensional cross-linked electroactive film on the electrode surface between pendant N-hydroxysuccinimide groups and lysines of the enzyme. The improved stabilisation afforded by the enzyme is attributed to the protective arms of the polymer chain preventing attack by proteases, and also due to the enzyme's size, it is physically confined behind the membrane thereby making it less susceptible to thermal denaturation.

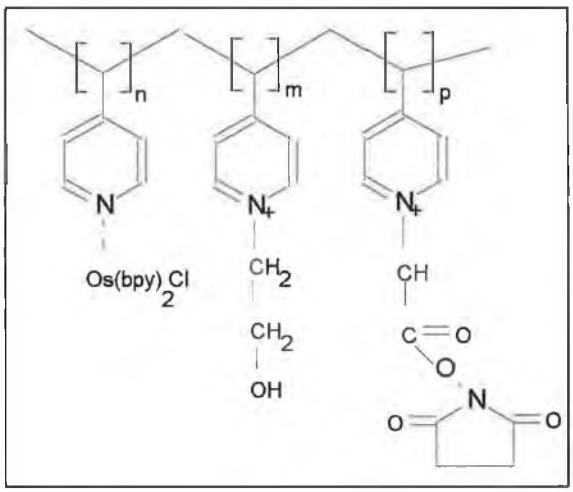

Figure 4.2. Redox 'polymeric wire' of PVP (poly(vinylpyridine)) complexed with $[Os(bpy)_2Cl]^{+/2+}$. The uncomplexed pyridines of the PVP are quaternised with NHS (N-hydroxysuccinimide) that forms amide bonds with both lysines on the enzyme surface and with the crosslinking agent (triethylenetetraamine).

Competition between the desired aminolysis of N-hydroxysuccinimide groups and their spontaneous hydrolysis, have lead to huge variation between films and also due to the N-hydroxysuccinimide groups being capable of reacting with primary amines and water. This was overcome by using a commercially available water-soluble diepoxide poly(ethylene glycol)diglycidyl ether (PEG) [49]. Crosslinking was achieved via the reaction of the epoxide with the pendant amine functions of the polymer and also with the amine functions of the enzyme. This redox 'epoxy cement' between the poly(vinylpyridine) complex and $Os(bpy)_2Cl$ and a diepoxide progressed slowly under near-physiological conditions and could be prepared with or without enzyme, at least 48 hours in advance, remaining essentially unreacted. PEG

(approx. 40 Å long when extended), poly(vinylpyridine) and the $Os(bpy)_2$ complex are highly water soluble and result in a highly swollen gel-like redox polymer structure allowing permeation of both substrate and products relatively easily. Electron diffusion can be explained by random polymer chain motions, bringing the redox sites closer together and allowing 'electron hopping' to occur. Modification of this design include complexing a highly water soluble poly(1-vinylimidazole), (PVI) complex with $[Os(bpy)_2Cl]^+$ and crosslinking with the PEG [50]. These PVI_n-Os polymers did not require quaternisation with bromoethyl-amine, hence the synthesis was simplified somewhat. These complexes also have lower redox potentials than the PVP based complexes, thereby reducing the risk of electrooxidisable interferants.

4.4.3. Ferrocene containing redox mediators for biosensor use

The most widely exploited family of mediators remains that based on ferrocene, with second order rate constants for glucose oxidase mediation quoted in the range 2×10^4-3×10^6 l mol^{-1} s^{-1}. Ferrocenes have redox potentials which are much lower than 0.6 V, and are used in an attempt to reduce interference by other electroactive species in the sample [51]. Okamato et al. [52] designed a highly flexible ferrocene-containing siloxane polymer, which exhibited rapid transfer kinetics. Electron transfer occurred via the reduced flavin co-factor of several oxidases. Several stable amperometric biosensors based on these polymeric systems were constructed [53, 54]. Calvo and co-workers [55] developed a ferrocene containing acrylamide-acrylic acid co-polymer, using either glucose oxidase or horseradish peroxidase enzymes. Later, a polycationic redox hydrogel was constructed [56] by derivatisation of poly(allylamine) with ferrocene carboxaldehyde, and crosslinking the resulting redox polymer with glucose oxidase, using epichlorohydrin. Foulds and Lowe [57] developed a glucose biosensor by anodically forming a redox active polymeric film of pyrrole with the glucose enzyme, which was physically entrapped within the ferrocene containing polypyrrole film. A water-soluble, inclusion complex involving dimethylferrocene and hydroxypropyl-β cyclodextrin, (HPCD) was developed by Luong *et al.* [58], and was used as a glucose biosensor. A simple and rapid redox gel formulation by a one-step procedure was recently developed [59], which involved a copolymerisation reaction of vinylferrocene with acrylamide and methylenebisacrylamide. HPCD was again used, this time to convert the insoluble

vinylferrocene (VF) into a water soluble VF-HPCD inclusion complex, which allowed the copolymerisation reaction to proceed in aqueous solution, while polyacrylamide was used to improve the mechanical stability and degree of crosslinking withinthe polymer matrix. The polyacrylamide based gel, being of high water content, offers a more suitable environment for enzyme stability and activity. Long-term stability of the enzyme-based redox gel electrodes was a problem, however, and currents dropped considerably during the course of one week.

4.4.4. Electrochemically deposited polymers for biosensor applications

Electrochemical polymerisation is an attractive method for the immobilisation of redox enzymes at electrode surfaces, as it allows precise control over the amount of enzyme immobilised and the spatial distribution is well defined and also that multilayer structures can be produced. Lowe *et al.* [60] described work on the immobilisation of glucose oxidase in an electrochemicaly grown film of polypyrrole. A theoretical model for such an amperometric biosensor was described by Bartlett and Whitaker [61]. They were able to distinguish between direct electrochemical reaction of the product of the enzyme reaction at the electrode and reaction throughout the film on the polymer used for immobilisation. The amount of mediator which was oxidised at the supporting electrode decreased with an increase in the rate of electron transfer between the mediator and polymer and with increase in the thickness of the polymer membrane for a given diffusion coefficient and polymer. An advantage of using electrochemically deposited polymers, is that deposition can be followed by monitoring the charge passed, and thus be reproduced from batch to batch. The thickness of the immobilised layer, should be controllable to precise limits. Better mediation kinetics have been achieved by grafting ferrocene moieties onto the polypyrrole backbone [57], or inclusion of other mediators into the polymeric network [62].

4.4.5. Layer thickness and enzyme loading; affects on kinetic parameters

The transport kinetics may be influenced by polymer layer thickness, enzyme loading, or even by the use of selective membranes. Hall and Hall [51] described a theoretical model, which highlights the importance of membrane thickness and enzyme loading on signal response with respect to sensitivity and reproducibility. Increasing membrane thickness advantageously results in lower background current and a greater overall change in current (hence greater

sensitivity to small changes in concentration). They also described how reproducibility of a sensor in which the enzyme is immobilised within a polymer layer depends not only on the manner in which it was deposited, but also on the molecular weight and the composition of the polymer.

4.4.6. Membrane technology

Biosensors which accommodate mediators to shuttle electrons between electrode and enzyme, generally suffer from problems such as leaching of the mediator from the electrode surface or instability of the enzyme and interference from other species present in the solution. The use of membranes that permit preferential transport of substrate and products while posing as a selective barrier to interfering electroactive species has been studied quite extensively. Traditionally, materials such as tracing paper and gelatin were used, and recently have been revived in a study carried out by Evtugyn *et al.* [63]. Gold coated or charged dialysis membranes [64], a bilayer system made of Nafion with cellulose acetate or collagen [65] and a multi-layer electrode system using (HRP) as an interferant eliminating layer [66], have also been used. Luong *et al.* [67] and Deng *et al.* [68] both constructed a glucose biosensor using Nafion to act as a protective membrane against potential interfering agents such as uric and ascorbic acid. However, while these membranes may enhance the stability of the enzyme and protect it from interferences, they all exhibit reduced sensitivity, due to oxygen competition and slower response rates.

4.4.7. Mediator fine-tuning towards an improved biosensor design

A comprehensive study was carried out by Grätzel and co-workers [69,70] on non-physiological redox-active mediators. This involved investigating the physiochemical and electro-chemical properties of a range of group VIII metals which were complexed with a bipyridine ligand. Several factors are necessary of any given mediator, for its use in amperometric biosensors.Some of the more important ones being:

- a high k_{med} value; this is necessary parameter to minimise competition with oxygen
- a low redox potential, thereby reducing the number of potential interferants

- chemical stability in both oxidised and reduced form
- insensitivity to pH and ionic strength changes .

This study was performed on tris(4,4-substituted 2,2'-bipyridine) complexes of iron$^{(III)}$, ruthenium$^{(III)}$and osmium$^{(III)}$ with the aim of elucidating an efficient mediator for the flavoprotein glucose oxidase and other redox active proteins. The mediator in its oxidised state would replace the requirement of molecular oxygen, by accepting electrons from the reduced form of the enzyme. Rate constants (i.e. k_{med} values) were calculated for over twenty complexes. Typical values of $10^{+5} \rightarrow 10^{+6}$ M^{-1} s^{-1} were found, indicating fast electron transfer kinetics. $Os(DMO\text{-}bpy)_3$ where (DMO-bpy) represents 4,4,-dimethoxy-2,2,bipyridine had a value k_{med} of $2.5 \times 10^{+6}$ M^{-1} s^{-1}, at a standard electrode potential of 225 mV in PBS. A slight modification of this compound; $Os(dm\text{-}bpy)_2(DMO\text{-}bpy)$, yielded a k_{med} value of $6.0 \times 10^{+6}$ M^{-1} s^{-1} but at an operating potential (E^0_{PBS}) of 400 mV, where dm-bpy represents dimethyl-bipyridyl. Such a potential is too negative to be of any use as a mediator, even though it has favourable electron transfer kinetics. The ideal range of standard redox potentials for amperometric biosensors is 0-300 mV (vs SCE). At potentials greater than 300 mV, the electrode being poised correspondingly above the redox potential of the complex, would be subject to serious electrochemical interferences in a biological medium (e.g. from urate and ascorbate) with unacceptably high background currents.

The pH and ionic strength dependence on the mediation of GOD by $Os^{(III)}$bpy complexes, infer that the anionic groups close to the enzymes active site control the extent of mediation. Maximum activity was obtained at high pH (in the range 7.5-9.5) with a sharp drop in activity in acidic conditions, closely associated with the pK_a of GOD ($pK_a \approx 4$) and the pKa of Os(bpy) complexes ($pK_a \approx 3.5$). Increasing ionic strength exhibits a decrease in the pseudo-first order rate constant (k_f). The overall mediation reaction appears to be influenced by changes in the tertiary and quaternary structure of GOD and possibly structural re-arrangements of the redox couple. In general, the tris(4,4-substituted-2,2'bipyridine) complexes of $Os^{(III)}$ and $Ru^{(III)}$ and $Fe^{(III)}$, which are all soluble in aqueous solutions are quite bulky molecules, yet exhibit rapid electron transfer kinetics. Studies such as these are required for a greater understanding towards mediator design in purpose built biosensor electrodes.

4.5. BIOSENSORS FOR ENVIRONMENTAL MONITORING

A number of comprehensive reviews have recently been published [71,72], concerning the use of biosensors for environmental health monitoring and control. Recent environmental concerns have resulted in an increased awareness of the need for the development of rapid, inexpensive techniques, to carry out continuous monitoring and control of pollution in water, soil and air. Time and the expense involved are the two major limitations, considered before any analytical investigation is carried out. Limited resources dictate the need for fast and cost-effective analytical technologies that can increase the number of analyses performed and decrease the time required to carry them out. Biosensors appear to fit these requirement quite well; generally, they are cheap, portable and have rapid response rates.

The vast majority of biosensor applications are used essentially for the detection of their substrates. The most advanced of these, the glucose biosensor, is now commercially available; demands for such sensor type being driven by the biomedical field where the need for a quick, simple and easy to use test method, can be used by the general practitioner and diabetic patients.

Enzyme-based sensors developed for environmental monitoring have involved measurements of either (i) the activity of an enzyme stimulated by the presence of a specific pollutant or (ii) by the disturbance of the activity of an enzyme by pollutants [73]. Development of such biosensors call for much higher sensitivity and for a greater tolerance of the biosensor design. Enzyme sensors based on inhibition require more rigorous control of substrate concentration and enzyme activity and also that the inhibition should be reversible.

4.5.1. Toxin sensors

Albery and co-workers [74] have studied the mechanism of oxidation/reduction of horse heart cytochrome c oxidase and its natural cofactor cytochrome C for the sensing of respiratory poisons. The required amplification was achieved by constructing a sensor in which the toxic substance inhibits the enzyme catalysed reaction. Cytochrome c is a haem-containing protein, which transfers electrons in the mitochondrial respiratory chain. The resulting biosensor was

used to detect for the presence of azide, cyanide and hydrogen sulphide, all specific inhibitors of the enzyme (in the μmolar range). However the lack of stability of the immobilised enzyme and the complex requirements of the system such as presence of lipid, restricted its application. Recently Kauffmann et al. [75] have developed a modified version of this biosensor, which incorporated charged lipids; (asolectins) to mimic the biological membrane environment. They observed enhanced electroactivity and reversibility of inhibition, with a LOD of 0.5 μM at neutral pH.

Smit and Cass [76] have demonstrated an enzyme-based dual-working electrode system for the detection of cyanide. These investigators chose the haem-containing glycoprotein horse radish peroxidase (HRP), as their biological sensing element. The dual-electrode system described exploits the electron transfer catalysing properties of peroxidase by oxidising the enzyme via the generation of hydrogen peroxide at a primary electrode and reducing it through the reduction of ferrocenium at a secondary electrode; hence the enzymatic activity occurs close to the electrode surface. This sensor detected cyanide levels of 2 μM and could be operated at temperatures between 5 - 40 °C.

Another study performed by Smit and Rechnitz [77] demonstrated the attractiveness of biosensors for continuous monitoring of toxic substances. Their simple design involved another oxidase enzyme, tyrosinase. This enzyme contains a pair of cupric ions which are assumed to act as the active site for electron exchange. Like cytochrome oxidase, oxygen plays an integral part in the functions of tyrosinase and can be competitively inhibited by toxins such as cyanide. Ferrocyanide was chosen as the natural substrate for tyrosinase which shuttles electrons from tyrosinase to oxygen. This system was 'reagentless' in the sense that it consumes only oxygen and hence demonstrate its effectiveness as a respiratory sensor capable of detecting poisons such as cyanide which compete competitively with oxygen. The regeneration of this sensor was an attractive feature for continuous monitoring as cyanide could be removed by replacing the electrode in buffer solution.

The number of biosensors for environmental applications [72] and the variety and innovation demonstrated for detection of significant pollutants, indicate that biosensors will almost certainly be among the analytical methods used for monitoring our environment.

4.6. METHODS USED TO STUDY CHARGE TRANSPORT WITHIN MULTILAYER BIOSENSORS

In most films, electrochemical charge transport is thought, as proposed originally by Kauffmann [78], to occur by an electron self-exchange reaction between neighbouring oxidised and reduced sites. This electron hopping process is mathematically representable by diffusion laws in which an apparent diffusion coefficient, D_{app}, for charge transport is introduced to measure its rate [79]. A variety of electrochemical techniques have been applied to study charge transport processes, including cyclic voltammetry (CV), rotating disk voltammetry (RDV) and potential step techniques.

4.6.1. Cyclic voltammetry

Cyclic Voltammetry (CV) has become increasingly popular as a means of studying redox states in many areas [80]. It consists of cycling the potential of an electrode, which is immersed in an unstirred solution and measuring the resulting current. The potential of the working electrode is controlled relative to the reference electrode. A typical CV is illustrated in Figure 4.3. The important parameters being the anodic peak current (i_{pa}), the cathodic peak current (i_{pc}), the anodic peak potential (E_{pa})and the cathodic peak potential (E_{pc}). Peak currents are usually measured by extrapolation of the baseline current.

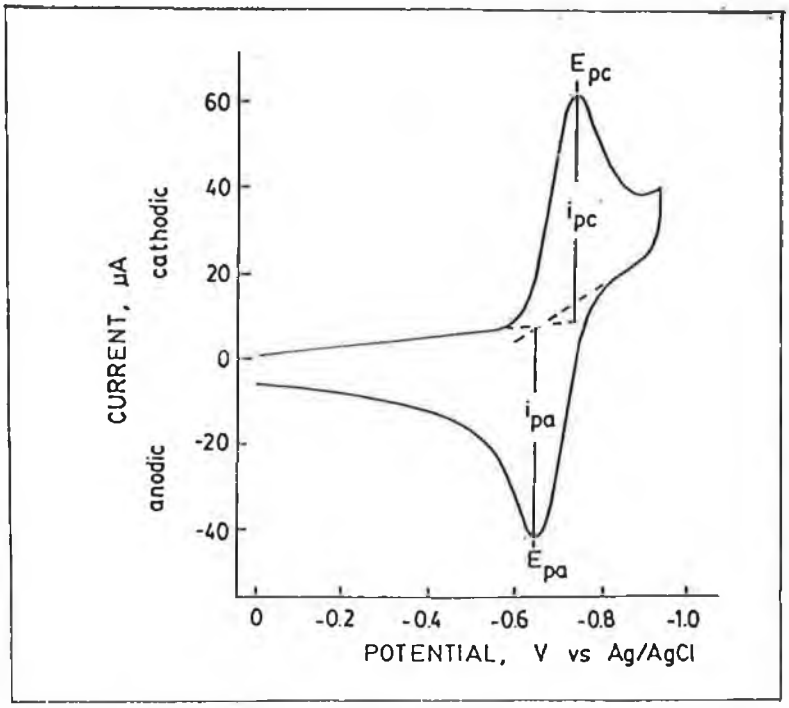

Figure 4.3. A typical cyclic voltammogram

A redox couple in which both species rapidly exchange electrons with the working electrode is termed an electrochemical reversible couple. The formal reduction potential (E^0) for a reversible couple is given by:

$$E^0 = (E_{pa}+E_{pc})/2 \qquad (4.4.)$$

Peak currents for a reversible system are described by the *Randles-Sevcik* equation:

$$i_p = 269n^{3/2}AD^{1/2}C\nu^{1/2} \qquad (4.5.)$$

where n, is the number of electrons transferred in the process, A is the surface area of the electrode (cm^2), D is the diffusion coefficient ($cm^2\ sec^{-1}$), C is the concentration (mol L^{-1}), and ν is the scan rate ($V\ sec^{-1}$).

This technique is most useful as a qualitative diagnostic tool of homogenous chemical reactions. It can rapidly scan over a wide potential range which demonstrates its effectiveness and versatility for observing redox behaviour. CV can generate a species in the forward scan then probe its fate in the backward scan, all in a matter of seconds. It can also generate useful information regarding the stability of the product of the electrode reaction.

4.6.2. Rotating Disk Voltammetry

Rotating disk voltammetry (RDV) can be used to probe the mechanism and position of the reaction zone within the layer of the electrocatalytic reaction [81]. It can yield information relating to the kinetics of electron transfer between redox active sites in polymer coatings and redox species, the permeation rates of the redox species through the polymer film and electron conducting rates through the electroactive polymer film. In RDV, the spinning disk drags with it the layer of liquid at its surface, thus ensuring a continuous flux of matter to the electrode surface. The layer of liquid that is dragged by the rotating disk has a certain thickness, P, often called the 'fluid boundary layer'. Molecules will be pulled into this fluid boundary layer, react, and then proceed to the outer area of the disk by centrifugal forces (ω). The fluid at the disk surface is then replenished by an upward flow normal to the surface by fresh solution .The thickness of this fluid layer is represented by P:

$$\mathbf{P = 3(\nu/\omega)^{1/2}} \qquad (4.6.)$$

where ν is the kinematic viscosity (viscosity /density) ($cm^2\ s^{-1}$) and ω is the angular velocity (usually > 10 sec^{-1}).

Scanning the voltage results in a current that follows a step-shaped curve, the height of which is proportional to the concentration of the active species. For a steady state current to be established in a stirred solution, one must scan slowly or pause sufficiently after each step for any transient to decay. Once this has occurred kinetic control may belong to the charge transfer reaction:

$$\mathbf{I = nFAk_fC^s} \qquad (4.7.)$$

where C^s is the concentration at the surface of the rotating disk electrode.

4.6.3. Potential step techniques

4.6.3.1. Chronopotentiometry

Chronopotentiometry involves controlling the current between the working and reference electrode and measuring the change in potential [82,83]. At the start of an experiment, only the reactants are present and can be detected at a relatively oxidative potential. Upon application of a current, the concentration of the reactant will decrease as it is reduced, and the working electrode potential will become increasingly more negative as the concentration of the reduced species increases.

For a reversible process, the potential can be described by the Nernst equation

$$\mathbf{E = E^0 + (RT/nF)\, lnC_{ox\,(0,t)}/C_{red\,(0,t)}} \qquad (4.8.)$$

where E^0 is the standard potential of the substance analysed and $C_{ox\,(0,t)}$ and $C_{red\,(0,t)}$ are the concentrations of the oxidised and reduced species respectively.

After a certain time, the concentration of the oxidised species becomes close to zero and according to the equation the electrode potential should be very high and negative. The time taken from the start of electrolysis to where change in potential is observed, is usually very rapid and is known as the transition time (τ). Under conditions of linear diffusion in an unstirred solution the transition time (τ) is given by the Sand's equation:

$$\mathbf{\tau^{1/2} = \pi^{1/2} nFAD^{1/2}\, C^0/2i_0} \qquad (4.9.)$$

where i_0 is the current density (Amps).

4.6.3.2. Chronoamperometry

In chronoamperometry, the current is recorded after the application of a potential. When the potential becomes sufficiently negative (due to diffusion of the substance during the reduction process), the concentration of the electrolysed substance at the electrode surface decreases to zero. The rate of change of current is given by the following (Cottrell) equation.

$$\mathbf{i = nFAD^{1/2}C^{0}/(\pi t)^{1/2}} \qquad (4.10)$$

where C^0 is the concentration of the substance under analysis and t is the electrolysis time

4.6.3.3. Chronocoulometry

The measurement of current has more recently been replaced by measurements of charge transferred during the electrolysis at constant potential. This method has been called chronocoulometry and the relationship expressing the rate of change of charge ,Q, is :

$$\mathbf{Q = 2nFAD^{1/2}C^{0}t^{1/2}/\pi^{1/2}} \qquad (4.11.)$$

This technique is particularly useful in studies on adsorption of electroactive substances and kinetic studies.

4.7. REFERENCES

1. Gorton, L. *Electroanalysis* **7** (1995) 23-45.
2. Thompson, M.; Krull, U. J. *Anal. Chem.* **63** (1991) 393A-405A.
3. Clarke Jr. L. C.; Lyons, C. *Annals New York Academy of Sciences* (1969) 29-45.
4. Scheller, F.; Schubert, F.; Pfeiffer, D.; Hintsche, R.; Dransfeld, I.; Rennberg, R.; Wollenberger, U.; Riedel, K.; Pavlova, M.; Kühn, M.; Müller, H-G.; Tan, P.M.; Hoffman, W.; Moritz, W. *Analyst* **114** (1989) 653-662.
5. Bond, A. M. *Anal. Proc.* **30** (1993) 219-226.
6. Palmisano, F.; Guerrieri, A.; Quinto, M.; Zambonin, P. G. *Anal. Chem.* **65** (1995) 1005-1009.
7. Pravda, M.; Jungar, C. M.; Iwuoha, E. I.; Smyth, M. R.; Vytras, K.; Ivaska, A. *Anal. Chim. Acta.* **304** (1995) 127-138.
8. Rohde, E.; Dempsey, E.; Smyth, M. R.; Vos J. G.; Emons, H. *Anal. Chim. Acta.* **278** (1993) 5-16.
9. Doherty, A. P.; Stanley, M. A.; Vos, J. G. Analyst 120 (1995) 2371-2376.
10. Simonian, A. L.; Badalian, I. E.; Berezov, T. T.; Smirnova, I. P.; Khaduev, S. H. *Anal. Letters*, **27** (1994) 2849-2860.
11. Ortega, F.; Cuevas, J.L.; Centenera, J. I.; Domínguez, E. *J. Pharm. Biomed. Anal.* **10** (1992) 789-796.
12. Nordling, M.; Elmgren, M.; Stahlberg, J.; Pettersson, G.; Linquist, S. E. *Anal. Biochem.* **214** (1993) 389-396.
13. O'Shea, T. J.; Lunte, S. M. *Anal. Chem.* **66** (1994) 307-311.
14. Cornish Bowden, A.; Wharton, C. W. *Enzyme Kinetics* , Chapt **1**., Irl. Press, Washington DC.
15. Szuc, A.; Hitchens, G. D.; Bockris, J. O. M. *Bioelectrochemistry and Bioenergetics*, **21** (1989) 133-148.
16. Goldstein, L. Kinetic Behaviour of Immobilised enzyme systems from *Methods in Enzymology* Vol. **XLIV**.
17. Albery, W. J.; Bartlett, P. N.; Svanberg, L. R. 'New electrochemical techniques applied to medicine and biology, 443-474, from *Charge and Field Effects in Biosystems*, Allen, M. J.; Usherwood, P. N. R.

18. Davis, G. *Biosensors* **1** (1985) 161-178.

19. Turner, A. P. F.; Karube, I.; Wilson, G. S. *Biosensors; Fundamentals and Applications* Oxford University Press (1986).

20. Palmer, T. *Understanding Enzymes* Third Ed., Ellis-Horwood Series in Biochemistry and Biotechnology.

21. Eddowes, M. J.; Hill, H. A. O. *J. Amer. Chem. Soc.*, **101** 16 (1979) 4461-4464.

22. Murray, R. W. *Introduction to Chemistry of Molecularly Designed Electrode Surfaces*, Chapt.2, Pub. J. Wiley & sons. Inc.

23. Schmehl, R. H.; Murray, R. W. *J. Electroanal. Chem.* **152** (1983) 97-109.

24. Merz, A.; Bard, A. J. *J. Amer. Chem. Soc.* **100** (1978) 3222-3223.

25. Van der Mark, M. R,; Miller,L. L. J. Amer. Chem. Soc. 100 (1978) 3223-3225.

26. Shigehara, K.; Oyama, N.; Anson, F. C. *J. Amer. Chem. Soc.* **103** (1981) 2552-2558.

27. Calvert, J. M.; Meyers, T. J. *Inorg. Chem.* **20** (1981) 27-33.

28. Wrighton, M. S. *Science*, **231** (1986) 32-37.

29. Pickup, P. G.; Murray, R. W. *J. Amer. Chem. Soc.* **105** (1983) 4510-4514.

30. Abruña, H. D.; Denisevich, P.; Umaña, M.; Meyers, T. J.; Murray, R. W. *J. Amer Chem. Soc.* **103** (1981) 1-5.

31. Kelly, D.; Vos, J. G. *Electroactive Polymer Electrochemistry*, Vol.**2**, Chapt.8, Plenium Press (1996) Editor, Lyons, M. E. G.

32. Evans, G. P. *Advances in Electrochemical Engineering*, Vol. **1**, Chapt 1, VCH Publishers (1990).

33. Facci, J. S.; Schnehl, R. H.; Murray, R. W. *J. Amer. Chem. Soc.* **104** (1982) 4959-4960.

34. McCarley, R.L;. Thomas, R. E.; Irene, E. A.; Murray, R. W. *J. Electrochem. Soc.* **137** (1990) 1485-1490.

35. Diaz, A. F.; Castillo, J.; Kanazawa, K.K.; Logan, J. A.; Solomon, M.; Fajardo, D , *J. Electroanal. Chem.* **133** (1982) 233-239.

36. Oyama, N.; Anson, F. C. *Anal. Chem.* **52** (1980) 1192-1198.

37. Oyama, N.; Anson, F. C. *J. Electrochem. Soc.* **127** (1980) 640-647.

38. Martin, C. R.; Rhoades, T. A.; Ferguson, J. A. *Anal. Chem.* **54** (1982) 1639-1641.

39. Szentirmay, M. N.; Martin, C. R. *Anal. Chem.* **56** (1984) 1898-1902.

40. Kauffman, F.B.; Schroder, A. H.; Engler, E. M.; Kramer, S. R.; Chambers, J. Q. *J. Amer. Chem. Soc.* **102** (1980) 483-488.
41. Murray, R. W.; Daum, P. *J. Electroanal. Chem.* **103** (1979) 289-294.
42. Nowak, R. J.; Schultz, F. A.; Umaña, M.; Lam, R.; Murray, R. W. *Anal. Chem.* **52** (1980) 315-321.
43. Heller, A. *Acc. Chem. Res.* **23** (1990) 128-134.
44. Marcus R. A.; Sutin, N. *Biochimica. et Biophysica Acta.* **811** (1985) 265-322
45. Sakura, S.; Buck, R. P. *Bioelectrochem. Bioenerg.* **28** (1992) 387-400.
46. Crumbliss, A. L.; Hill, H. A.; Page, D. J. *J. Electroanal. Chem.* **206** (1986) 327-331.
47. Degani, Y.; Heller, A. *J.Amer. Chem. Soc.* **111** (1989) 2357-2358.
48. Gregg, B. A.; Heller, A. *Anal. Chem.* **62** (1990) 258-263.
49. Gregg, B. A.; Heller, A. *J.Phys. Chem.* **95** (1991) 5970-5975.
50. Ohara, T. J.; Rajagopalan, R.; Heller, A. *Anal. Chem.* **65** (1993) 3512-3517.
51. Hall, E. A. H.; Gooding, J. J.; Hall, C. E. *Mikrochim. Acta.* **121**, (1995) 119-145.
52. Hale, P. D.; Inagaki, T.; Karan, H. I.; Okamoto, Y.; Skotheim, T. A. *J. Amer. Chem. Soc.* **111** (1989) 3482-3484.
53. Hale, P. D.; Boguslavsky, L. I.; Inagaki, T.; Karan, H. I.; Lee, H. S.; Skotheim, T. A.; Okamoto, Y. *Anal. Chem.* **63** (1991) 677-682.
54. Hale, P. D.; Lee, H. S.; Okamoto, Y. *Anal. Lett.* **26** (1993) 1-16.
55. Calvo, E. J.; Danilowicz, C.; Diaz, L. *J. Chem. Soc. Faraday Trans.* **89** (1993) 377-384.
56. Calvo, E. J.; Danilowicz, C.; Diaz, L. *J. Electroanal. Chem.* **369** (1994) 279-282.
57. Foulds, N. C.; Lowe, C. R. *Anal. Chem.* **60** (1988) 2473-2478.
58. Groom, C. A.; Luong, J. H. T. *Biosensors and Bioelectronics*, **9** (1994) 305-313.
59. Bu, H.; Mikkelsen, S. R.; English, A. M.; *Anal. Chem.* **67** (1995) 4071-4076.
60. Foulds, N. C.; Lowe, C. R. *J. Chem. Soc. Faraday Trans.* **1** (1986) 1259-1264.
61. Bartlett, P. N. Whitaker, R. G. *J. Electroanal. Chem. 224* (1987) 27-35.
62. Kjiya, Y.; Sugai, H.; Iwakura, C.; Yoneyama, H. *Anal. Chem.* **63** (1991) 49-54.
63. Budnikov, H. C.; Evtugyn, G. A. *Electranalysis*, **8** (1996) 817-820.
64. Lobel, E.; Rishpon, J. *Anal. Chem.*, **53** (1981) 51-53.
65. Bindra, D. S.; Wilson, G. S. *Anal. Chem.*, **61** (1989) 2566-2570.
66. Maidan, R.; Heller,A. *Anal. Chem.*, **64** (1992) 2889-2896.

67. Brown, R. S.; Luong, J. H. T. *Anal. Chim. Acta*. **310** (1995) 419-427.

68. Liu. H.; Deng, J. *Anal. Chim. Acta*. **300** (1995) 65-70.

69. Zakeeruddin, S. M.; Fraser, D. M.; Nazeeruddin, M-K.; Gratzel, M. *J. Electroanal. Chem.* **337** (1992) 253-283.

70. Fraser, D. M.; Zakerruddin, S. M.; Gratzel, M. *J. Electroanal. Chem*. **359** (1993) 125-139.

71. Rogers, K. R.; Williams, L. R. *Trends Anal. Chem*. **14** (1995) 295-299.

72. Karube, I.; Nomura, Y. Arikawa, Y. *Trends. Anal. Chem*. **14** (1995) 289-294.

73. Gaisford, W. C.; Rawson, D. M. *Meas. Control* **22** (1989) 183-186.

74. Albery, W. J.; Cass, A. E. G.; Mangold, B. P.; Shu, Z. X. *Biosensors and Bioelectronics*, **5** (1990) 397-413.

75. Amine, A. Alafandy, M. Kauffmann, J-M. Pekli, M. N. *Anal. Chem*. **67** (1995) 2822-2827.

76. Smit, M. H.; Cass, A. E. G. *Anal. Chem.* **62** (1990) 2429-2436.

77. Smit, M. H.; Rechnitz, G. A. *Anal. Chem.* **65** (1993) 380-385.

78. Kauffmann, B.; Engler, E. M. *J. Amer. Chem. Soc.* **101** (1979) 547-549.

79. Daum, P.; Lenhart, J. R.; Rolinson, D.; Murray, R. W. *J. Amer. Chem. Soc.* **102** (1980) 4649-4653.

80. Heinman, W. R.; Kissinger, P. *Amer. Lab*. **15** (1982) 29-38

81. Vassos, B. H.; Ewing, G. W. *Electroanalytical Chemistry*, Chapt.11, J. Wiley & sons. Inc.(Publishers).

82. Bond, A. M. *Modern Polarographic Methods in Analytical Chemistry*, Chapt.8, Marcel, Dekker Press.

83. Galus, Z. *Fundamentals of Electrochemical Analysis*, Chapt.2 Ellis Horwood Ltd.(Publishers).

CHAPTER 5

REAGENTLESS TYROSINASE ELECTRODE FOR THE DETECTION OF RESPIRATORY POISONS

5.1 INTRODUCTION

The catalytic activity of enzymes is not only very selective for their substrates but can also be very sensitive to the presence of inhibitors. The amplifying nature imparted by enzymes, coupled to the sensitivity of many amperometric devices, provides us with the opportunity of developing sensitive and selective biosensor devices for the detection of toxins at submolar concentrations.

The use of the redox species, $[Os(bpy)_2Cl]Cl^{+/0}$, $[Os(bpy)_2(MeIm)Cl]^{2+/+}$ and $[Fe(CN)_6]^{4-/3-}$, where bpy is 2,2-bipyridine and MeIm is N-methylimidazole, as electron mediators in the enzymatic reduction of oxygen by tyrosinase was investigated in solution. Co-immobilisation of both enzyme and an osmium redox mediator in a hydrogel on a glassy carbon electrode results in a biosensor for the 'reagentless' addressing of enzyme activity, consuming only oxygen present in the solution.

Biosensors offer a number of advantages over conventional analytical techniques: high specificity, simplicity, portability and low cost. In this chapter, an immobilised enzyme inhibition biosensor is described for the detection of tyrosinase inhibitors, such as sodium azide, using this approach. The enzyme inhibition biosensor was capable of detecting levels as low as 5×10^{-6} mol dm^{-3} in solution and may in the future prove to be useful in environmental monitoring applications as an early warning poison sensor.

5.1.1. Osmium and Group VIII metal redox polymers for biosensor applications

Osmium and many other group VIII metal complexes are a versatile family of molecules which can undergo oxidation state changes, are strong visible light absorbers, are photochemically active and are catalysts for a wide range of reactions [1]. These complexes, when attached to a solid support, have great potential in applications such as redox catalysts, chemical analysis, solar energy conversion, optical storage devices and electrochromic displays [2].

Pioneered by Heller [3,4], considerable effort has been expended on the establishment of direct electrical communication between redox enzymes and metal electrode surfaces by use of these osmium redox complexes. Such complexes can penetrate the enzymes sufficiently deep and can shuttle electrons from the active site of the enzyme to the electrode and have been applied for use as amperometric biosensors [5]. Polyanionic enzymes can be electrostatically complexed with polycationic redox polymers such as osmium- and ruthenium-based polymers, with typical values of 100-200 redox centers and several hundred cationic sites. These redox polymers demonstrate fast electron transfer kinetics, are rugged and have suitable potential in the 0.2-0.5 V (vs SCE) range [3].

In the presence of an enzyme and a cross-linking agent, the polycationic polymer forms an insoluble cross-linked film containing covalently bound enzyme on the surface of an electrode. The need for a membrane to contain the enzyme is eliminated in the resulting electrode [5]. Modifications to Hellers [3] original design include: use of a commercially available water-soluble diepoxide as cross-linking agent; poly(ethyleneglycol)-diglycidyl ether, PEG [6]. This compound reacts with the primary amine functions on the redox polymer and the enzyme. Other modifications include: alteration of the polymer backbone from Poly(4-vinyl-pyridine), PVP to Poly(1-vinylimidazole), PVI. This improved the polymer properties resulting in a water soluble redox hydrogel, which adhered well to the electrode surface without the need for quaternisation and had lower operating potentials, which reduced the risk of electrooxidisable interferants [7]. Recently [8], this particular biosensor design has been used for subcutaneous monitoring of glucose in rats and it is envisaged that this biosensor design will assist biomedical monitoring processes.

5.1.2. Tyrosinase

Tyrosinase (polyphenol oxidase: EC 1.14.18.1) is an enzyme commonly found in nature. It is mainly involved in the biosynthesis of melanin and other polyphenolic compounds. The postulated catalytic enzyme reactions of tyrosinase are shown where D(red) normally represents an o-diphenol (catecholase activity) or a mono-phenol activity (cresolase

activity) and met-Tyr and deoxy-Tyr are the oxidised Cu^{II}-Cu^{II}, where the binuclear copper sites are bridged by an endogenous ligand and co-ordinatively bound to three histidine ligands and reduced Cu^{I}-Cu^{I} forms of the enzyme copper active site, respectively [9,10]. The mechanisms of enzyme action is a modified ping-pong reaction where the enzyme copper sites are reduced by the substrate D(red) and re-oxidised by oxygen [11]:

$$\textbf{D(red) + met-Tyr} \rightarrow \textbf{D(ox) + deoxy-Tyr} \qquad \text{(i)}$$

$$\textbf{deoxy-Tyr + } \mathbf{O_2} \rightarrow \textbf{oxy-Tyr} \qquad \text{(ii)}$$

$$\textbf{oxy-Tyr + D(red)} \rightarrow \textbf{met-Tyr + D(ox) + } \mathbf{H_2O} \qquad \text{(iii)}$$

Kubowitz [12] established the involvement of copper as the prosthetic group in tyrosinase. Little is known, however, of the molecular structure of tyrosinase, due to the heterogeneity of tyrosinase preparations. Bacterial tyrosinase are normally obtained from a large number of the *Streptomyces* strains. The molecular weight appears to vary from 29,000-41,000 Da, and differ substantially from other tyrosinases in their substrate specificity.

Of all the studies carried out on tyrosinases, most research has been devoted to mushroom tyrosinase (*Agaricus bisporus)*. It is composed of four polypeptide chains (two heavy chains and two light chains) differing in their amino acid composition. It has a total molecular weight of approximately 1.2×10^5 Da and contains two of the binuclear copper active sites per molecule [11]. More information is known about Neurospora tyrosinase which consists of a single polypeptide chain of 407 amino acids with a molecular weight of 46,000 Da. It also contains a binuclear copper complex [11]. Copper proteins provide well characterized examples in which the unusual electronic structures of their active sites contribute to rapid long range electron transfer reactivity. Solomon [9] has carried out extensive spectral studies on the oxidized form of tyrosinase, i.e. oxytyrosinase, and has correlated spectral data with bonding calculations to develop a detailed description of the

electronic structure of its active sites. It has a rather unusual electronic structure compared with other copper containing proteins which may reflect its importance as a biological catalyst.

5.1.3. Atomic Absorption Spectrometry (AAS) studies

Duckworth and Coleman [13] and Jolley and co-workers [14] have used AAS and UV absorbance detection (involving the oxidation of tyrosinase using hydrogen peroxide) methods for the rapid analysis of the copper content in tyrosinases. No sample preparation was necessary, and by simply preparing a standard curve, the total enzyme copper was evaluated. Both research groups used flame AAS, which requires quite large sample volumes to achieve good sensitivity.

Graphite Furnace AAS was used in this study to analyse the copper content in tyrosinase (*Agaricus bisporus*). This form of atomisation has several advantages over the conventional flame method. Firstly, the sample is dispensed (usually 5-20 μl) in a small graphite tube, which is then heated electrically by increasing the temperature stepwise. The process of drying, thermal decomposition of the matrix and thermal dissociation into free atoms (atomization) can then be separated. In flame AAS, the sample is nebulised into the flame, and the above process of drying to the dissociation stage occurs within the flame. These processes, which are in part equilibrium reactions will depend on the temperature of the flame and must occur within a few milliseconds, else the sample will have passed out of the light path. Chemical interference is a major problem in flame AAS, whereas in graphite furnace AAS, much of the matrix components and interfering substances can be removed before atomization. By reducing the gas stream through the graphite tube during atomization the free atoms remain in the light beam for up to a thousand times longer than with flame AAS. Consequently, a larger number of sample atoms are stimulated to light absorption; hence this technique is very useful for small sample volumes or for determining trace amounts of metals in samples.

5.2. EXPERIMENTAL

5.2.1. Apparatus for Atomic Absorption analysis

The graphite furnace AAS equipment consisted of a Perkin-Elmer 2380 AAS and a Perkin-Elmer HGA-50 Programmer which was interfaced with a Gold Star computer. A pyrolytic coated graphite tube was used which allows greater sensitivity and longer lifetimes than the standard high density graphite tubes. A copper hollow cathode lamp (HCL) with optimum sensitivity at $\lambda = 324$ nm and a lamp current of 15 mA were used.

5.2.2. Reagents and Materials

Tyrosinase (polyphenol oxidase E.C.1.14.18.1) from *Agaricus bisporus* was obtained from Sigma. Enzyme activities studied included 8,300 units/mg solid and 3,900 units/mg solid. 1000 mg/L Copper sulphate standard solutions were supplied by Merck (Darmstad, Germany) and analytical grade nitric acid by B.D.H. (Poole, England). All water used was purified using a Milli-Q filtration system (Millipore, Bedford, MA, USA).

$[Os(bpy)_2Cl]Cl^{+/0}$ and $[Os(bpy)_2MeIm]PF_6^{2+/+}$ where $(bpy)_2$ = 2,2-bipyridine and MeIm = N-methylimidazole, were kindly donated by Dr. Dónal Leech, (Université de Montréal, Montréal, Québéc). 0.05 M PB, pH 7.4, was prepared using analytical grade disodium hydrogen phosphate and dihydrogen sodium phosphate (Riedel-de Haën) The oxidised form of $[Os(bpy)_2MeIm]PF_6^{2+/+}$ was prepared immediately before use by oxidation of a suspension of the reduced complex in P.B. with PbO_2. Stock solutions of Ferricyanide (Aldrich) were prepared fresh daily in P.B. Sodium azide solutions (Aldrich) were prepared fresh daily in distilled water.

5.2.3. Standard solution preparation

To avoid any extraneous peaks, all glassware was soaked in a 20% nitric acid solution for 24 hours. Standard solutions were prepared by diluting the copper stock solution (1000 mg/L) in a 1% nitric acid solution to the appropriate volume required. The range chosen was 0-150 ppb Cu. The tyrosinase samples were simply dissolved in a 1% nitric acid solution.

5.2.4. Procedure for Atomic Absorption analysis

20 µl of either standard or sample were dispensed into the graphite tube which was then heated resistively by passing a current through it. The sample was first dried at a low temperature (110 ^{0}C), followed by pyrolysis at 900 ^{0}C. This step destroys any organic matter that produces smoke and scatters the light source during measurement. The smoke from pyrolysis and any solvent vapours were flushed out with argon and finally the sample was rapidly thermally atomised at a high temperature. (Table 5.1). The entire time from drying of the sample to analysis takes less than 2 minutes to perform. Water (recommended temperature of 20 ^{0}C) was pumped at a rate of 900 ml/min around the graphite tube to approach room temperature quickly between analyses. If the water is too cold or flowing to fast, atmospheric moisture may condense on the contacts or windows and cause attenuation of the sample light beam.

Stage	**Temperature** (°C)	**Rate** (ml/min)	**Ramp** (seconds)	**Hold-Time** (seconds)
Drying	110	300	5	40
Charring	900	300	5	40
Atomisation	2200	10	1	10
Clean-up	2400	300	1	5

Table 5.1. Conditions for Graphite Furnace AAS.

5.2.5. Apparatus for Electrochemical experiments

Electrochemical experiments were performed using a Pine Instruments AFC BPI BiPotentiostat coupled to a BioAnalytical Systems (BAS) X-Y recorder. Either a 0.5 ml micro-cell or a 2 ml one compartment thermostatted cell was used in all experiments. The electrochemical cell consisted of a Ag/AgCl reference electrode (BAS, 3 mol dm^{-3} KCl) a Pt wire counter electrode (Aldrich), and a 3 mm diameter glassy carbon working electrode purchased from BAS or constructed in-house by embedding a glassy carbon rod (V-25, Atomergic Chemetals) in a glass tube using spurr low viscosity epoxy (Polyscience) and contacting the unexposed side to a copper wire with a silver epoxy (Epoxy Technology). Rotating disk electrode experiments were performed using an EG & G Princeton Applied Research electrochemical analyser, connected to a Philips PM 8621 x-t recorder. A rotating glassy carbon disk working electrode (RDE) of 3 mm in diameter, was obtained from Metrohm AG 628 rotator and was used for all RDE experiments.

5.2.6. Redox polymer modified electrode preparation

Redox polymer modified electrodes containing coordinatively bound tyrosinase were prepared using polyoxyethylene bis(glycidyl ether), PEG, from Sigma, as the crosslinking agent. The structures of the redox polymer and the crosslinking agent used are illustrated in Figure 5.1. Aliquots of the redox polymer (1 mg/ml in water), followed by aliquots of PEG (2.5 mg/ml in water) and finally tyrosinase (2.5 mg/ml in PB) were pipetted onto the surface of a glassy carbon electrode. The subsequent hydrogel formed was allowed to dry in a solvent saturated chamber for a least 48 hours before use. The RDE was prepared as for the cyclic voltammetry experiments, with 5 μl volumes of each of the materials described being drop-coated onto the electrode surface and dried in a water saturated chamber as before.

5.2.7. Homogenous inhibition studies

Homogenous inhibition of the tyrosinase enzyme was investigated using OsMeIm redox couple as mediator and sodium azide as a model inhibitor of this enzyme, in 0.05 mol dm^{-3} P.B., pH 7.4. Small volumes of concentrated azide solutions (to minimise volume changes and hence variations in the concentration of both enzyme and mediator) were added successively to a solution (2 ml) of osmium mediator (1 ×10-4 mol dm^{-3}) and enzyme. The solution was magnetically stirred (300 rpm) for 1 minute following each addition, slow scans i.e. 5, 2 and 1 mV/s cyclic voltammograms were recorded following a 1 minute equilibrium period.

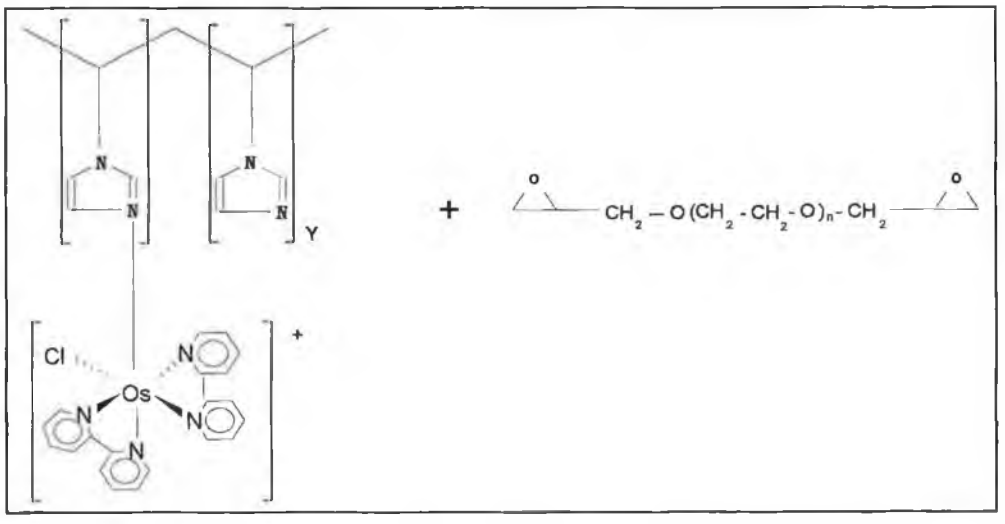

Figure 5.1. $[Os(bpy)_2PVI_YCl]^+$ redox polymer and polyoxyethylene bis(glycidyl ether) as the crosslinking agent.

5.3. RESULTS AND DISCUSSION

5.3.1. Atomic Absorption analysis for the estimation of the copper content in the tyrosinase enzyme

The concentration of Copper in the tyrosinase enzyme was estimated by two methods:(i) standard curve and (ii) standard additions for both enzymes activities. Using the standard curve method the copper content in the tyrosinase sample of activity 8,300 units/mg solid was evaluated by extrapolating from both the peak area and peak height curves. The value obtained was then corrected to the amount of copper per gram of sample. Values of 26.78 μg/g and 28.06 μg/g were obtained for the peak area and peak heights respectively. For the lower activity enzyme sample of 3,900 units/mg solid values of 8.005 μg/g and 8.73 μg/g were obtained. These results correlate well with those from the higher activity sample.

The method of standard additions is used extensively in AAS. The advantage of standard additions over normal standardisation is that the performance of a specific procedure can be checked under operating conditions to detect flaws and bias in a method. It can reveal errors arising from the way the sample was treated or from the presence of other elements and or compounds in the matrix. The copper content in the tyrosinase sample of activity 8,300 units/mg solid as evaluated by this method gave 75.09 μg/g and 82.86 μg/g (i.e. μg Cu per gram of tyrosinase) for the peak area and peak height respectively.

Volume of copper added. (ul)	Height (A.U.)	S.D.	% S.D.	Area (A.U.)	S.D.	% S.D.
0	0.137 0.138 0.137 0.138	0.001	0.4	0.962 0.982 0.963 0.955	0.01	1.2
50	0.280 0.275 0.284 0.286	0.005	1.7	1.973 2.017 2.043 2.052	0.04	1.8
100	0.421 0.408 0.428 0.414	0.009	2.1	3.072 2.998 3.144 3.011	0.07	2.2
150	0.547 0.552 0.548 0.538	0.006	1.1	4.036 4.107 4.134 4.041	0.049	1.2

Table 5.2. Data obtained for the method of standard additions for the estimation of the copper content in the tyrosinase enzyme with an activity of 8,300 units/mg solid (1:8 dilution of enzyme)

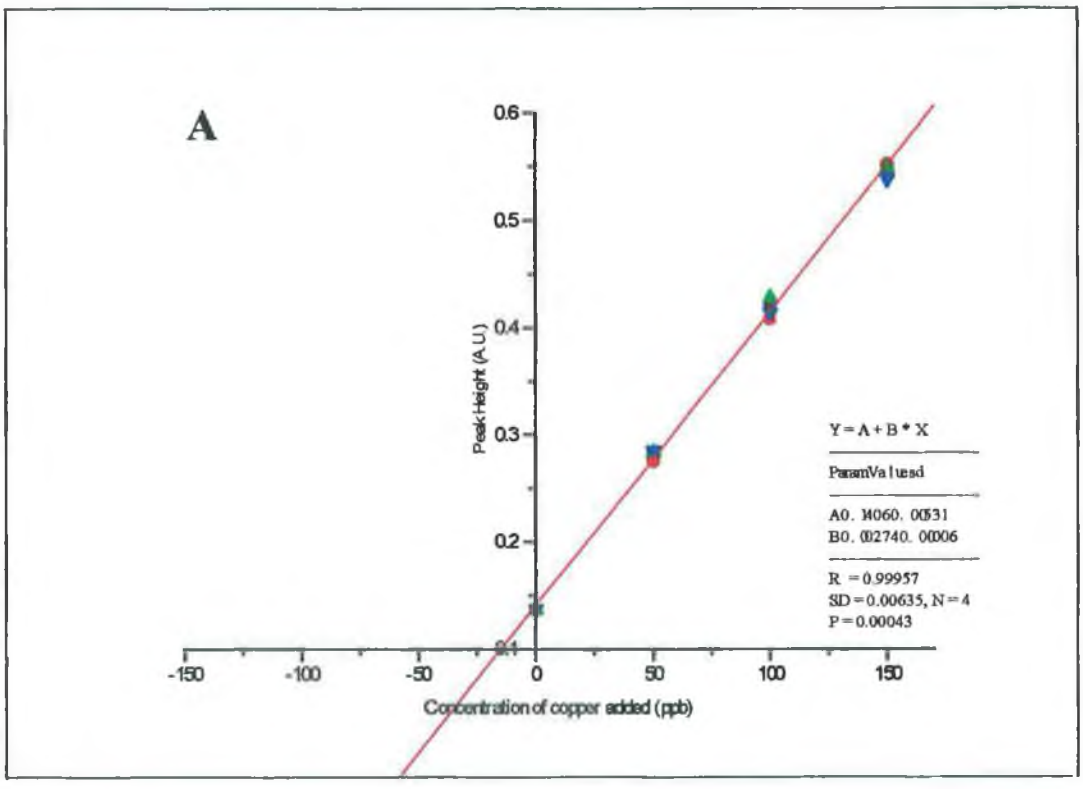

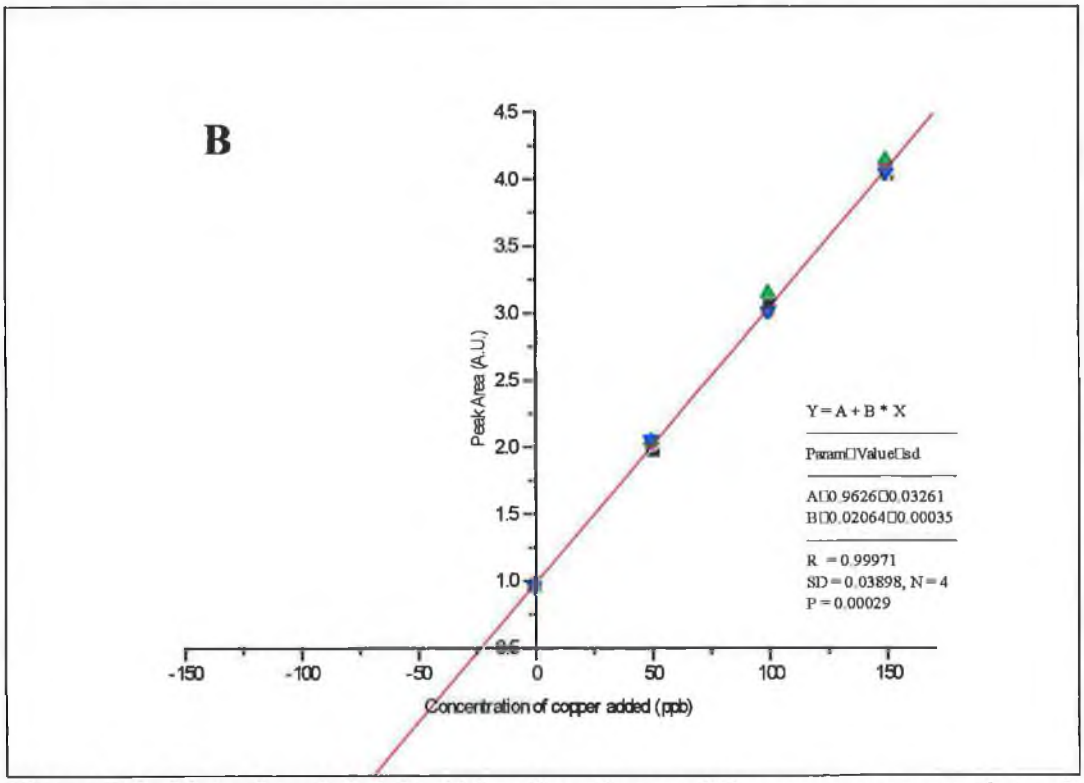

Figure 5.2. Plot of peak height (A) and peak area (B) versus concentration of copper added for the estimation of the copper content in tyrosinase of activity 8,300 units/mg solid, using the method of standard additions.

Using the method by Jolley *et al.* [14] the average of the above results gave a concentration of 0.35 μmoles of tyrosinase per mgram of protein. (Figure 5.2). The 3,900 units/mg solid tyrosinase sample revealed values of 38.29 μg/g and 34.58 μg/g for the peak area and peak height respectively. This value represents a tyrosinase concentration of 0.1675 μmoles/mg. These values calculated are used in the kinetic experiments carried out in the electrochemical section for the estimation of the concentration of tyrosinase used in each experiment.

5.3.2. Osmium based redox compounds as artificial mediators

Osmium and many other group VIII metal complexes are both physically and chemically robust, which makes them ideal candidates for the study of charge mediation in solution or within polymeric films [15]. Charge mediation by the mediators (a) $[Os(bpy)_2Cl]Cl^{+/0}$,

Os(bpy), (b) $[Os(bpy)_2(MeIm)PF_6]^{2+/+}$, OsMeIm, and (c) ferricyanide were investigated in order to allow mechanistic elucidation and some kinetic parameters to be evaluated. Ferricyanide and Osbpy were chosen for the investigation because of their well characterised reversible voltammetry and for the preliminary investigation of the effect the charge on the redox couple on the interaction of the tyrosinase enzyme with electron donors. Optimisation procedures for the mediated oxidation of $[Os(bpy)_2$ with tyrosinase in solution (homogenous case) were also investigated, this involved investigating the effect of varying parameters such as pH, ionic strength and temperature. The OsMeIm complex was selected as a model monomeric compound for the polymeric system that was used for the co-immobilisation of enzyme and osmium electron donor in a hydrogel on the electrode surface. The OsMeIm model monomer exhibited stable reversible voltammetry, that was independent of pH, during the course of the experiments. The voltammetric response, however, tended to degrade if the oxidise form of the monomer was stored at room temperature in P.B. over extended periods (several days). Fresh solutions of the oxidised species were therefore prepared daily or as required. Cyclic voltammetry was used to study the electroactivity of these redox reactions and to investigate the rate of charge transport in these artificial mediators. Typical slow scan cyclic voltammograms of each are illustrated in Figure 5.3.

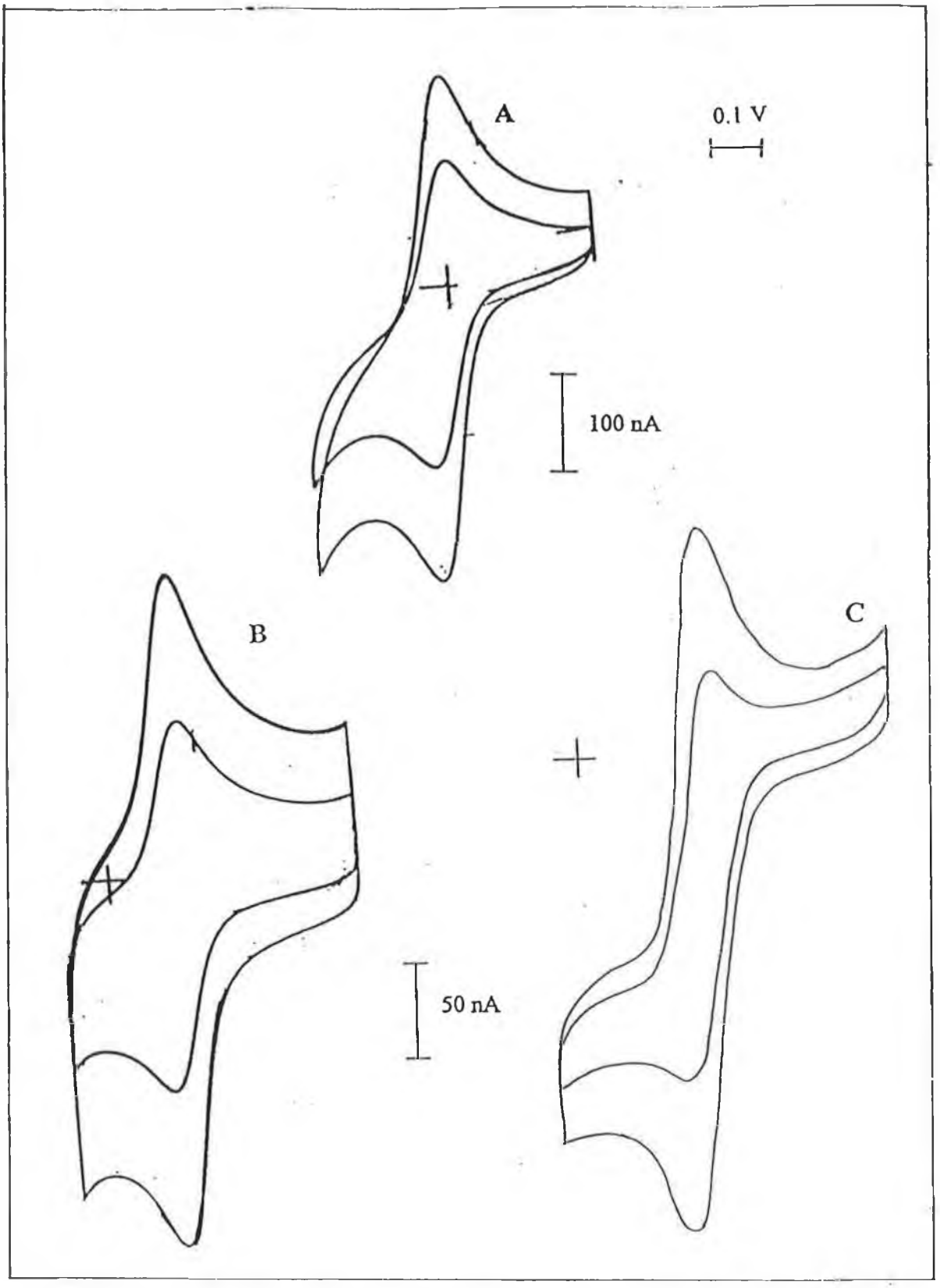

Figure 5.3. Typical slow scan (2,5 mV/s) cyclic voltammograms of 1 $\times 10^{-4}$ mol dm^{-3} solutions of (A); Os(bpy), (B); Os(bpy)MeIm, and (C) Ferricyanide redox couples. Scanning was started at + 300 mV (A), + 500 mV (B) and + 400 mV (C). Crosshairs represent (0,0).

5.3.3. Redox behaviour of tyrosinase

In this study, the natural monophenol and diphenol enzyme substrates are replaced by an electrochemically reversible redox couple which, in the reduced state, can act as an enzyme electron donor. The tyrosinase enzyme has a reduction potential (vs Ag/AgCl) of approximately 310 mV [16], while direct reduction of oxygen at the glassy carbon electrodes utilised in this study begins at approximately -200 mV (vs AgAgCl). Useful electron donors should thus have a reduction potentials between 0 mV and 250 mV in order to yield a response sufficiently removed from the direct reduction current of oxygen while also exhibiting an adequate driving force for the reduction of the enzyme.

Electrochemical switching of the system to an active state is achieved by reduction of the redox complex which can then mediate electron transfer to the enzyme, as depicted in the scheme below, resulting in an electrochemical signal for the enzyme mediated reduction of oxygen.

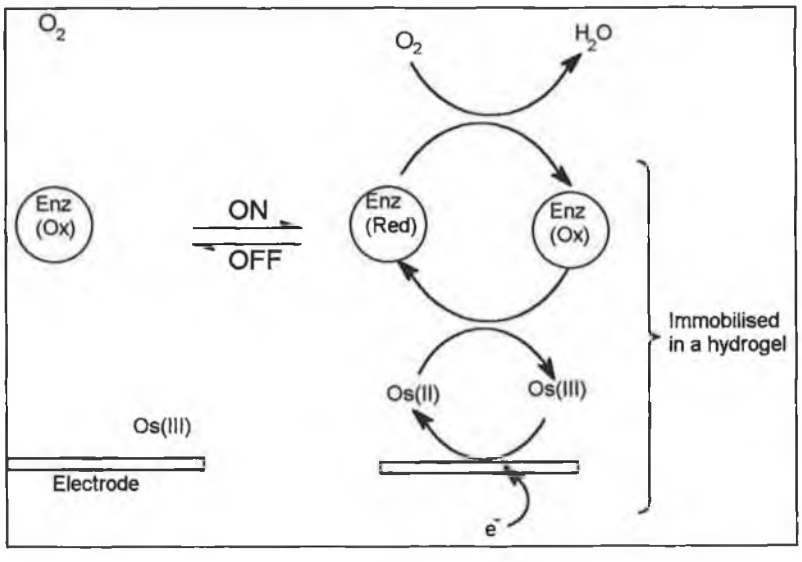

Figure 5.4. Catalytic scheme for the electrochemical sampling of the tyrosinase activity is achieved by switching the potential of the electrode negative of the reduction potential for the osmium redox couple, thereby initiating the catalytic cycle.

5.3.3.1. Determination of kinetic parameters for a reversible electron transfer system

Diffusion coefficients (D_{med}) for the three mediators were evaluated from the variation of peak current with sweep rate according to the Randles-Sevcik equation:

$$i_p = 2.687 \times 10^5 (n)^{3/2} A D^{1/2}_{CT} C v^{1/2} \qquad (5.1)$$

where i_p is the peak current (Amp), n is the number of electrons transferred, A is the area of the electrode (cm^2), D_{CT} is the diffusion coefficient, C is the concentration of the artificial mediator studied, (mol cm^{-3}) and ν is the scan rate (V s^{-1}). See Table 5.3 below.

Mediator	Diffusion coefficient D_{med} (cm^2 s^{-1})
$[Os(bpy)_2(MeIm)PF_6]^{2+/+}$	3.247×10^{-6}
$[Os(bpy)_2Cl]Cl^{+/0}$	6.776×10^{-6}
$[Fe(CN)_6]^{4-/3-}$	5.604×10^{-6}

Table 5.3. Estimation of diffusion coefficients (D_{med}) for the artificial mediators investigated.

The kinetics of interaction between the enzyme and the electron donors $[Fe(CN)_6]^{4-/3-}$, (Osbpy), and (OsMeIm) which exhibit pH independent formal redox potentials of 180 mV, - 20 mV and 130 mV (vs Ag/AgCl) respectively in P.B., pH 7.4 were studied. Typical slow scan cyclic voltammograms (CVs) of 1×10^{-4} mol dm^{-3} $OsMeIm^{2+}$ (A) and $Osbpy^{+}$ (B) in oxygenated P.B. at a glassy carbon electrode both before and following the addition of tyrosinase are shown in Figure 5.5, demonstrating the catalytic enzyme activity for the mediated reduction of oxygen in the presence of the electron donor (an EC' catalytic redox mechanisms). As is apparent from the voltammogram, the enzyme is inactive in the presence of the oxidised redox couple.

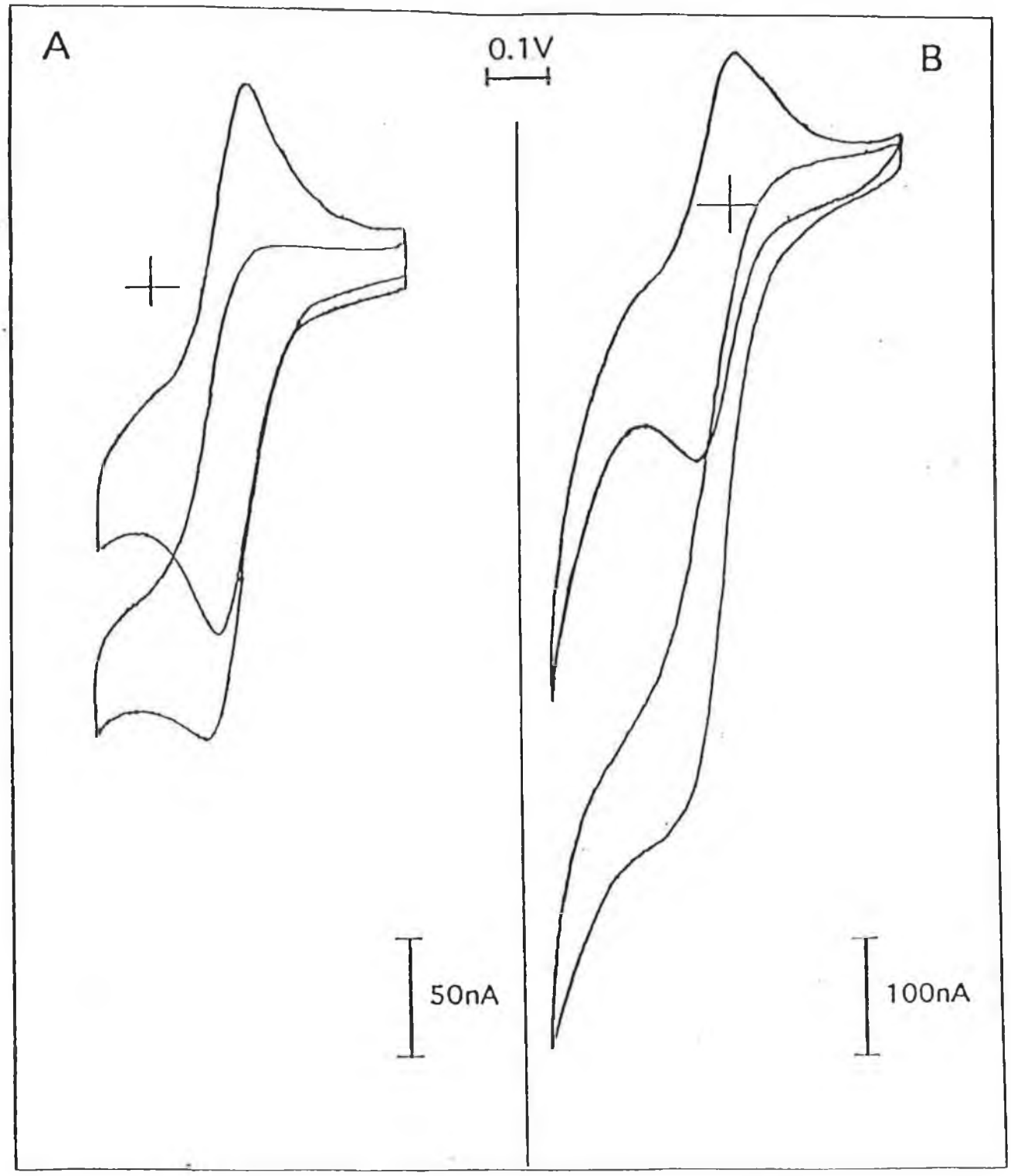

Figure 5.5. Slow scan (2 mV/s) cyclic voltammetry of 1×10^{-4} mol dm^{-3} OsMeIm (A) and Osbpy (B) redox couples both before and after the addition of 0.7×10^{-6} mol dm^{-3} (A) and 1.04×10^{-6} mol dm^{-3} (B) of tyrosinase to the 0.05 mol dm^{-3} phosphate buffer electrolyte (pH 7.4). Scanning was started at potentials of + 400 mV (A) and + 300 mV (B). Crosshairs represent (0,0).

According to the theory developed by Nicholson and Shain [17] for a reversible electron transfer reaction for an immobilised species the peak current is directly proportional to the scan rate as diffusion is not involved. A working curve in which the ratio of the catalytic peak current to the reversible peak current was plotted as a function of the kinetic parameters, $(k_f/a)^{1/2}$, was constructed. k_f is the pseudo first order rate constant and $a= nF\nu/RT$.

For values of k_f/a larger than ≈ 1.0, the plot is essentially linear, for values of $k_f/a < 0.06$ the peak ratio of i_k/i_d is fairly insensitive to changes in k_f/a. This plot is used to accurately determine kinetic rate data for any reversible system. Using the values obtained for k_f from the Nicholson and Shain plot for each of the polymers investigated at various concentrations, and by plotting these values against different enzyme concentrations, the second order rate constant (k_{med}) can be obtained from the slope of the linear plot.

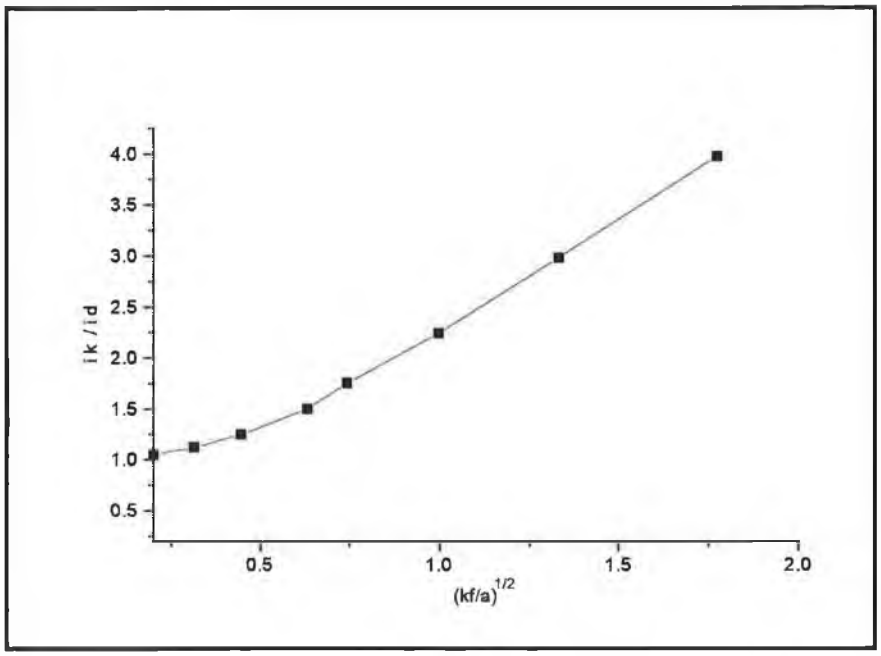

Figure 5.6. Theoretical plot of the ratio of the kinetic to diffusion-controlled peak current, i_k/i_d, versus the kinetic parameter $(k_f/a)^{1/2}$ [17].

Homogenous second order rate constants (k_{med}) for the interaction between the redox couples and the enzyme were evaluated at various scan rates using the approach of Cass *et al.* [18], based on the theory of Nicholson and Shain [17], for steady state voltammetry. While a low concentration of electron donor (1×10^{-4} mol dm^{-3}) and enzyme (0.1 to 1.5 $\times$ 10^{-6} mol dm^{-3}) was utilised in an attempt to maintain saturation oxygen levels (the effective electron-accepting concentration of oxygen in solution is approximately 1×10^{-3} [19], it is recognised that uncertainties in the evaluation of the rate constants can occur using this approach [20]. However, values for the rate constant obtained for rapid kinetics (greater than 1×10^{4} dm^3 $mol^{-1}s^{-1}$) are assumed to be accurate within an order of magnitude.

An alternative method for the evaluation of the second order rate constant is based on the use of the closed-form solution for the current-potential catalytic wave, where the catalytic limiting current (i_k) can be described by equation (5.2) below [21].

$$\mathbf{i_k = nFAC_{med}(2D_{med}k_{med}[E])^{1/2}} \qquad (5.2)$$

where n is the number of electrons transferred, F is the Faraday constant, A is the area of the electrode, C_{med} is the bulk mediator concentration, [E] is the total enzyme concentration, and D_{med} is the diffusion coefficient for the mediator in solution (Table 5.4).

This method for the determination of k_{med} ignores the contribution from the diffusion current of the mediator and is valid provided that the catalytic current is dependent on mediator and enzyme concentration as described above, and is independent of substrate (oxygen) concentration. The second order rate constants evaluated using these approaches were similar and are tabulated in Table 5.4.

Mediator	k_{med} (dm^3 mol^{-1} s^{-1})a	k_{med} (dm^3 mol^{-1} s^{-1})b
Osbpy	3.0 (±1.6) × 10^5	0.9 (±0.2) × 10^5
OsMeIm	0.3 (±0.2) ×10^5	0.4 (±0.1) × 10^5
$[Fe(CN)6]^{4-}$	2.3 (±1.4) ×10^5	0.8 (±0.3) × 10^5

Table 5.4. Rate constants for the reaction between the mediator and tyrosinase.

a: second order rate constant determined by the method of Nicholson and Shain [16],
b: second order rate constant determined by using equation (5.2).

Slightly lower values for the rate constants were obtained using equation (5.2), compared to the method of Cass *et al.* [18], which correlates with the findings reported by other researchers for the glucose oxidase mediated oxidation of glucose by osmium bipyridine complexes [22]. The values obtained for the rate constants are indicative of rapid electron transfer demonstrating the usefulness of these complexes as electron donors for the development of an enzyme inhibition sensor.

The rate constant obtained for the model monomeric complex, OsMeIm, is almost an order of magnitude lower than that obtained for the similar Osbpy redox couple. This decrease in rate constant could be attributed to the effect of the increased positive charge on the monomer or steric effects introduced by the addition of an N-methylimidazole group compared to the Osbpy complex.

5.3.3.2. Enzyme Kinetic analysis

The K_m for the redox couples were evaluated from the slow scan CV's using the plateau of the steady state reduction currents. These currents were measured at - 100 mV, + 100 mV and + 200 mV for Osbpy, OsMeIm and $[Fe(CN)_6]^{4-}$ respectively. The K_m values were

then evaluated using the Eadie Hofstee transformation of the Michaelis-Menten equation (5.3) and the Hanes method, equation (5.4.).

$$i_0 = -K_m (i_0/[S]) + i_{max} \quad (5.3)$$

where $i_0 = nFl\nu_0$, where l is the thickness of the diffusion layer and ν_0 is the initial velocity, when very little of the substrate has reacted, Km is the Michaelis-Menten constant (mol dm^{-3}), [S] is the substrate concentration (mol dm^{-3}) and i_{max} is the maximum current obtained for a particular enzyme concentration.

$$[S]/i_0 = [S]/i_{max} + K_m/i_{max} \quad (5.4)$$

Mediator	K_m (Eadie-Hofstee) (mol dm^{-3})	K_m (Hanes) (mol dm^{-3})
Osbpy	38 (±9) × 10^{-6}	32(± 55) × 10^{-6}
OsMeIm	45 (±20)× 10^{-6}	40 (±27) × 10^{-6}
$[Fe(CN)_6]^{4-}$	34 (±17)× 10^{-6}	33(±13) × 10^{-6}

Table 5.5. Michaelis-Menten constant (K_m) estimated using (i) Eadee-Hofstee and (ii) Hanes methods respectively.

All experiments were carried out in conditions of oxygen saturated buffer. The Hanes analysis of the experimental results gave comparable values for the K_m using the Eadie-Hofstee method, but yielded larger errors in the regression analysis of the linear transformation. Deviations from the straight line Eadie-Hofstee and Hanes plots were observed both at low and high redox couple concentrations, in particular for the OsMeIm redox species, probably because of diffusional limitations and non-saturating co-substrate (oxygen) conditions, respectively. Reported K_m values for the enzymatic oxidation by oxytyrosinase of the monophenolic substrates p-hydroxybenzoate and p-hydroxybenzaldehyde were 55 × 10^{-6} and 28 × 10^{-6} mol dm^{-3}, respectively, while the K_m

for oxidation of the diphenolic substrates 3,4-dihydroxybenzoate and 3,4-dihydroxybenzaldehyde are 0.57×10^{-3} and 0.33×10^{-3} respectively [23]. Tyrosinase oxidation of the physiological substrates L-Tyrosine and L-Dopa has a K_m of approximately 0.3×10^{-3} and 0.5×10^{-3} mol dm $^{-3}$, respectively [24].

5.3.3.3. Effect of Temperature, pH and Ionic Strength

The effect of temperature, pH and ionic strength on the ratio of the catalytic current (i_k) to the diffusional peak current (i_d) obtained in the presence and absence of enzyme, respectively was examined for the OsMeIm complex. The catalytic ratio remains relatively constant between the pH values of 5.0 and 7.5 studied, as reported for the reaction of tyrosinase with other substrates [24]. A slight increase in the catalytic ratio is observed upon decreasing electrolyte solution pH (while maintaining constant ionic strength) to pH 5.0 (Figure 5.7).

An increase in the i_k/i_d ratio of approximately 2.5% per degree Celsius was observed for the OsMeIm monomer upon increasing the temperature, for temperatures up to at least 40°C (Figure 5.8). Similar results were observed for the Osbpy complex. All subsequent experiments were carried out at room temperature and at a pH of 7.4. No enzymatic degradation was observed using these conditions during experiments of up to 12 hours duration on the same solution.

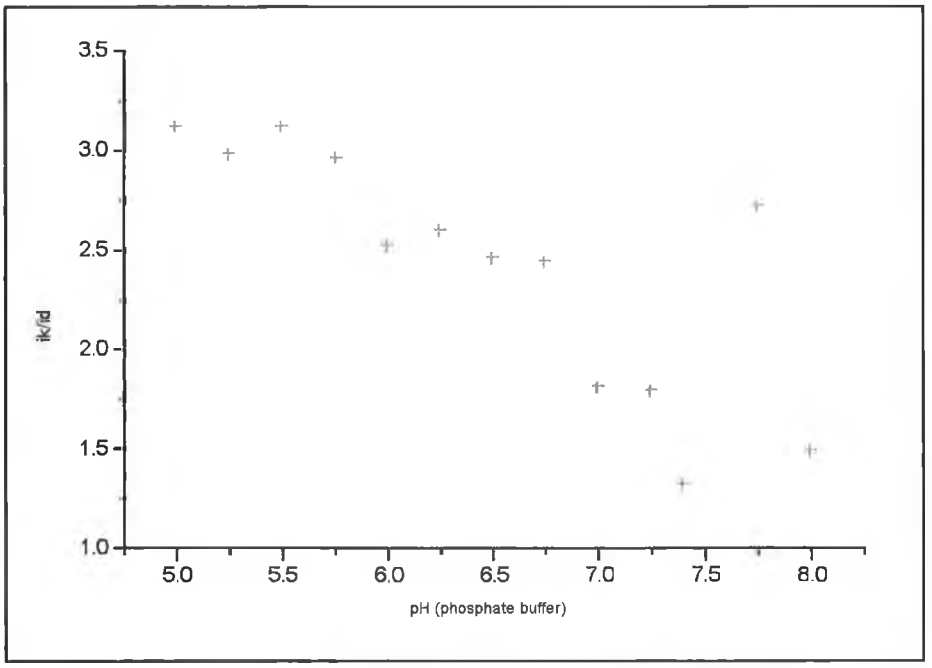

Figure 5.7. The change in the catalytic ratio i_k/i_d, where i_k is the catalytic current obtained in the presence of enzyme and mediator and i_d is the diffusion current observed in the presence of mediator alone, with electrolyte pH (0.05 mol dm^{-3} phosphate buffer) observed using the OsMeIm mediator and slow scan CV (2 mV/s). Tyrosinase and OsMeIm concentrations were 0.2×10^{-6} mol dm^{-3} and 1×10^{-4} mol dm^{-3} respectively. Crosshairs represent the average of three experiments.

Increasing the ionic strength of the solution by addition of sodium chloride led to a decrease in the catalytic ratio for both the OsMeIm and the Osbpy redox species, as shown in Figure 5.9., with a more pronounced decrease observed for the more highly charged OsMeIm species. The decrease in catalytic ratio with increasing ionic strength could therefore indicate shielding of an electrostatic interaction between the positively charged osmium electron donors and the negatively charged tyrosinase enzyme. The results obtained for the second order rate constant however indicate that the charge on the redox species is not a controlling factor in the kinetics of the mediator interaction with tyrosinase. Further studies using similarly sized osmium redox species possessing permanently charged and ionizable groups would help elucidate the factors involved in the interaction of electron donors with tyrosinase.

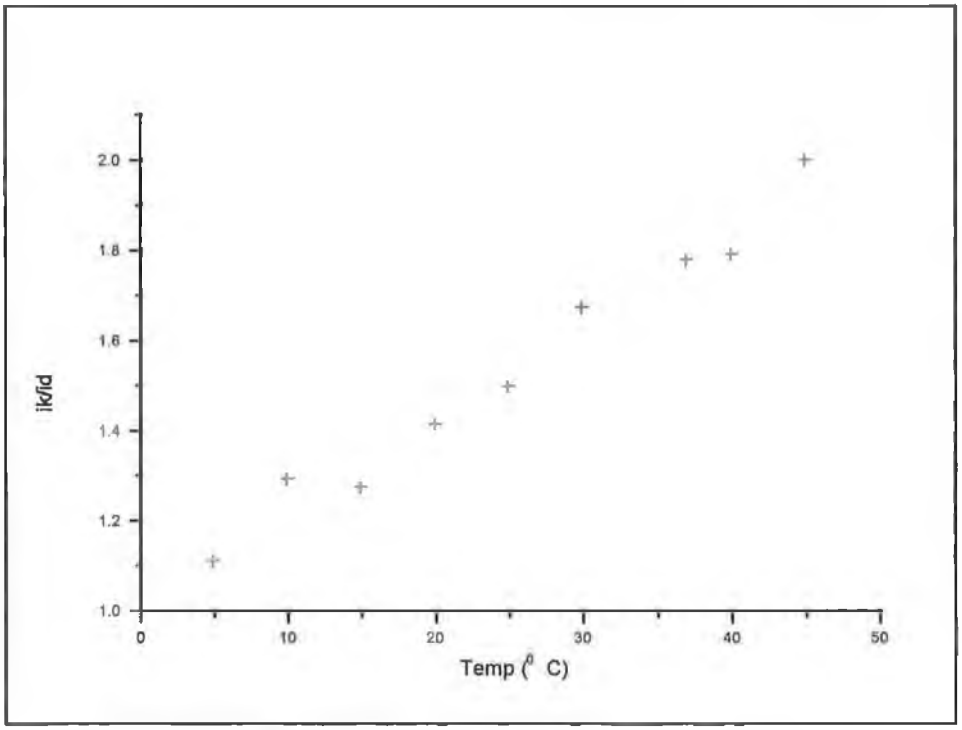

Figure 5.8. The change in catalytic ratio i_k/i_d observed on the tyrosinase activity and MeIm mediator in solution with increasing temperature (in 0.05 mol dm^{-3} phosphate buffer). Scan rate for the cyclic voltammetry was 5 mV/s. Crosshairs represent the average of three experiments.

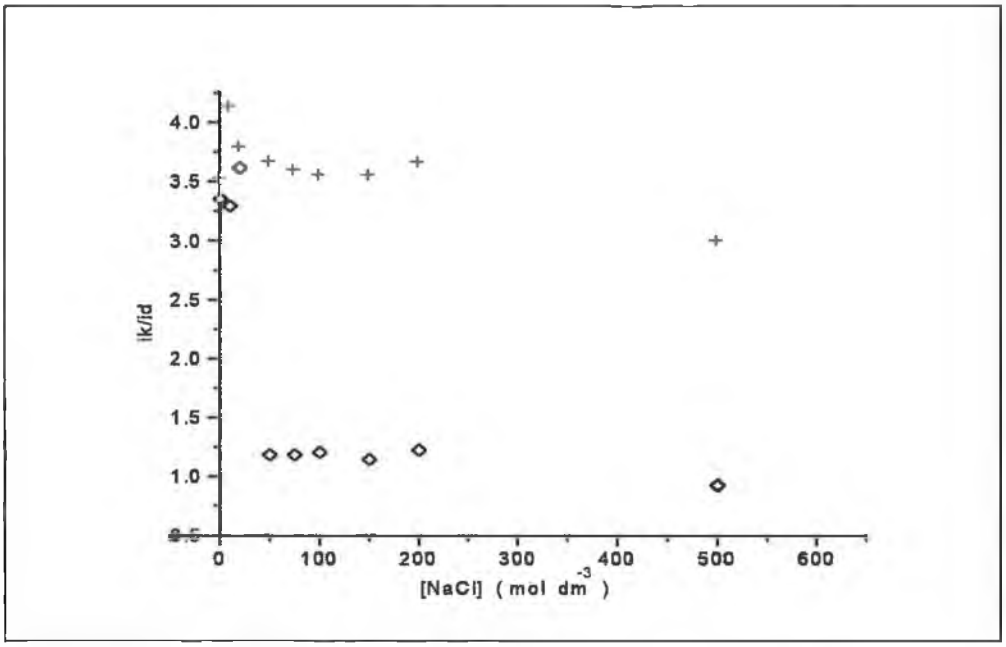

Figure 5.9. Variation of the catalytic current (i_k/i_d) upon increasing concentration of NaCl to a background electrolyte solution of P.B., pH 7.4, for the Osbpy(+) and OsMeIm (◊) mediators. Mediators concentration was 1 $\times 10^{-4}$ mol dm $^{-3}$ and tyrosinase concentration were 0.16 $\times$ 10 $^{-6}$ mol dm^{-3} (+) and 0.19 $\times$ 10^{-6} mol dm^{-3} (◊) respectively. Scan rate for the cyclic voltammogram was 2 mV/s, where the data are represented as the average of three experiments.

5.3.3.4. Homogenous inhibition of the tyrosinase enzyme using the complex $Os(bpy)_2(MeIm)]PF_6^{2+/+}$ as mediator with sodium azide as a model inhibitor

The addition of increased concentrations of azide inhibitor resulted in a measurable decrease in the slow scan rate catalytic currents. Normalised inhibition curves for azide, such as that depicted in Figure 5.10, could be plotted from the slow scan CV data, demonstrating the utility of this method for monitoring enzyme inhibition.

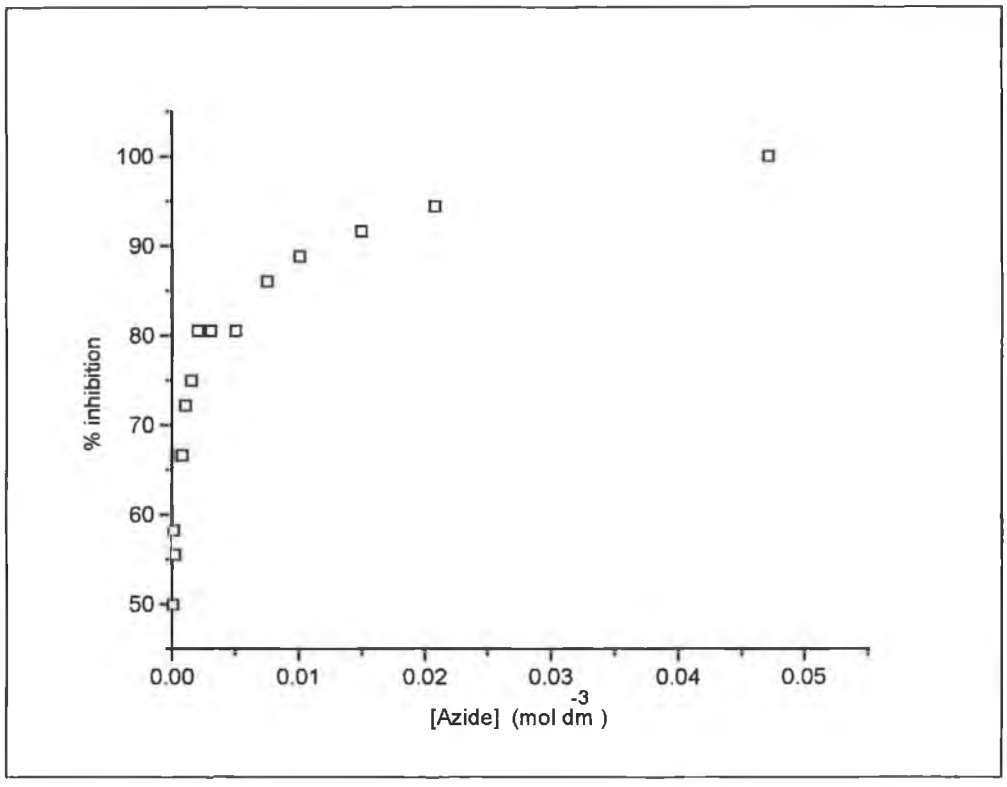

Figure 5.10. Inhibition curve for sodium azide using 1×10^{-4} mol dm^{-3} OsMeIm mediator and 0.17×10^{-6} mol dm^{-3} tyrosinase. Normalisation of the inhibition curve was achieved by calculating $[\{1-(i_{inh}-i_d)/(i_k-i_d)\}\times 100]$, where i_{inh} represents the inhibition current obtained upon addition of the inhibitor to the solution containing the mediator and enzyme, i_k is the catalytic current for the same solution in the absence of inhibitor and i_d the diffusion current for the mediator alone. (n= 2).

5.3.3.5. Immobilised enzyme inhibition electrode - Heterogeneous inhibition

Diffusion coefficients of the immobilised redox polymer, $[Os(bpy)_2(PVI)_{10}Cl]Cl$ (OsPVI), where bpy is the 2,2'-bipyridine ligand and $(PVI)_{10}$ is the poly-N-vinylimidazole indicating a ratio of coordinated redox sites to free pendant groups of 1:10, were evaluated using the Randles-Sevcik equation (5.1). Concentrations of OsPVI from 0.5-1.5 mg/ml were studied. The results obtained, demonstrate greatest diffusion of charge through the polymer film for concentrations of 0.5-1.0 mg/ml. More accurate estimations using Chronocoulometry or Chronoamperometry are necessary to compare with these values obtained. These values, however, indicate that diffusion is limited at higher polymer concentrations, due to the increase in redox centers within the film. It appears that these sites are more densely packed together, and as the concentration is increased an almost impermeable layer is produced. (Table 5.6).

(OsPVI) concentration. (mg/ml)	**Diffusion Coefficient. ($cm^2 s^{-1}$)**
0.5	9.95×10^{-6}
1.0	9.95×10^{-6}
1.5	6.021×10^{-6}

Table 5.6. Diffusion coefficients for the (OsPVI) polymer estimated using the Randles-Sevcik equation (5.1).

The co-immobilisation of both enzyme and electron donor in a stable film on the electrode surface was necessary for the application of these enzyme inhibition electrodes as portable, "reagentless" biosensors. Co-immobilisation of both the tyrosinase enzyme and the osmium mediator was achieved using an approach devised by Ohara *et al.* [7, 25] for the construction of mediated glucose biosensors. In this approach the osmium redox polymer

and the enzyme were crosslinked with PEG in phosphate buffer on the electrode surface. The crosslinker reacts with both the free imidazole nitrogen of the polymer and the enzyme amino groups to produce a stable hydrogel on the electrode surface. Slow drying of the drop-coated electrode in a water saturated atmosphere for a period of at least 48 hours was found to yield stable, active films of immobilised enzyme/electron donor. The formal redox potential for the immobilised osmium redox couple in P.B., pH 7.4 was 220 mV (vs Ag/AgCl), which compares well to that obtained by other researchers for the OsPVI co-immobilised in a hydrogel containing the enzyme glucose oxidase [7] and with the value obtained for the monomer.

The response observed for the enzyme/mediator immobilised electrode remains stable provided sufficient oxygen is present in solution. Modified electrodes prepared by drop-coating the redox polymer and the PEG crosslinker on the electrode surface did not exhibit catalytic currents for the reduction of oxygen. Typical CVs of decreasing reduction current upon the addition of the inhibitior; azide are illustrated in Figure 5.11. The decrease in the reduction current apparent upon addition of the inhibitor indicates that the activity is retained upon immobilisation and that the mediation of electron transfer from the polymeric osmium redox couple to the enzyme active site occurs in the hydrogel. The shape of the modified electrode cyclic voltammetric waves also change from that of a sigmoidal shape, normally observed for electrocatalytic reactions, before addition of inhibitor to a waveshape normally observed for a surface-modified redox polymer upon increasing the inhibitor concentration, again indicating inhibition of catalytic activity.

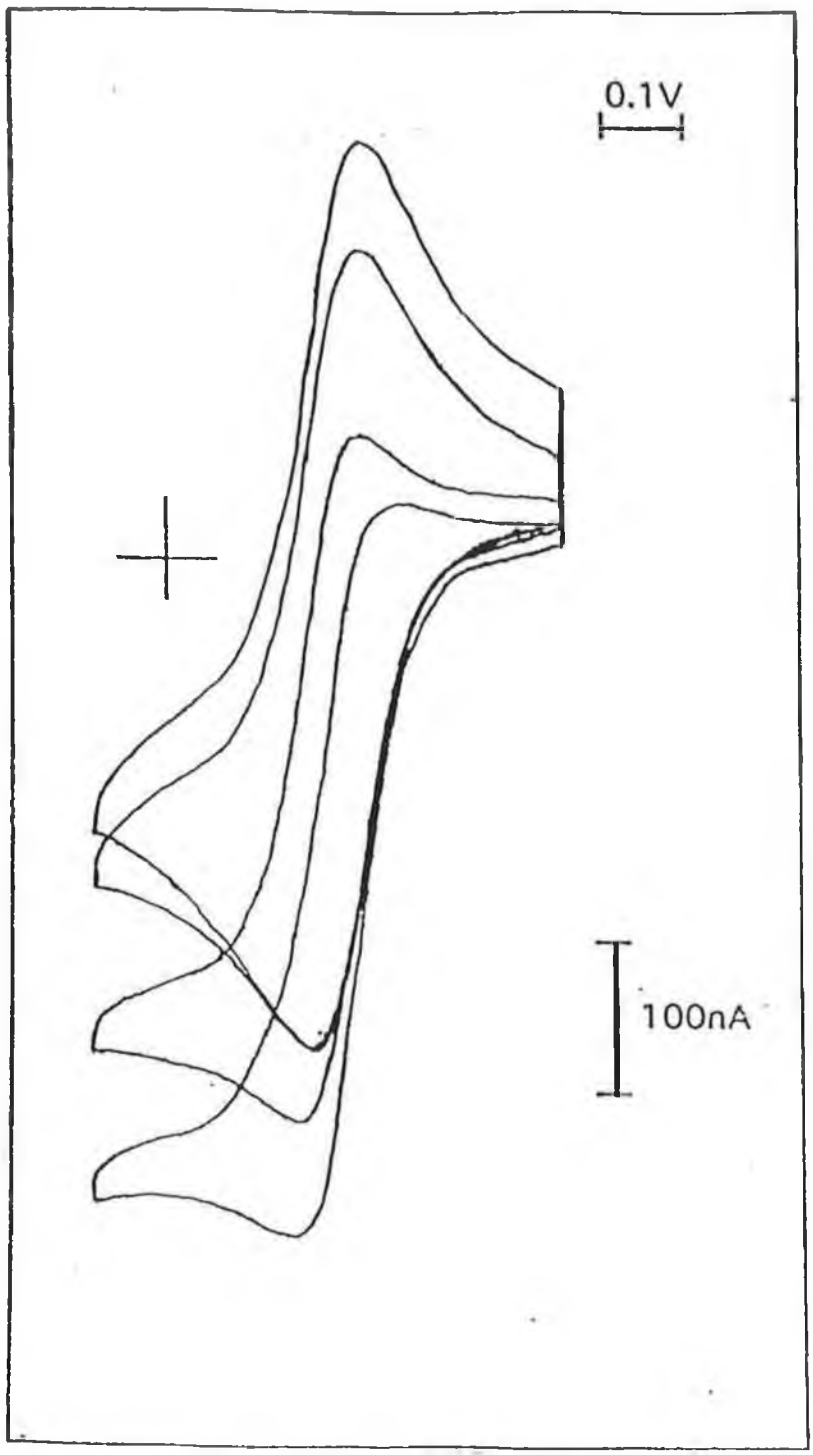

Figure 5.11. Slow scan cyclic voltammogram (2 mV/s) obtained at a modified electrode prepared by drop coating 10 μl $OsPVI_{10}$ (1 mg cm^{-3}), 5 μl of tyrosinase (0.45×10^{-6} mol dm^{-3}) and 10 μl of PEG linker(2.5 mg cm^{-3}) onto a glassy carbon electrode and allowing the mixture to dry for 48 hours. The voltammograms were obtained (in ascending order) upon addition of 0, 0.22, 3.5 and 25×10^{-3} mol dm^{-3} of sodium azide to phosphate buffer (0.05 mol dm^{-3}, pH 7.4).

Reproducible inhibition curves could be obtained from the voltammetric data from different polymeric films by normalising the inhibition response, as in Figure 5.12, by assuming that 25 × 10^{-3} mol dm^{-3} of azide represents 100% inhibition of the enzyme. The hydrogel enzyme electrode was capable of detecting azide inhibitor concentrations as low as 5 × 10^{-6} mol dm^{-3} using the conditions shown in Figure 5.11.

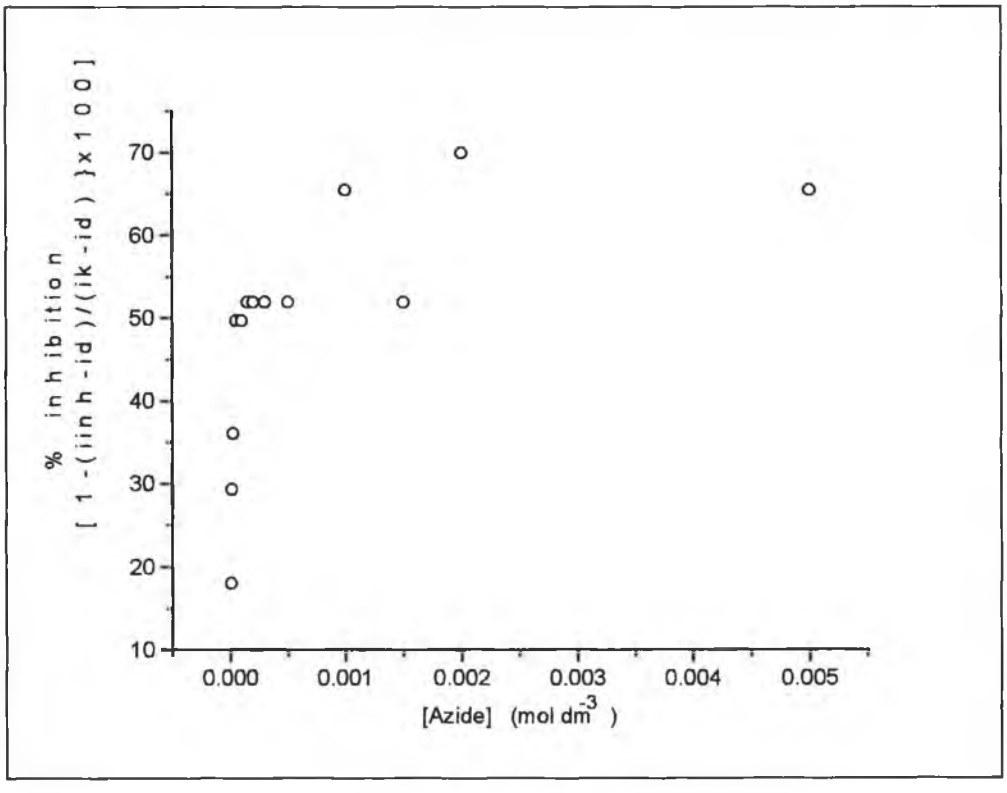

Figure 5.12. Inhibition curve for sodium azide for the modified electrode used in Figure 5.11. Normalisation of the inhibition curve was achieved by assuming that 25× 10^{-3} mol dm^{-3} of inhibitor represents 100% inhibition.

5.3.3.6. Effect of enzyme concentration on inhibition

A series of enzyme electrodes were prepared by pipetting different volumes of enzyme stock solution (0.45 × 10^{-6} mol dm^{-3}) onto the electrode surface. The ratio of the linker to enzyme was varied within the series, while keeping the polymer concentration constant.

No greater than 45 % inhibition was obtained (Figure 5.13.). Heller *et al.* [26] observed that the sensors response was controlled by adequate electron transfer between the enzyme and the polymer, such as an electron transferring collision of chain process occurring, thus a delicate balance between the enzyme : polymer exists.

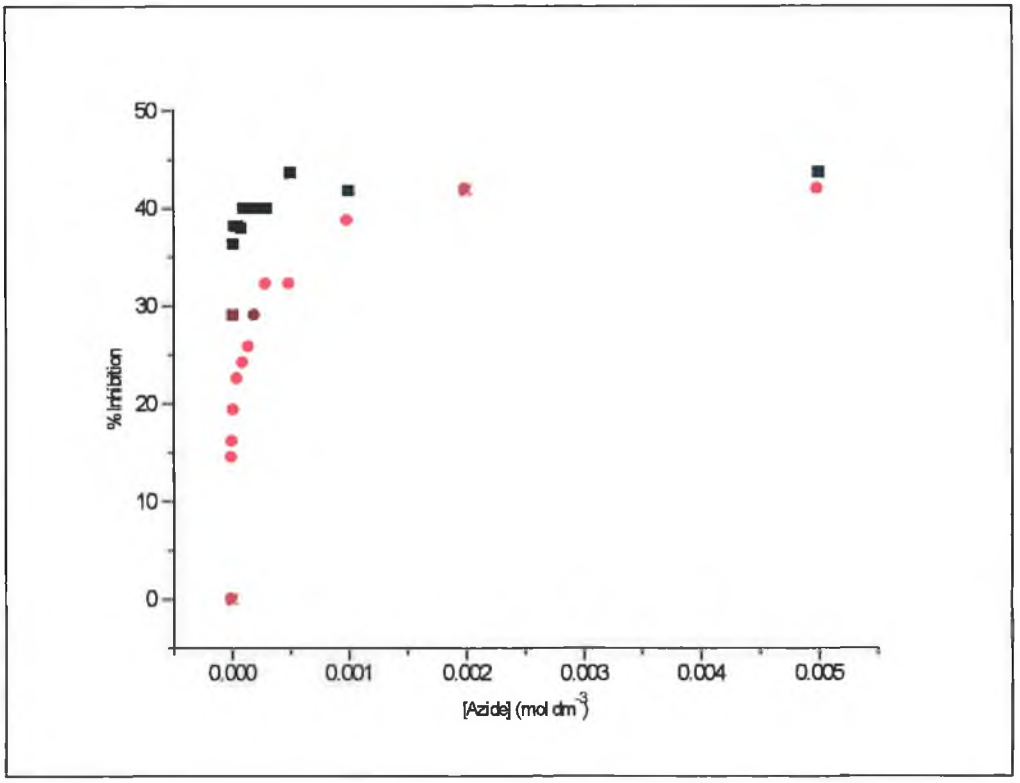

Figure 5.13. Effect of enzyme concentration on inhibition for slow scan cyclic voltammetry (2 mV s^{-1}). Electrodes were prepared by pipetting volumes of 5 µl of (OsPVI); (1.0 mg dm^{-3}), 5 µl PEG crosslinker (2.5 mg dm^{-3}) and 10 µl of tyrosinase (0.45 × 10^{-6} mol dm^{-3}) as represented by the closed square, while volumes of 5 µl of (OsPVI) (1.0 mg dm^{-3}), 10 µl PEG crosslinker (2.5 mg dm^{-3}) and 5 ul of tyrosinase (0.45 × 10^{-6} mol dm^{-3}) are represented by the closed circle, onto a glassy carbon electrode as before.(n = 2)

5.3.3.7. Effect of polymer concentration on inhibition

The extent of inhibition varied considerably with redox polymer concentration. A polymer concentration of 0.5 mg/ml demonstrated only 30 % inhibition while up to 100 %

inhibition was observed for a polymer concentration of 1.0 mg/ml inhibition upon the addition of 0.001 mol dm^{-3} sodium azide. Higher redox polymer concentrations of 1.5 mg/ml were also investigated, but in these experiments, the inhibition currents fluctuated considerably. This may be explained by assuming that: at increased concentration there is a more dense network of redox polymeric sites, which surround the enzyme and restrict the access of other ions into the film. Steric hindrance by this excess of polymer sites protect the enzyme from azide attack yet manifest limitations on charge transport properties.

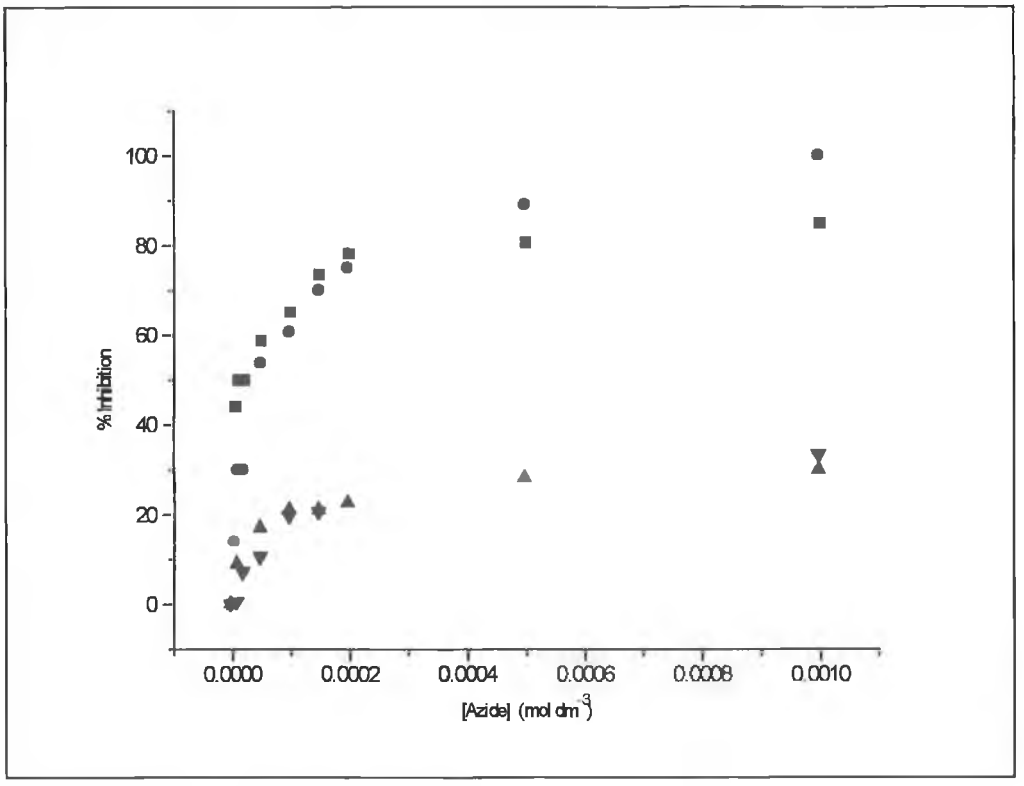

Figure 5.14. The effect of polymer concentration on the inhibition of tyrosinase activity obtained for slow scan cyclic voltammetry. The modified electrode consisted of 5 µl of tyrosinase (0.45×10^{-6} mol dm^{-3}) and 5 µl of PEG linker (2.5 mg dm^{-3}) with 5 µl $OsPVI_{10}$ (0.5 mg dm^{-3}) represented by the closed triangles and 5 µl $OsPVI_{10}$ (1.0 mg dm^{-3}) as represented by the closed square and circle.(n = 2).

5.3.4. Determination of the kinetic parameters of the tyrosinase electrode using rotating disk electrode experiments (RDE)

All rotating disk electrode experiments were performed in an electrochemical cell containing 3 cm^3 of 0.05 M P.B., pH 7.4 solutions. The modified electrode was allowed to equilibrate in the P.B. solution for approximately 30 minutes, or until a steady state was reached, prior to performing any electrochemical experiments. The electrode was then rotated at slow speeds for 5-10 minutes to allow any unbound enzyme or polymer to fall off prior to RDE experiments. The electrochemical cell was fully aerated by bubbling oxygen from a controlled flow-cell at a flow rate of 40 ml/min and was maintained throughout all experiments.

In Figure 5.4, the general kinetic scheme for the immobilised tyrosinase electrode was illustrated. In this model, it is assumed that the enzyme layer is sufficiently thin, so that no concentration polarisation of the substrate, S in the external solution occurs, and that the substrate has a partition coefficient K and a diffusion coefficient D_s in the film. Thus the surface concentration of substrate in the film is Ks_∞ , where s_∞ is the bulk concentration of the substrate. The enzyme catalysed oxidation of S is assumed to occur throughout the film, and can be described by standard Michaelis-Menten kinetics, where K_m and k_{cat} have their usual meaning [27].

Lyons *et al.* [28] and Iwuoha *et al.* [29] have described that the catalytic current can be achieved at infinite rotation speeds in RDE, where there is no mass transfer effects. The catalytic current can be obtained from the intercept of the Koutecky-Levich (KL) equation:

$$\mathbf{1/I_s = 1/I_{Lev}\ \omega^{-1/2} + 1/I_{cat}} \qquad (4.5)$$

where I_s is the steady state current of the RDE, I_{Lev} is the Levich current, which is diffusion controlled and can be denoted by: $I_{Lev} = 0.2nFAD^{2/3}\nu^{-1/6}s_\infty$, I_{cat} is the catalytic

current (μA), ω is the rotational speed (rpm) and ν is the kinematic viscosity of the buffer medium ($cm^2\ s^{-1}$).

Preliminary results revealed an increase in steady state current as the rotation speed of the enzyme electrode was increased. Typical plots are illustrated in Figure 5.15. This indicates that the enzyme layer is not lost to the bulk solution as was described by Iwuoha et al. [29].

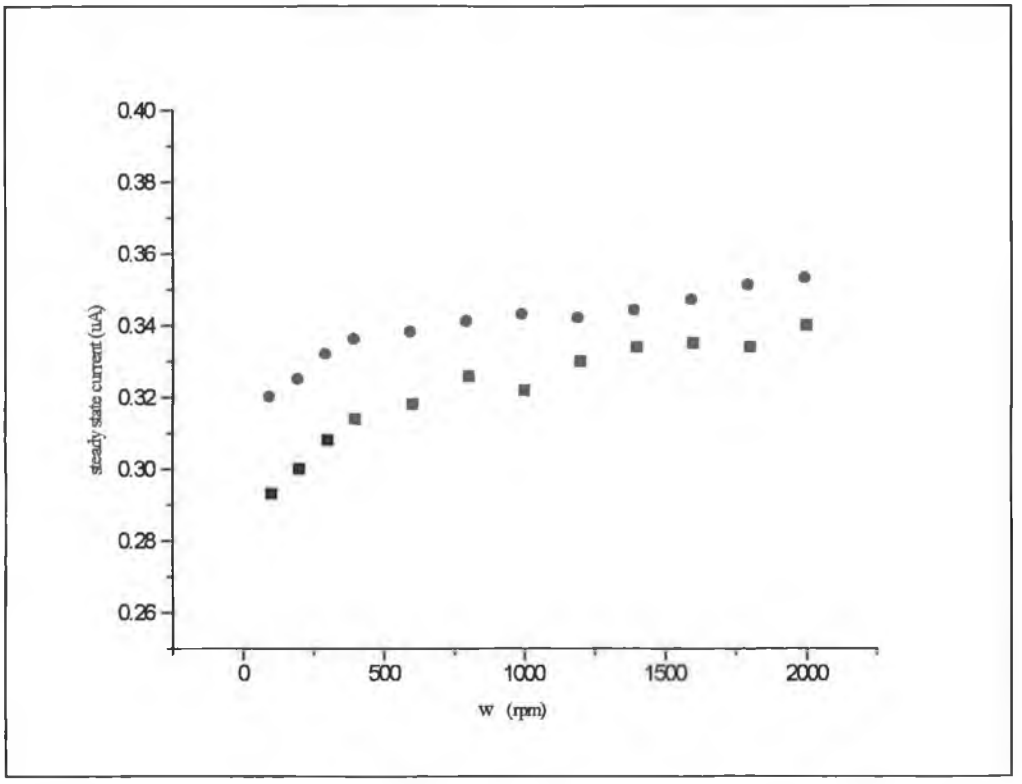

Figure 5.15. Typical plots of increasing steady state current with increasing rotational speed for RDE experiments in an aerated cell of 0.05 M phosphate buffered solutions (n= 2).

When Koutecky-Levich plots of $1/I_s$ vs. $\omega^{-1/2}$ at different oxygen concentrations are carried out, then it is possible to evaluate the kinetic parameters K_m and k_{cat} from the Lineweaver-Burke plots of the intercept of the Koutecky-Levich plots. [30]. Typical Koutecky-Levich plots are illustrated in Figure 5.16, with linear slopes for 4 different oxygen tensions.

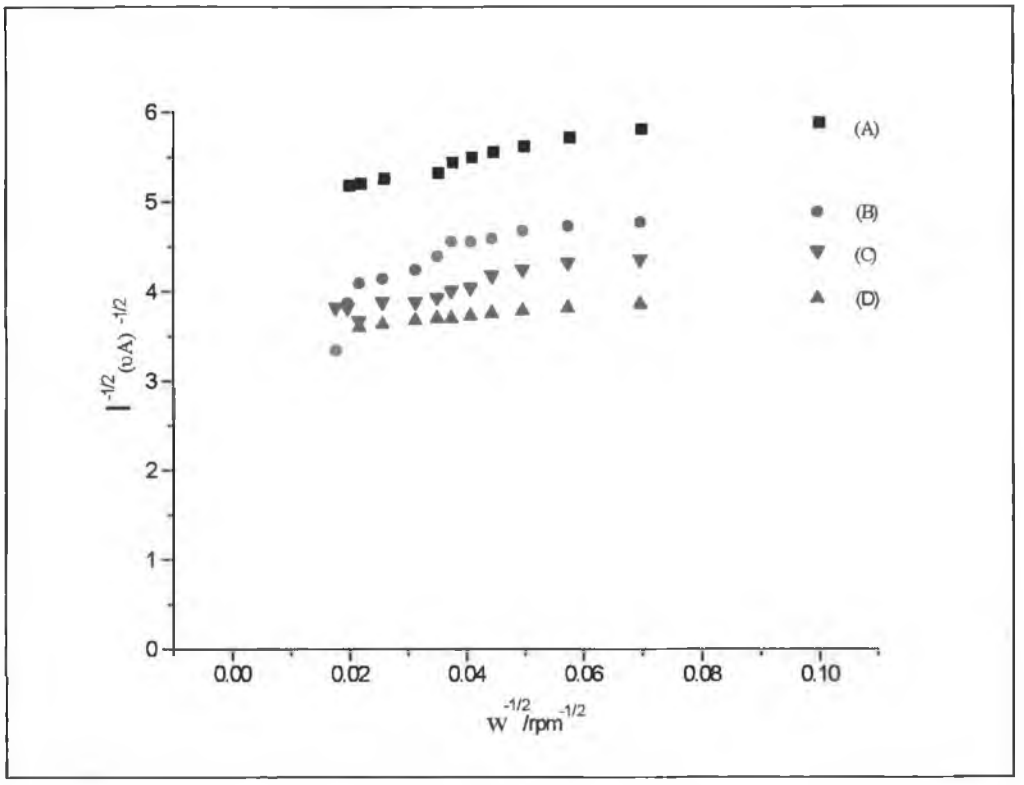

Figure 5.16. Koutecky-Levich plot of the (OsPVI)/tyrosinase based biosensor for different oxygen tensions. Results are shown for oxygen tensions of 6 lb/inch^2 (A), 10 lb/inch^2 (B), 14 lb/inch^2 (C) and 21 lb/inch^2 (D) which was bubbled into an electrochemical cell containing 0.05 M phosphate buffer, pH 7.4, (n=2).

However, a non-linear plot was obtained for the Lineweaver-Burk plot, which may indicate inefficient enzyme kinetics. These preliminary experiments suggest that stirring serves primarily as a means to maintain the oxygen concentration at the solution-film interface [31]. From the slopes of these plots, values for the Diffusion coefficient (D_S) can be calculated and compared with those obtained by cyclic voltammetry.

In these preliminary experiments for the estimation of k_{cat} and K_m, no attempt was made to estimate the film thickness. Furthermore, it is anticipated that the stability of this particular biosensor design is not sufficiently strong for RDE-based experiments, as the biosensing layer was often disturbed during rotational experiments, which often meant the cession of these experiments. The difficulty in obtaining results for k_{cat} and K_m indicate that a protective membrane layer, such as a dialysis membrane or cellulose tri-nitrate

membrane layer as described by Budnikov *et al.* [31] will be necessary to contain the enzyme layer in place. Cooper *et al.* [32] have used a nylon membrane, and results indicate that the presence of this gasket has not perturbed the hydrodynamics of the rotating disc experiments significantly. They describe similar results for the mass transport in the solution to that at the bare electrode surface.

5.4. CONCLUSION

An immobilised enzyme/mediator-modified electrode for the 'reagentless' detection of enzyme activity, consuming only oxygen present in the electrolyte solution is described. Sampling of enzyme activity is achieved by supplying a sufficiently reducing potential to the modified electrode to effect the electrochemical reduction of the immobilised osmium redox species. This tyrosinase based sensor is capable of detecting any modulator of enzyme activity. The use of the electrode as an enzyme inhibition sensor is demonstrated by the detection of the tyrosinase inhibitor, azide, and provides an attractive alternative approach for its detection. The model system described here reacts rapidly (within seconds) upon the introduction of azide in the submicromolar range.

As the basis for its sensing is on the biological action of a toxin rather than on its molecular structure, it is envisaged to extend the system for the detection of other inhibitors of tyrosinase such as cyanide.

Future research should include a more detailed investigation for the determination of inhibition kinetics in the modified electrode, for the optimisation of the response to inhibitors. This should also include studies containing a protective membrane layer to contain the enzyme which may enable an improved estimation of catalytic constants k_{cat} and the K_m.

5.5. REFERENCES

1. Forster, R. J.; Vos, J. G. *Macromolecules* **23** (1990) 4372-4377.
2. Gould, S.; Leasure, R. M.; Meyer, T. *J. Chemistry in Britain* (1995) 891-893.
3. Heller, A. *Acc. Chem. Res.* **23** (1990) 128-134.
4. Heller, A. *Angew. Chem. Int. Ed. Engl.* **29** (1990) 82-84.
5. Gregg, B. A.; Heller, A. *Anal. Chem.* **62** (1990) 256-163.
6. Gregg, B. A.; Heller, A. *J. Phys. Chem.* **95** (1991) 5970-5975.
7. Ohara, T. J.; Rajagopalan, R.; Heller, A. *Anal. Chem.* **65** (1993) 3512-3517.
8. Csöregi, E.; Schmidtke, D. W.; Heller, A. *Anal. Chem.* **67** (1995) 1240-1244.
9. Solomon, E. I.; Lowery, M. D. *Science*, **259** (1993) 1575-1580.
10. Himmelwright, R. S.; Eickman, N. C.; LuBien, C. D.; Lerch, K.; Winkler, M. Solomon, E. I. *J.Amer. Chem. Soc.* **102** (1980) 7339-7344.
11. Mayer, A.M.; Harel, E. *Phytochem.* **18** (1979) 193-215.
12. Kubowitz, F. *Biochem. Z.* **229** (1938) 32-57.
13. Duckworth, A.W.; Coleman, J. E. *Anal. Biochem.* **34** (1970) 382-386.
14. Jolley, R.L.; Makino, N.; Evans, L.E.; Mason, H.S. *J. Biol .Chem.* **249** (1974) 335-345.
15. Forster, R. J.; Vos, J. G. *J. Electrochem. Soc.* **139** (1992) 1503-1509.
16. Furbee, J. W. Jr.; Thomas, C. R.; Kelly, R. S.; Malachowski, M. R. *Anal. Chem.* **65** (1993) 1654-1657.
17. Nicholson, R. S.; Shain, I. *Anal. Chem.* **36** (1964) 706-723.
18. Cass, A. E. G.; Davis, G.; Francis, G. D.; Hill. H. A. O.; Higgins, I. J.; Aston, W. J.; Plotkin, E. V.; Scott, L. D. L.; Turner, A, P. L. *Anal. Chem.* **62** (1984) 667-671.
19. Smit, M. H. ; Rechnitz, G. A. *Anal. Chem.* **62** (1990) 2429-2436.

20. Zakeeruddin, S. M.; Fraser, D. M.; Nazeeruddin, M. K.; Grätzel, M. *J. Electroanal. Chem.* **337** (1992) 253-283.
21. Cooper, J. M.; Bannister, J. V.; McNeil, C. J. *J. Electroanal. Chem.* **312** (1991) 155-163.
22. Fraser, D. M.; Zakeeruddin, S. M.; Grätzel, M. *J. Electroanal. Chem.* **359** (1993) 125-139.
23. Makino, N.; Mason, H. S. *J. Biol. Chem.* **248** (1973) 5731-5735.
24. Rivas, G.; Solis, V. M. *Bioelectrochem. Bioenerg.* **29** (1992) 19-28.
25. Ohara, T. J.; Rajagoplan, R. Heller, A. *Anal. Chem.* **66** (1994) 2451-2457.
26. Lumley-Woodyear, T.; Rocca, P.; Lindsay, J.; Dror, Y.; Freeman. A.; Heller, A. *Anal. Chem.* **67** (1995) 1332-1338.
27. Bartlett, P. N.; Whitaker, R. G. *J. Electroanal. Chem.* **224** (1987) 27-35.
28. Lyons, M. E. G.; Lyons, C. H.; Michas, A.; Bartlett, P. N. *J. Electroanal. Chem.* **351** (1993) 245-258.
29. Iwuoha, E. I.; Smyth, M. R.; Lyons, M. E. G. *J. Electroanal. Chem.* **390** (1995) 35-45.
30. Weibel, M. K.; Bright, H. J. *J. Biol. Chem.* **246** (1971) 2743-
31. Mell, L. D.; Maloy, J. T. *Anal. Chem.* **47** (1975) 299-307.
32. Budnikov, H. C.; Evtugyn, G. A. *Electroanalysis.* **8** (1996) 817-820.
33. Cooper, J. M.; Alvarez-Icaza, M.; McNeil, C. J.; Bartlett, P. N. *J. Electroanal. Chem.* **272** (1989) 57-70.

CHAPTER 6

CONCLUSIONS AND FUTURE TRENDS

6.1. CONCLUSIONS

This thesis has dealt with some capillary electrophoretic separations and the development of a biosensor for pharmaceutical and biomedically related applications.

CE is now firmly established as a viable option for the analysis of a wide variety of pharmaceutical compounds [1]. The versatility of CE, its minimal buffer solution consumption, and high efficiency separations achieved using inexpensive capillaries are just some of the benefits offered by CE. These features among others, will ensure its importance as an analytical method, capable of complementing or even presenting as an alternative method among the classical established methodologies.

The utility of CE for the analysis of several NSG-peptoid combinatorial libraries was evaluated in Chapter 2. Combinatorial libraries involve the rapid generation of a large number of compounds with diverse physical and chemical characteristics. The screening and identification for bioactive components and suitable pharmacokinetics is the driving force behind the generation of these libraries, in the hope of discovering new drug molecules. Peptide libraries have been synthesised and used in drug research; however, their metabolic instability, owing to proteolysis and their poor absorption characteristics, often render them poor drug candidates [2]. Non-synthetic libraries, i.e. NSG-peptoids, are structurally similar; however, they are far more likely to become useful therapeutic agents than peptide-based libraries.

The initial investigation involved developing a CE separation method for one particular NSG-peptoid library, CHIR 4580.1, and assessing the utility of this method for the separation of five other structurally diverse libraries. Various parameters affecting the separation of the individual peptoids were examined. This included investigating the effect of the run buffer pH, ionic strength and several buffer additives.

It was found that a mixed-mode system, involving both an ion-pairing agent (heptane sulphonic acid) and a cyclodextrin (methyl-β cyclodextrin) was necessary to achieve optimum separation. While the time required for separation was quite long, compared to the majority of CE separations, the diverse range of functionalities attached to the peptoid backbone structure must be considered. This method developed for the separation of CHIR 4580.1 was successfully applied to three other libraries with only minor modifications being made.

The remaining problematic libraries resolved using yet another mixed-mode system, involving cyclodextrin and a micelle. While complete resolution of these libraries was not achieved, this cyclodextrin-modified MEKC system, appears to be quite promising for the separation of these highly hydrophobic molecules. A brief investigation involving bile salts was also carried out to asssess their ability to separate these bulky hydrophobic peptoid libraries. While the time required for separation was greatly reduced, the number of individual peptoids actually separated remained similar to what was obtained with the cyclodextrin-modified MEKC system.

Finally a look at some individual NSG-peptoid markers were investigated. While only a brief study was carried out, these markers offer an insight towards the migration behaviour of individual peptoids within a given library and may be used as internal standards for CE method development of combinatorial libraries. These can be used in conjunction with or as an alternative to the classical markers such as Sudan III or Sudan IV for SDS micellar-based systems.

Chapter 3 utilises CE with diode array detection to provide additional spectral information for the identification of the unstable intermediate compounds, produced during the oxidation of L-tyrosine and L-dopa, during melanogenesis. A century has passed, and yet this pathway remains uncertain and still challenges various research communities. The significance of this pathway stems from its social and cosmetic

importance to a more serious level, involving the formation of malignant melanomas at a cellular level.

The enzymatic oxidation of L-tyrosine by tyrosinase was found to depend on the concentration of tyrosinase used, with optimum production of intermediate compounds being formed within 5 minutes when an activity of 44 units/mg solid was used. The tyrosinase enzyme loses activity following prolonged incubation and outside the pH range of 6-8; hence chemical oxidation, involving sodium periodate is more suitable. Short capillaries and high voltages facilitated the rapid analysis of the products of L-dopa oxidation, with run times generally less than 4 minutes. The diode array spectra of several unstable intermediate compounds formed were illustrated and their identity postulated. Use of an internal standard is recommended to minimise problems associated with drifting migration times, and two possible candidates are presented.

In addition, electrochemical studies were performed to elucidate some of the electrochemical characteristics of the final product, melanin, formed during the melanogenesis pathway. While the structure of melanin is still unknown, it is thought to be composed of pyrrole units randomly linked forming a hygroscopic polymer or mixture of polymers and was assessed as a potential biopolymer for sensor/biosensor-based applications. The effect of buffer pH on the voltammetric behaviour of L-dopa, and the durability of the polymeric film was assessed using cyclic voltammetry. The effect of different electrolyte ions, perchlorate and sulphate-based electrolytes were also investigated. The rate of charge propagation through these electrochemically prepared films was measured using chronocoulometry, and the results obtained were compared with other polymer systems. The use of a melanin biopolymer offers a new and challenging concept in sensor/biosensor-based applications.

Finally the rationale of electrically 'wiring' redox enzyme to an electrode via redox polymers was introduced in Chapters 4 & 5. Modified electrodes employing redox mediators to shuttle electrons to the electrode surface, demonstrating rapid electron

transfer kinetics was discussed. The high specificity of enzymes for their substrates and the high selectivity of these for target species has received considerable attention in recent years.

In Chapter 5, the development of an electrically 'wired' tyrosinase enzyme inhibition inhibition electrode was described. This involved use of osmium-based redox compounds as artificial mediators. Optimisation procedures of the mediated oxidation of $[Os(bpy)_2Cl]Cl^{+/0}$ with tyrosinase, involved investigating the effect of varying parameters such as pH ionic strength and temperature, using cyclic voltammetric analysis. Various kinetic parameters for the interaction of the enzyme with the various electron donors, were evaluated. Based on these parameters, the inhibition of tyrosinase enzyme using sodium azide as a model inhibitor was investigated for both the homogenous and the heterogenous case. The model system described, reacts quickly upon the introduction of azide and was capable of detection of levels as low as 5×10^{-6} mol dm^{-3} in solution. As the basis for its sensing is on the biological action of a toxin rather than on its molecular structure, it is envisaged that this system amy be used for the detection of other inhibitors of tyrosinase, such as cyanide, and may be used as an early warning poison sensor.

6.2. FUTURE TRENDS

The small dimensions of the separation capillary (typically 10-100 μm in diameter) make detection a particular problem in CE. Of all the detection techniques developed for CE, fluorescence shows the greatest promise for introduction to automated commercial systems, giving increased sensitivity for compounds with appropriate fluorophores. Other detection modes, such as electrochemical techniques offer considerable utility for CE applications. Amperometric detection provides excellent sensitivity for the small dimensions associated with CE, while offering a high degree of selectivity towards electroactive species.

Heller *et al.* [3] have recently extended the idea of wiring a redox enzyme to an electrode and was coupled with an HPLC for the determination of four biologically important substances. The enzyme-electrode offered good selectivity, high selectivity, low detection limits and was stable over a period of seven days of continuous operation. O'Shea et al. [4] have described a chemically modified microelectrode using glucose oxidase for the selective determination of glucose as a detector for CE. One of the drawbacks associated with chemically modified electrodes for electrochemical detection in conjunction with CE was that the optimal run buffer for the CE separations was very often not compatible with the electrolyte conditions necessary for the maximum detector response. A modified version of this system was recently described [5] which involved using a membrane-based on-column mixer for the separation and detection of several amino acids. An extension of the work carried out in this thesis would be to co-immobilise different redox modifiers for multifunctional based operations i.e. for the detection of respiratory poisons as an alternative to the conventional modes commonly employed, which would extend this already rapidly growing list of CE applications.

6.3. REFERENCES

1. Altria, K. D.; Elgey, J.; Lockwood, P.; Moore, D. *Chromatographia* **42** (1996) 332-342.
2. Desai, M. C.; Zuckermann, R. N.; Moos, W. H. *Drug Dev. Res.* **33** (1994) 174-188.
3. Yang, L.; Janie, E.; Huang, T.; Gitzen, J.; Kissinger, P. T.; Vreek, M.; Heller, A. *Anal. Chem.* **67** (1995) 1326-1331.
4. O'Shea, T. J.; Lunte, S. M. *Anal. Chem.* **66** (1994) 307-311.
5. Zhou, J.; Lunte, S. M. *Anal. Chem.* **67** (1995) 13-18.

Appendix

List of Publications

1. Electrically 'Wired' Tyrosinase Enzyme Inhibition Electrode for the Detection of Respiratory Poisons. Gemma Robinson, Donal Leech and Malcolm R. Smyth Electroanalysis 7, 10 (1995) 952-957.
2. Development of a Capillary Electrophoretic Separation of an NSG-Peptoid Combinatorial Library. Gemma M. Robinson, Malcolm R. Smyth, and Craig, E. Lunte. J. Chromatogr. (1997). Submitted for publication.
3. Application of Capillary Electrophoresis to the Separation of Structurally Diverse NSG-Peptoid Combinatorial Libraries. Gemma M. Robinson, Malcolm R. Smyth and Craig E. Lunte. J. Chromatogr. (1997). Submitted for publication.
4. Determination of Products and Intermediates of L-dopa Oxidation using Capillary Electrophoresis with Diode Array Detection. Gemma M. Robinson and Malcolm. R. Smyth. (manuscript in preparation).
5. Transport and kinetic studies in melanin, and its suitability as a sensor component. Gemma M. Robinson, Emmanuel I. Iwuoha, Malcolm R. Smyth. (manuscript in preparation).

Seminar and Poster Presentations

A. 'Biomedical Applications of Capillary Electrophoresis Linked to Microdialysis Sampling and Electrochemical Detection'. Malcolm R. Smyth and Gemma M. Robinson. At the Symposium on Capillary Electrophoresis on 'Applications of Capillary Electrophoresis in Medicine', (Queens University Belfast, 1995).
B. 'Capillary Electrophoretic Analysis of Peptoid Combinatorial Libraries'. Poster presentation by Gemma M. Robinson at The Fifth International Workshop on Bioanalysis at The University of Kansas, Lawrence, Kansas, USA (1996).